

AN INVESTIGATION OF THE POWER SPECTRAL DENSITY OF ATMOSPHERIC TURBULENCE

by

GERHARDT C. CLEMENTSON

B.S. U.S. Military Academy, 1942
M.S. California Institute of Technology, 1945
S.M. Massachusetts Institute of Technology, 1948

SUBMITTED IN PARTIAL FULFILLMENT OF THE
REQUIREMENTS FOR THE DEGREE OF
DOCTOR OF SCIENCE
at
MASSACHUSETTS INSTITUTE OF TECHNOLOGY
1950

Signature of Author

Thesis Supervisor

Chairman, Departmental Committee on Graduate Students

Aero
Thesis
1950



May 12, 1950

Prof. Joseph S. Newell
Secretary of the Faculty
Massachusetts Institute of Technology
Cambridge 39, Massachusetts

Dear Professor Newell:

In accordance with the regulations of the faculty, I hereby submit a thesis entitled, "An Investigation of the Power Spectral Density of Atmospheric Turbulence," in partial fulfillment of the requirements for the degree of Doctor of Science.

Respectfully yours,

ACKNOWLEDGMENT

The author wishes to express his gratitude and appreciation to the following persons and organizations who aided directly or indirectly in the development of this thesis:

To Dr. C. S. Draper, who in a large measure is directly responsible for the opportunity for carrying on this investigation.

To the United States Air Forces for supplying the airplane used in this investigation and for assigning the author to Massachusetts Institute of Technology for graduate training.

To Professor R. C. Seamans, Jr., for his helpful and constructive supervision and encouragement.

To Dr. J. H. Laning, Jr. and Dr. Elmer Frey for many helpful and practical suggestions.

To the staff of the Tracking Control Project of the Instrumentation Laboratory for invaluable technical assistance and suggestions.

To the personnel of the Bedford Flight Facility of the Instrumentation Laboratory, M.I.T., for wholehearted cooperation and assistance with the flight test phases of this investigation.

To Miss Alice Wood and Miss Maryann Harris for the arduous task of correlating and computing the flight test records.

To Mr. L. E. Payne and his associates of Jackson & Moreland for editing and reproducing the manuscript.

This thesis was prepared while assigned as a graduate student from U.S.A.F.I.T. under the auspices of D.I.C. Project-6445-T-31 and sponsored by the Office of Air Research and the Armament Laboratory, Engineering Division, Air Materiel Command, through Contract No. W33-038-ac-13969, Project No. RR-3.

TABLE OF CONTENTS

	<u>Page</u>
ABSTRACT	vii
Chapter 1 INTRODUCTION	1
A. Summary of Previous Work	1
B. The Requirements for This Investigation	2
Chapter 2 ELIMINATION OF INSTRUMENTATION SYSTEM DYNAMICS FROM THE TEST DATA	4
Chapter 3 THE PROBLEM OF ELIMINATING THE FORWARD VELOCITY OF THE INSTRUMENTATION SYSTEM FROM THE REDUCED DATA	7
Chapter 4 DISCUSSION OF RESULTS	9
Chapter 5 CONCLUSIONS AND SUGGESTIONS FOR FURTHER RESEARCH	16
A. Conclusions	16
B. Recommendations and Suggestions for Further Research	16
Appendix I GENERALIZED HARMONIC ANALYSIS	18
A. Fourier Transform Pairs	18
B. Mathematical Theorems Related to the Study of Atmospheric Turbulence	20
C. Statistical Analysis of Time Series	23
D. The Harmonic Analysis of Random Functions	25
Appendix II INPUT - OUTPUT STATISTICAL RELATIONSHIP	27
Appendix III THE SAMPLING PROBLEMS INVOLVED IN THE APPLICATION OF THE THEORY OF A GENERALIZED HARMONIC ANALYSIS TO A FINITE NUMBER OF RECORDS OF FINITE LENGTH	31
A. The General Problem of Estimating the Correlation Function	34
B. The Sampling Problem of a Random Function of Time	35
C. Sample Size Criteria	38
D. Reasonable Estimate of the Correlation Function	41

TABLE OF CONTENTS
(continued)

	<u>Page</u>
Appendix IV METHODS OF APPROXIMATION USED IN OBTAINING THE POWER SPECTRAL DENSITIES	46
A. Method No. 2	47
B. Method No. 3	49
Appendix V AIRCRAFT PERFORMANCE FUNCTIONS	52
A. General	52
B. Basic Assumptions and Definitions Used in the Development of Performance Functions	53
C. Assumptions for the Determination of the Statistical Properties of Rough Air	53
D. Longitudinal Response Equations	55
E. Lateral Response Equations	58
F. The Test Airplane	60
G. Stability Derivatives Used in Computation of Airplane Performance Function	64
Appendix VI DESCRIPTION OF FLIGHT TEST INSTRUMENTATION	66
A. General	66
B. The Flight Test Instrumentation	66
Appendix VII DESIGN OF A CORRELATION COMPUTER	75
Appendix VIII BIBLIOGRAPHY	84
Appendix IX GLOSSARY	86
Appendix X BIOGRAPHICAL SKETCH	89
FLIGHT TEST SUPPLEMENT	90

TABLE 1		
Meteorological Condition	Mean Power of θ Response [(CF) $_{\theta\theta}$ (0)] in [deg/sec] ²	Root-Mean Square of $\dot{\theta}$ Response [(RMS)($\dot{\theta}$)] in [deg/sec]
Unstable air mass	.0987	.3142
Water - land discontinuities	.1672	.4089
Thunderstorms	.1038	.3222
Mountainous terrain	.1224	.3499

influences the airplane primarily in roll, could not be determined with the degree of certainty possible for the longitudinal data due to the inadequate length of the records. However, on the basis of this limited data, a tentative conclusion can be made that the spectrum of this lateral component is not essentially different from the longitudinal component.

Chapter 1

INTRODUCTION

A. Summary of Previous Work

In some respects, turbulence has been exhaustively investigated, and one may justifiably question the need or desire for an additional investigation. However, as is shown later, there is a great need for data on atmospheric turbulence of the type herein presented. In order to appreciate this distinction, it is desirable that one review the history of the study of turbulence that affects this problem.

The most extensive program carried out by any agency within the United States for the study of atmospheric turbulence has been conducted by the National Advisory Committee for Aeronautics. Unfortunately, this program was aimed primarily toward obtaining a statistical survey of air loads on airplanes in flight. This data, in general, forms a statistical survey of the statics of extreme values (peak amplitudes only determined) of turbulent air, and in no way can be used to determine a statistical survey of the dynamics of turbulent air. The correlation function, which is introduced later, is a statistical parameter that measures the importance of the dynamics of a random process and is the basis of this investigation. The N.A.C.A. data cannot be used to obtain a correlation function for two reasons:

1. The performance function or frequency response spectrum of the aircraft from which the data was measured are not known.
2. Since only peak values of the output response were determined, nothing is known about the airplane response as a continuous function between peaks. Consequently the dynamics of the output function is completely unknown.

In general, the present investigation is a practical application of Wiener's general theory.^{(2)*} However, this work was not, until recently in an unrestricted classification; and the original idea and proposal for making this investigation is a direct result of the lectures of Dr. Yuk Wing Lee⁽²²⁾ of the Electrical Engineering Department at the Massachusetts Institute of Technology.

* See list of references in Appendix VIII for references in parentheses.

In terms of the end result (the power spectral density of the turbulent air mass) this investigation is essentially the same as the correlation method of determining boundary layer turbulence. An excellent report on this modern statistical theory of turbulence has been written by Monsieur Bass⁽¹³⁾. The primary difference between the study by Monsieur Bass and this investigation (other than the obvious difference in scale) is that the turbulence he considers can be measured directly. In this investigation, it is necessary to measure the response of a sensing vehicle, the airplane, to the turbulence, and by the direct application of the Wiener - Lee theory, determine the input power spectral density.

This work is an extension of a larger program in airplane dynamic research. The first and pioneering program was conducted by the Cornell Aeronautical Laboratory at Buffalo, New York. In this program, the frequency response of an airplane was determined directly by sinusoidally oscillating the flight controls. The second program, conducted at the Instrumentation Laboratory, M. I. T., determined the frequency response indirectly by making a harmonic analysis of the airplane response to measured pulses. The present program leans heavily on the two former programs for the frequency response characteristics of the airplane and from this data conducts a generalized harmonic analysis of turbulent air.

B. The Requirements for This Investigation

The design of automatic control equipment for aircraft has, in the past, been based primarily on steady-state performance characteristics. In the preliminary design state, very little consideration was given to the fact that under certain meteorological conditions, the aircraft and its control equipment would also be subjected to random inputs caused by the turbulence of the atmosphere. In general, the effect of turbulence was taken into consideration in the flight test stages of the design by modifications to the existing design. In some cases these modifications were successful; and an excellent control system was obtained. However, in other cases, modifications were not so successful.

The usual specifications were that the control equipment meet a certain required steady-state performance, and be well-behaved in turbulent air. This latter requirement was not too important because the pilots were always available to take over the controls.

However, the day of the completely controlled aircraft in all types of weather is not too far off. When this day arrives, the equipment must be properly designed to meet certain minimum requirements under all weather conditions. In addition, since the primary means of control will be automatic, it is highly desirable to

realize the optimum designs for average weather conditions.

The term "optimum design for the average condition" needs more careful definition. Since the design is to be optimized for the average condition, it is evident that the design problem belongs in the general field of the statistics of dynamic elements.

Norbert Wiener⁽²⁾ has solved this general problem for the case of a linear system subjected to random and controlled inputs. He has shown that for a given stationary random process and a given class of controlled inputs, there exists a unique design of the mechanism which will minimize the integral squared error. However, in order to determine this optimum design, one must first determine the correlation functions of the controlled inputs and the random inputs.

In addition to automatic control equipment, there is also the problem of stabilizing an airborne platform in turbulent air. In order to realize a good design, the spectrum of the turbulent air mass must be known. To meet this dual requirement, this investigation was undertaken.

The object of this investigation is to obtain the power spectral density of turbulent air for use in the design of control equipment and stabilized airborne platforms for aircraft.

Chapter 2

ELIMINATION OF INSTRUMENTATION SYSTEM DYNAMICS FROM THE TEST DATA

The problem of determining the power spectral density of the velocity components of a turbulent air mass is basically a general measurement problem, wherein the output response of a sensing element is known and the input forcing function is desired. In the usual measurement problem, the input is either periodic or of finite duration, and consequently, is amenable to ordinary harmonic analysis. However, the velocity components of turbulent air are neither periodic nor of finite duration. In fact, they constitute a continuous infinite random set of functions. As is pointed out in Appendix I, it is not possible to obtain a harmonic analysis of such a random function directly. Instead, one must make use of the auto-correlation function* and its Fourier transform, the power spectral density.

In Appendix II, it is shown that the output response of a linear system to a randomly varying input is very simply related when the output and the input are described statistically by their auto-correlation function. In the time domain, the relation is given by a convolution integral as follows:

$$[(CF)_{oo}(\tau)] = \int_{-\infty}^{\infty} [(CF)_{(UIR)}(t)][(CF)_{ii}(t + \tau)] dt \quad (2-1)$$

where

$$[(CF)_{oo}(\tau)] = \lim_{T \rightarrow \infty} \frac{1}{2T} \int_{-T}^T q_{out}(t) q_{out}(t + \tau) dt$$

* The auto-correlation function is defined as the correlation of a function of time with itself when displaced along the time axis. The cross-correlation function is defined as the correlation of two different functions of time when displaced along the time axis.

$$[(CF)_{ii}(\tau)] = \lim_{T \rightarrow \infty} \frac{1}{2T} \int_{-T}^T q_{in}(t) q_{in}(t + \tau) dt$$

$$[(CF)_{(UIR)}(\tau)] = \int_{-\infty}^{\infty} [(UIR)(t)][(UIR)(t + \tau)] dt$$

This expression can be reduced to a simpler form in the frequency domain by taking the Fourier transform of Eq. (2-1) to give:

$$[(PSD)_{oo}(\omega)] = \left| (PF)_{()} [q_{in} q_{out}] \right|^2 [(PSD)_{ii}(\omega)] \quad (2-2)$$

where

$$[(PSD)_{oo}(\omega)] = \int_{-\infty}^{\infty} [(CF)_{oo}(\tau)] \cos \omega \tau d\tau$$

$$[(PSD)_{ii}(\omega)] = \int_{-\infty}^{\infty} [(CF)_{ii}(\tau)] \cos \omega \tau d\tau$$

$$\left| (PF)_{()} [q_{in} q_{out}] \right|^2 = \int_{-\infty}^{\infty} [(CF)_{(UIR)}(\tau)] \cos \omega \tau d\tau$$

Equation (2-2) is the basis for eliminating the instrumentation system dynamics. The performance function used in this equation is the product of the aircraft instrumentation performance function and the airplane performance function.

In order to simplify as much as possible the data reduction problem, all airplane response data was measured with the controls locked. If this were not done, the airplane would be simultaneously acted upon by two forcing functions and the problem of data reduction and flight test instrumentation would be considerably increased.

The simplification, due to locked controls, is in itself a compromise between reliability of the correlation function obtained and ease of reducing the resulting data. This compromise arises from the fact that the airplane differential equations of motion are in general non-linear, but can be linearized in terms of small oscillations about an equilibrium airspeed. With the controls locked, the airplane eventually ends up in a tight spiral with the airspeed building up. Since the equilibrium point is now non-existent, the record must be terminated. In the flight test program, all records were terminated by a roll-off.

In the case of the longitudinal response data, this compromise was quite satisfactory since record lengths of 20 to 30 response times* were obtained. In the lateral response data, these record lengths were only 4 to 5 response times and not of sufficient length to constitute reliable samples.

In future programs, it will be highly desirable to consider the installation of an autopilot to maintain the equilibrium condition. This arrangement will give more reliable sampling, but has the disadvantage that the instrumentation system performance function becomes a closed loop enclosing the airplane and autopilot, and consequently will be more difficult to determine. In this respect, a proposal has been made by the Flight Research Group of the Cornell Aeronautical Laboratory to calibrate the airplane by flying over a concentrated thermal disturbance such as occurs over an open hearth blast furnace. If this method of calibration proves successful, the addition of an autopilot to the instrumentation system constitutes no additional problem.

* (RT), Response time is defined as the time required for the airplane response to decrease to and remain less than 5 percent of its maximum output magnitude.

Chapter 3

THE PROBLEM OF ELIMINATING THE FORWARD VELOCITY OF THE INSTRUMENTATION SYSTEM FROM THE REDUCED DATA

At a fixed point in space, the instantaneous velocity of an air particle in a turbulent air mass can be described by a randomly varying vector. To describe the state of turbulence at this fixed point in space, one must know both the time history of the vector at the given point as well as the variation at a given instant of time of the velocity vectors with any three spatial coordinates. However, in this investigation only the variation of the velocity vector in two directions at a given instant of time is important in disturbing the airplane. These two variations are:

1. The change of the normal component of the velocity vector as a function of the distance along the flight path of the airplane.
2. The change of the partial derivative of the normal component of the velocity vector with respect to spanwise distance as a function of the distance along the flight path of the airplane.

The variation of the velocity vector with time at a fixed point in space is assumed negligible for the following reason:

The lowest airplane velocity used in these tests was 299 ft/sec. The tail length of the airplane is 25.9 ft. Hence, at a fixed point in space, the airplane can be influenced at the most by 0.1 second of the time history of the air mass velocity vector. It is assumed that no significant change in the velocity vector occurs in this short an interval.

Consequently, the random forcing function in the longitudinal case is assumed to be given by the spatial distribution of the vertical component of the air mass velocity along the flight path. This forcing function appears distributed in time due to the motion of the airplane through the air mass.

The response of the airplane to the turbulent air mass is measured as a continuous function of time. This data is then reduced, by the method already presented in Chapter 2, to a power spectral density of the vertical component of the air mass. This power spectral density represents the spectrum of the correlation function of the

turbulent air mass as it appeared to an airplane flying at the test airspeed. To another airplane flying faster through the air mass, the turbulence would be compressed in time; and consequently the bandwidth of the power spectral density would be increased. This effect, however, can be compensated for.

In Appendix I, a general relation is derived for the Fourier transform of a function that is changed in scale, i.e.;

$$[\text{FT}(\omega)][q(at)] = \frac{1}{a} [\text{FT}(\frac{\omega}{a})][q(t)]$$

In this particular case:*

$$q(t) \stackrel{\Delta}{=} [(\text{CF})_{qq}(\tau)]$$

$$a \stackrel{\Delta}{=} V_A \stackrel{\Delta}{=} \text{True velocity of the airplane in feet per second.}$$

Applying this relation to the power spectral density of the air mass under the test conditions, one obtains

$$[(\text{PSD})(\omega)][\text{CF}(V_A\tau)] = \frac{1}{V_A} [(\text{PSD})(\frac{\omega}{V_A})][\text{CF}(\tau)]$$

Hence, if the test power spectral density curve is scaled in both coordinates by the true velocity of the airplane under the test conditions, a general curve is obtained that can be applied to any airplane for which the frequency response is known at any applicable airspeed.

* The symbol $\stackrel{\Delta}{=}$ means "equal by definition."

Chapter 4
DISCUSSION OF RESULTS

In the entire flight test program, more than one thousand feet of oscillograph recordings were taken. This program consisted of six flights that represented four different meteorological conditions of the atmosphere, as follows:

Condition No. 1

Unstable Air Mass	Flight #85
Towering Cumulous	Flight #86
Hot Summer Day	

Condition No. 2

Hot summer day, ground thermals obtained by flying over water-land discontinuities from Lowell, Mass. to Newburyport, Mass.	Flight #87
	Flight #89

Condition No. 3

Low thunderstorms	
High ground winds	Flight #90
Cold front passage	

Condition No. 4

High ground winds over mountainous terrain – "White Mountains"	Flight #91
--	------------

Although this data cannot be assumed to be representative samples of atmospheric turbulence as a whole, it certainly is representative of a large group of turbulent air in which military and civilian flights must be conducted under normal operations.

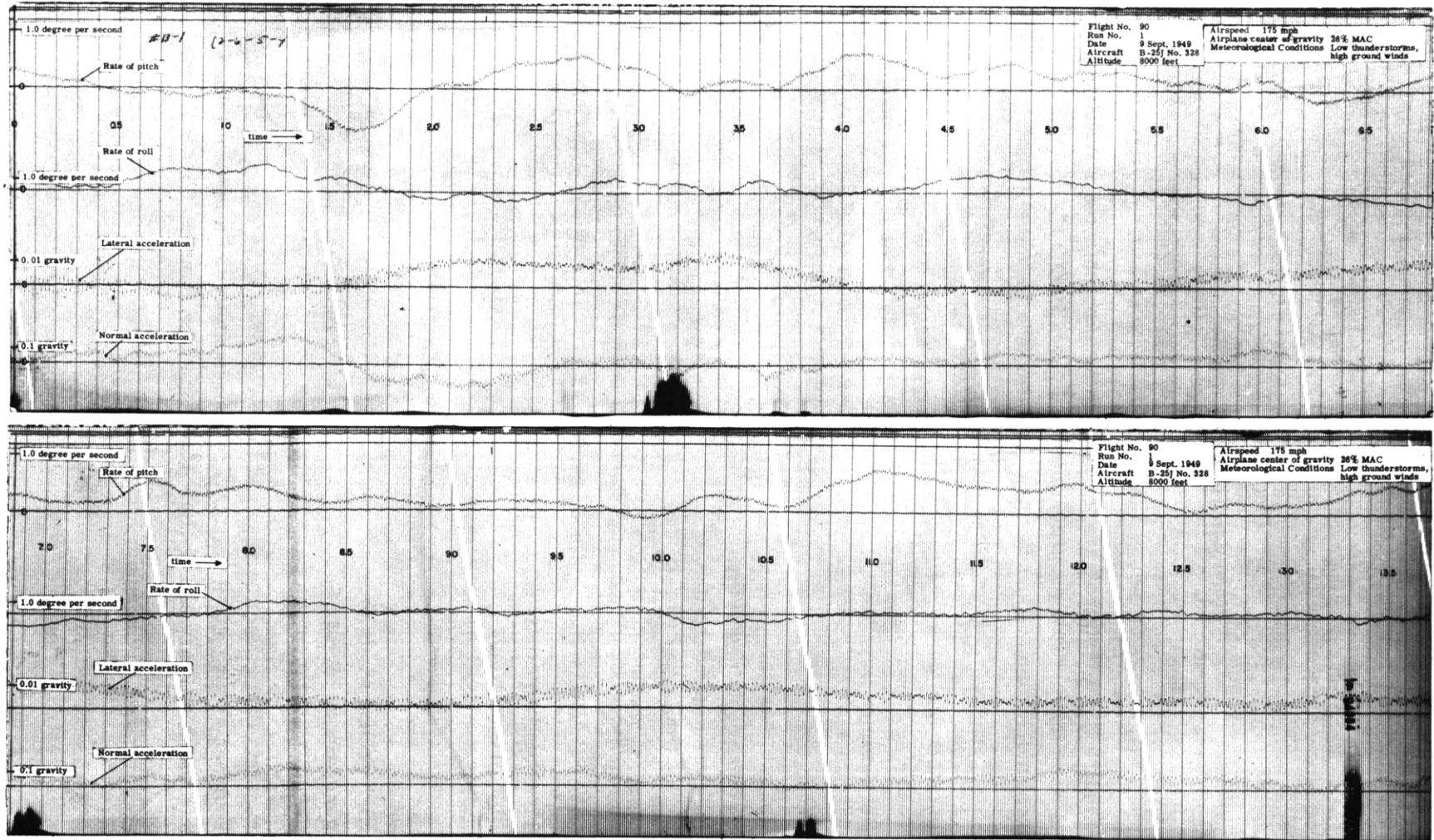


FIG. 4-1 SAMPLE FLIGHT TEST DATA.

Because it was felt that, on the average, most persons would be interested primarily in the final results of this investigation, the entire group of flight test records were published in a supplement and only one sample record presented in Fig. 4-1. For those persons who are interested in the entire group, the flight test data supplements are available through the Instrumentation Laboratory, M.I.T., by request.

Although four output response variables of the airplane were measured, only two were analyzed because of an unavoidable delay in construction of the correlation computer. The rate of pitch response, $\dot{\theta}$, of the airplane was analyzed completely for all recorded data. The entire set of data is plotted in Fig. 4-2, which is

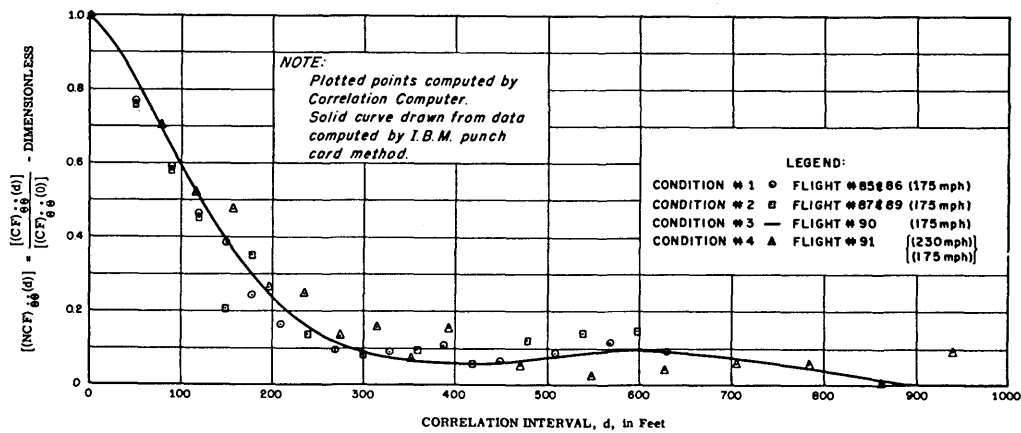


FIG. 4-2 THE NORMALIZED REDUCED CORRELATION FUNCTION OF THE RESPONSE OF A B-25J AIRPLANE TO ATMOSPHERIC TURBULENCE FOR FOUR DIFFERENT METEOROLOGICAL CONDITIONS.

a normalized correlation function reduced to eliminate the true velocity of the airplane. The plot is indeed remarkable when one recalls that it represents six flights on different days under four different meteorological conditions. This plot is the basis for the conclusion drawn that, other than a difference of mean power (or intensity) of the gust, the atmospheric turbulence for the set of conditions tested is a stationary random process, and can be adequately described by a single reduced power spectral density curve. The mean power and root mean square of the output response for each condition is given in Table 4-1.

Figure 4-3 presents all three spectrums involved in computing the power spectral density of the atmospheric turbulence. The three curves were plotted on the same graph in order to graphically illustrate how the dynamics of the airplane

TABLE 4-1

	Meteorological Condition	Mean Power of $\dot{\theta}$ Response $[(CF)_{\dot{\theta}}(0)]$ in $[\text{deg}/\text{sec}]^2$	Root-Mean-Square of $\dot{\theta}$ Response $[(\text{RMS})(\dot{\theta})]$ in $[\text{deg}/\text{sec}]$
1.	Unstable air mass	.0987	.3142
2.	Water-land discontinuities	.1672	.4089
3.	Thunderstorms	.1038	.3222
4.	Mountainous terrain	.1224	.3499

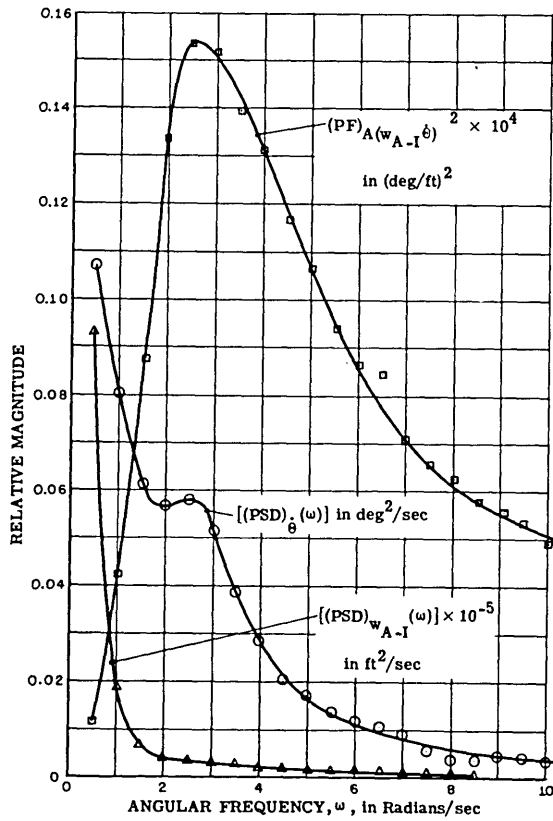


FIG. 4-3 COMPARISON OF FREQUENCY SPECTRUM OF OF AVERAGE OF ALL FLIGHT TEST LONGITUDINAL DATA AT 175 m.p.h.

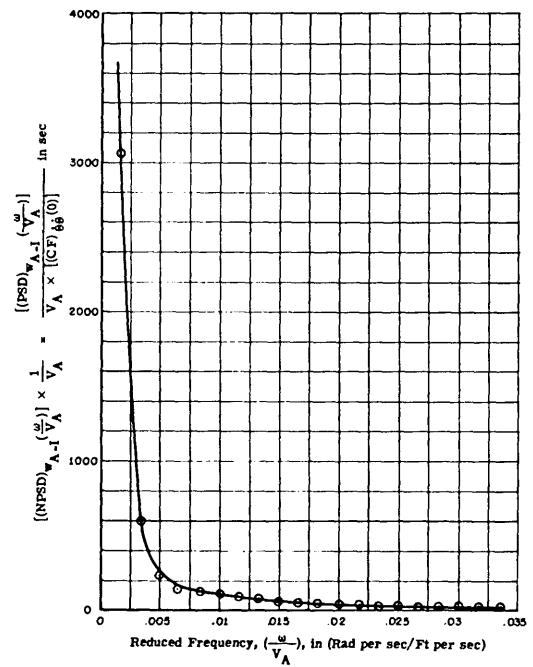


FIG. 4-4 REDUCED-NORMALIZED POWER SPECTRAL DENSITY OF VERTICAL VELOCITY COMPONENT OF ATMOSPHERIC TURBULENCE

were eliminated from the response data. The power spectral density of the airplane output response is the Fourier transform of Fig. 4-2 for a true airplane velocity of 299 ft/sec and has already been corrected for the dynamics of the rate of pitch gyro. The power spectral density of the input turbulence is the output spectrum divided by the square of the magnitude of the performance function of the airplane.

Figure 4-4 is the reduced power spectral density of the vertical velocity component of atmospheric turbulence for the conditions tested. To use this curve for a given true velocity and for one of the tested meteorological conditions, multiply the ordinate by both the airplane true velocity in feet per second and the mean power given by Table 4-1; then, multiply the abscissa by the airplane true velocity in feet per second. This data can be used to optimize a given airplane control system.

Since the airplane performance function has been linearized for an equilibrium airspeed, it is necessary to consider a number of optimum systems for the range of airspeed desired, and then to choose a compromise design. This formidable task can be made somewhat easier by an airplane control system simulator such as has been developed by the Tracking Control Project of the Instrumentation Laboratory, M.I.T. This method would require the design of two filters and a "white noise" generator.⁽²⁶⁾ One filter must be designed to approximate the airplane performance function ratio given in Appendix V. The purpose of this filter is to modify the existing airplane simulator to obtain the airplane frequency response function to atmospheric turbulence. The second filter must be designed so that the square of the magnitude of its performance function approximates the atmospheric turbulence power spectral density curve. A preliminary check seems to indicate that a first-order network gives a satisfactory approximation. If the "white noise" generator is then connected in chain with the two filters, this output signal can be added to the airplane simulator control signal to simulate the statistical effect of atmospheric turbulence on the system.

Figure 4-5 is the reduced rate of roll response correlation function of the airplane for Condition No. 3. This curve was computed by I.B.M. methods and smoothed as indicated in Appendix IV.

Figures 4-6 and 4-7 are the reduced data from Fig. 4-5. It is noticed that the power spectral density curve of the lateral turbulence shows an apparent peak at the "Dutch Roll" oscillation of the airplane. This peak is not considered characteristic of the atmospheric turbulence, but represents instead an indication of the uncertainty of the data in this case. This uncertainty arises from two main sources:

1. The lateral airplane performance functions are not as reliably known as the longitudinal performance functions. This can be

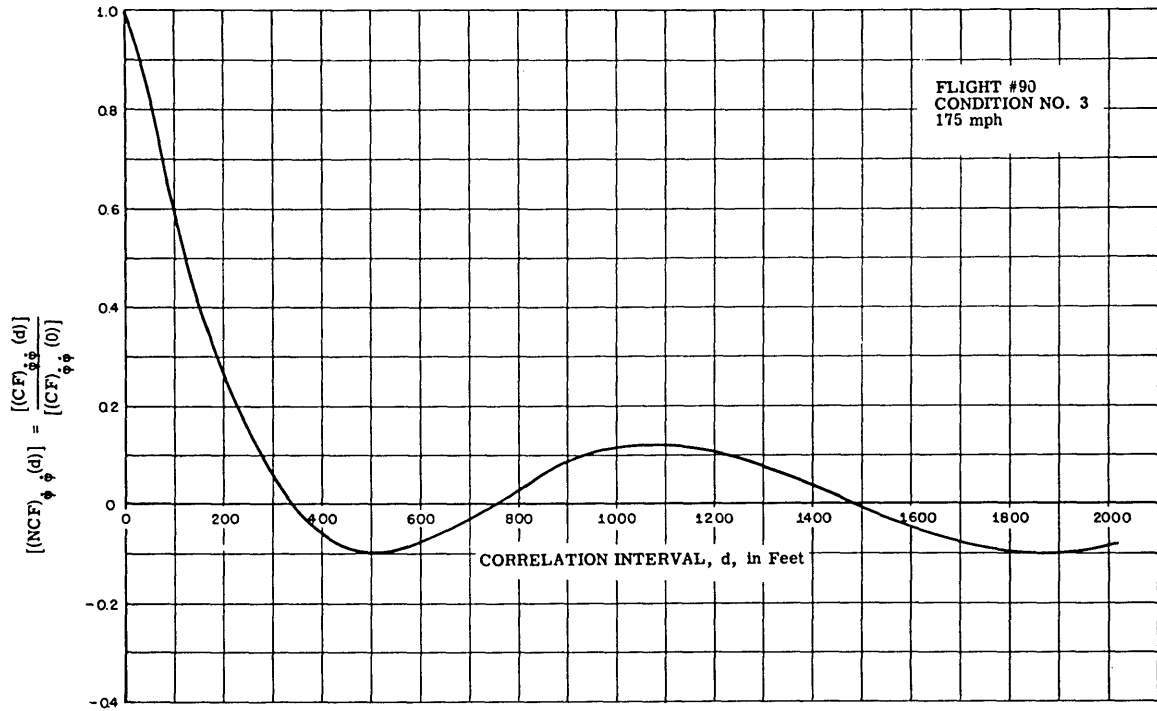


Fig. 4-5 THE NORMALIZED REDUCED CORRELATION FUNCTION OF THE RATE OF ROLL RESPONSE OF A B-25J AIRPLANE TO ATMOSPHERIC TURBULENCE FOR METEOROLOGICAL CONDITION NO. 3

- attributed to the general difficulty of accurately measuring a system performance function that has a large resonance peak.
2. The sampling errors in the recorded data for the lateral response are much larger than for the longitudinal response due to the fact that the average record length in this case is only three to four times the lateral response time, $(RT)_{(lat)}$, of the airplane. A dotted curve has been drawn on Fig. 4-7 to indicate the best estimate from this limited data of the lateral power spectral density.

The frequency spectrums in Figs. 4-3 and 4-6 are not shown for frequencies below $1/2$ radian per second because of lack of data as to their behavior in this region. No information was obtained in this region for two reasons:

1. The airplane fixed control performance functions were not determined below $1/2$ radian per second.

- The length of the airplane response records was not sufficient to include frequencies below 1/2 radian per second.

This lack of data at the low frequencies is not a serious obstacle to the use of the over-all results because the major problems of stabilization of aircraft systems arise for forcing frequencies above 1/2 radian per second.

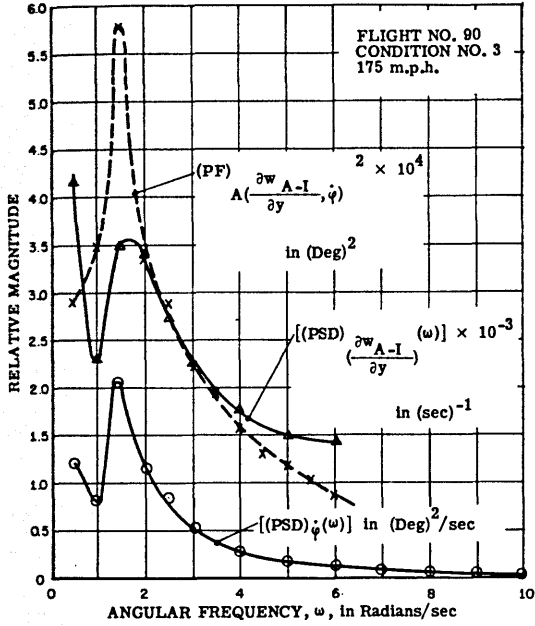


FIG. 4-6 COMPARISON OF FREQUENCY SPECTRUM OF LATERAL FLIGHT TEST DATA

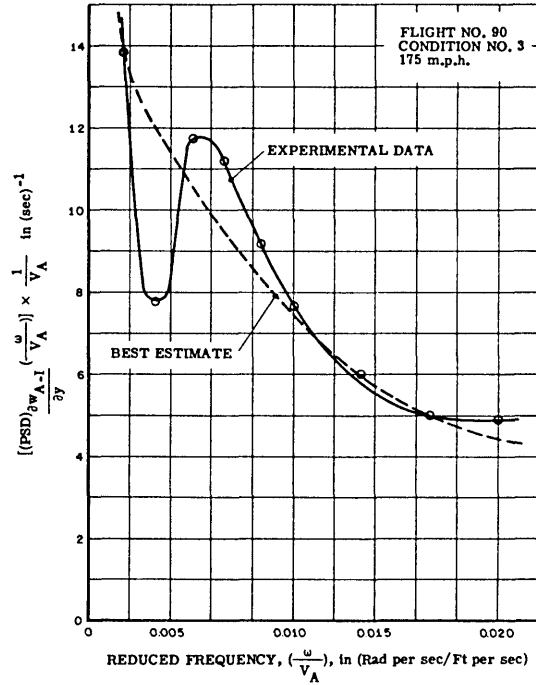


FIG. 4-7 REDUCED POWER SPECTRAL DENSITY OF SPANWISE RATE OF CHANGE OF VERTICAL VELOCITY COMPONENT OF ATMOSPHERIC TURBULENCE

Chapter 5

CONCLUSIONS AND SUGGESTIONS FOR FURTHER RESEARCH

A. Conclusions

On the basis of results obtained in this investigation, the following conclusions are presented:

1. Atmospheric turbulence is a stationary random process that can be statistically described by a single reduced power spectral density curve.
2. For the limited set of meteorological conditions tested, a single power spectral density curve reduced only by the airplane true velocity has been determined.
3. The power spectral density of the lateral forcing function velocity components is apparently not significantly different from that of the longitudinal components.
4. A correlation computer of the type designed for this thesis is an invaluable aid for conducting this type of statistical study.

B. Recommendations and Suggestions for Further Research

1. This study should be expanded to include a much larger set of meteorological conditions. In case the turbulence appears to have a scale difference in correlation distance through the air mass, it is suggested that a characteristic length be determined for each large meteorological condition that could be used to reduce the correlation function of the turbulence to a unique function in terms of a non-dimensional distance through the air mass. The non-dimensional distance could be obtained by dividing the correlation distance by the characteristic length for each meteorological condition.
2. The correlation computer should be re-designed to operate from a magnetic tape. This would be potentially faster, more accurate, and simpler to operate.

3. A compact, portable measuring system that records on a magnetic tape should be designed so that it can be used to obtain future records of an airplane response to turbulent air.
4. A method for obtaining the performance function for the airplane response to turbulent air should be evolved that does not require the use of theoretical correction factors to the airplane fixed control performance functions.
5. An investigation should be made of the long period response and the lateral response of the airplane by means of an airplane controlled by an auto-pilot.

Appendix I

GENERALIZED HARMONIC ANALYSIS

Introduction

The theory of a generalized harmonic analysis was presented by Norbert Wiener in 1930 ⁽²⁾. Since this investigation is primarily a practical application of this general theory, only so much of the theory as is directly connected to this effort will be presented here. No attempt is made to present the rigorous theory, rather a conscious attempt has been made to present in a heuristic engineering manner the practical application and usefulness of the theory. Any and all over-simplifications in this respect are solely the responsibility of the author.

As Norbert Wiener has pointed out ⁽¹⁾, the theory of a generalized harmonic analysis is a natural and compatible union of two widely different fields of scientific endeavor, statistical analysis of time series, and communication engineering. The primary tools used from each field are the theory of correlation from the field of statistics and the theory of transient analysis of dynamic systems from the field of communication engineering. A short discussion is given on each of these tools in order to lead to the general theory.

A. Fourier Transform Pairs

If $q(t)$ is a periodic function of period T_1 , the following equations constitute the analysis and synthesis of $q(t)$ in terms of harmonics of the fundamental period T_1 .

$$[\text{FSC}] [q(t)] = \frac{1}{T_1} \int_{-\frac{T_1}{2}}^{\frac{T_1}{2}} q(t) e^{-j\frac{2\pi n t}{T_1}} dt \quad (\text{I} - 1)$$

$$q(t) = \sum_{n=-\infty}^{n=\infty} [\text{FSC}] [q(t)] e^{j\frac{2\pi n t}{T_1}} \quad (\text{I} - 2)$$

where

$[\text{FSC}] \triangleq$ Fourier series coefficient.

If $q(t)$ is non-periodic, it is possible to analyze and synthesize the function by a continuous spectrum rather than discrete line spectra as in the case of a periodic function. The transform pair for the continuous spectrum can be developed as the limiting case from Eqs. (I - 1) and (I - 2) as the fundamental period, T_1 , becomes infinite. However, this limit must be taken properly to obtain a usable transform pair.

From Eq. (I - 1) consider the following limit,

$$\lim_{T_1 \rightarrow \infty} \left\{ \int_{-\frac{T_1}{2}}^{\frac{T_1}{2}} q(t) e^{-j\frac{2\pi n t}{T_1}} dt \right\} = L_1 \quad (\text{I} - 3)$$

but (7)

$$\left| \int_{-\frac{T_1}{2}}^{\frac{T_1}{2}} q(t) e^{-j \frac{2\pi n t}{T_1}} dt \right| \leq \int_{-\frac{T_1}{2}}^{\frac{T_1}{2}} |q(t)| dt$$

In order to ensure that the limit L_1 of Eq. (I - 3) remain finite, it is necessary

to stipulate that $\lim_{T_1 \rightarrow \infty} \left\{ \int_{-\frac{T_1}{2}}^{\frac{T_1}{2}} |q(t)| dt \right\}$ be finite.

However, when this condition is met,

$$\lim_{T_1 \rightarrow \infty} \left\{ \frac{1}{T_1} \int_{-\frac{T_1}{2}}^{\frac{T_1}{2}} q(t) e^{-j \frac{2\pi n t}{T_1}} dt \right\} = 0 .$$

To avoid this difficulty, the direct Fourier transform is defined as:

$$[\text{FT}] [q(t)] = \lim_{\substack{T_1 \rightarrow \infty \\ n \rightarrow \infty}} \left\{ T_1 [\text{FSC}] [q(t)] \right\} \quad (\text{I} - 4)$$

or, in the limit:

$$[\text{FT}] [q(t)] = \int_{-\infty}^{\infty} q(t) e^{-j\omega t} dt \quad (\text{I} - 5)$$

where

$$\omega = \lim_{\substack{T_1 \rightarrow \infty \\ n \rightarrow \infty}} \left\{ \frac{2\pi n}{T_1} \right\} .$$

Now, substituting Eq. (I - 4) into Eq. (I - 2):

$$q(t) = \lim_{\substack{T_1 \rightarrow \infty \\ n \rightarrow \infty}} \sum_{n=-\infty}^{\infty} \frac{[\text{FT}] [q(t)]}{T_1} e^{j \frac{2\pi n t}{T_1}}$$

but

$$\lim_{T_1 \rightarrow \infty} \left\{ \frac{1}{T_1} \right\} = \lim_{\omega_1 \rightarrow 0} \left\{ \frac{\omega_1}{2\pi} \right\} = \lim_{\Delta\omega \rightarrow 0} \left\{ \frac{\Delta\omega}{2\pi} \right\}$$

and in the limiting case,

$$q(t) = \frac{1}{2\pi} \int_{-\infty}^{\infty} [\text{FT}] [q(t)] e^{j\omega t} d\omega \quad (\text{I} - 6)$$

with its Fourier transform pair already obtained as

$$[\text{FT}] [q(t)] = \int_{-\infty}^{\infty} q(t) e^{-j\omega t} dt$$

B. Mathematical Theorems Related to the Study of Atmospheric Turbulence

1. The Shift Theorem⁽¹²⁾

$$\begin{aligned} \int_{-\infty}^{\infty} q(t+\tau) e^{-j\omega t} dt &= e^{j\omega\tau} \int_{-\infty}^{\infty} q(t+\tau) e^{-j\omega(t+\tau)} d(t+\tau) \\ &= e^{j\omega\tau} [\text{FT}] [q(t)] \quad . \end{aligned}$$

Hence:

$$[\text{FT}] [q(t+\tau)] = e^{j\omega\tau} [\text{FT}] [q(t)]$$

2. The Multiplication Theorem⁽¹⁰⁾

If

$$[\text{FT}] [q_1(t)] \stackrel{\Delta}{=} \int_{-\infty}^{\infty} q_1(t) e^{-j\omega t} dt$$

$$[\text{FT}] [q_2(t)] \stackrel{\Delta}{=} \int_{-\infty}^{\infty} q_2(t) e^{-j\omega t} dt$$

and

$$q_1(t) = \frac{1}{2\pi} \int_{-\infty}^{\infty} [\text{FT}] [q_1(t)] e^{j\omega t} d\omega$$

$$q_2(\tau) = \frac{1}{2\pi} \int_{-\infty}^{\infty} [\text{FT}] [q_2(t)] e^{j\omega t} d\omega \quad .$$

Then, consider:

$$\begin{aligned}
q(\tau) &= \frac{1}{2\pi} \int_{-\infty}^{\infty} \overline{[\text{FT}][q_1(t)]} \{[\text{FT}][q_2(t)]\} e^{j\omega\tau} d\omega & (\text{I} - 7) \\
&= \frac{1}{2\pi} \int_{-\infty}^{\infty} [\text{FT}][q_2(t)] e^{j\omega\tau} d\omega \int_{-\infty}^{\infty} q_1(t) e^{j\omega t} dt
\end{aligned}$$

where $\overline{[\text{FT}][q_1(t)]}$ is the complex conjugate of $[\text{FT}][q_1(t)]$.

Since $q_1(t)$ and $q_2(t)$ both have transforms, the order of integration may be interchanged so that

$$q(\tau) = \int_{-\infty}^{\infty} q_1(t) dt \frac{1}{2\pi} \int_{-\infty}^{\infty} [\text{FT}][q_2(t)] e^{j\omega(\tau+t)} d\omega$$

or

$$q(\tau) = \int_{-\infty}^{\infty} q_1(t) q_2(t+\tau) dt . \quad (\text{I} - 8)$$

Equating the right-hand sides of Eqs. (I - 7) and (I - 8):

$$\frac{1}{2\pi} \int_{-\infty}^{\infty} \overline{[\text{FT}][q_1(t)]} [\text{FT}][q_2(t)] e^{j\omega\tau} d\omega = \int_{-\infty}^{\infty} q_1(t) q_2(t+\tau) dt \quad (\text{I} - 9)$$

Eq. (I - 9) is known as the multiplication theorem.

For the special case that $q_1(t) = q_2(t) = q(t)$, one obtains,

$$\frac{1}{2\pi} \int_{-\infty}^{\infty} |[\text{FT}][q(t)]|^2 e^{j\omega\tau} d\omega = \int_{-\infty}^{\infty} q(t) q(t+\tau) dt . \quad (\text{I} - 10)$$

Eq. (I - 10) can be further specialized for $\tau = 0$ to obtain Parseval's theorem

$$\frac{1}{2\pi} \int_{-\infty}^{\infty} |[\text{FT}][q(t)]|^2 d\omega = \int_{-\infty}^{\infty} q^2(t) dt .$$

3. The Convolution Integral ⁽¹²⁾

The output response of a linear mechanism to any input function beginning at "a" units in the past can be written in terms of a convolution integral by applying the principal of superposition, that is

$$q_o(t) = \int_{-a}^t [q_i(\sigma)] [(UIR)(t-\sigma)] d\sigma$$

where $[(UIR)(t)] \triangleq$ Unit impulse response of the mechanism.

Now let,

$$t - \sigma = \tau$$

then

$$q_o(t) = - \int_{t+a}^0 [q_i(t-\tau)] [(UIR)(\tau)] d\tau$$

and

$$q_o(t) = \int_0^{t+a} [(UIR)(\tau)] [q_i(t-\tau)] d\tau .$$

However, for a realizable physical system, $[(UIR)(\tau)] = 0$ for $\tau < 0$, hence

$$q_o(t) = \int_{-\infty}^{t+a} [(UIR)(\tau)] [q_i(t-\tau)] d\tau$$

and for an infinite time process

$$a \rightarrow \infty .$$

Hence

$$q_o(t) = \int_{-\infty}^{\infty} [(UIR)(\tau)] [q_i(t-\tau)] d\tau . \quad (I - 11)$$

4. Change of Scale (12)

If $q(t)$ has the Fourier transform $[FT][q(t)]$, and the symbol "a" is a constant, or a second variable which is independent of t and ω , then

$$\int_{-\infty}^{\infty} q(\tau) e^{-j\omega\tau} d\tau = [FT(\omega)] [q(t)]$$

or

$$\int_{-\infty}^{\infty} q\left(a \frac{\tau}{a}\right) e^{-j\omega a \left(\frac{\tau}{a}\right)} d\left(a \frac{\tau}{a}\right) = [\text{FT}(\omega)] [q(t)].$$

Upon substitution of

$$t = \frac{\tau}{a}$$

and

$$\omega = u a$$

this becomes:

$$\int_{-\infty}^{\infty} q(at) e^{-j\omega t} dt = \frac{1}{a} [\text{FT}\left(\frac{\omega}{a}\right)] [q(t)]$$

or

$$[\text{FT}(\omega)] [q(at)] = \frac{1}{a} [\text{FT}\left(\frac{\omega}{a}\right)] [q(t)] \quad (\text{I} - 12)$$

C. Statistical Analysis of Time Series

1. The Correlation Function

In general, the functions that have been considered so far are either periodic or bounded, and converge at infinity at a sufficient rate for the integral of the absolute value of the function to be finite. However, there are a large class of functions that are neither periodic nor converge at infinity. To handle this class of random functions, one must resort to a statistical analysis.

A tool which the statistician often employs to measure the degree of dependence between two sets of variables is the correlation coefficient (KC) defined as:

$$[(\text{KC})_{xy}]_N = \frac{\frac{1}{N} \sum_{i=1}^N (x_i - (\text{av})x_i) (y_i - (\text{av})y_i)}{\sqrt{\frac{1}{N} \sum_{i=1}^N [x_i - (\text{av})x_i]^2 \cdot \frac{1}{N} \sum_{i=1}^N [y_i - (\text{av})y_i]^2}}$$

where $(\text{av})x_i$ and $(\text{av})y_i$ are average values of x_i and y_i , respectively.

If the values of x_i are all assumed to be discrete points of a continuous function of time measured at equal time intervals; and if all the values of y_i are assumed to be the same set shifted by an integral number of intervals, one can define a serial correlation coefficient (SKC) as:

$$[(SKC)_{x_1 x_{1+n}}(n)]_N = \frac{\frac{1}{N} \sum_1^N (x_1) (x_{1+n})}{\sqrt{\left[\frac{1}{N} \sum_1^N (x_1)^2\right] \left[\frac{1}{N} \sum_1^N (x_{1+n})^2\right]}} \quad (I - 13)$$

where $(av)x_1$ and $(av)x_{1+n}$ have been assumed zero for convenience.

Now let the number of variates, N , in the time series increase without limit. Let it be assumed that the statistical properties of the series approach definite limits, (or that the series is in statistical equilibrium). In this case,

$$\lim_{N \rightarrow \infty} \left\{ \frac{1}{N} \sum_1^N (x_1)^2 \right\} = \lim_{N \rightarrow \infty} \left\{ \frac{1}{N} \sum_1^N (x_{1+n})^2 \right\}$$

and consequently the numerator by itself is now a measure of correlation. Wiener has defined the auto-correlation function to be the following limit:

$$[(CF)_{xx}(n)]_{\infty} = \lim_{N \rightarrow \infty} \frac{1}{2N+1} \sum_{i=-N}^{i=N} x_i x_{i+n} \cdot \quad (I - 14)$$

When the time interval between successive variates in the series is decreased indefinitely, the auto-correlation function for the continuous case is defined as:

$$[(CF)_{qq}(\tau)]_{\infty} = \lim_{T \rightarrow \infty} \left\{ \frac{1}{2T} \int_{-T}^T q(t) q(t+\tau) dt \right\} \cdot \quad (I - 15)$$

2. Properties of the Auto-Correlation Function

a.

Consider:

$$[q(t) \pm q(t+\tau)]^2 \geq 0$$

or:

$$[q(t)]^2 + [q(t+\tau)]^2 \geq 2q(t)q(t+\tau)$$

and, averaging both sides:

$$\begin{aligned} & \lim_{T \rightarrow \infty} \left\{ \frac{1}{2T} \int_{-T}^T [q(t)]^2 dt + \frac{1}{2T} \int_{-\infty}^{\infty} [q(t+\tau)]^2 dt \right\} \\ & \geq \lim_{T \rightarrow \infty} \left\{ \pm \frac{2}{2T} \int_{-T}^T q(t)q(t+\tau) dt \right\} \end{aligned}$$

but, for a stationary random process:

$$\lim_{T \rightarrow \infty} \left\{ \frac{1}{2T} \int_{-T}^T [q(t)]^2 dt \right\} = \lim_{T \rightarrow \infty} \left\{ \frac{1}{2T} \int_{-T}^T [q(t+\tau)]^2 dt \right\} .$$

Hence,

$$[(CF)(0)] \geq \pm [(CF)(\tau)]$$

or

$$[(CF)(0)] \geq |[(CF)(\tau)]| \quad (I - 16)$$

b.

$$[(CF)(\tau)] = \lim_{T \rightarrow \infty} \frac{1}{2T} \int_{-T}^T q(t)q(t+\tau) dt .$$

Define

$$s = t + \tau$$

or

$$t = s - \tau$$

and

$$dt = ds .$$

Then

$$[(CF)(\tau)] = \lim_{T \rightarrow \infty} \frac{1}{2T} \int_{-T}^T q(s-\tau) q(s) ds = [(CF)(-\tau)] . \quad (I - 17)$$

D. The Harmonic Analysis of Random Functions

Although the Fourier transform of a stationary random function does not exist, it

does have a correlation function whose transform does exist. The Fourier transform of the correlation function is called the power spectral density, and is defined as follows:

$$[(\text{PSD}) (\omega)] = \int_{-\infty}^{\infty} [(\text{CF}) (\tau)] e^{-j\omega\tau} d\tau \quad (\text{I} - 18)$$

and

$$[(\text{CF}) (\tau)] = \frac{1}{2\pi} \int_{-\infty}^{\infty} [(\text{PSD}) (\omega)] e^{j\omega\tau} d\omega .$$

Since the auto-correlation function is an even function of time, this reduces to,

$$[(\text{PSD}) (\omega)] = 2 \int_0^{\infty} [(\text{CF}) (\tau)] \cos \omega\tau d\tau \quad (\text{I} - 19)$$

and

$$[(\text{CF}) (\tau)] = \frac{1}{\pi} \int_0^{\infty} [(\text{PSD}) (\omega)] \cos \omega\tau d\omega .$$

The following properties of the power spectral density, (PSD), are useful:

1. $[(\text{PSD}) (0)] = 2 \int_0^{\infty} [(\text{CF}) (\tau)] d\tau$
2. $[(\text{PSD}) (\omega)] = [(\text{PSD}) (-\omega)]$
3. From Eq. (I - 10),

$$\begin{aligned} \lim_{T_1 \rightarrow \infty} \left\{ \frac{1}{T_1} \int_{-\frac{T_1}{2}}^{\frac{T_1}{2}} q(t)q(t+\tau) dt \right\} &= \lim_{T_1 \rightarrow \infty} \left\{ \frac{1}{T_1} \frac{1}{2\pi} \int_{-\infty}^{\infty} |[\text{FT}] [q(t)]|^2 e^{j\omega\tau} d\omega \right\} \\ &= \lim_{T_1 \rightarrow \infty} \left\{ \frac{1}{2\pi} \int_{-\infty}^{\infty} T_1 |[\text{FSC}] [q(t)]|^2 e^{j\omega\tau} d\omega \right\} . \end{aligned}$$

Then, taking the direct transform of each side,

$$[(\text{PSD}) (\omega)] [q(t)] = \lim_{T_1 \rightarrow \infty} \left\{ T_1 |[\text{FSC}] [q(t)]|^2 \right\} . \quad (\text{I} - 20)$$

Appendix II

INPUT - OUTPUT STATISTICAL RELATIONSHIPS

Since the correlation function measures the statistical importance of the dynamics in a random function of time, one may equally well develop the input-output statistical relationship from the point of view of applying the theory of correlation to the convolution integral or one may choose to develop these relationships as an averaging process of the system output as given by the convolution integral. The latter approach is used here because the author wishes to emphasize the importance of thinking in terms of the dynamics of the system first, and the statistical analysis of these dynamic relationships as a later specialization.

In Appendix I, it was shown that the output response of a linear system can be written in terms of the convolution of the system unit impulse response and any known input forcing function, that is:

$$q_{\text{out}}(t) = \int_{-\infty}^{\infty} [(\text{UIR})(\sigma)] [q_{\text{in}}(t-\sigma)] d\sigma \quad (\text{II} - 1)$$

where σ is a dummy variable of integration.

A similar equation for the output displaced in time by the interval, τ , is:

$$q_{\text{out}}(t+\tau) = \int_{-\infty}^{\infty} [(\text{UIR})(\nu)] [q_{\text{in}}(t-\nu+\tau)] d\nu \quad (\text{II} - 2)$$

where ν is a dummy variable of integration.

These two equations can be applied to any bounded input whether it is finite or infinite. When the input is a random function, the output, although also random, will include the dynamics of the system. In the particular application of investigating atmospheric turbulence, one cannot measure the input directly, but one can measure the airplane response; consequently, the analysis starts from determining the auto-correlation function of the output. The auto-correlation function of the output is defined as:

$$[(\text{CF})_{\text{oo}}(\tau)] = \lim_{T \rightarrow \infty} \frac{1}{2T} \int_{-T}^T q_o(t) q_o(t+\tau) dt . \quad (\text{II} - 3)$$

Substituting Eqs. (II - 1) and (II - 2) into Eq. (II - 3) gives,

$$\begin{aligned}
[(CF)_{oo}(\tau)] &= \left[\lim_{T \rightarrow \infty} \frac{1}{2T} \int_{-T}^T dt \int_{-\infty}^{\infty} [(UIR)(\sigma)] [q_1(t-\sigma)] d\sigma \right] \left[\int_{-\infty}^{\infty} [(UIR)(v)] [q_1(t-v+\tau)] dv \right] \\
&= \int_{-\infty}^{\infty} [(UIR)(v)] dv \int_{-\infty}^{\infty} [(UIR)(\sigma)] d\sigma \lim_{T \rightarrow \infty} \frac{1}{2T} \int_{-T}^T [q_1(t-\sigma)] [q_1(t-v+\tau)] dt \\
&= \int_{-\infty}^{\infty} [(UIR)(v)] dv \int_{-\infty}^{\infty} [(UIR)(\sigma)] d\sigma [(CF)_{ii}(\tau+v-\sigma)] \quad .
\end{aligned}$$

However,

$$[(PSD)_{oo}(\omega)] = \int_{-\infty}^{\infty} [(CF)_{oo}(\tau)] e^{-j\omega\tau} d\tau$$

or,

$$[(PSD)_{oo}(\omega)] = \int_{-\infty}^{\infty} d\tau \int_{-\infty}^{\infty} [(UIR)(v)] dv \int_{-\infty}^{\infty} [(UIR)(\sigma)] d\sigma [(CF)_{ii}(\tau+v+\sigma)] e^{-j\omega\tau}$$

Now let,

$$\tau + v - \sigma = s \quad .$$

Then,

$$\begin{aligned}
[(PSD)_{oo}(\omega)] &= \int_{-\infty}^{\infty} ds \int_{-\infty}^{\infty} [(UIR)(v)] dv \int_{-\infty}^{\infty} [(UIR)(\sigma)] d\sigma [(CF)_{ii}(s)] e^{-j\omega(s+\sigma-v)} \\
&= \int_{-\infty}^{\infty} [(UIR)(v)] e^{j\omega v} dv \int_{-\infty}^{\infty} [(UIR)(\sigma)] e^{-j\omega\sigma} d\sigma \int_{-\infty}^{\infty} [(CF)_{ii}(s)] e^{-j\omega s} ds
\end{aligned}$$

but:

$$(PF) () [q_{in}q_{out}] = \int_{-\infty}^{\infty} [(UIR)(t)] e^{-j\omega t} dt \quad .$$

Hence,

$$[(PSD)_{oo}(\omega)] = \overline{(PF)} () [q_{in}q_{out}] (PF) () [q_{in}q_{out}] [(PSD)_{ii}(\omega)]$$

or

$$[(\text{PSD})_{\text{oo}}(\omega)] = \left| (\text{PF}) () [q_{\text{in}}q_{\text{out}}] \right|^2 [(\text{PSD})_{\text{ii}}(\omega)] . \quad (\text{II} - 4)$$

This equation is the mathematical basis for the calculation of the power spectral density of atmospheric turbulence from the airplane response power spectral density.

In the discussion of the sampling problems involved in the determination of the output auto-correlation function, the statistical input-output relationship in the time domain is useful. This relationship is obtained as follows:

From Eq. (I - 10), since

$$(\text{PF}) () [q_{\text{in}}q_{\text{out}}] = \int_{-\infty}^{\infty} [(\text{UIR}) (t)] e^{-j\omega t} dt$$

one obtains

$$\frac{1}{2\pi} \int_{-\infty}^{\infty} \left| (\text{PF}) () [q_{\text{in}}q_{\text{out}}] \right|^2 e^{j\omega\tau} d\omega = \int_{-\infty}^{\infty} [(\text{UIR}) (t)] [(\text{UIR}) (t+\tau)] dt .$$

If we define

$$[(\text{CF}) (\text{UIR}) (\tau)] \triangleq \int_{-\infty}^{\infty} [(\text{UIR}) (t)] [(\text{UIR}) (t+\tau)] dt \quad (\text{II} - 5)$$

then

$$[(\text{CF}) (\text{UIR}) (\tau)] = \frac{1}{2\pi} \int_{-\infty}^{\infty} \left| (\text{PF}) () [q_{\text{in}}q_{\text{out}}] \right|^2 e^{j\omega\tau} d\omega$$

and its direct transform is:

$$\left| (\text{PF}) () [q_{\text{in}}q_{\text{out}}] \right|^2 = \int_{-\infty}^{\infty} [(\text{CF}) (\text{UIR}) (\tau)] e^{-j\omega\tau} d\tau .$$

Define:

$$\overline{[\text{FT}] [q_1(t)]} \triangleq \left| (\text{PF}) () [q_{\text{in}}q_{\text{out}}] \right|^2 \quad (\text{II} - 6)$$

$$[\text{FT}] [q_2(t)] \triangleq [(\text{PSD})_{\text{ii}}(\omega)] . \quad (\text{II} - 7)$$

If Eqs. (II - 6) and (II - 7) are substituted in the multiplication theorem given by Eq. (I - 9) in Appendix I, and in addition identify terms in the resulting equation with the following relationships,

$$\begin{aligned}
[(\text{PSD})_{oo}(\omega)] &= |(\text{PF})_{oo}(\omega)|^2 [(\text{PSD})_{ii}(\omega)] \\
[(\text{CF})_{oo}(\tau)] &= \frac{1}{2\pi} \int_{-\infty}^{\infty} [(\text{PSD})_{oo}(\omega)] e^{j\omega\tau} d\omega \\
[(\text{CF})_{(UIR)}(t)] &= \frac{1}{2\pi} \int_{-\infty}^{\infty} |(\text{PF})_{oo}(\omega)|^2 e^{j\omega t} d\omega \\
[(\text{CF})_{ii}(\tau)] &= \frac{1}{2\pi} \int_{-\infty}^{\infty} [(\text{PSD})_{ii}(\omega)] e^{j\omega\tau} d\omega
\end{aligned}$$

Then, one obtains:

$$[(\text{CF})_{oo}(\tau)] = \int_{-\infty}^{\infty} [(\text{CF})_{(UIR)}(t)] [(\text{CF})_{ii}(t+\tau)] dt . \quad (\text{II} - 8)$$

This relationship is used to estimate the interval of significant correlation of the airplane response data.

Appendix III

THE SAMPLING PROBLEMS INVOLVED IN THE APPLICATION OF THE THEORY OF A GENERALIZED HARMONIC ANALYSIS TO A FINITE NUMBER OF RECORDS OF FINITE LENGTH

Introduction

In the practical application of the theory presented in Appendices I and II, records of finite length must always be used. From these records it is desired to obtain the best estimate of the correlation function and the power spectral density of the entire group of data from which a limited number of samples are available.

There are two techniques for the solution of this sampling problem:

1. A reasonable method of averaging the approximate correlation functions based on a finite sample which will be a consistent estimate of the correlation function of the entire group,
2. A reasonable method of averaging the Fourier Series coefficients computed from the finite records to obtain a consistent estimate of the power spectral density of the entire group according to equation (I-20), i.e.,

$$[(\text{PSD}) (\omega)] [q(t)] = \lim_{T_1 \rightarrow \infty} \left\{ T_1 \left| [\text{FSC}] [q(t)] \right|^2 \right\}$$

Both methods are theoretically valid approaches to the sampling problem but the amount of work involved in the second approach is considerably greater than that in the first method. For example⁽⁶⁾, suppose one chooses to reduce a given finite record by measuring M data points at equal increments of time. Then, by employing a straight line approximation to the time curve between each successive point, an approximate harmonic analysis⁽⁸⁾ can be obtained as follows:

$$\begin{aligned}
[\text{FSC}] [q(t)] \cong \frac{\Delta t}{T_1} \left[\frac{\sin \frac{\pi n}{T_1} \Delta t}{\frac{\pi n}{T_1} \Delta t} \right]^2 \left\{ \sum_{m=0}^{m=M} q_n(m\Delta t) \cos \frac{2\pi n}{T_1} m\Delta t \right. \\
\left. - j \sum_{m=0}^{m=M} q_m(m\Delta t) \sin \frac{2\pi n}{T_1} m\Delta t \right\} \quad (\text{III} - 1)
\end{aligned}$$

To compute $\frac{M}{2}$ harmonics, there are required M^2 multiplications and M^2 additions.

If the length of the records is assumed to be at least 30 times a response time, (RT), of the dynamic element in the function of time being analyzed, then

$$M\Delta t = 30(\text{RT})$$

(The desirability of meeting this requirement on a record length is discussed further under the sampling problem of correlation functions.)

The correlation function for a discrete time series is defined as:

$$[(\text{CF})_{xx}(m)] \cong \frac{1}{M-m} \sum_0^{M-m} x_i x_{i+m}$$

Figure III-1, which is a graphical illustration of convolution required to obtain the output correlation function, shows that the interval of significant correlation is approximately equal to the response time of the mechanism plus the interval of significant correlation of the input function. For an approximate criteria, one can assume the interval of significant correlation is not much greater than one response time (RT). Hence, there will be approximately $\frac{1}{30} M^2$ multiplications and $\frac{1}{30} M^2$ additions required to compute the correlation function. In addition, to compute the power spectral density according to the equation*

$$[(\text{PSD})(\omega)] [q(t)] \cong \Delta\tau \left[\frac{\sin \frac{\omega\Delta\tau}{2}}{\frac{\omega\Delta\tau}{2}} \right]^2 \left\{ 2\text{CF}(n\Delta\tau) \cos \omega n\Delta\tau - \text{CF}(0) \right\} \quad (\text{III} - 2)$$

for $\frac{M}{2}$ frequencies, $\frac{1}{2} \frac{M^2}{30}$ multiplications and $\frac{1}{2} \frac{M^2}{30}$ additions are necessary. Hence, to determine the power spectral density by first computing the correlation function, the amount of work has been decreased by approximately $\frac{1}{20}$. It is for

* See Appendix IV.

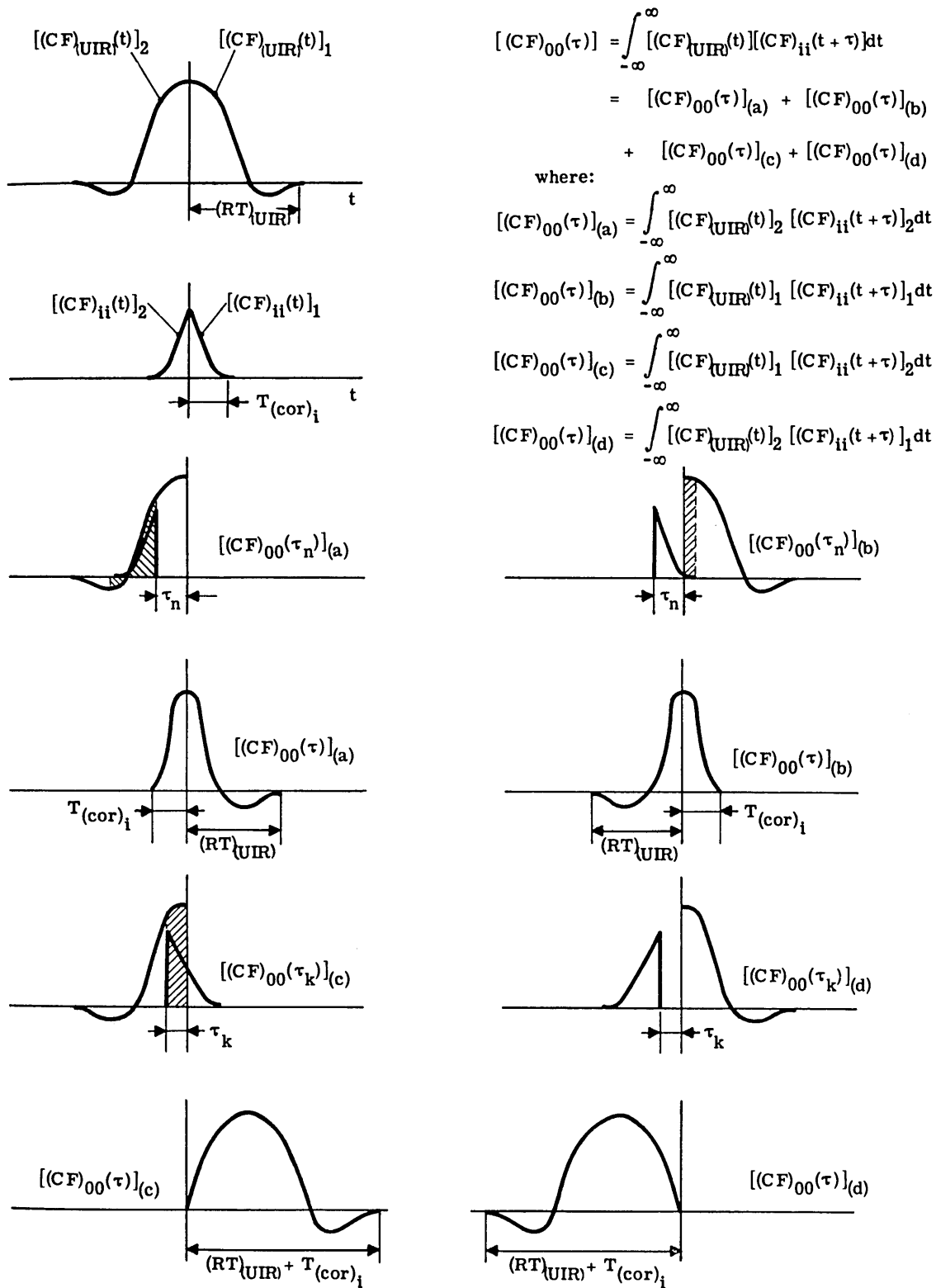


FIG. III-1
ILLUSTRATION OF A METHOD OF OBTAINING THE OUTPUT CORRELATION
FUNCTION BY GRAPHICAL CONVOLUTION.

this reason that the first method was used exclusively.

A. The General Problem of Estimating the Correlation Function

Since the correlation function is defined for the infinite sequence only, it is necessary to consider methods of estimating the correlation function from finite samples of the random function. In any sampling problem, the size of the sample is of prime importance, and consequently a criteria for determining sample size is the first consideration.

It has often been suggested that if one selects the sample lengths of the time series so that the total length is greater than 20 to 30 times the interval of significant correlation, then the correlation function can be estimated by an approximate one based on the finite limits. This criteria is objectionable for two reasons. First, the interval of significant correlation cannot be determined until data has been actually correlated, and hence this criteria cannot be used as a gauge in determining, a priori, the minimum length of the data record. Second, the question of the interval of apparent significant correlation is dependent upon the size of sample due to sampling errors. Consequently, some criteria must be given for determining what is a significant correlation and what is a sampling error. It is felt that these two objections must be resolved before one can discuss a reasonable estimate of the correlation function.

If the sampling distribution of serial correlation coefficients were known, these sampling values could be used as in the case of random sampling to determine the best estimate of the correlation function. Unfortunately, the theory of sampling have not as yet been extended to the general case of time series. The difficulty lies in the fact that the individual members are stochastically dependent on time and the order of the individuals in each sample is important. This is not true in the case of random sampling. Special solutions of the sampling distribution of the serial correlation coefficient of a circular* time series, wherein the variates are normally distributed, have been worked out⁽²⁷⁾⁽²⁸⁾, but the general applicability of these solutions is highly questionable in the case of a continuous function of time,

* The term "circular" means that the first and last terms of the series are identical.

because no criteria are given for selecting the interval between data points to be correlated. To be more specific, since a continuous function of time has within any finite record (no matter how short) an infinite set of points from which a time series can be selected to represent the continuous function, unless some criteria is given for the selection of these points, their number cannot be a measure of the size of the sample. This question of sample size is important since it gives an idea as to the proper method to weigh the sample serial correlation functions. The problem of determining a qualitative measure of the size of a time sample as well as the significant correlation can best be examined by means of an idealized theory.

B. The Sampling Problem of a Random Function of Time

It has been shown in Appendix II that for a linear system excited by any input for which a correlation function exists, the output correlation function can be written as:

$$[(CF)_{oo}(\tau)]_{\infty} = \int_{-\infty}^{\infty} [(CF)_{(UIR)}(t)]_{\infty} [(CF)_{11}(t+\tau)]_{\infty} dt \quad (III - 3)$$

where

$$[(CF)_{(UIR)}(t)]_{\infty} = \int_{-\infty}^{\infty} [(UIR)(\tau)] [(UIR)(\tau+t)] d\tau$$

For the purpose of gaining an insight into the sampling problem of the output serial correlation function, let the input be defined as a random sequence of delta functions where the delta function is defined as

$$\lim_{e \rightarrow 0} \begin{cases} \delta(t) = 0 \text{ for } (t < -\frac{e}{2}) \text{ or } (t > +\frac{e}{2}) \\ \delta(t) = \frac{1}{e} \text{ for } (-\frac{e}{2} < t < \frac{e}{2}) \end{cases}$$

then,

$$q_1(t) \stackrel{\Delta}{=} \lim_{N \rightarrow \infty} \sum_{n=-N}^{n=+N} a_n \delta(t - t_n)$$

where

$$t_{-n} \stackrel{\Delta}{=} -t_n$$

The coefficients a_n are independent random variables with zero mean and the same probability distribution; and the time increments, $(t_n - t_{n-1})$ are independent random variables and have the same probability distribution. For these assumptions it can be shown⁽²²⁾ that for the infinite process,

$$[(CF)_{ii}(\tau)]_{\infty} = \frac{[(MS)(a_n)]}{[t_n - t_{n-1}]_{av}} \delta(\tau)$$

where

$$[(MS)(a_n)] = \frac{1}{n} \sum_{-\infty}^{\infty} a_n^2$$

However, the approximate correlation function of a finite sample of this infinite set of delta functions is,

$$[(CF)_{ii}(\tau)]_T = \sum_{i=0}^{i=N} b_i \delta(\tau - \tau_i)$$

Hence, there exists spurious correlations of the input entirely due to sampling. This sample correlation function that consists of a finite set of delta functions reduces to a single delta function at the origin when the sample length is infinite. The longer the sample the more dense becomes the set until in the limit the delta functions at all points different from the origin overlap and the average is zero. In the case of the random set of delta functions the proper average to be used for the sample is not clear, but one can obtain an idea of the interval of significant correlation. This interval is useful to obtain an estimate of the errors in sampling for $[(SKC)(\tau)]_T = 0$.

In this example, for the infinite sequence since

$$[(CF)_{oo}(\tau)]_{\infty} = \int_{-\infty}^{\infty} [(CF)_{(UIR)}(t)]_{\infty} [(CF)_{ii}(t+\tau)]_{\infty} dt$$

then,

$$[(CF)_{oo}(\tau)]_{\infty} = \frac{[(MS)(a_n)]}{[t_n - t_{n-1}]_{av}} [(CF)_{(UIR)}(\tau)]_{\infty}$$

If the response time (RT) of the system is defined as the time for the output to decrease to and remain less than 5 percent of its peak magnitude, then:

$$[(CF)_{(UIR)}(RT)]_{\infty} \cong [(CF)_{oo}(RT)]_{\infty}$$

This is illustrated graphically in Fig. III-1.

Hence, in the case for which the input consists of a random sequence of delta functions, any correlation greater than 5 percent at $\tau = (RT)$ is largely an error due to random sampling.

For atmospheric turbulence the disturbances will not be delta functions. In reference 24 it is shown from experimental data that the average gust is close to 10 chord lengths. From this information, the average time duration of a gust for the B-25 airplane is approximately:

$$[t_{dr}]_{av} \cong \frac{2(10\bar{C})}{299} = .67 \text{ sec (175 mph, 10,000 ft)}$$

where

$[t_{dr}]_{av}$ is the average gust duration time

\bar{C} is the chord length of the airplane.

On this basis, one can anticipate that the significant correlation interval of the gusts is about 1.0 second. Combining this knowledge with a knowledge of the response time of the system, the significant correlation interval of the airplane response should be approximately:

$$T_{(cor)o} = (RT)_{airplane} + 1.0 \text{ sec}$$

For a B-25J⁽³⁾ at 175 mph and 26 percent M.A.C. and neglecting long period effects (see Appendix V):

$$W_n = 2.4 \text{ rad/sec}$$

$$DR = 0.7$$

$$(RT)_{A(Long.)} \cong 3(CT)_{A(Long.)} = 1.8 \text{ sec}$$

$$(CT)_{A(Long.)} = \frac{1}{(DR)W_n} \approx 0.6$$

where $(CT)_{A(Long.)}$ is the characteristic time of the longitudinal response of the airplane. Consequently, there should be no significant correlation in the longitudinal case beyond 2.8 seconds.

In the lateral response, for a first approximation, one can neglect the roll subsidence and consider the correlation determined primarily by the "Dutch Roll" mode. For a B-25J⁽⁴⁾ at 175 mph and 26 percent M.A.C.:

$$W_n = 1.4 \text{ rad/sec}$$

$$DR = 0.15$$

$$(RT)_{A(Lat.)} \cong 3(CT)_{A(Lat.)} = 15 \text{ sec}$$

where $(CT)_{A(Lat.)}$ is the characteristic time of the lateral response of the airplane. Consequently, there should be no significant correlation beyond 16 seconds.

C. Sample Size Criteria

It has been previously pointed out that the length of the record cannot be a measure of size of the sample. Rather, one must use a measure that includes the relative importance of the dynamic time constants of the series. If the number of random disturbances can be spotted on the record, this could be used as a measure of size. However, in many cases these disturbances cannot be separately counted. In this case, the number of response times, (RT), in the total length will on the average accomplish the same purpose. The response time is a measure of the interval in which the system dynamics are important. Hence, any choice of data points within this interval are on the average largely dependent upon each other due to the system dynamics. On the other hand if we assume that each disturbance is independent of each other, then data points selected at intervals greater than a response time are primarily related by the random nature of the disturbing input and to a very small degree by the system dynamics. Hence, the number of response times of the airplane included in the measured record is proposed as a measure of sample size.

By reasoning from the results of random sampling, one would expect that for long records the distribution of serial correlation coefficients should be nearly symmetrical and a mean based upon weighing each serial correlation coefficient by its length is a reasonable estimate. By the term "large" one should mean more than 20 to 30 disturbances, and hence the length of records should be in general 20 to 30 times the response time (RT) of the dynamic element relating the random

generating functions to the output functions. Since the length of the significant correlation interval will be closely related to the (RT) of the dynamic element, this criteria agrees very well with that given by Mr. Bubb⁽¹⁰⁾ for an approximate correlation function. However, from a knowledge of the response time of the system this criteria can, a priori, be used as a rule for determining the length of record which will on the average have a minimum sampling error (i.e., a large sample).

As a guide to further research on turbulent air as well as a check on the reliability of this proposed sample length criteria, an actual check of the effect of record length on the sample correlation function was made. The original record, which was 57 seconds long, was divided into four equal parts. The first quarter, the first half, the first three-quarters, and then the entire record were correlated and the results plotted as shown in Fig. III-2. The first quarter, which is only 7 response times of the rate of pitch response of a B-25J is extremely erratic and fails to converge properly. The first half, which is 14 response times, is improved somewhat but is still unreliable. However, the three-quarter length and the full length indicate convergent correlation functions that are in reasonable agreement. These results experimentally verify the criteria that the record length should be at least from 20 to 30 response times of the airplane. Contrast these results with that shown in Fig. III-3, which is the correlation function of the rate of roll response of the airplane. In this case, the correlation function determined from the entire record available is erratic and fails to converge. This is due to the fact that the response time of the airplane in roll is 16 seconds and consequently, this record is only 4 response times. The roll data records are of insufficient length and therefore this data is not as reliable as the longitudinal response data.

It might be pointed out here that if the "long period" response data of the airplane, which has a response time of approximately 5 minutes were desired, one should obtain continuous records of from 100 to 150 minutes. This presents a rather difficult instrumentation problem.

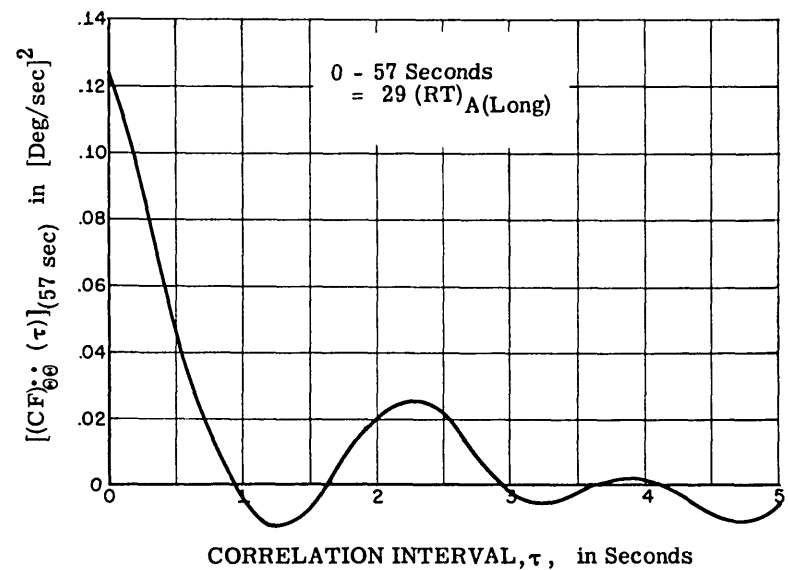
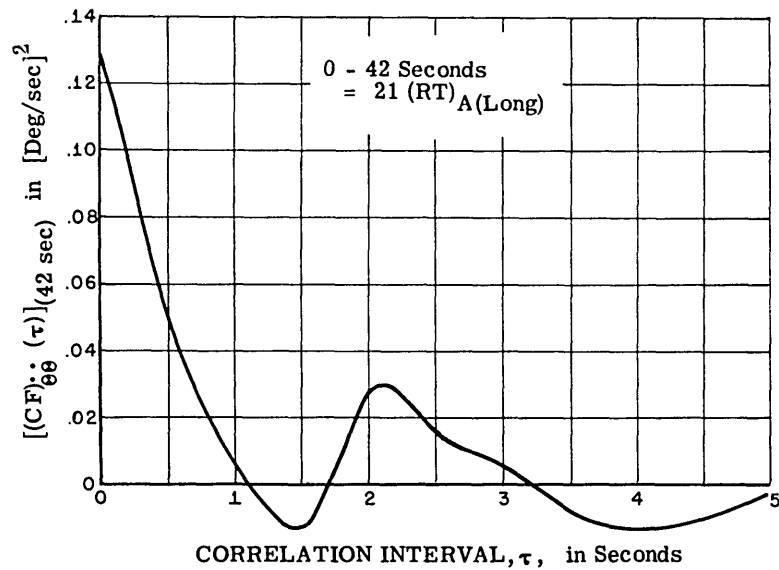
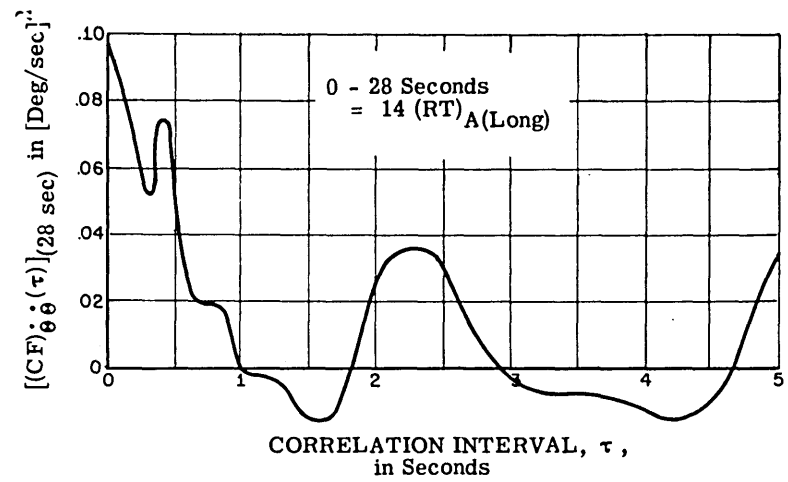
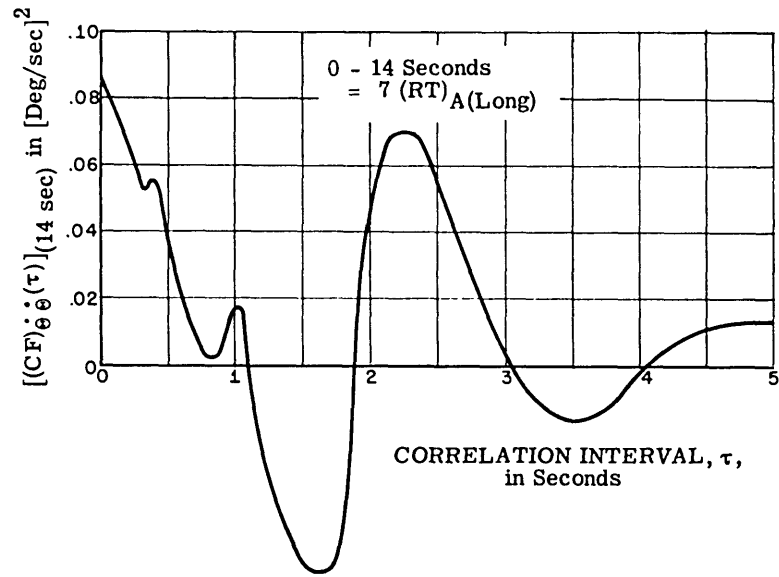


FIG. III-2 ILLUSTRATION OF EFFECT OF SAMPLE LENGTH ON CONVERGENCE OF THE CORRELATION FUNCTION

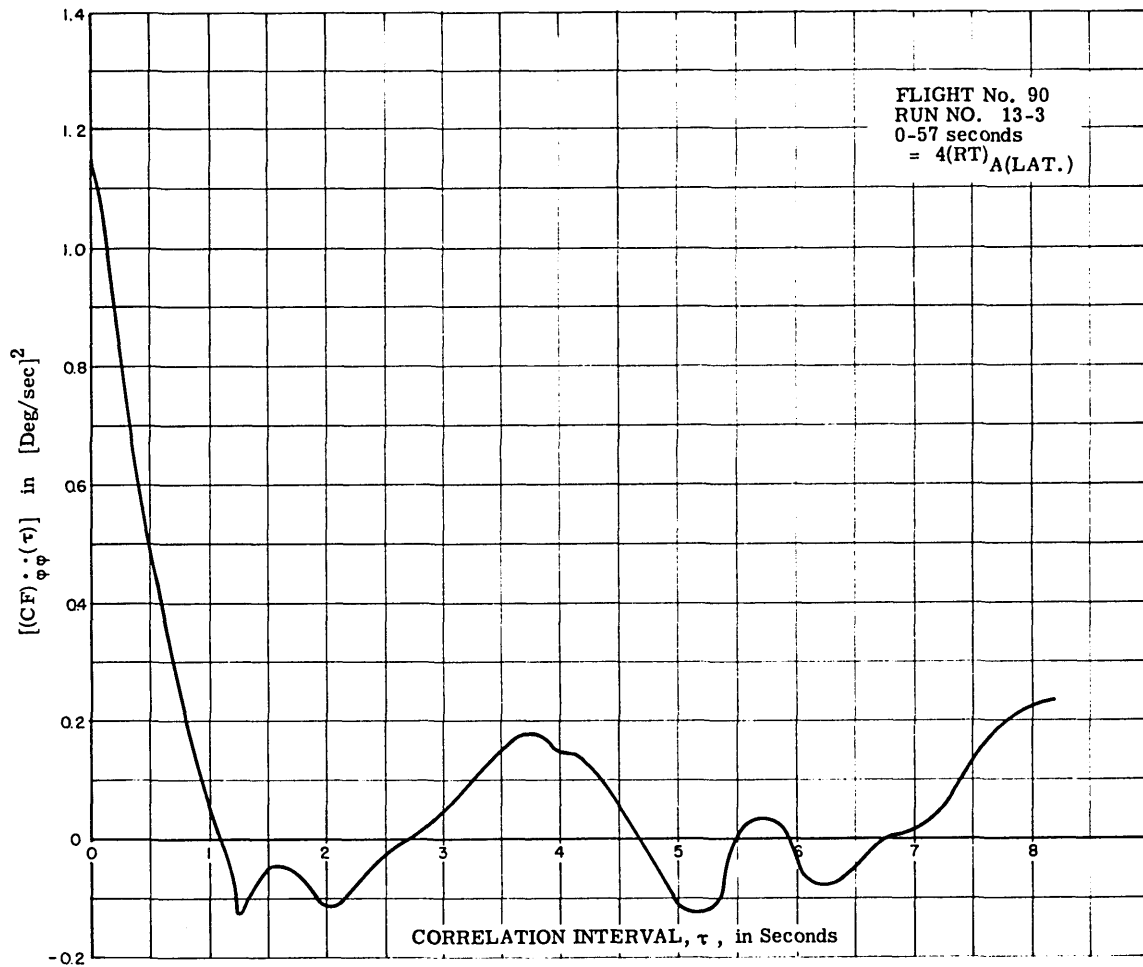


FIG. III-3 ILLUSTRATION OF LACK OF CONVERGENCE OF SAMPLE CORRELATION FUNCTION FOR RATE OF ROLL RESPONSE OF B-25J AIRPLANE DUE TO INSUFFICIENT LENGTH.

D. Reasonable Estimate of the Correlation Function

The approximate correlation function (with finite limits) is a measure of covariance of a time series with itself under shifts in time, and as such includes not only a measure of the stochastic dependence but also the change in standard deviation of each section of the time sequence as the sequence is shifted. It is only for the infinite limit where the standard deviations are constant under shifts in time (stationary process) that the correlation function is a true measure of correlation. One can therefore define a large sample as one wherein the mean value and the standard deviation does not change more than 5 percent at the largest

significant value of the correlation interval. For large samples, the most reasonable estimate of the correlation function will be found by weighing each covariance by the length of the interval and averaging over all samples.

In case the standard deviation does change more than 5 percent, the best method of averaging cannot be definitely specified because the sampling distribution is not known. One might weigh each sample serial correlation coefficient by its length and average over all samples, but this would be equivalent to assuming a symmetrical distribution of the serial correlation coefficients. From the general results obtained in random sampling theory it seems that this might be a poor assumption. Another possibility would be to weigh and average the covariance and the standard deviations for each sample separately and consider a reasonable estimate of the serial correlation coefficients for all samples to be the ratio of these averages. This method is easier to apply and in this investigation was assumed to be the most reasonable estimate; i.e.,

$$[(CF)_{qq}(\bar{\tau})]_{\infty} \cong \frac{\overline{[(Covar) q(t) q(t+\tau)]_{T_n-\tau}}}{\sqrt{\overline{[(Var) q(t)]_{T_n-\tau}} \overline{[(Var) q(t+\tau)]_{T_n-\tau}}}}$$

where

$\overline{[(Var) q(t)]_{T_n}}$ is the weighted mean of the variance or mean power of $q(t)$ over N records in a given flight

$$\Delta = \frac{1}{\sum_0^N T_n} \sum_0^N \int_0^{T_n} [q(t)]^2 dt$$

$\overline{[(Covar) q(t) q(t+\tau)]_{T_n-\tau}}$ is the weighted mean of the covariance of $q(t)$ and $q(t+\tau)$ over N records in a given flight

$$\Delta = \frac{1}{\sum_0^N (T_n-\tau)} \sum_0^N \int_0^{T_n-\tau} q(t) q(t+\tau) dt$$

$\overline{[(\text{Var})q(t)]_{T_n-\tau}}$ is the weighted mean of the variance of $q(t)$ as a function of the correlation interval τ

$$\Delta \equiv \frac{1}{\sum_0^N (T_n-\tau)} \sum_0^N \int_0^{T_n-\tau} [q(t)]^2 dt$$

$\overline{[(\text{Var})q(t+\tau)]_{T_n-\tau}}$ is the weighted mean of the variance of $q(t+\tau)$ as a function of the correlation interval, τ

$$\Delta \equiv \frac{1}{\sum_0^N (T_n-\tau)} \sum_0^N \int_0^{T_n-\tau} [q(t+\tau)]^2 dt$$

T_n is the length of the n-th sample

N is the total number of samples.

However, this presents increased computational work that may or may not be justified depending upon the relative magnitude of the sampling errors involved. To check whether or not this refinement was justified, the data for Flight No. 90 was reduced by three methods:

1. Best estimate obtained by correcting for both the change of mean square and mean with respect to an arbitrary base line as a function of the correlation interval.
2. Approximation to the best estimate based on correcting for only the change in mean of each record with respect to the same arbitrary

base line as a function of the correlation interval.

3. Approximation based on correcting the covariance of the entire set of records for the flight by the mean of the entire set with respect to the same arbitrary base line at zero correlation interval.

The results are presented in Figs. III-4 and III-5. From these figures it is seen that the difference is, at the most, no greater than 3 percent and consequently

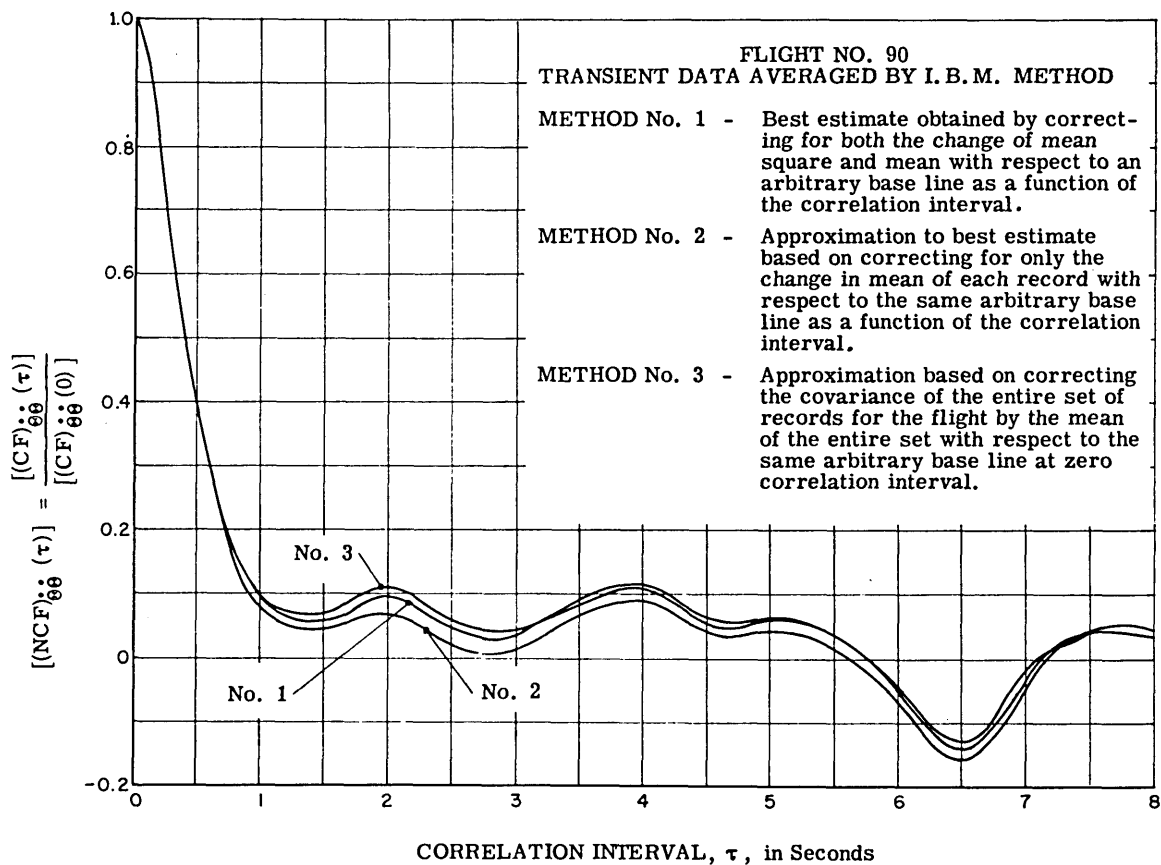


FIG. III-4 COMPARISON OF THREE METHODS OF COMPUTING THE CORRELATION FUNCTION FOR RATE OF PITCH RESPONSE, θ

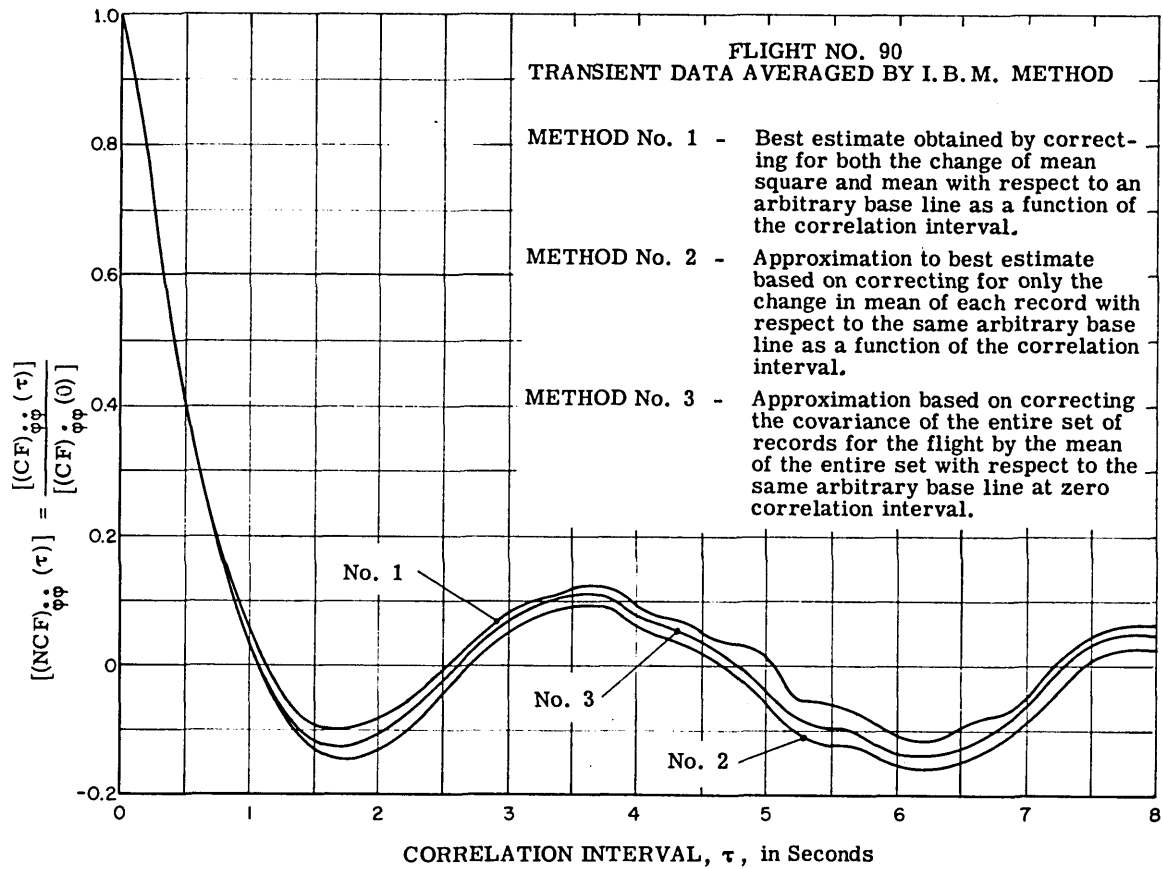


FIG. III-5 COMPARISON OF THREE METHODS OF COMPUTING THE CORRELATION FUNCTION FOR THE RATE OF ROLL RESPONSE, $\dot{\phi}$

this refinement in the computation is not justified. All the remaining flights were computed by the simplest method indicated by Method 3.

Appendix IV

METHODS OF APPROXIMATION USED IN OBTAINING THE POWER SPECTRAL DENSITIES

It has been shown by Wiener⁽¹⁾ that the power spectral density and the correlation function in addition to being Fourier transforms of each other are also even functions of frequency and the correlation time interval, respectively. Hence, the transform pairs reduce to:

$$[(\text{PSD}) (\omega)] = 2 \int_0^{\infty} [(\text{CF}) (\tau)] \cos \omega \tau \, d\tau \quad (\text{IV-1})$$

$$[(\text{CF}) (\tau)] = \frac{1}{\pi} \int_0^{\infty} [(\text{PSD}) (\omega)] \cos \omega \tau \, d\omega \quad (\text{IV-2})$$

There are three methods available for accomplishing these transforms on experimental data:

1. By approximation of the entire range of the experimental data with an analytical equation and obtaining the transform in the closed form.
2. By approximation of the experimental data by a series of analytical segments and obtaining the transform as the summation of the transforms of the segments.
3. By appropriately combining methods 1 and 2 to obtain the best fit.

For the data obtained in this investigation, Method 1 seems to be the least desirable since it was shown in Appendix III that the correlation function of the output is, in general, a convolution and cannot be reasonably approximated throughout its entire range by an analytical expression.

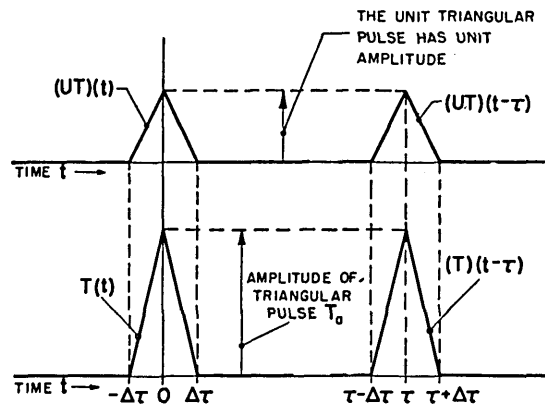
In the longitudinal response, no correlation exists beyond 3.0 seconds except for primarily sampling errors. Hence, in this case transforming the data by the second method is preferred.

In the lateral response, correlation should exist to 16 seconds. However, it is not advisable to attempt to correlate this data for the full time interval because the correlation function at 8 seconds is already becoming erratic. The lateral data can be best approximated by the third method.

A. Method No. 2

In reference 8 a general method of approximating transforms that is based upon an isosceles triangle approximation to the true curve is presented. Although more refined approximations are possible and may in some cases increase the degree of approximation by giving curved segments between the data points that more nearly fit the experimental curve, this additional refinement is, in general, not justified. Therefore, the only method of transforming analytical line segments considered in this thesis is the straight line segment system.

The triangular pulse used for approximating the experimental curve is defined in Fig. IV-1. This triangular pulse leads to approximating the experimental curve curve by a series of chords, as shown in Fig. IV-2.



BY DEFINITION, THE UNIT AND GENERAL PULSES ARE SYMMETRICAL AND HAVE A COMMON TIME DURATION OF $2 \Delta \tau$

CONSEQUENTLY

$$T(t-\tau) = T_0 [(UT)(t-\tau)]$$

FIG. IX-1 DEFINITION OF UNIT TRIANGULAR PULSE AND GENERAL TRIANGULAR PULSE.

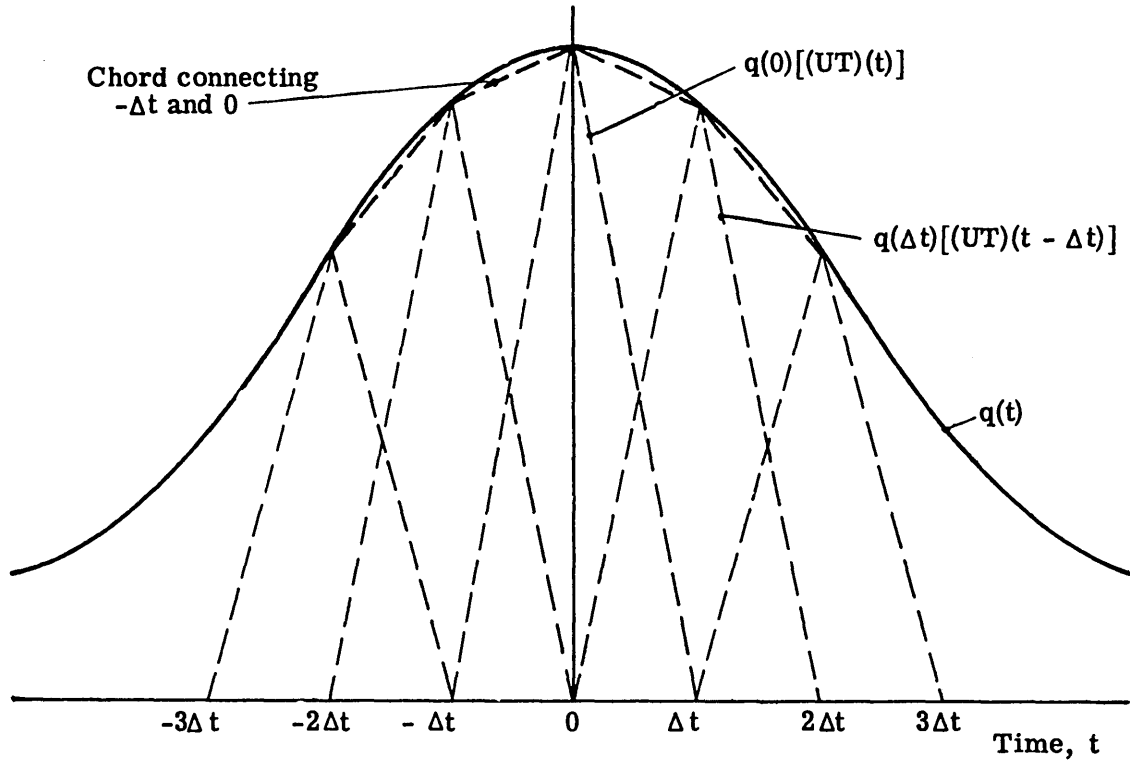


FIG. IV-2. THE TRIANGULAR PULSE METHOD OF APPROXIMATION

Then,

$$q(t) \cong q(0) [(UT)(t)] + \sum_{n=-N}^{n=N} q(n\Delta t) [(UT)(t - n\Delta t)] \quad (IV-3)$$

and

$$[FT][q(t)] \cong q(0) [FT][(UT)(t)] + \sum_{n=-N}^{n=N} q(n\Delta t) [FT][(UT)(t - n\Delta t)] \quad (IV-4)$$

but, by the shift theorem:

$$[FT][(UT)(t - n\Delta t)] = e^{-jn\omega\Delta t} [FT][(UT)(t)]$$

where ω is measured in radians per second.

Since $q(t)$ is an even function of time, Eq. IV-4 reduces to:

$$[\text{FT}] [q(t)] \cong \Delta t \left[\frac{\sin \frac{\omega \Delta t}{2}}{\frac{\omega \Delta t}{2}} \right]^2 \left\{ 2 \sum_{n=0}^{n=N} q(n\Delta t) \cos (\omega n \Delta t) - q(0) \right\} . \quad (\text{IV-5})$$

This result can now be applied to the transform pair given by Eqs. IV-1 and IV-2 to give:

$$[(\text{PSD}) (\omega)] \cong \Delta \tau \left[\frac{\sin \frac{\omega \Delta \tau}{2}}{\frac{\omega \Delta \tau}{2}} \right]^2 \left\{ 2 \sum_{n=0}^{n=N} \text{CF}(n\Delta t) \cos \omega n \Delta t - \text{CF}(0) \right\} \quad (\text{IV-6})$$

$$[\text{CF} (\tau)] \cong \frac{\Delta \omega}{2\pi} \left[\frac{\sin \frac{\tau \Delta \omega}{2}}{\frac{\tau \Delta \omega}{2}} \right]^2 \left\{ 2 \sum_{n=0}^{n=N} (\text{PSD}) (n\Delta \omega) \cos \tau n \Delta \omega - (\text{PSD}) (0) \right\} \quad (\text{IV-7})$$

B. Method No. 3

The correlation function of the lateral response has a damped sinusoidal response for all values of $\tau > 1.0$ seconds. Hence, the lateral response correlation function can be approximated by:

$$[(\text{CF})_{\dot{\varphi}\dot{\varphi}} (\tau)] = [(\text{CF})_{\dot{\varphi}\dot{\varphi}} (\tau)]_{(\text{osc})} + [(\text{CF})_{\dot{\varphi}\dot{\varphi}} (\tau)]_{(\text{rem})} . \quad (\text{IV-8})$$

The remainder component is transformed by the triangular approximation method the same as the correlation function for the longitudinal case. The oscillatory component is transformed in the closed form from the following equation which is to be fitted to the experimental curve.

$$[(\text{CF})_{\dot{\varphi}\dot{\varphi}} (\tau)]_{(\text{osc})} = A_{(\text{osc})} e^{-(\text{DR}) \omega_n t} \sin \left\{ \omega_n \sqrt{1 - (\text{DR})^2} t + (\text{PA})_{(\text{osc})} \right\} \quad (\text{IV-9})$$

Then

$$\begin{aligned}
[\text{FT}] [(\text{CF})_{\ddot{\varphi}\varphi}(\tau)]_{(\text{osc})} &= 2 \operatorname{Re} \left[\frac{A_{(\text{osc})} \sin(\text{PA})_{(\text{osc})}}{(\text{CT})_{(\text{osc})}} \left\{ \frac{1 + j(\text{CT})_{(\text{osc})}\omega}{(\omega_n^2 - \omega^2) + j 2(\text{DR})\omega_n\omega} \right\} \right] \\
&= \frac{2A_{(\text{osc})} \sin(\text{PA})_{(\text{osc})}}{(\text{CT})_{(\text{osc})}} \left[\frac{[\omega_n^2 - \omega^2] + [2(\text{DR})\omega_n] (\text{CT})_{(\text{osc})} \omega^2}{[\omega_n^2 - \omega^2]^2 + [2(\text{DR})\omega_n]^2 \omega^2} \right]
\end{aligned} \tag{IV-10}$$

where

$$(\text{CT})_{(\text{osc})} \stackrel{\Delta}{=} \frac{\sin(\text{PA})_{(\text{osc})}}{\omega_n [\sqrt{1 - (\text{DR})^2} \cos(\text{PA})_{(\text{osc})} + (\text{DR}) \sin(\text{PA})_{(\text{osc})}]}$$

$$(\text{PA})_{(\text{osc})} \stackrel{\Delta}{=} -t_d \sqrt{1 - (\text{DR})^2} \omega_n .$$

For the B-25J airplane flying at 175 mph and 8,000 feet altitude from data extracted from reference 4, the following parameters are determined to fit Eq. IV-9 to the experimental data shown in Fig. IV-3.

$$\text{DR} = 0.15$$

$$\omega_n = 1.4 \text{ rad/sec}$$

From Fig. IV-3 for $t_d = 1.8$ sec, the phase angle, $(\text{PA})_{(\text{osc})} = 143$ degrees, $(\text{CT})_{(\text{osc})} = - .615$ and the amplitude $A_{(\text{osc})} = .269$.

When these values are substituted into Eq. IV-9, one obtains

$$[(\text{CF})_{\ddot{\varphi}\varphi}(\tau)]_{(\text{osc})} = .211 e^{-.21t} \sin \left\{ 79.5t + 143^\circ \right\} \tag{IV-11}$$

and, the Fourier Transform of Eq. IV-11 which is given by Eq. IV-10 is given by:

$$[\text{FT}] [(\text{CF})_{\ddot{\varphi}\varphi}(\tau)]_{(\text{osc})} = .43 \left[\frac{1.258\omega^2 - 1.96}{(\omega^2 - 1.96)^2 + (.1764)\omega^2} \right] \tag{IV-12}$$

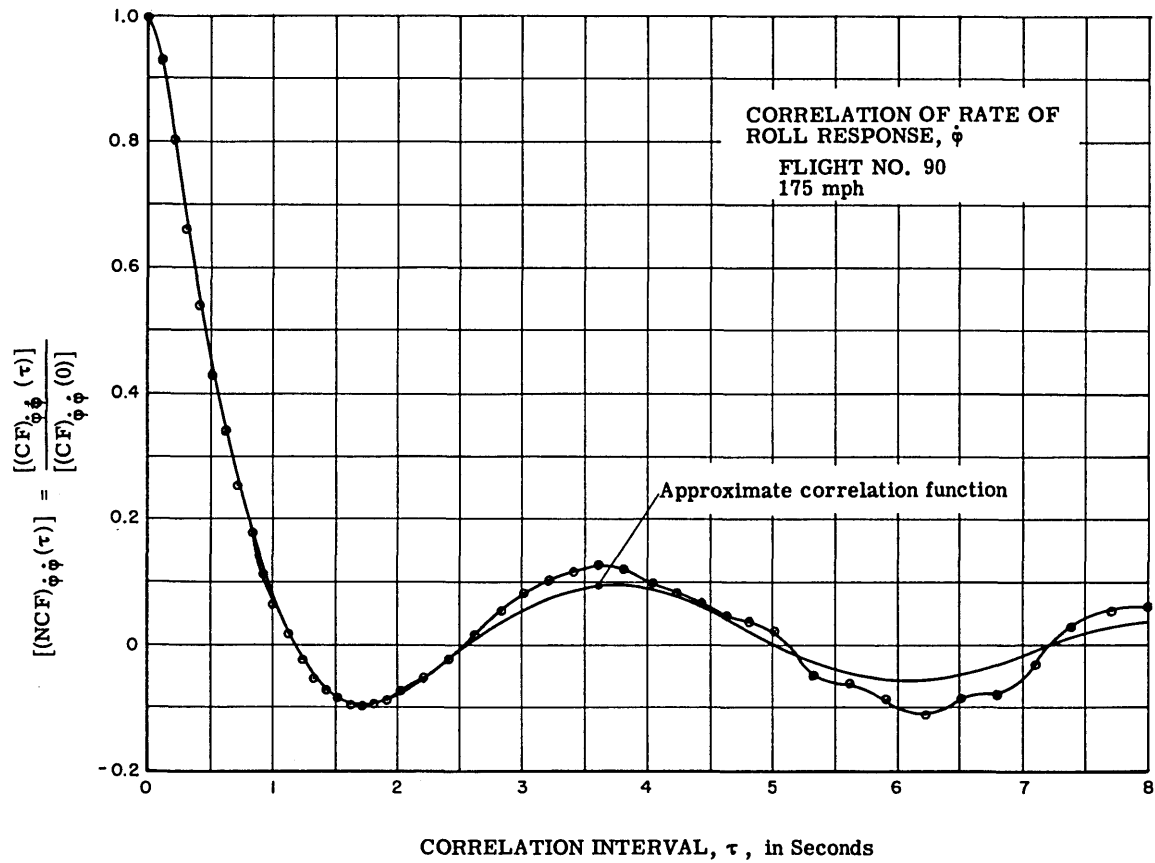


FIG. IV-3 COMPARISON OF BEST ESTIMATE OF EXPERIMENTAL NORMALIZED CORRELATION FUNCTION WITH THE APPROXIMATION USED TO COMPUTE THE POWER SPECTRAL DENSITY FOR THE LATERAL RESPONSE DATA

The lateral response power spectral density can then be computed by:

$$[(PSD)_{\dot{\phi}\dot{\phi}}(\omega)] = [FT] [(CF)_{\dot{\phi}\dot{\phi}}(\tau)]_{(osc)} + [FT] [(CF)_{\dot{\phi}\dot{\phi}}(\tau)]_{(rem)} \cdot$$

Appendix V
AIRCRAFT PERFORMANCE FUNCTIONS

A. General

In Appendix II, the general input-output statistical relationship was developed as:

$$[(\text{PSD})_{\text{oo}}(\omega)] = \left| (\text{PF})_{()} [] \right|^2 [(\text{PSD})_{\text{ii}}(\omega)] \quad (\text{V-1})$$

In this section the performance functions of the airplane are derived. These performance functions are used to compute the power spectral density of the input from the output power spectral density.

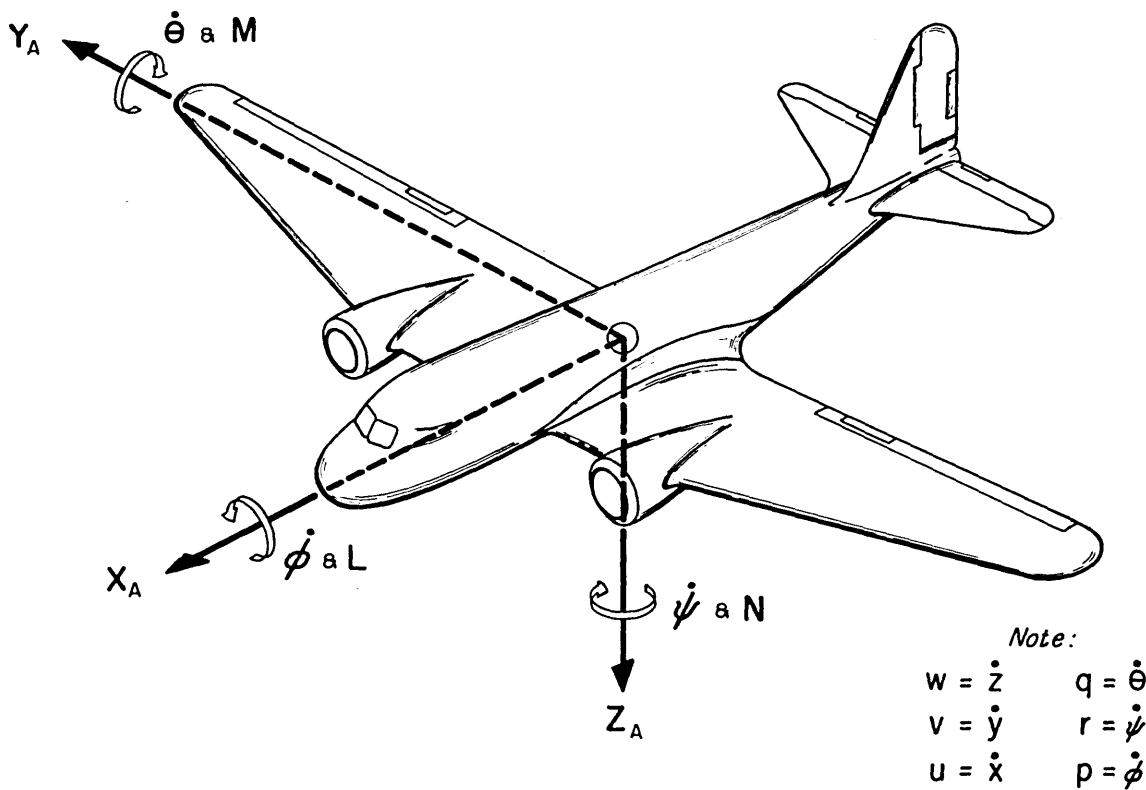


FIG. V-1 RIGHT-HAND AIRPLANE AXIS SYSTEM AS DEFINED BY N.A.C.A.

B. Basic Assumptions and Definitions Used in the Development of Performance Functions

In this analysis, the N. A. C. A. Standard Airplane Axes and definitions of displacements are used. (See Fig. V-1).

The derivation of the classical linearized equations of motion of an airplane for small oscillations about a point of equilibrium is not pertinent to this investigation, and consequently only the end results of this theory are presented here⁽¹¹⁾.

C. Assumptions for the Determination of the Statistical Properties of Rough Air

There are two principal types of rough air, namely, thermals and wind gusts. The rough air thermal is characterized by variations of the air mass principally in the vertical direction. Gusts are characterized by variations of wind in the horizontal direction. Each presents a problem to the controlled aircraft at different conditions. The thermals are encountered mostly between 1,000 and 20,000 feet, and gusts primarily close to the ground. However, as far as the airplane is concerned they present similar problems. This analysis deals primarily with thermals, but can be extended easily to include considerations of gusts.

A cross sectional view of the velocity distribution of a rough air thermal is assumed to be as shown in Fig. V-2.

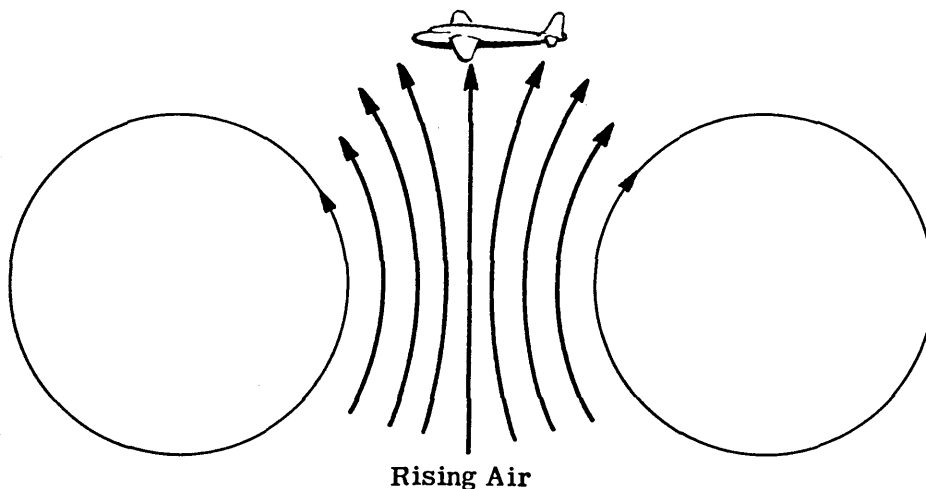


FIG. V-2 CROSS-SECTIONAL VIEW OF A SIMPLIFIED THERMAL

The rough air thermal makes itself apparent to the airplane in two principal ways:

1. There will be a change in the relative normal velocity of the airplane with respect to the air mass, i. e. ,

$$\Delta w_{[A-P](norm)} = w_{A-I}$$

2. There will be a variation in the magnitude of the normal velocity of the air mass spanwise, i. e. ,

$$\Delta \dot{\phi}_{[A-P]} = \frac{\partial w_{[A-I](norm)}}{\partial y}$$

Rough air acts on the airplane like a load disturbance on a servo except that the summation points are in velocities instead of torques or forces. This is true because aerodynamic forces are generated by the relative velocities between the body and the air mass.

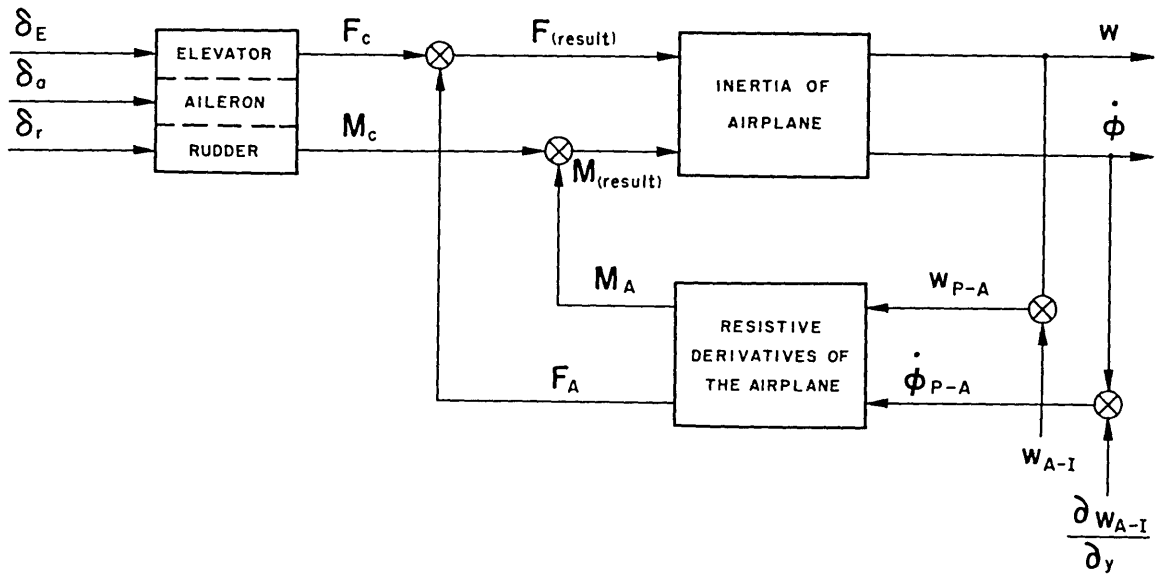


FIG. V-3 AIRPLANE FUNCTIONAL DIAGRAM FOR ANALYSIS OF RESPONSE TO ATMOSPHERIC TURBULENCE

Referring to Fig. V-3, it is evident that by proper manipulation of the equations of motion of the airplane, one can develop the following performance functions:

$$(PF)_A[\delta_E, \dot{\theta}] \quad (V-2)$$

$$(PF)_A[w_{A-I}, \dot{\theta}] \quad (V-3)$$

$$(PF)_A[\delta_a, \dot{\phi}] \quad (V-4)$$

$$(PF)_A\left[\frac{\partial w_{A-I}}{\partial y}, \dot{\phi}\right] \quad (V-5)$$

The important point to note is that since Eqs. (V-1) and (V-2), and Eqs. (V-3) and (V-4) encompass the same loop respectively in their transfer functions, they have identical denominators. The first and third functions can be measured directly on the airplane. The second and fourth can then be computed theoretically. Hence, the rough air performance functions can be determined within engineering tolerances.

D. Longitudinal Response Equations

Neglecting non-steady airflow effects, the longitudinal response of an airplane for fixed controls is composed of two damped oscillations. One is a lightly damped long period motion that is called the "Long Period Oscillation." The second, usually near critical damping and having a period of about two seconds, is called the "Short Period Oscillation."

It was pointed out in Appendix III that in order to obtain a reliable estimate of the correlation function, which included the long period oscillation, one must have a record length of from 100 to 150 minutes. A recording system designed to accommodate a time interval of this length would lose completely the fine detail in the short period oscillation. Hence, to obtain a correlation function that includes both long

and short period effects would require two recorders with provisions for synchronizing the records. The total correlation function would then be obtained as follows:

$$[(CF)_{qq}(\tau)]_{A(total)} = \lim_{T \rightarrow \infty} \frac{1}{2T} \int_{-T}^T [q_{(SP)}(t) + q_{(LP)}(t)] [q_{(SP)}(t + \tau) + q_{(LP)}(t + \tau)] dt$$

where

$$[(CF)_{qq}(\tau)]_{A(total)} \triangleq \text{Correlation function of the total airplane response}$$

$$q_{(SP)} \triangleq \text{Short period response}$$

$$q_{(LP)} \triangleq \text{Long period response}$$

or

$$[(CF)(\tau)]_{total} = [(CF)(\tau)]_{(SP)} + [(CF)(\tau)]_{(LP)} + [(CCF)(\tau)]_{(SP)(LP)} + [(CCF)(\tau)]_{(LP)(SP)}$$

where

$$[(CCF)(\tau)] \triangleq \text{Cross-correlation function}$$

Since the undamped natural periods of these two oscillations are of the order of 60 to 1, the long period oscillation will, from a practical standpoint, appear as a constant when correlated with the short period oscillation. Hence, to a high degree of approximation these two cross-correlation functions are negligible and one can write:

$$[(CF)(\tau)]_{A(total)} \cong [(CF)(\tau)]_{(SP)} + [(CF)(\tau)]_{(LP)} \quad (V-6)$$

This equation permits the auto-correlation of the two oscillations separately. However, for the purpose for which this data is intended the long period effects can be considered negligible. Consequently, the recording system was designed to measure short period effects only. Because the recording system accommodated only short period effects, the longitudinal equations of motion, which neglect the long period oscillation, are presented.

Neglecting long period effects, the longitudinal equations of motion reduce to:⁽¹¹⁾

$$\begin{aligned} -\dot{w}Z_{\dot{w}} - U_0 \dot{\theta} + \dot{w} - wZ_w &= \delta Z_{\delta e} + w_{A-I} Z_w + \dot{w}_{A-I} Z_{\dot{w}} \\ \ddot{\theta} - \dot{\theta}M_{\dot{\theta}} - \dot{w}M_{\dot{w}} - wM_w &= \delta M_{\delta e} + w_{A-I} M_w + \dot{w}_{A-I} M_{\dot{w}} \end{aligned}$$

where

$U_o \triangleq$ Equilibrium airspeed in feet per second

$M(\cdot) \triangleq \frac{1}{I_{yy}} \frac{\partial M}{\partial (\cdot)}$

$Z(\cdot) \triangleq \frac{1}{m} \frac{\partial Z}{\partial (\cdot)}$

$I_{yy} \triangleq$ Moment of inertia of the airplane about the Y axis in slug-feet²

$m \triangleq$ Mass of the airplane in slugs.

$w_{A-I} \triangleq$ Vertical velocity of the air mass with respect to inertial space.

the dot over a variable represents the Newtonian derivative with respect to time.

For zero initial conditions at a stable equilibrium flight, the Fourier transform of the above set of differential equations gives the following set of complex algebraic equations:

$$[(j\omega)(1 - Z_{\dot{w}}) - Z_w]w - [U_o] \dot{\theta} = \delta Z_{\delta} + [Z_{\dot{w}}(j\omega) + Z_w] w_{A-I}$$

$$-[M_{\dot{w}}(j\omega) + M_w]w - [(j\omega) - M_{\dot{\theta}}] \dot{\theta} = \delta M_{\delta} + [M_{\dot{w}}(j\omega) + M_w] w_{A-I}$$

where the variables are now a function of the angular frequency, ω .

This set of equations can now be solved to obtain the following performance functions:

$$(\text{PF})_{A(\delta_E \dot{\theta})} = \frac{(j\omega)M_{\delta} + (Z_{\delta}M_w - Z_wM_{\delta})}{\Delta_{A(\text{Long})}} \quad (\text{V-7})$$

$$(\text{PF})_{A(w_{A-I} \dot{\theta})} = \frac{(j\omega)[M_{\dot{w}}(j\omega) + M_w]}{\Delta_{A(\text{Long})}} \quad (\text{V-8})$$

where:

$$\Delta_{A(\text{Long})} = \begin{vmatrix} [(1 - Z_{\dot{w}})(j\omega) - Z_w] & - U_o \\ -[M_{\dot{w}}(j\omega) + M_w] & [(j\omega) - M_{\dot{\theta}}] \end{vmatrix} \quad (\text{V-9})$$

The performance function given by Eq. (V-2) can be measured experimentally. This experimental data can then be used in conjunction with Eqs. (V-2) and (V-3) to compute the performance function corresponding to the theoretical Eq. (V-3). For example:

$$\left| (\text{PF})_{A(w_{A-I} \dot{\theta})} \right|^2 = \left| \frac{(\text{PF})_{A(w_{A-I} \dot{\theta})}(\text{Theor})}{(\text{PF})_{A(\delta_E \dot{\theta})}(\text{Theor})} \right|^2 \left| (\text{PF})_{A(\delta_E \dot{\theta})}(\text{Exp}) \right|^2 \quad (\text{V-10})$$

The longitudinal experimental performance functions were taken from data presented in reference 3 and multiplied by the following modifying ratios to obtain the longitudinal rough air performance function:

$$\left| \frac{(\text{PF})_{A(w_{A-I} \dot{\theta})}(\text{Theor})}{(\text{PF})_{A(\delta_E \dot{\theta})}(\text{Theor})} \right|^2 = \left[\frac{M_w^*}{M_\delta}(\omega) \right]^2 \left[\frac{(\omega)^2 + \left(\frac{M_w}{M_w^*} \right)^2}{(\omega)^2 + \frac{1}{(\text{CT})_{A(\delta \dot{\theta})}^2}} \right] \quad (\text{V-11})$$

where

$$(\text{CT})_{A(\delta \dot{\theta})} \triangleq \frac{M_\delta}{(M_w Z_\delta - M_\delta Z_w)}$$

E. Lateral Response Equations

For the assumptions already noted, the lateral equations of motion are:

$$\begin{aligned} \dot{v} + U_O \dot{\psi} - v Y_v - \varphi Y_\varphi &= 0 \\ \ddot{\varphi} - v L_v - \dot{\varphi} L_\varphi - \dot{\psi} L_\psi &= \delta_a L_{\delta a} + \frac{\partial w_{A-I}}{\partial y} L_\varphi \\ \ddot{\psi} - v N_v - \dot{\varphi} N_\varphi - \dot{\psi} N_\psi &= \delta_a N_{\delta a} + \frac{\partial w_{A-I}}{\partial y} N_\psi \end{aligned} \quad (\text{V-12})$$

Taking the Fourier transform for zero initial conditions, one obtains,

$$[(j\omega) - Y_v] v + [U_o] \dot{\psi} + \left[-\frac{Y_\varphi}{(j\omega)}\right] \dot{\varphi} = 0$$

$$[-L_v] v + [-L_\dot{\psi}] \dot{\psi} + [(j\omega) - L_\dot{\varphi}] \dot{\varphi} = \delta_a L_{\delta a} + \frac{\partial w_{A-I}}{\partial y} L_\dot{\varphi} \quad (V-13)$$

$$[-N_v] v + [(j\omega) - N_\dot{\psi}] \dot{\psi} + [-N_\dot{\varphi}] \dot{\varphi} = \delta_a N_{\delta a} + \frac{\partial w_{A-I}}{\partial y} N_\dot{\varphi}$$

This set of algebraic equations can now be solved to obtain the following performance functions:

$$\begin{aligned} (PF)_A(\delta_a \dot{\varphi}) &= \frac{(j\omega)^2 [-L_{\delta a}] - (j\omega)[N_{\delta a} N_\dot{\psi} - Y_v L_{\delta a} - L_a N_\dot{\psi}]}{\Delta_A(Lat)} \\ &+ \frac{U_o [L_v N_{\delta a} - N_v L_{\delta a}] + Y_v [N_{\delta z} L_\dot{\psi} - L_{\delta a} N_\dot{\psi}]}{\Delta_A(Lat)} \end{aligned} \quad (V-14)$$

$$\begin{aligned} (PF)_A\left(\frac{\partial w_{A-I}}{\partial y} \dot{\varphi}\right) &= \frac{(j\omega)^2 [-L_\dot{\varphi}] - (j\omega)[N_\dot{\psi} L_\dot{\psi} - L_\dot{\psi} N_\dot{\varphi} - L_\dot{\varphi} Y_v]}{\Delta_A(Lat)} \\ &+ \frac{U_o [N_\dot{\psi} L_v - L_\dot{\psi} N_v] + Y_v [N_\dot{\psi} L_\dot{\psi} - N_\dot{\varphi} L_\dot{\psi}]}{\Delta_A(Lat)} \end{aligned} \quad (V-15)$$

where:

$$\Delta_A(Lat) \triangleq \begin{vmatrix} [(j\omega) - Y_v] & [U_o] & \left[-\frac{Y_\varphi}{(j\omega)}\right] \\ [-L_v] & [-L_\dot{\psi}] & [(j\omega) - L_\dot{\varphi}] \\ [-N_v] & [(j\omega) - N_\dot{\psi}] & [-N_\dot{\varphi}] \end{vmatrix} \quad (V-16)$$

and, as in the longitudinal case:

$$\left| \frac{(\text{PF})_{A\left(\frac{\partial w_{A-I}}{\partial y}\dot{\varphi}\right)(\text{Theor})}}{(\text{PF})_{A(\delta_a\dot{\varphi})(\text{Theor})}} \right|^2 = \left| \frac{(j\omega)^2 + (j\omega)\left[L_{\dot{\psi}}\frac{N_{\dot{\varphi}}}{L_{\dot{\varphi}}} - N_{\dot{\psi}} - Y_v\right] - U_o\left[L_v\frac{N_{\dot{\varphi}}}{L_{\dot{\varphi}}} - N_v\right] - Y_v\left[L_{\dot{\psi}}\frac{N_{\dot{\varphi}}}{L_{\dot{\varphi}}} - N_{\dot{\psi}}\right]}{(j\omega)^2 + (j\omega)\left[N_{\dot{\psi}}\frac{N_{\delta_a}}{L_{\delta_a}} - N_{\dot{\psi}} - Y_v\right] - U_o\left[L_v\frac{N_{\delta_a}}{L_{\delta_a}} - N_v\right] - Y_v\left[L_{\dot{\psi}}\frac{N_{\delta_a}}{L_{\delta_a}} - N_{\dot{\psi}}\right]} \right|^2 \quad (\text{V-17})$$

This theoretical correction factor multiplied by experimental aileron response data gives the lateral rough air performance function. The experimental aileron response data was obtained from reference 4.

F. The Test Airplane

The airplane used in this investigation was a USAF B-25J, under bailment contract to the Instrumentation Laboratory, Massachusetts Institute of Technology. The airplane was, prior to these tests, stripped of all its guns, turrets, and bombing equipment as shown in Fig. V-4.

For these tests, the airplane was ballasted to 26 percent M. A. C. In addition, hydraulic shut-off valves were used between the front and rear main fuel tanks in order to keep the change in longitudinal center of gravity and moment of inertia of the airplane with fuel consumption to a negligible amount.

To simplify the data reduction and computation of the airplane performance functions, it was desirable to record the airplane response to the turbulent air with



FIG. V-4 B-25J AIRPLANE U.S.A.F. No. 44-30328

the flight path controls locked. The control locks used are shown in Figs. V-5 and V-6. The elevator lock was previously designed by Mr. Clifford Muzzey for a double stop used in determining the airplane performance function by the pulse technique. The results of this investigation are presented in reference 3. The aileron and rudder locks were designed for use as control stops to determine the lateral performance functions by the pulse technique. The results of this investigation are given in reference 4.

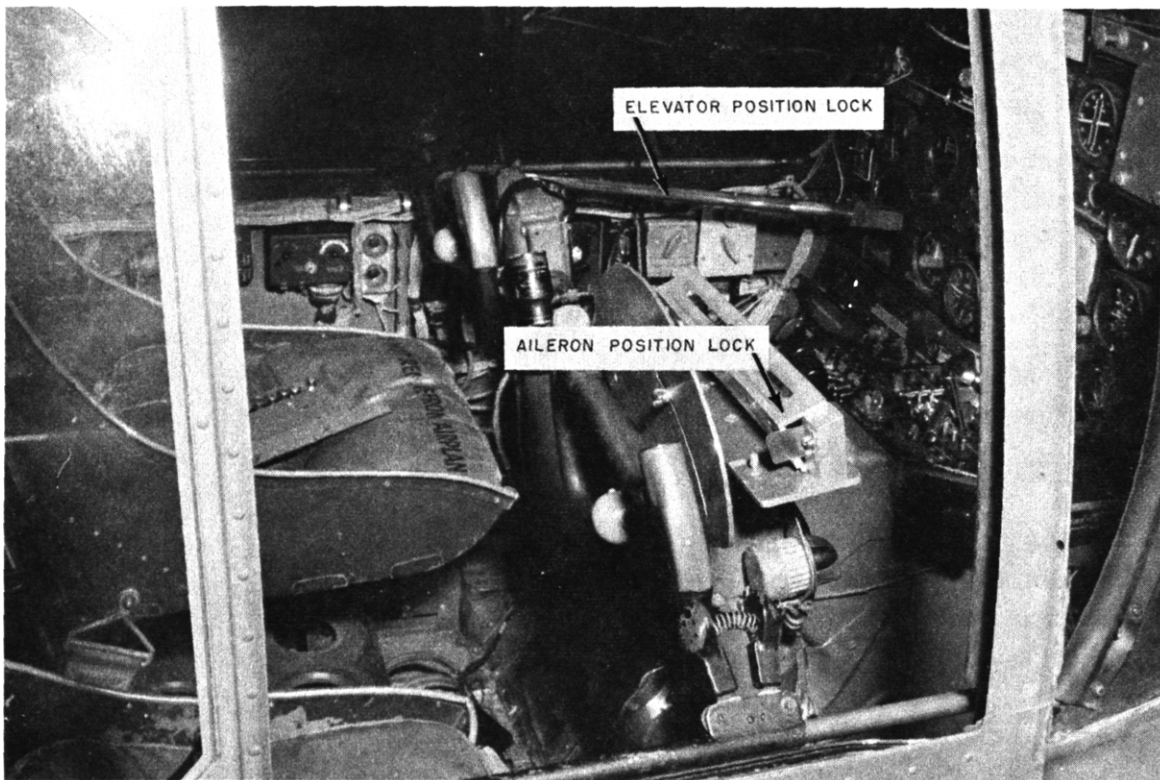


FIG. V-5 ELEVATOR AND AILERON CONTROL POSITION LOCKS

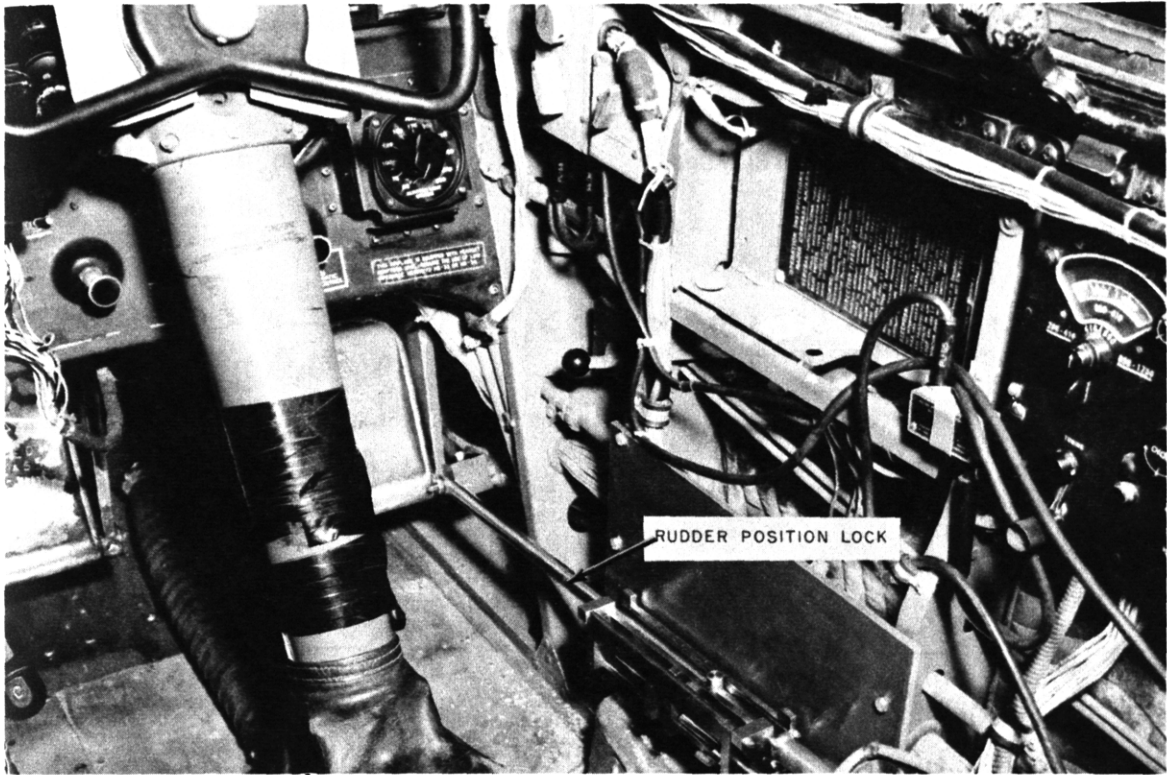


FIG. V-6 THE RUDDER POSITION LOCK

Physical Data

$I_{yy} = 64,000 \text{ slug ft}^2$ (measured)	$\text{Area}_{(\text{wing})} \triangleq s_w = 610 \text{ ft}^2$
$I_{xx} = 63,000 \text{ slug ft}^2$ (estimated)	$\text{Chord}_{(\text{wing})} \triangleq c_w = 9.67 \text{ ft}$
$I_{zz} = 120,000 \text{ slug ft}^2$ (estimated)	$\text{Span}_{(\text{wing})} \triangleq b = 67.56 \text{ ft}$
Wt. = 26,000 lbs. (measured)	$\text{Area}_{(\text{tail})} \triangleq s_t = 132.5 \text{ ft}^2$
C.G. = 26 percent MAC (measured)	$\text{Length}_{(\text{tail})} \triangleq l_t = 25.9 \text{ ft}$

G. Stability Derivatives Used in Computation of Airplane Performance Functions

Condition No. 1

(175 mph, 26 percent M. A. C., 8,000 ft., Press. Alt.)

<u>Longitudinal</u>	<u>Lateral</u>
$M_{\delta} = \left(\frac{dC_M}{d\delta_E} \right) \frac{s_w c_w}{I_{yy}} q_o = -9.8 (1/\text{sec}^2)$	$L_{\delta a} = \left(\frac{dC_l}{d\delta a} \right) \frac{s_w b}{I_{xx}} q_o = -3.7 (1/\text{sec}^2)$
$Z_{\delta} = \left(\frac{dC_M}{d\delta_E} \right) \frac{s_w c_w}{m l_t} q_o = -30.4 (ft/\text{sec}^2)$	$N_{\delta a} = \left(\frac{dC_n}{d\delta a} \right) \frac{s_w b}{I_{zz}} q_o = .148 (1/\text{sec}^2)$
$M_w = \left(\frac{dC_M}{d\alpha} \right) \frac{s_w c_w}{I_y U_o} q_o = -0.0128 (1/\text{ft-sec})$	$L_v = \left(\frac{dC_l}{d\beta} \right) \frac{s_w b^2}{I_{xx} U_o} q_o = -.0081 (1/\text{ft-sec})$
$Z_w = - \left(\frac{dC_L}{d\alpha} \right) \frac{s_w q_o}{m U_o} = -1.065 (1/\text{sec})$	$N_v = \left(\frac{dC_n}{d\beta} \right) \frac{s_w b}{I_{zz} U_o} q_o = .0063 (1/\text{ft-sec})$
$M_w^{\cdot} = - \left(\frac{dC_L}{d\alpha} \right) n_t \frac{d\varepsilon}{d\alpha} \frac{l_t^2 s_t q_o}{I_{yy} U_o^2}$ $= -0.00176 (1/\text{ft})$	$L_{\phi}^{\cdot} = \frac{dC_l}{d\left(\frac{pb}{2U_o}\right)} \frac{s_w b^2}{2U_o I_{xx}} q_o = -3.63 (1/\text{sec})$
$M_{\theta}^{\cdot} = -(1.2) \left(\frac{dC_L}{d\alpha} \right) n_t \frac{s_t l_t^2}{I_y U_o} q_o$ $= -1.72 (1/\text{sec})$	$N_{\phi}^{\cdot} = \frac{dC_n}{d\left(\frac{pb}{2U_o}\right)} \frac{s_w b}{2U_o I_{zz}} q_o = -.11 (1/\text{sec})$
	$L_{\phi}^{\cdot} = \frac{dC_l}{d\left(\frac{pb}{2U_o}\right)} \frac{s_w b^2}{2I_{xx}} q_o = .53 (1/\text{sec})$

where

$$q_o = \frac{1}{2} \rho U_o^2$$

ρ = air mass density

$$N_{\psi}^{\circ} = \frac{dC_n}{d\left(\frac{rb}{2U_o}\right)} \frac{s_w b^2}{2I_{zz}} q_o = -.603 \text{ (1/sec)}$$

Condition No. 2

(230 mph, 26 percent M.A.C., 8,000 ft., Press. Alt.)

Longitudinal

$$M_{\delta} = -16.95 \text{ (1/sec}^2\text{)}$$

$$Z_{\delta} = -52.6 \text{ (ft/sec}^2\text{)}$$

$$M_w = -.0218 \text{ (1/ft-sec)}$$

$$Z_w = -1.4 \text{ (1/sec)}$$

$$M_w^{\circ} = -0.00176 \text{ (1/ft)}$$

$$M_{\theta}^{\circ} = -2.26 \text{ (1/sec)}$$

Appendix VI

DESCRIPTION OF FLIGHT TEST INSTRUMENTATION

A. General

In this investigation, the airplane served as the sensing instrument for determining atmospheric turbulence. In order to record and interpret the data, however, it was necessary to, in turn, sense the response of the airplane and record this response as a continuous function of time. Consequently, the airplane and the flight test instrumentation, as a unit, constitutes the measuring system. As with all problems of measuring continuous functions of time, it is necessary not only to record and compensate for all environmental changes, but also to apply dynamic corrections to compensate for the dynamics introduced into the records by the measuring system. However, due to the random character of the input in this particular problem, it is necessary to know only the attenuation characteristics of the frequency response of the measuring system. Since the airplane and the flight test instrumentation operate in a chain, the frequency response of each unit may be determined separately and the over-all performance function determined as the product of the separate performance functions. The performance functions for the airplane are presented in Appendix V. The performance functions for the aircraft instrumentation are presented in this appendix.

B. The Flight Test Instrumentation

With the exception of the lateral accelerometer, the flight test recording equipment had been previously installed for the flight test programs in references 3 and

4. The recording equipment consisted of four basic units:

1. The Sensing Instruments
2. The Recording Amplifiers
3. The Recording Oscillograph
4. In-flight static calibration equipment.

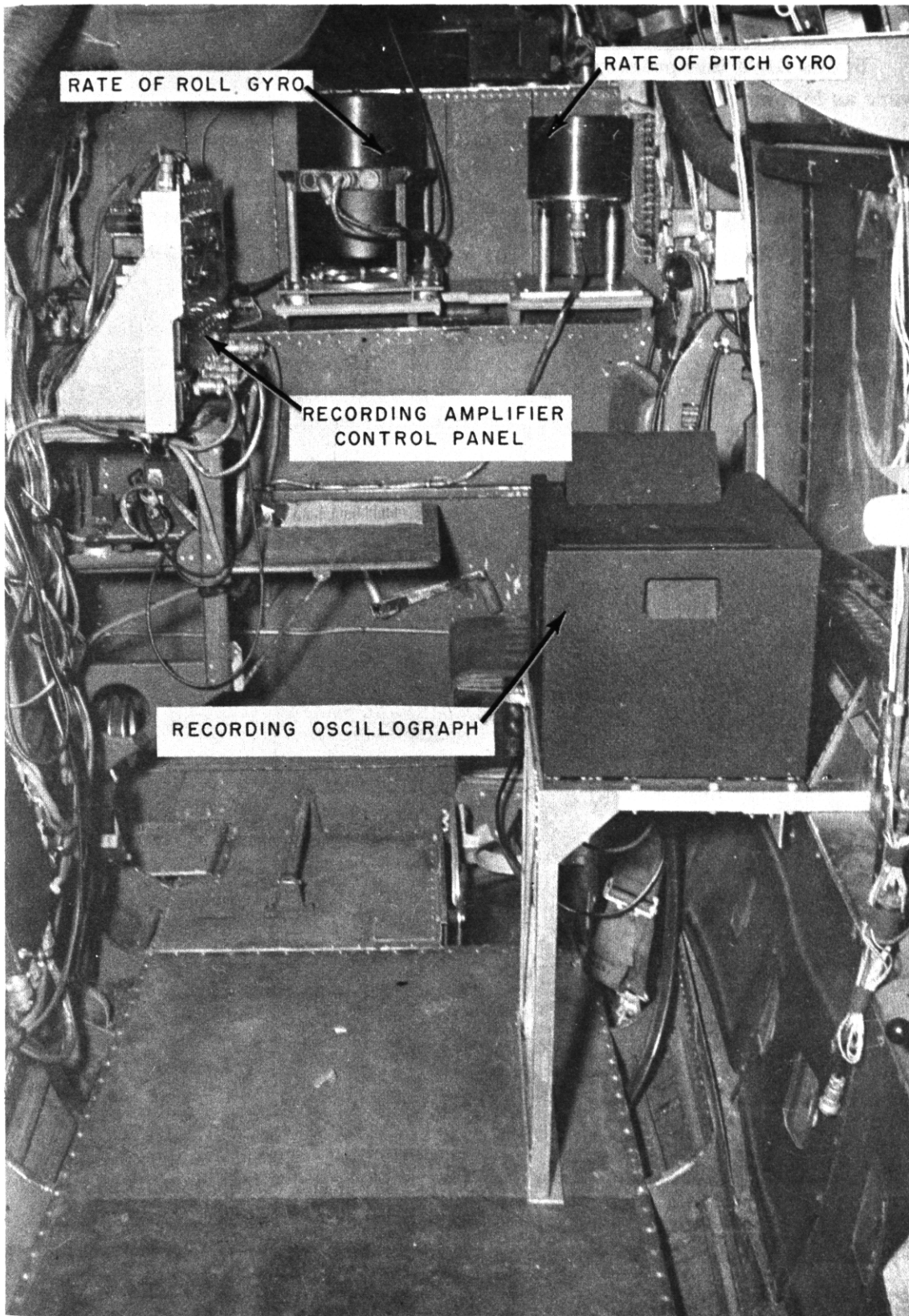


FIG. VI-1 VIEW OF INSTRUMENT RECORDING STATION FROM AFT HATCH

In this flight test program, the sensing instruments with their uncertainty levels were as follows:

- a. Rate of Pitch Indicator (± 1 mil/sec) (A-1 gunsight single-degree-of-freedom gyro modified for test work).
- b. Rate of Roll Indicator (± 1 mil/sec) (Same type as 1).
- c. Normal accelerometer ($\pm .01$ g) (Instrumentation Laboratory, M. I. T.) .
- d. Lateral accelerometer ($\pm .001$ g) (A-1 modified pendulous accelerometer).

Figures VI-1 and VI-2 show the location of these instruments in the aircraft.

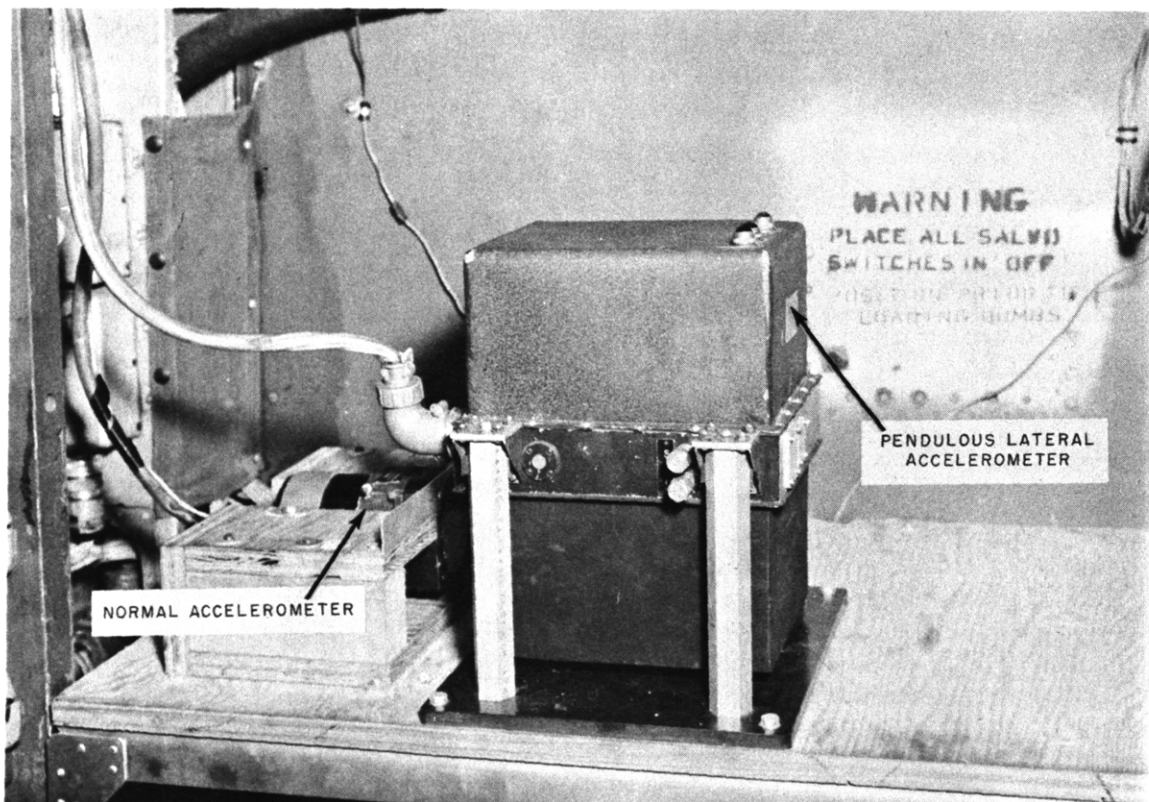


FIG. VI-2 VIEW OF BOMB-BAY ACCELEROMETER INSTALLATION
LOOKING FORWARD.

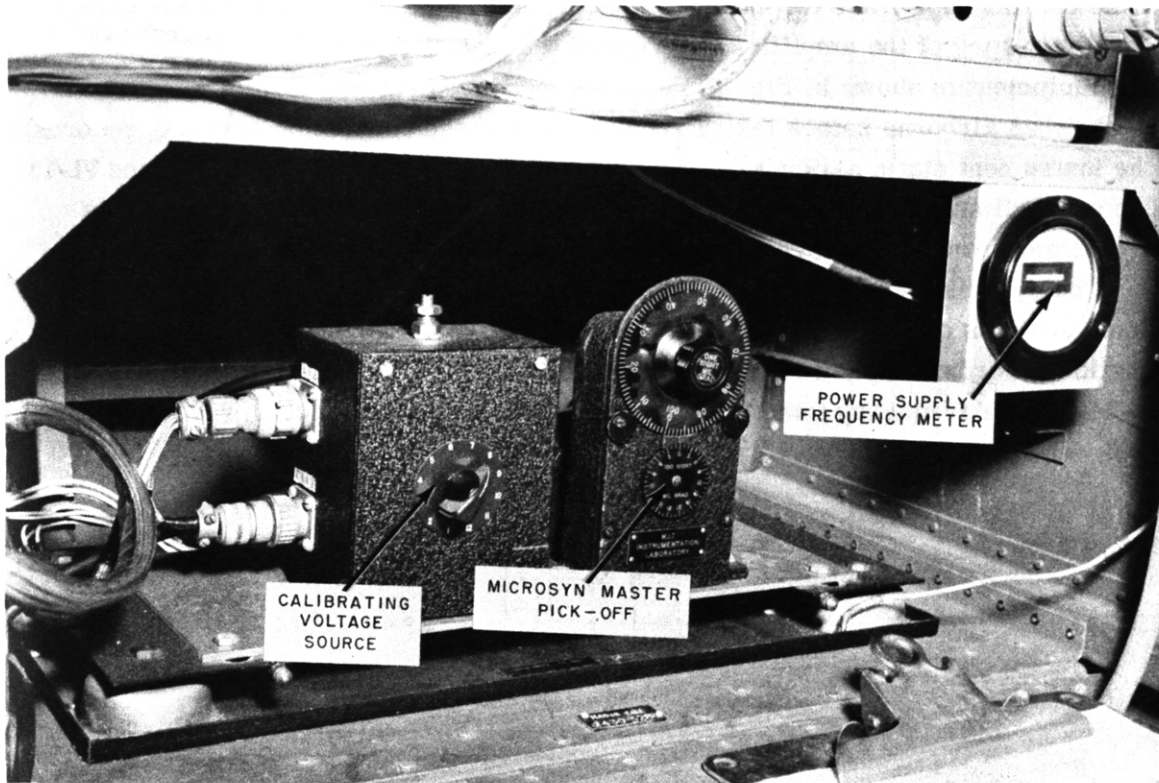


FIG. VI-3 VIEW OF IN-FLIGHT CALIBRATION EQUIPMENT

Figure VI-1 also shows the recording amplifiers and the recording oscillograph. Each amplifier performed three functions:

1. Amplified the a-c pickoff signal.
2. Demodulated the a-c signal.
3. Amplified the resulting d-c signal for recording on the oscillograph.

The output of each amplifier is controlled by 12 attenuation settings that adjust the oscillograph trace sensitivity.

The oscillograph is a 12-channel Consolidated Recording Oscillograph. The dynamics of the amplifier and oscillograph are negligible for the frequencies involved in the aircraft response.

The static calibration of each channel was accomplished in two steps. The first step was the calibration of each sensing instrument in terms of divisions on a master

pickoff. This measurement was not subject to change and consequently was made only at the beginning and end of the program. The second step was the calibration of the oscillograph trace for known displacements of the master pickoff for each attenuator setting of the amplifier. A view of the installation of the in-flight calibration equipment is shown in Fig. VI-3. This measurement was made twice each flight (when airborne before taking records, and at the conclusion of taking records). The instrument static calibrations are shown in Figs. VI-4, VI-7, VI-10, and VI-13. The over-all sensitivity indicated on each flight record was obtained from these figures and from the in-flight static calibrations.

The dynamic calibration for each sensing instrument was obtained from a harmonic analysis of the response of each instrument to a step-function. The step-function records are shown for each instrument in Figs. VI-5, VI-8, VI-11, and VI-14. Their frequency functions squared follow each step-function record in Figs. VI-6, VI-9, VI-12, and VI-15.

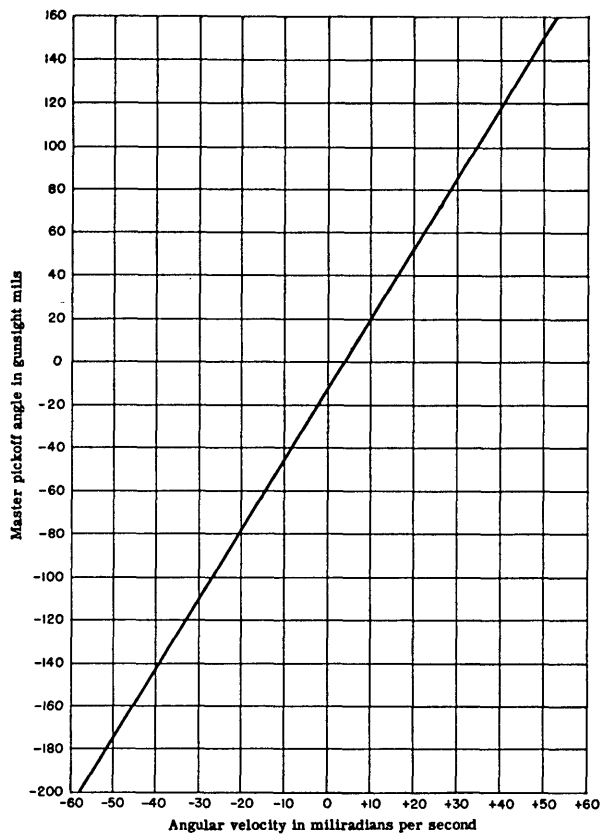


FIG. VI-4 STATIC CALIBRATION

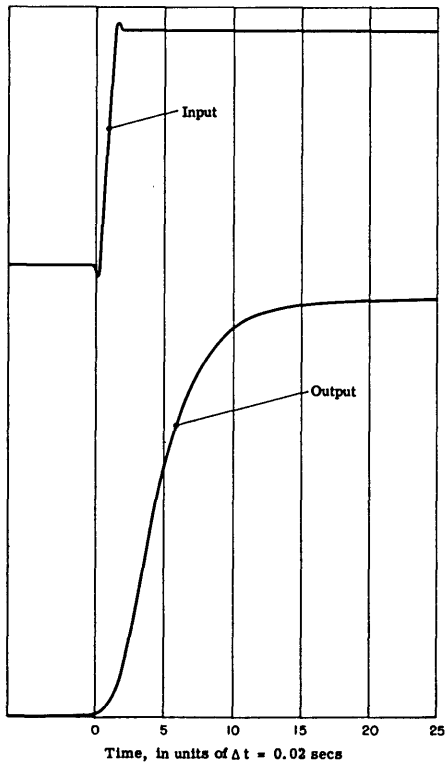


FIG. VI-5 INSTRUMENT RESPONSE TO A STEP FUNCTION

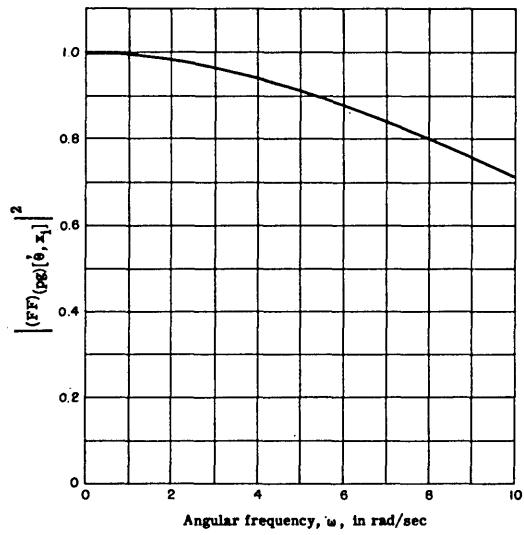


Fig. VI-6 INSTRUMENT FREQUENCY FUNCTION SPECTRUM

RATE OF PITCH GYRO CALIBRATION DATA

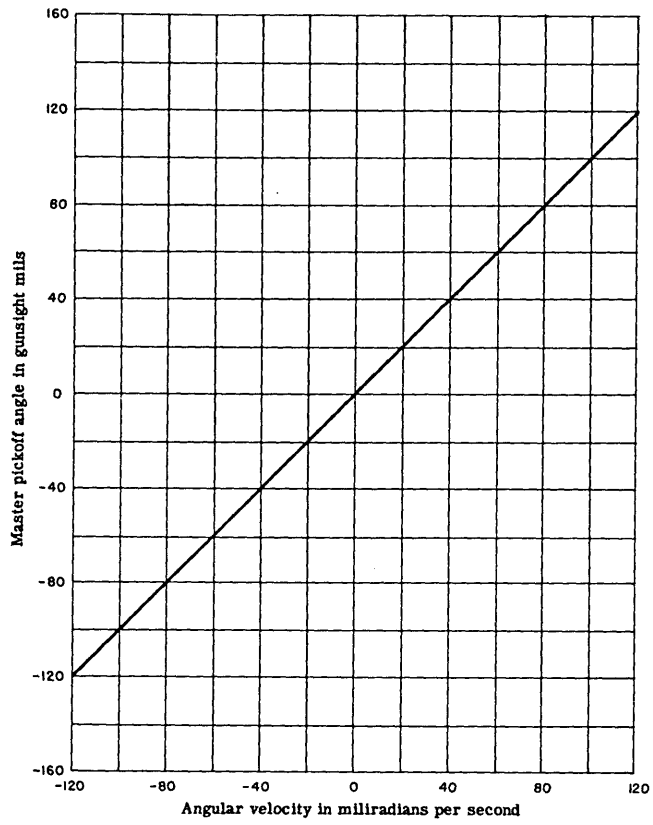


FIG. VI-7 STATIC CALIBRATION

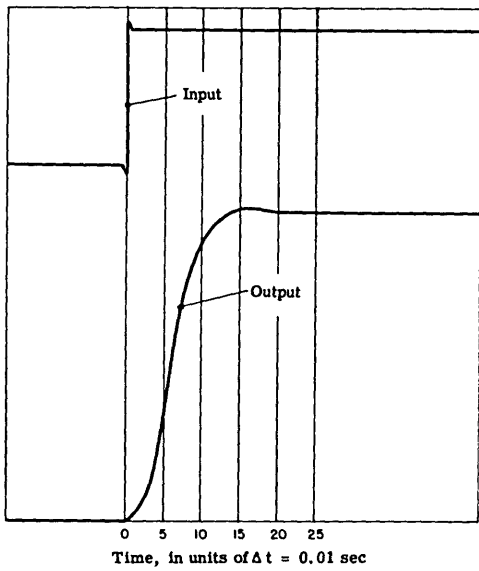


FIG. VI-8 INSTRUMENT RESPONSE TO A STEP FUNCTION INPUT

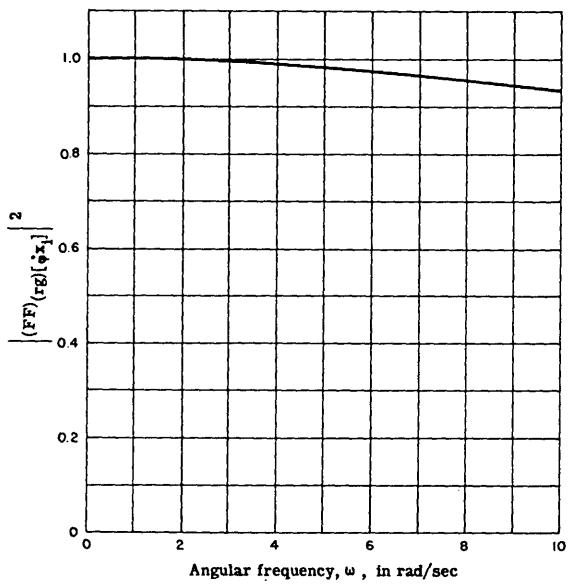


FIG. VI-9 INSTRUMENT FREQUENCY FUNCTION SPECTRUM

RATE OF ROLL GYRO CALIBRATION DATA

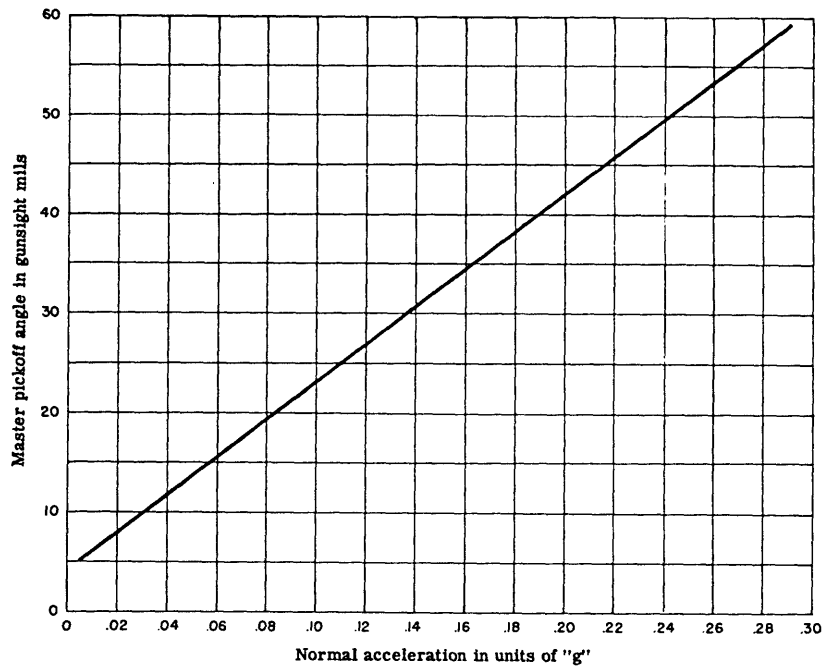


FIG. VI-10 STATIC CALIBRATION

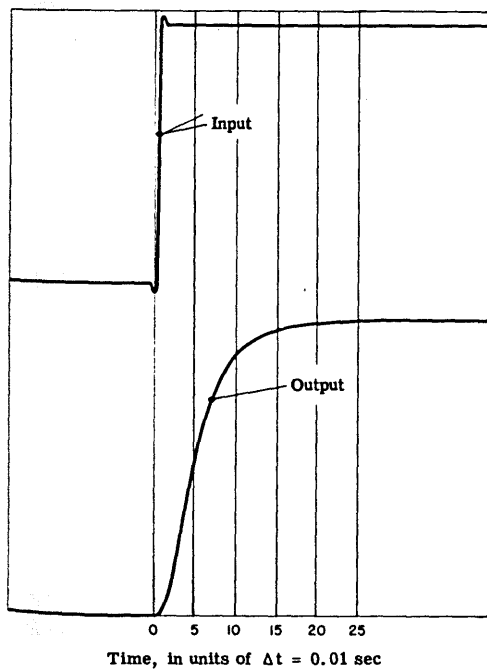


FIG. VI-11 INSTRUMENT RESPONSE TO A STEP FUNCTION

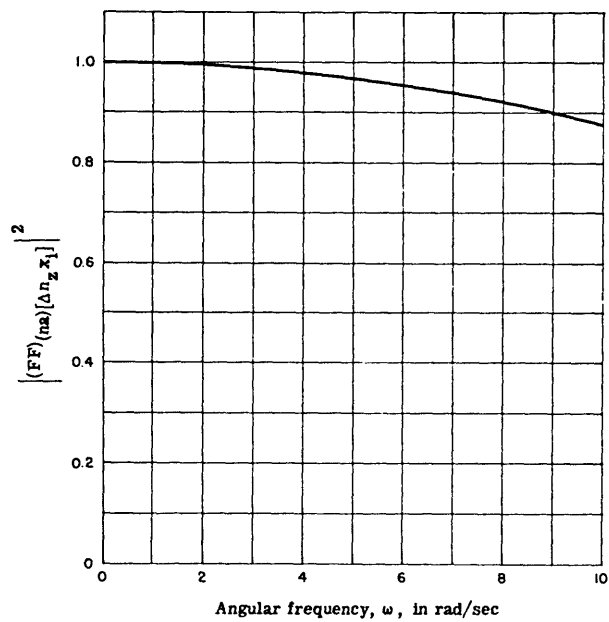


FIG. VI-12 INSTRUMENT FREQUENCY FUNCTION SPECTRUM

NORMAL ACCELEROMETER CALIBRATION DATA

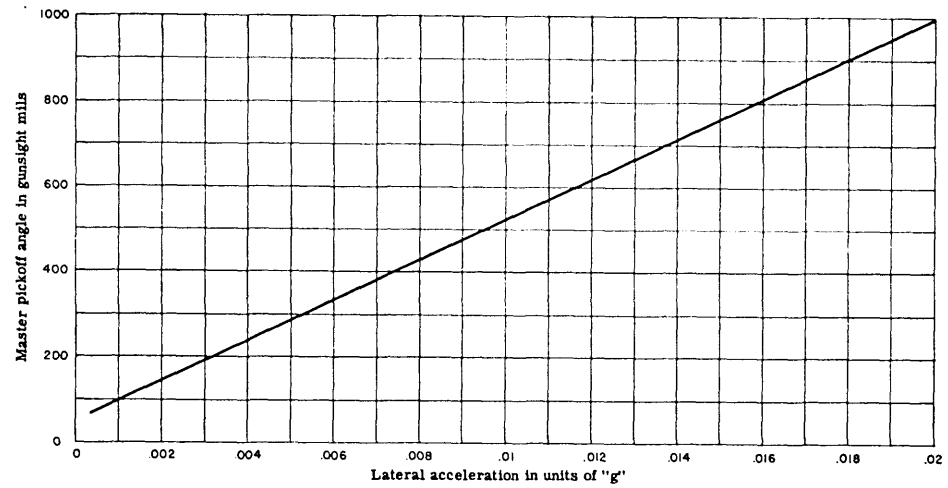


FIG. VI-13 STATIC CALIBRATION

74

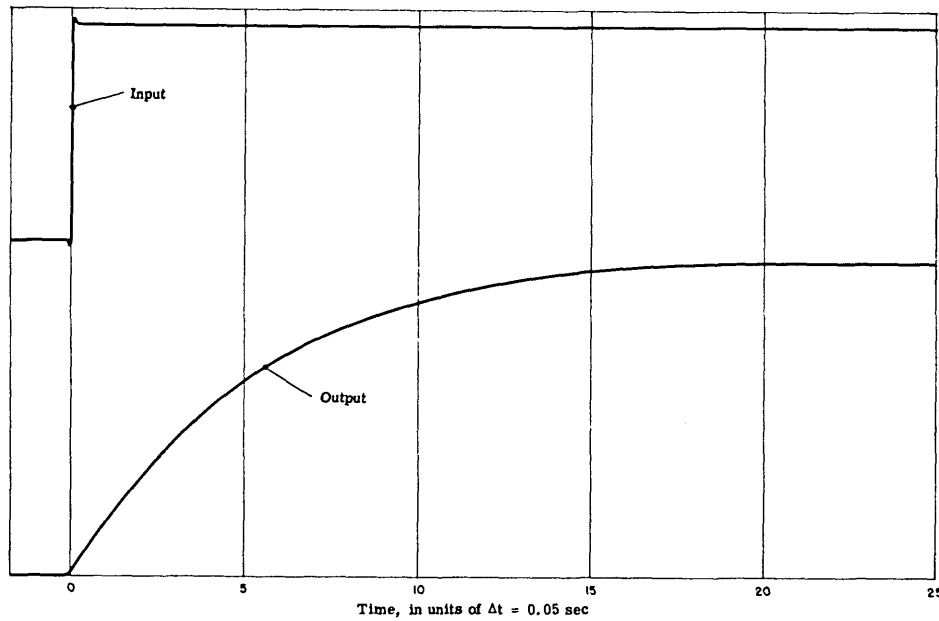


FIG. VI-14 INSTRUMENT RESPONSE TO A STEP FUNCTION

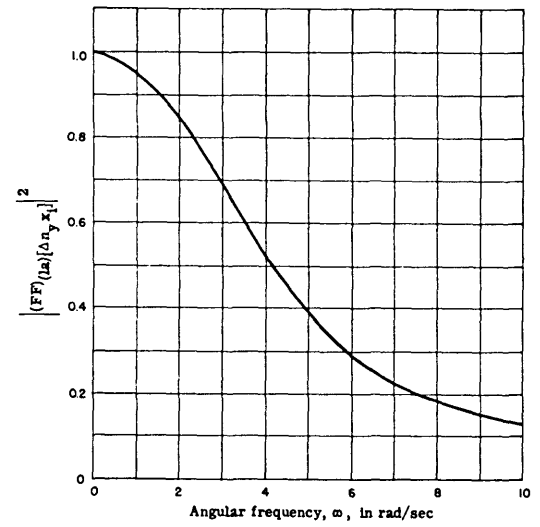


FIG. VI-15 INSTRUMENT FREQUENCY FUNCTION SPECTRUM

Appendix VII
DESIGN OF A CORRELATION COMPUTER

One of the greatest deterrents to the application of the random function theory is the tremendous amount of work involved in determining the correlation functions upon which the optimum design is based. In an attempt to reduce somewhat the amount of work required in this computation, a correlation computer was designed jointly with Mr. Hollander of the Instrumentation Laboratory, M. I. T.

The computer consists of four primary components:

1. The paper-drive system
2. The tracking system
3. The timing system
4. The integrating system

Figure VII-1 is a functional diagram of the computer.

The computer was designed as a general correlation computer for as many types of data as might be submitted. In addition to integrating the cross-product of the output of the two tracking arms, it also integrates the value and the squared value of the output of each arm.

Mathematically, the computer gives the following data for each record:

1. The time interval over which the integration was taken, with an uncertainty of ± 0.02 seconds, i. e. $(T - \tau)$.
2. The integral of the cross product of the output of both tracking arms, i. e.

$$\int_0^{T - \tau} f(t)f(t + \tau)dt = I_1$$

3. The integral of the square of the output from each tracker, i. e.,

$$I_2(\text{Position } \epsilon_1) = \int_0^{T - \tau} f^2(t)dt$$

$$I_2(\text{Position } \epsilon_2) = \int_0^{T - \tau} f^2(t + \tau)dt$$

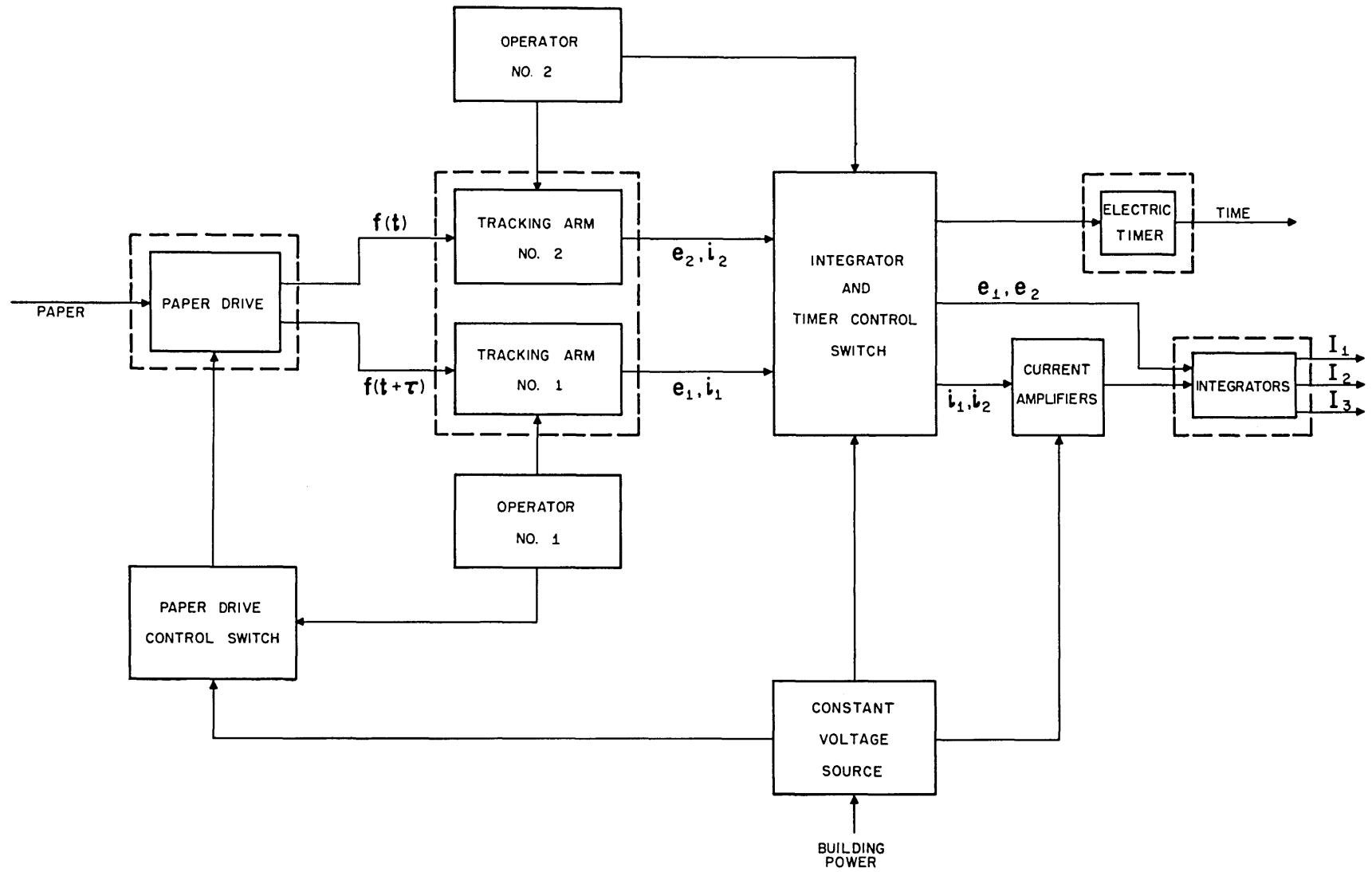


FIG. VII -1 FUNCTIONAL DIAGRAM OF CORRELATION COMPUTER

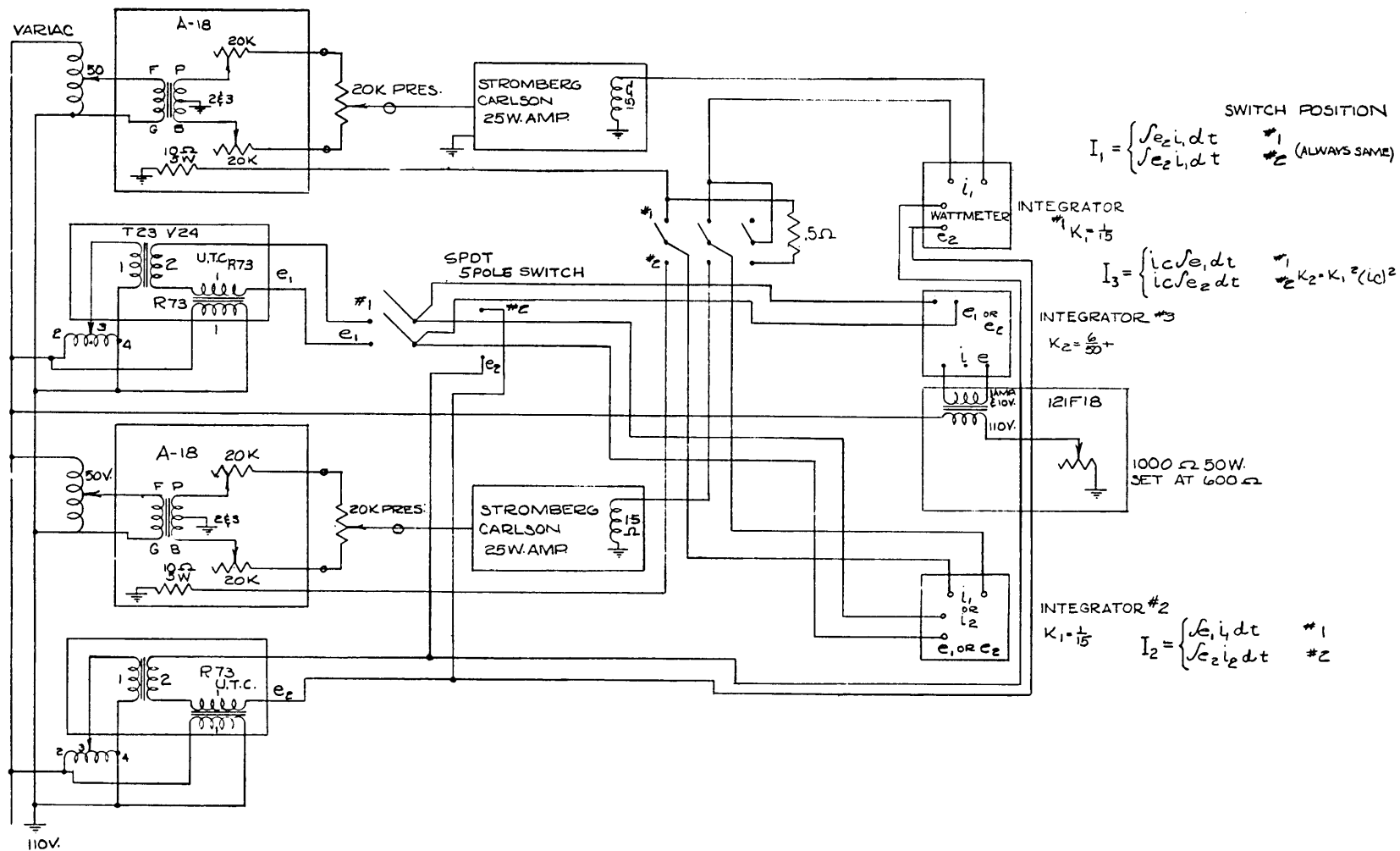


FIG. VII-2 CORRELATION COMPUTER WIRING DIAGRAM

4. The integral of the output from each tracker, i. e.

$$I_3(\text{Position } \epsilon_1) = \int_0^{T-\tau} f(t)dt$$

$$I_3(\text{Position } \epsilon_2) = \int_0^{T-\tau} f(t + \tau)dt$$

The details of the switching arrangement for obtaining these integrals are shown in Fig. VII-2.

Figures VII-3 and VII-4 are photographs of the computer in operation. Figure VII-5 shows the arrangement of the integrators and timer.

The computer requires two operators. Each operator tracks the records as the paper is driven at constant speed. The distance between tracking arms in indicated time determines the correlation interval. To each tracking arm a variac (voltage source) and a potentiometer (current source) are mechanically coupled. In this way a current and a voltage are obtained that are directly proportional to the displacement of the tracking arm. The variac output is applied directly to the voltage side of the integrator. However, in order to obtain the required sensitivity, it was found necessary to amplify the output of the potentiometers before applying the current to the integrators.

The integrators used are watt-second meters commercially obtainable. These instruments are laboratory meters used to adjust and regulate the watt-hour meters used to totalize power consumption. The time constants of the meters are not of concern in this application since one is not interested in an instantaneous value of the integral, but rather in the steady-state value after integrating the entire length of the record.

Integrator No. 1 integrates the product of the voltage from arm No. 2 of the current from arm No. 1. Integrator No. 2 integrates the product of the voltage and current from a given arm dependent upon the switch position. Integrator No. 3 integrates the product of the voltage from a given arm, dependent upon the switch position, and a constant current taken from a separate source.

Referring to Fig. VII-1 and Fig. VII-3, the operation of the computer can be explained as follows:

Operator No. 1 starts the paper drive by pressing foot switch No. 1. When the paper drive has come up to constant speed as indicated by the paper speed indicator, Operator No. 2 presses switch No. 2, starting the integrators and the clock simultaneously. The two operators then track the record until the end is reached at which time Operator No. 2 cuts the switch, stopping the integrators and the clock. While

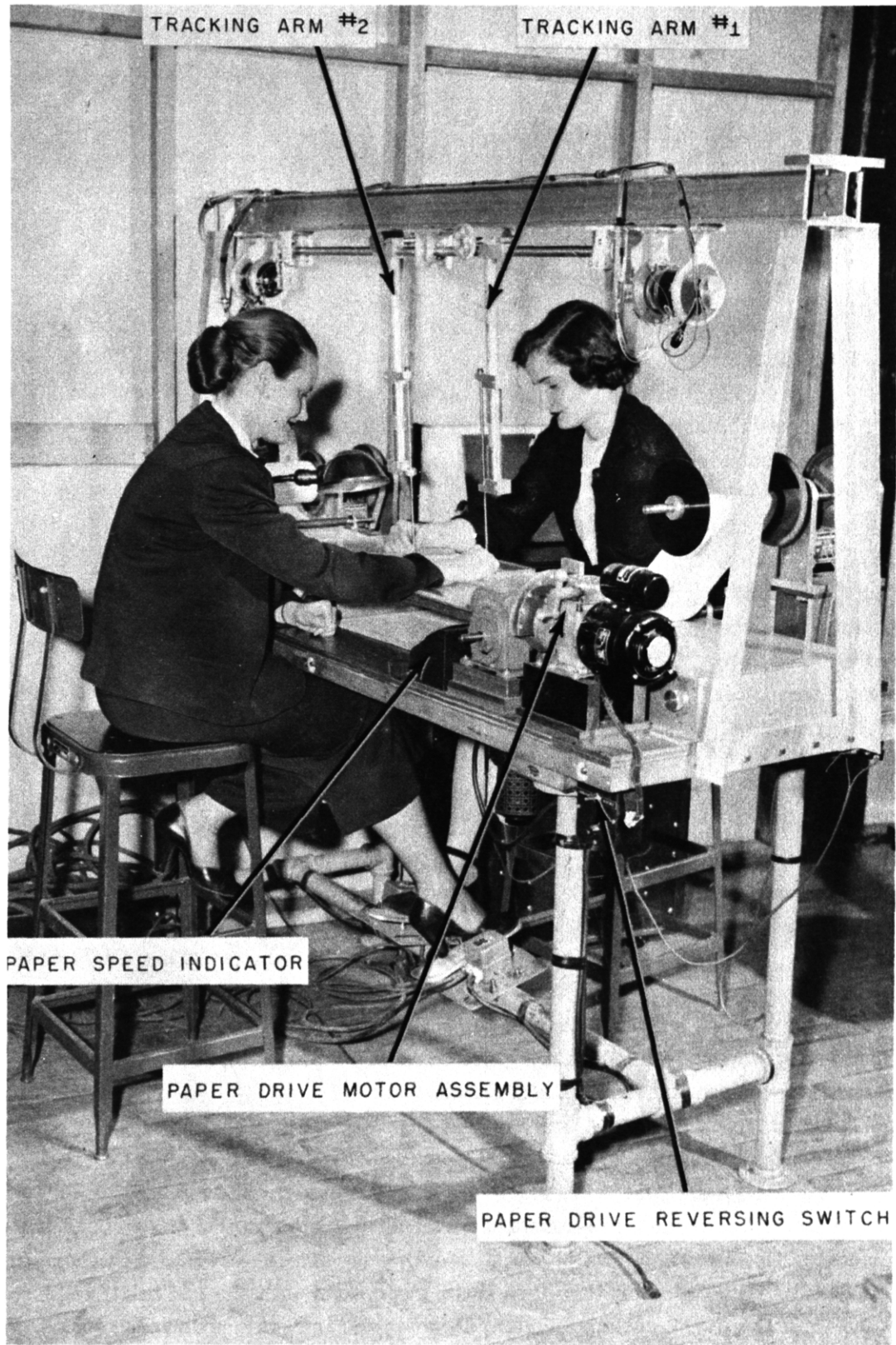


FIG. VII-3
LEFT-SIDE VIEW OF OPERATION OF CORRELATION COMPUTER

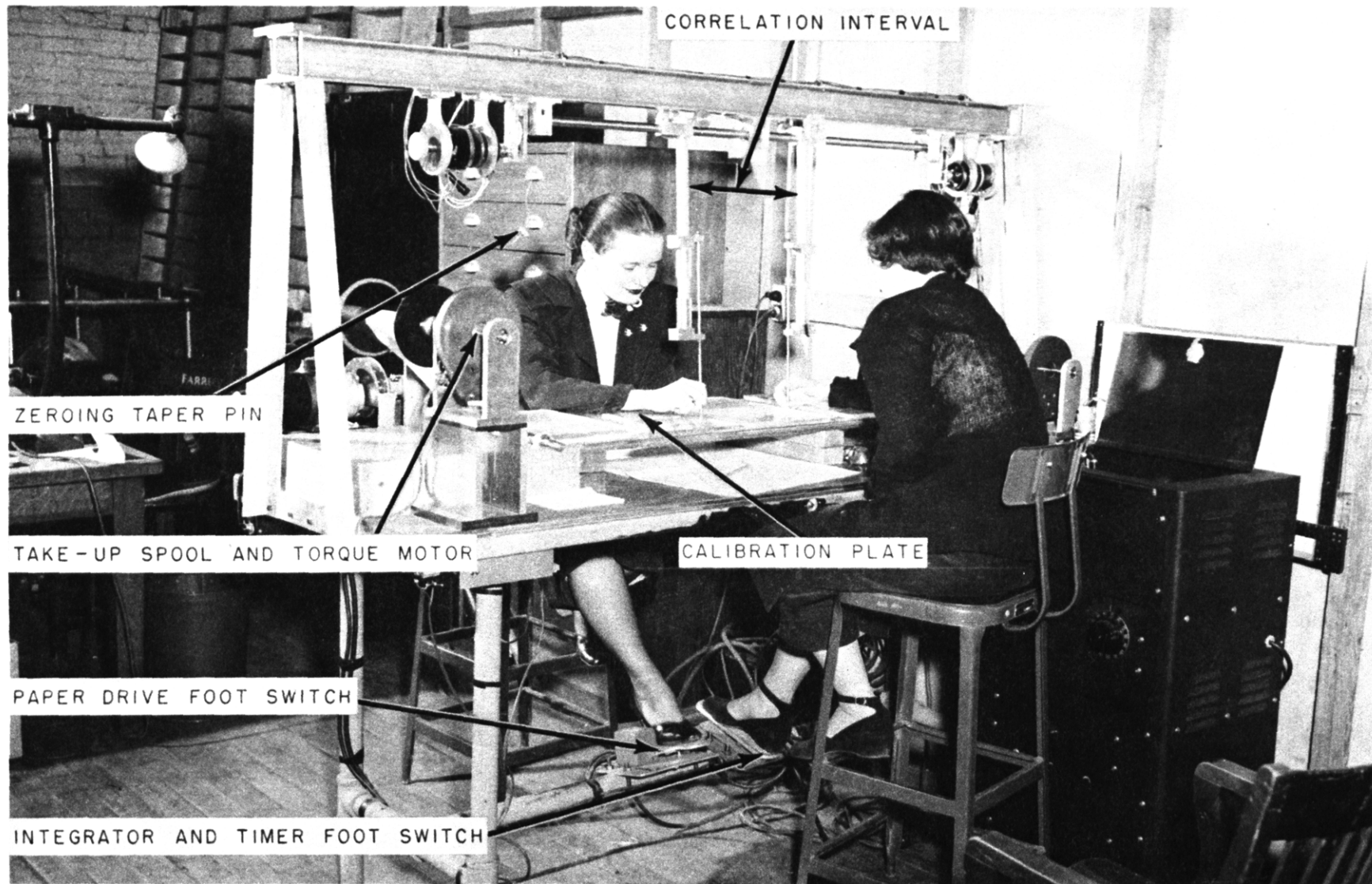


FIG. VII-4 RIGHT-SIDE VIEW OF OPERATION OF CORRELATION COMPUTER

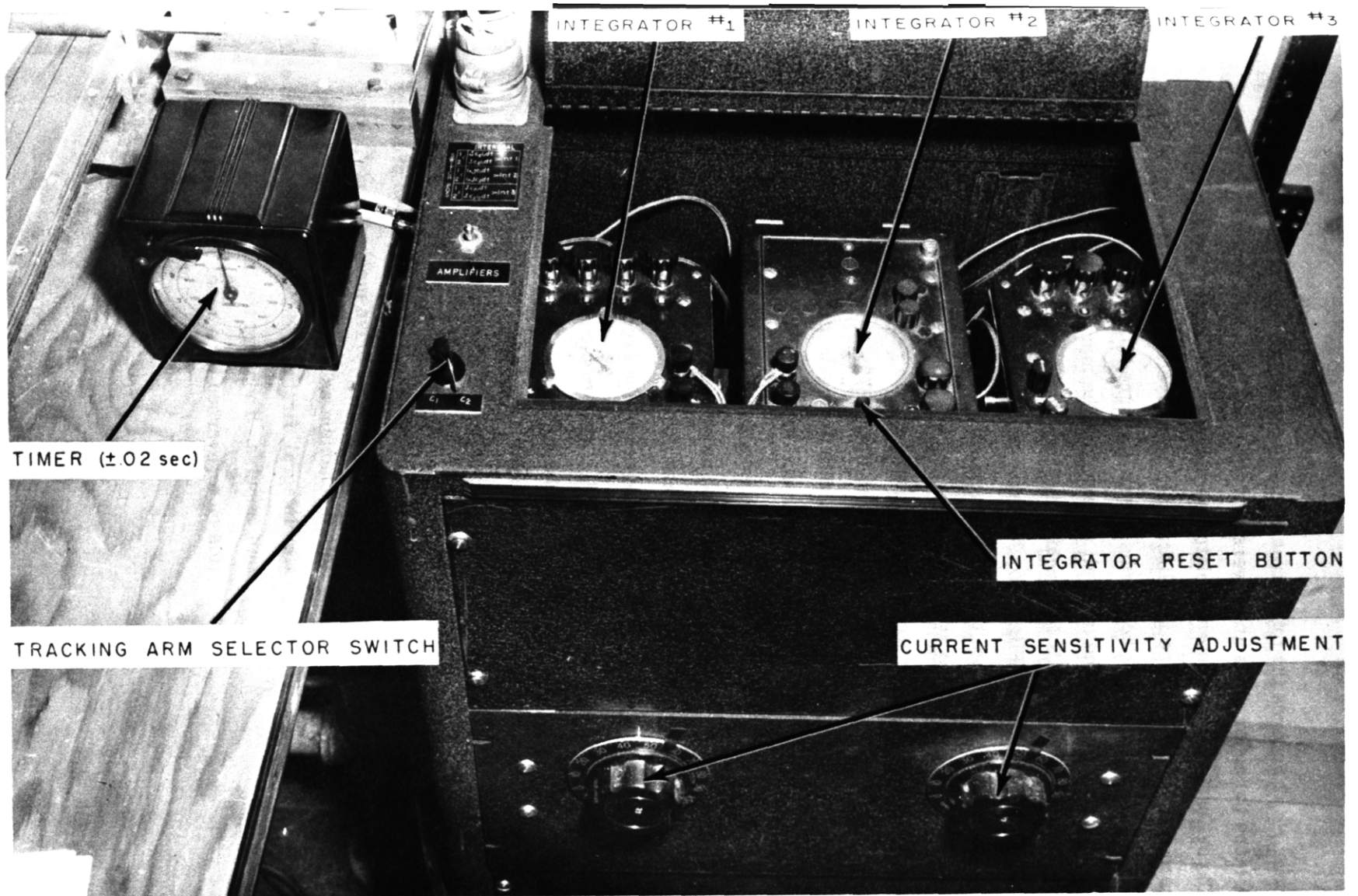


FIG. VII-5 VIEW OF INTEGRATOR CONSOLE AND ELECTRIC TIMER

Operator No. 2 records the totals from the integrators and the clock , Operator No. 1 stops the paper drive and reverses it for tracking in the opposite direction.

To calibrate the computer, a plate was made with holes drilled ± 1 inch from the zero point. The machine is calibrated in both directions by taking the integral of a 1-inch displacement of both arms over a measured time interval.

In order to check on the over-all accuracy of the machine, a run that had previously been totalized by I.B.M. machine methods was re-run on the computer.

The first set of data, Flight No. 90, was computed by selecting discrete points at 0.1-second intervals from the oscillograph records. The set of discrete points were then correlated on I.B.M. equipment. One run of this data was used to check the overall accuracy of the correlation computer. The results of this check are

shown in Fig. VII-6. The solid curve is the I.B.M. data and against this curve is plotted the results obtained from the correlation computer.

These results indicate that the correlation function as computed by the correlation computer was obtained to within 5 percent of the mean power of the record.

This correlation computer can in addition be used as a harmonic analyzer and a machine to compute the convolution integral. To use this mechanism as a harmonic analyzer, the product of one tracking arm can be integrated against the output of a sine generator properly geared to the paper drive mechanism. To use this mechanism as a computer for the convolution integral, first plot the system response to a unit impulse. Then plot the input forcing function on a reversed time base. The convolution

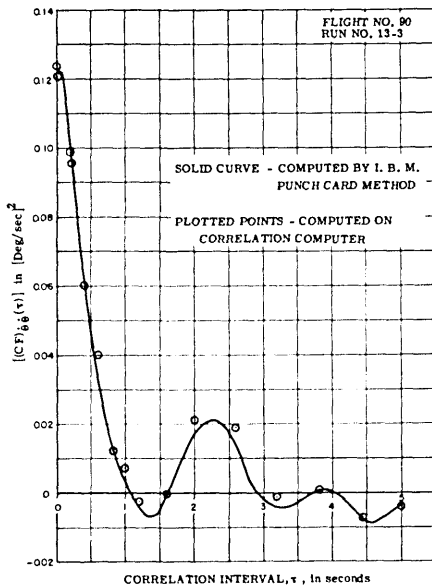


FIG. VII-6 COMPARISON OF CORRELATION FUNCTIONS OBTAINED BY I. B. M. AND CORRELATION COMPUTER REDUCTION

integral can then be obtained by tracking these two curves for a given convolution interval.

This machine was designed primarily to meet an existing need. That is, a method of correlating 4000 feet of data already recorded on oscillograph paper. However, it is not felt that this machine, as set up, is the optimum solution. Instead, it is believed that a faster and more accurate computer can be designed to correlate data recorded on a magnetic tape. In this case, the correlation interval can be established by using split pickups which can be displaced along the tape with respect to each other. In order to use this scheme, however, it will be necessary to utilize a carrier frequency and demodulate the output from the pickup heads before integrating. If this is not done, there will be only a limited number of points along the tape where the pickups can stop and still keep the carrier frequency between the two pickup signals in phase.

Appendix VIII

BIBLIOGRAPHY

1. Wiener, Norbert, "The Extrapolation, Interpolation and Smoothing of Stationary Time Series with Engineering Applications," John Wiley & Sons, Inc., New York, 1949.
2. Wiener, Norbert, "Generalized Harmonic Analysis," *Acta Mathematica*, Vol. 55, 1930, p. 273.
3. Muzzy, C.L., "Dynamic Response of a B-25J Airplane to Pulse Shape Elevator Disturbances," Instrumentation Laboratory, Massachusetts Institute of Technology, Engineering Memorandum No. 6445-E-27, July 1949.
4. Bain, J.B., Michailis, F.H., and Wootton, J.C., "Investigation of Aircraft Lateral Motion Performance Function by Pulse Technique," Thesis for M.S., M.I.T., 1949.
5. Campbell, G.F., "Dynamic Lateral Stability Flight Tests of a B-25J Airplane by the Forced Oscillation Method," Cornell Aeronautical Laboratory Report No. TB-405-F-7, 1947.
6. James, Nichols and Phillips, "Theory of Servomechanisms," Vol. 25, Massachusetts Institute of Technology, Radiation Laboratory Series, McGraw-Hill Book Company, Inc., New York, 1947.
7. Clementson, G.C., "Investigation of the Response of an Aircraft to a Finite Pulse Input," Thesis for M.S., 1948.
8. Seamans, R.C., Jr., Blasingame, B.P., and Clementson, G.C., "The Pulse Method for the Determination of Aircraft Dynamic Performance," *Journal of the Institute of Aeronautical Science*, Vol. 17, No. 1, Jan. 1950.
9. Loh, Yuan-Chiu, "Design of Linear Systems for Minimum Mean Integral Square Error," Thesis for Sc.D., 1949.
10. Bubb, F.W., "Theory of Best Automatic Control Systems for Predicting and Smoothing," Technical Report No. WURF-MGE-26, Washington University Research Foundation, 1948.
11. Durand, W.F., "Aerodynamic Theory," Vol. V, Div. N, Durand Reprinting Committee, C.I.T., Calif., 1943.
12. Gardner, M.F., and Barnes, J.L., "Transients in Linear Systems, Vol. 1," John Wiley & Sons, Inc., New York, 1945.

13. Bass, J., "Les methodes modernes du calcul des probabilities et leur appli-
cation au probleme de la turbulence," Rapport Technique No. 28, Groupement
pour le development des recherches aeronautiques, Paris, 1946.
14. Kenrick, G.W., "The Analysis of Irregular Motions with Applications to the
Energy Frequency Spectrum of Static and Telegraph Signals," Phil. Mag.,
Ser. 7, Vol. 7, pgs. 176-196, January 1929.
15. Alan E. Treloar, 1. "An Outline of Biometric Analysis" (1935), 2. "Random
Sampling Distribution" (1940), Burgess Pub. Co., Minneapolis, Minn.
16. Palmer O. Johnson, "Statistical Methods in Research," Prentice-Hall, New
York, 1949.
17. Dr. T. Koopmans, "Linear Regression Analysis of Economic Time Series,"
Haarlem-De Erven F. Bohm, N.V., 1937.
18. Tippett, L.H.C., M.Sc. (Lond.), "The Methods of Statistics," Williams and
Norgats, Ltd., Great Russell Street.
19. Kendall, M.G., "Contributions to the Study of Oscillatory Times-Series",
Cambridge Univ. Press (1946).
20. Davis, Harold T., "The Analysis of Economic Time Series," The Principia
Press Inc., Bloomington, Ind., 1941.
21. Treloar, Alan E., "Elements of Statistical Reasoning," John Wiley & Sons,
Inc., 1939.
22. Lee, Y.W., Lecture Notes of "Optimum Linear Systems," Presented by Prof.
Lee in the Department of Electrical Engineering, Massachusetts Institute of
Technology, 1948.
23. Rice, S.O., "Mathematical Analysis of Random Noise," Bell Telephone Tech-
nical Journal, July 1944 and January 1945.
24. Donely, Phillip, "Summary of Information Relating to Gust Loads on Air-
planes," N.A.C.A. Tech. Note, 1976, dated Nov. 1949.
25. Draper, C.S., "Generalized Concepts and Self-Defining Symbols for the De-
sign and Specification of Instrument Systems," Instrumentation Laboratory,
M.I.T., Cambridge, Mass., September 1949.
26. Lee, Y.W., and Stutt, C.A., "Statistical Prediction of Noise," Technical Re-
port No. 129, Research Laboratory of Electronics, Massachusetts Institute of
Technology, July 12, 1949.
27. Leipnitz, R.B., "Distribution of the Serial Correlation Coefficient in a Cir-
cularly Correlated Universe," The Annals of Math. Statistics, Vol. XVII
(1947) pp 80-87.
28. Anderson, R.L., "Distribution of the Serial Correlation Coefficient," The
Annals of Math. Statistics, Vol. XIII, (1942) pp 1-13.

Appendix IX

GLOSSARY

The system of notation used in this thesis was developed by Dr. C. S. Draper⁽²⁵⁾. However, in the development of the airplane performance functions it was felt that the standard N. A. C. A. notation was so firmly fixed in the aeronautical field that it would not be desirable to attempt to transcribe it.

The underlying philosophy of the Draper notation is to provide a set of symbols which in themselves will be a mnemonic tool which will define itself as well as designate its application.

SYMBOL	DEFINITION
$[(CF)_{qq}(0)]$	Mean power of a real function of time and is obtained as the average value of the function squared.
$[(CF)_{qq}(\tau)]_{\infty}$	Correlation function for an infinite continuous function of time.
$[(CF)_{x_i x_{i+n}}(n)]_{\infty}$	Correlation function for an infinite discrete time series.
C. G.	Center of gravity of the airplane.
$(CT)_{(osc)}$	Characteristic time of an oscillatory function.
(DR)	Damping ratio. The ratio of actual damping to the critical damping of a damped sinusoidal oscillation.
$(FF)_{()}[q_{in}q_{out}]$	$\frac{(PF)_{()}[q_{in}q_{out}]}{(S)_{()}[q_{in}q_{out}]}$
[FSC][q(t)]	Fourier series coefficient of a real function of time, q(t).
[FT(ω)][q(t)]	Fourier transform as a continuous function of the angular frequency, ω , of a real function of time.

$\overline{[FT(\omega)][q(t)]}$	Complex conjugate of the Fourier transform of a real function of time.
$I()$	Value of a designated definite integral.
I_{yy}	Moment of inertia of the airplane about its y axis.
j	$\sqrt{-1}$
$[(KC)_{xy}]_N$	Correlation coefficient between two samples of N variates.
n	Real integral number.
$(PA)_{(osc)}$	Phase angle of a damped sinusoidal oscillation.
$(PF)() [q_{in}q_{out}]$	Performance function of a designated system for the designated input and output. The function is equal to the Fourier transform of the Unit Impulse Response, $[(UIR)(t)]$ of the system.
$[(PSD)_q(\omega)]$	Power spectral density of a real function of time, $q(t)$. Most easily obtained as the Fourier transform of the correlation function of $q(t)$.
$q() (t)$	Real function of time which may be designated further by proper choice of subscript in place of the open parentheses.
$Re[]$	Real part of the complex function of the variable ω in the brackets.
$[RMS(q)]$	Root-mean-square value of a real function of time. It is equal to the square root of the mean power.
(RT)	Response time of a given dynamic system. Defined as the time required for the response to decrease to and remain less than 5% of its maximum output magnitude.
s	Dummy variable of integration with respect to time.
$[(SKC)_{x_i x_{i+n}}(n)]_N$	Serial correlation coefficient of a finite time series of total number N lagged by the interval of n variates.
$(S)() [q_{in}q_{out}]$	$\lim_{\omega \rightarrow 0} \left\{ (PF)() [q_{in}q_{out}] \right\}$
t	Newtonian time variable. In this report the units are in seconds.

T_1	Period of the fundamental frequency in a Fourier series expansion of a real function of time, $q(t)$.
$T_{(cor)}$	Time interval of significant correlation.
$[UIR_{()}(t - \tau)]$	Unit Impulse Response of a designated dynamic system delayed in time by the interval, τ . A unit impulse is defined as a delta function of unit area.
v	Airplane velocity response along Y axis.
V_A	True velocity of the airplane in feet per second.
w	Airplane velocity response along Z axis.
w_{A-I}	Vertical velocity component of a turbulent air mass with respect to inertial space.
$\frac{\partial w_{A-I}}{\partial y}$	Rate of change spanwise of the vertical velocity of a turbulent air mass with respect to inertial space.
$\delta ()$	Control angular deflection. Parentheses to be replaced by designated control. In Appendix III, only, this symbol is used to represent a delta function.
θ	Airplane rate of pitch response.
σ	Dummy variable of integration with respect to time.
ν	Dummy variable of integration with respect to time.
τ	Newtonian time interval.
$\dot{\phi}$	Airplane rate of roll response.
$\dot{\psi}$	Airplane rate of yaw response.
ω	Angular frequency in radians per second.
ω_n	Undamped natural frequency of a damped sinusoidal oscillation.
$\underline{\underline{\Delta}}$	Equal by definition.
∞	Symbol for a number which is allowed to increase without bound.

Appendix X
BIOGRAPHICAL SKETCH

Gerhardt Christopher Clementson was born in Blackearth, Wisconsin, on May 3, 1917. Shortly thereafter, his parents moved to Minneapolis, Minnesota, where he obtained his primary schooling. He was graduated from South High School in January of 1937.

In May of 1937, he enlisted in the 3rd Infantry, then stationed at Fort Snelling, Minnesota, and won a competitive assignment to the 7th Corps Area West Point Preparatory School. In March of 1938, he was appointed a cadet at the United States Military Academy, West Point, New York, by Congressman Henry G. Tiegen of the Minnesota 5th Congressional District as a result of his standing on a civil service competitive examination. He was graduated from the United States Military Academy with a degree of B.S. in May, 1942. After graduation, he was assigned to pilot flying training in the West Coast Training Command. On receiving his wings, he was assigned to the 4th Air Force as a trainee and later as an instructor pilot in the P-38 type aircraft.

In June of 1944, he was assigned to a refresher course at the U.S.A.F. Engineering School at Wright Field, and after completion was assigned to the California Institute of Technology to complete a course of study in compressibility effects in aerodynamics. He was elected to Sigma Xi, and awarded the degree of M.S. in June 1945. He was then assigned as a flight test pilot and engineer to the Flight Research Section of the Flight Test Division at Wright Field, Dayton, Ohio, where he specialized in stability and control flight testing.

In June of 1947, he applied for and was assigned to a course of study in Fire Control Instrumentation in the Aeronautical Department of the Massachusetts Institute of Technology where, in September of 1948, he was awarded the degree of Master of Science in Aeronautical Engineering. He then was granted a two-year extension of his tour of duty to complete a course of study leading to the degree of Doctor of Science in Instrumentation.

He is co-author of a paper published in The Journal of the Aeronautical Sciences Vol. 17, January, 1950, entitled "The Pulse Method for the Determination of Aircraft Dynamic Performance."

FLIGHT TEST SUPPLEMENT

The entire set of airplane response to turbulent air oscillograph records are published in this supplement in order that this data may be preserved in a form which might be useful to future investigators in this field.

FLIGHT NO. 85

DATE: 15 August 1949

Duration: 1:75 hours

AIRPLANE: B-25J No. 44-30328

CREW:

Pilot: C. Collins

Co-pilot: G. C. Clementson

Instr. T.O.: F. Smith

PURPOSE OF FLIGHT:

1. Instrument shakedown
2. Rough air data

AIRPLANE CONFIGURATION:

Gross Weight - 26,100 lb.

C. G. Percent MAC - 26.1

INSTRUMENTATION: Instrumentation installed for measuring normal acceleration, lateral acceleration, rate of pitch and rate of roll response to turbulent air. Stops installed for keeping controls (aileron, rudder and elevator) fixed on the trim condition of 175 m. p. h. I. A. S.

METEOROLOGICAL CONDITIONS: Unstable air mass, scattered towering cumulus.

FLIGHT PROCEDURE:

1. Airplane trimmed at 175 m.p.h. at 9,000 ft. P.A.
2. Controls stops adjusted to trim control positions.
3. Controls held fixed against stops and sensitivities adjusted on oscillograph.

4. Static calibration of oscillograph by master pickoff.
5. Rough air response measured at trim conditions.
6. Re-calibration of oscillograph.

RESULTS AND COMMENTS:

Noise level on oscillograph records excessive. Appears to be primarily engine and prop vibrations. Data can be used by smoothing obvious noise roughness.

FLIGHT NO. 86

DATE: 21 August 1949

DURATION: 1:5 hours

AIRPLANE B-25-J No. 44-30328

CREW:

Pilot: C. O. Bostrom

Co-pilot: G. C. Clementson

Instr. T.O.: F. Smith

PURPOSE OF FLIGHT:

1. Test of modified instrumentation vibration mounts.
2. Rough air data

AIRPLANE CONFIGURATION:

Gross Weight - 26,100 lb.

C. G. Percent M.A.C. - 26.1

INSTRUMENTATION: Same as No. 85

METEOROLOGICAL CONDITIONS: Hot Summer day, towering cumulus, thermal heating.

FLIGHT PROCEDURE: Same as No. 85

RESULTS: Normal accelerometer malfunctioned. Vibration mounts unsatisfactory. Will try complete removal of mounts and rigid tie-down on next flight.

FLIGHT NO. 87

DATE: 26 August 1949 DURATION: 1:25 hours

AIRPLANE: B-25J No. 44-30328

CREW:

Pilot: C. Collins

Co-pilot: G. C. Clementson

Instr. T.O.: R. Whistler

PURPOSE OF FLIGHT:

1. Test of rigid instrument mounts.
2. Rough air data

AIRPLANE CONFIGURATION:

Gross Weight - 26,100 lb.

C. G. Percent M.A.C. - 26.1

METEOROLOGICAL CONDITIONS:

Hot summer day, ground thermals obtained by flying over water-land discontinuities from Lowell, Mass., to Newburyport, Mass.

FLIGHT PROCEDURE:

Same as No. 85

RESULTS:

Rigid mounts reduce engine and prop. noise pick-up to an acceptable level. Instrumentation is satisfactory.

FLIGHT NO. 89

DATE: 2 September 1949 DURATION: 1:15 hours

AIRPLANE: B-25J No. 44-30328

CREW:

Pilot: C. O. Bostrom

Co-pilot: G. C. Clementson

Instr. T.O.: R. Whistler

PURPOSE OF FLIGHT:

1. Rough air data

AIRPLANE CONFIGURATION:

Gross Weight - 26,100 lb.

C. G. Percent M.A.C. - 26.1

METEOROLOGICAL CONDITIONS:

Same as Flight No. 87 .

FLIGHT PROCEDURE:

Same as No. 85

RESULTS:

Satisfactory records.

FLIGHT NO. 90

DATE: 9 September 1949

DURATION: 2.0 hours

AIRPLANE: B-25J No. 44-30328

CREW:

Pilot: C. O. Bostrom

Co-pilot: G. C. Clementson

Instr. T.O.: R. Whistler

PURPOSE OF FLIGHT:

1. Rough air data

AIRPLANE CONFIGURATION:

Gross Weight - 26,100 lb.

C. G. Percent M.A.C. - 26.1

METEOROLOGICAL CONDITIONS: Cold front passage, low thunderstorms,
high ground winds.

FLIGHT PROCEDURE: Same as No. 85.

RESULTS: Satisfactory records.

FLIGHT NO. 91

DATE: 16 September 1949 **DURATION:** 2:5 hours

AIRPLANE: B-25-J No. 44-30328

CREW:

Pilot: C. O. Bostrom

Co-pilot: G. C. Clementson

Instr. T.O.: R. Whistler

PURPOSE OF FLIGHT:

1. Rough air data at two different airspeeds, 175 and 230 m.p.h.

AIRPLANE CONFIGURATION:

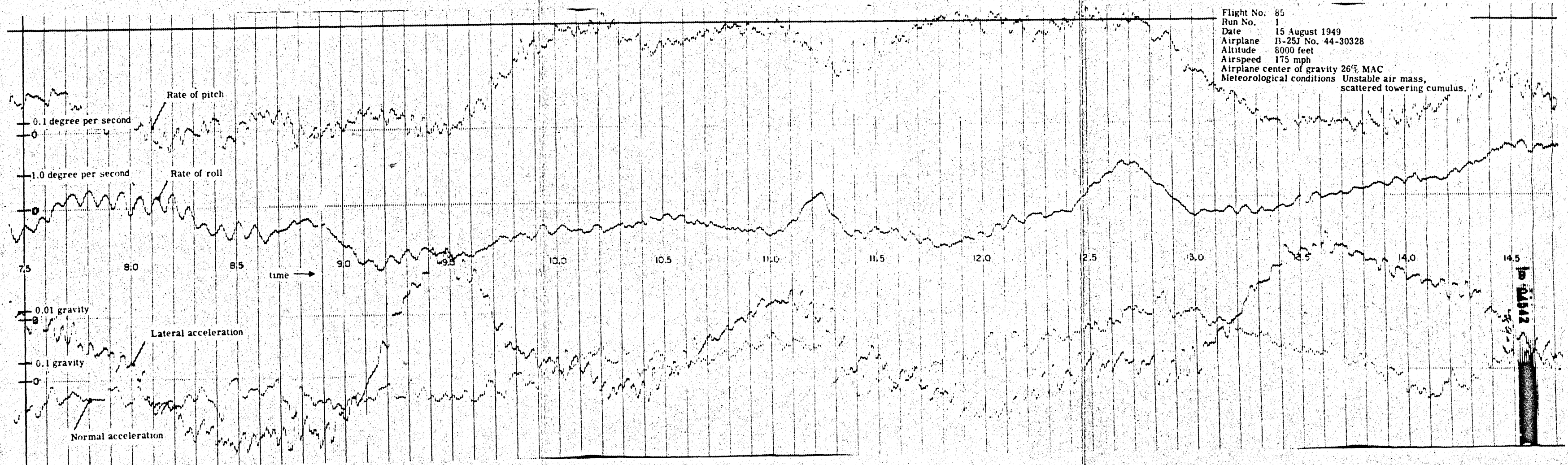
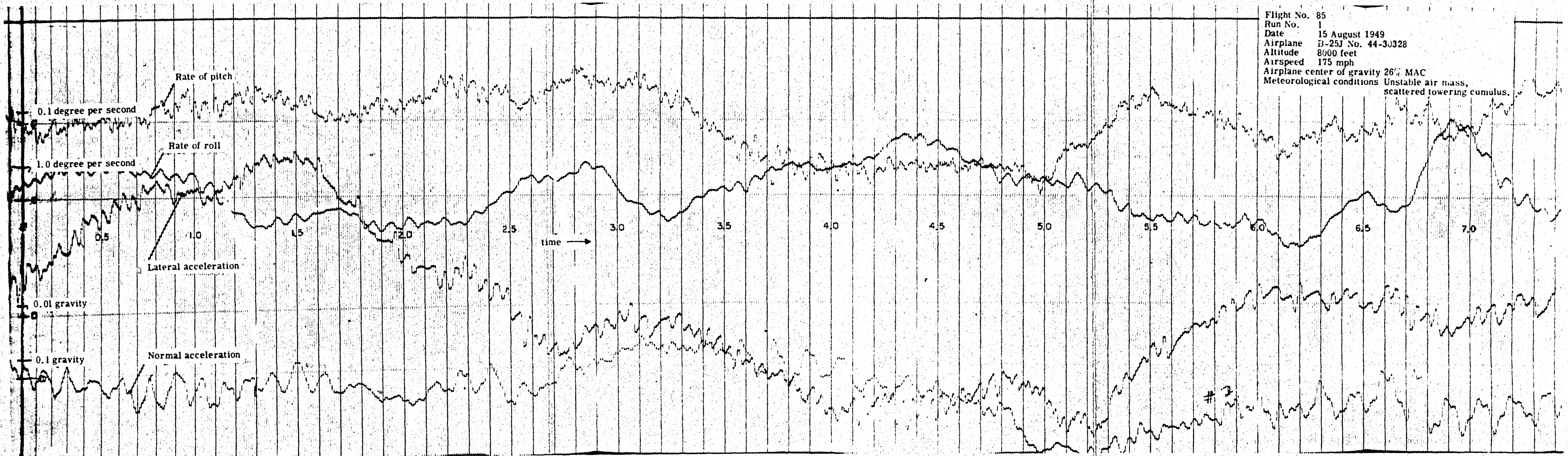
Gross Weight: 26,100 lb.

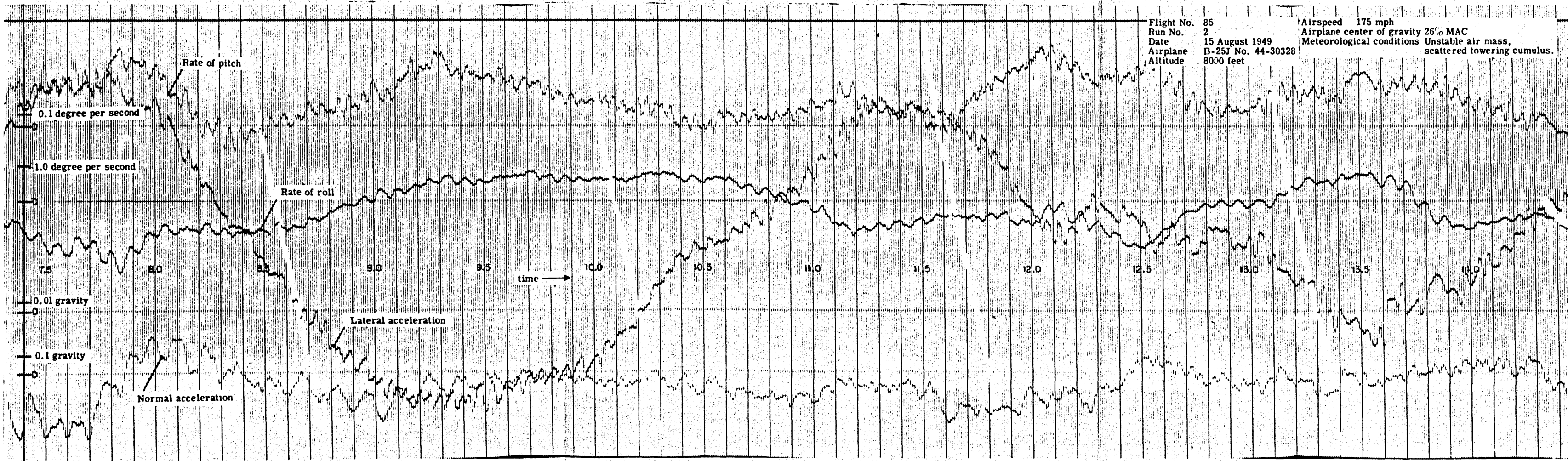
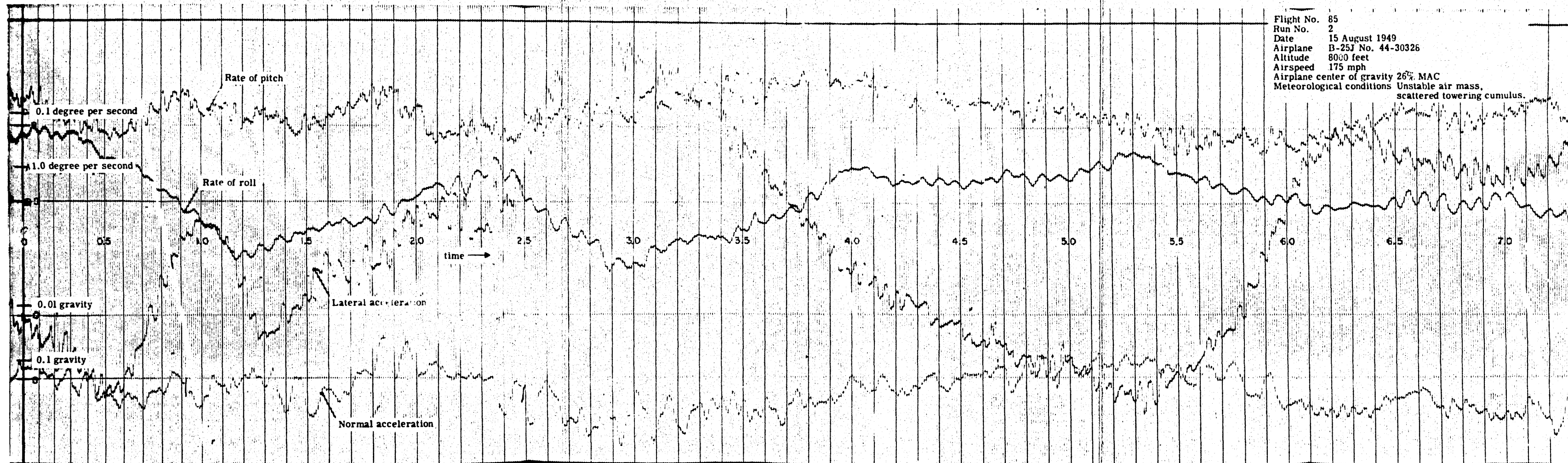
C. G. Percent M.A.C. - 26.1

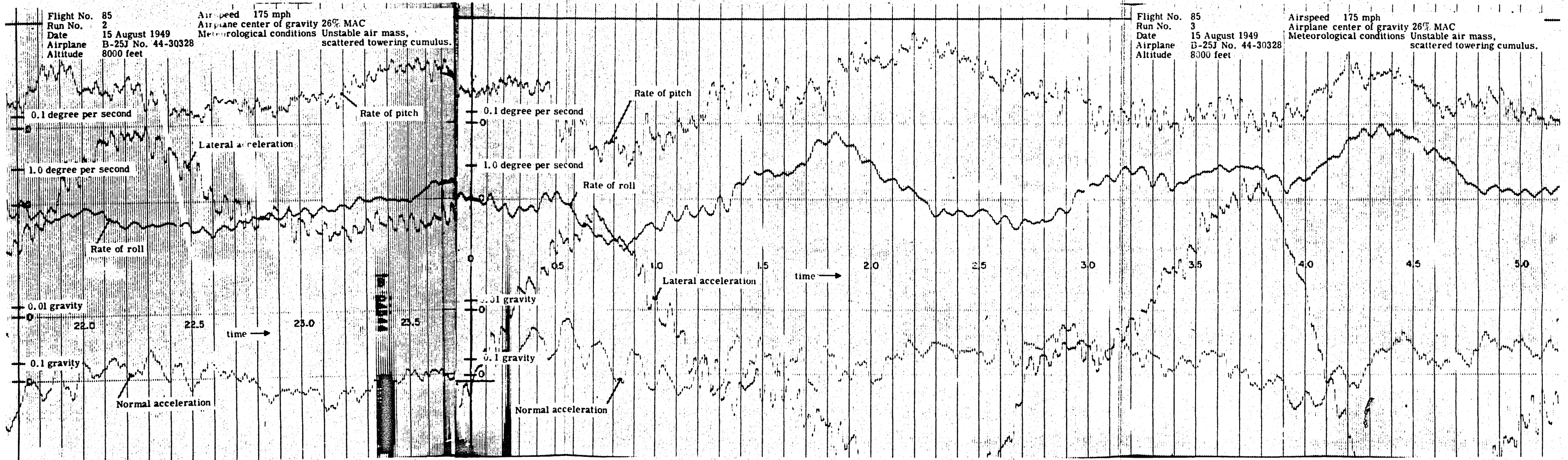
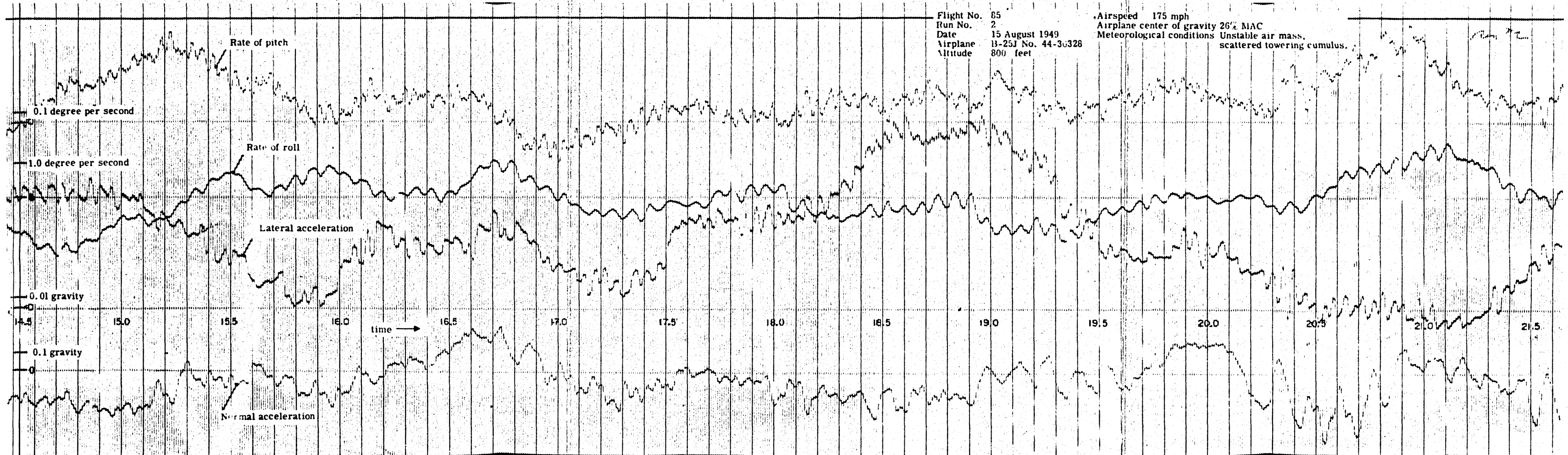
METEOROLOGICAL CONDITIONS: High ground winds, flown over mountain terrain.

FLIGHT PROCEDURE: Same as No. 85.

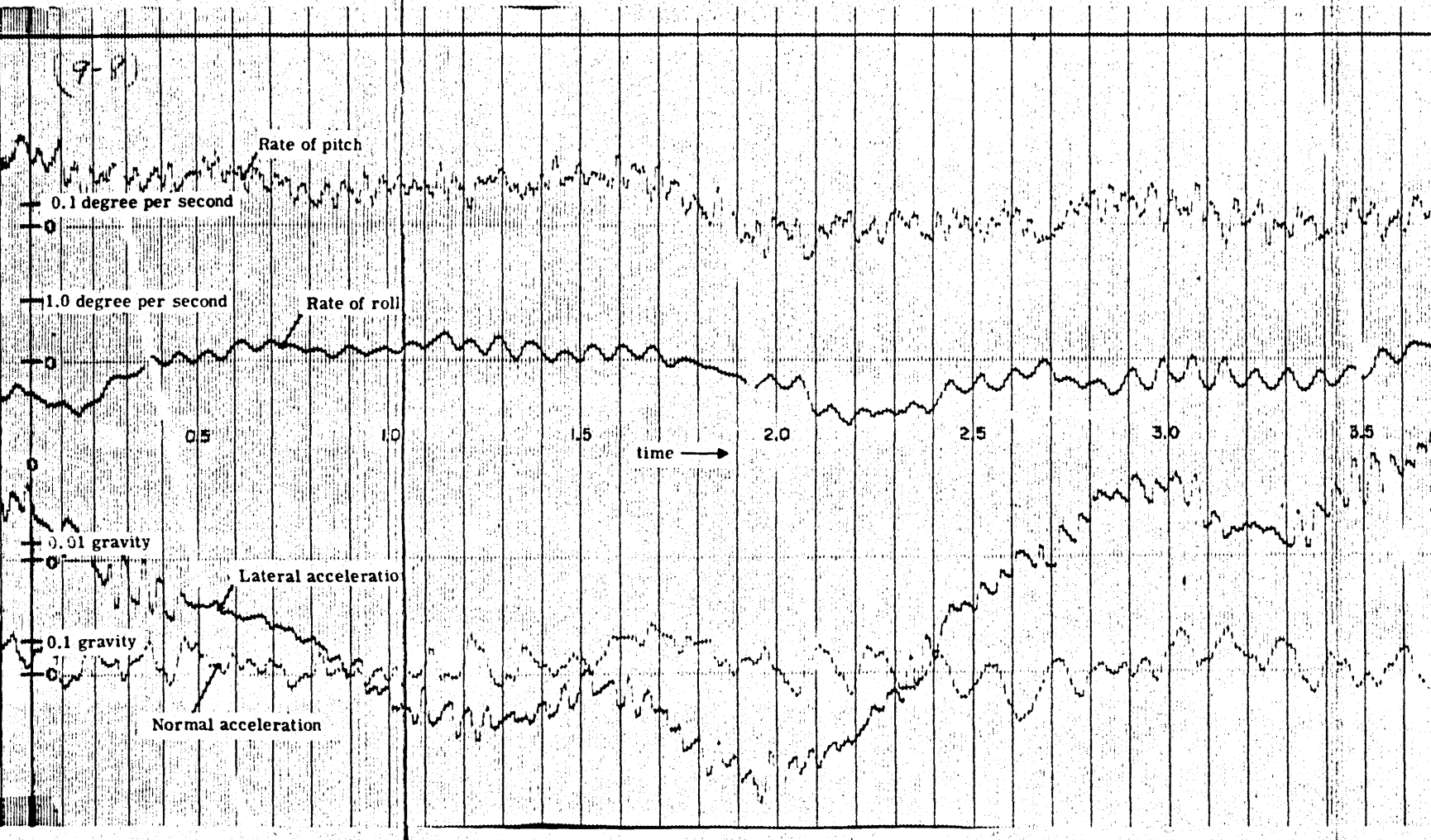
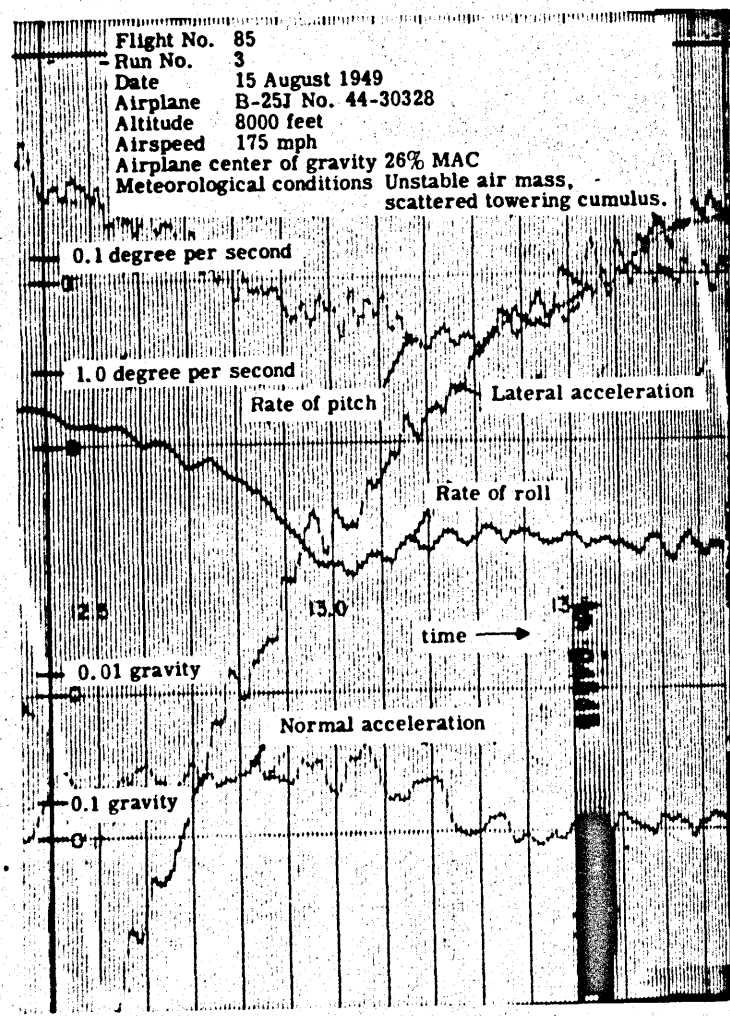
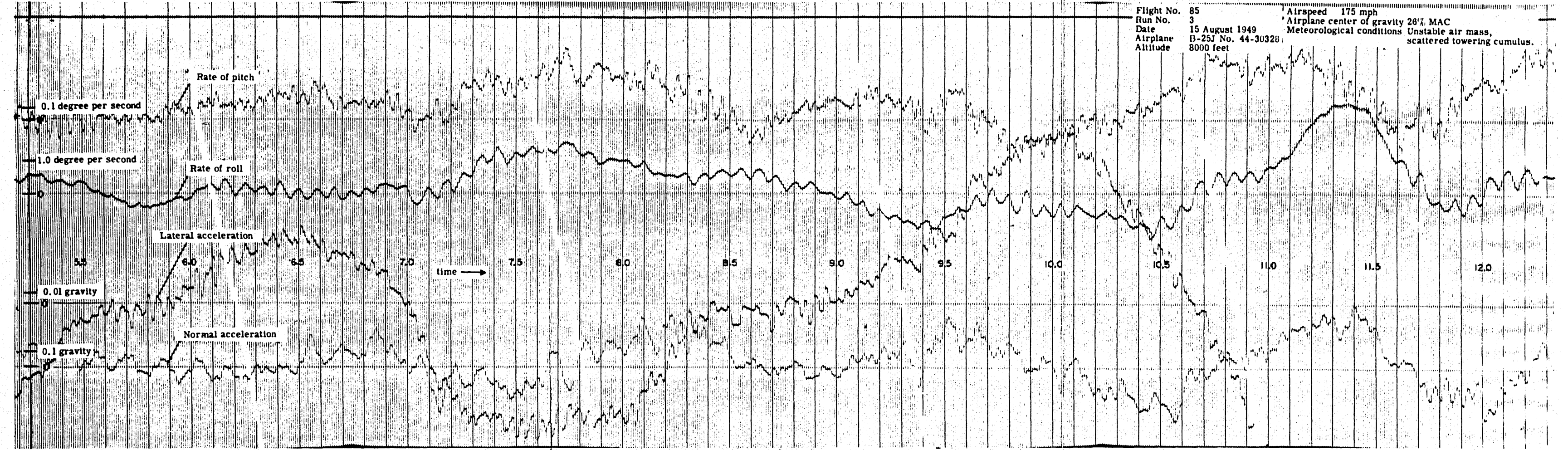
RESULTS: Satisfactory records.



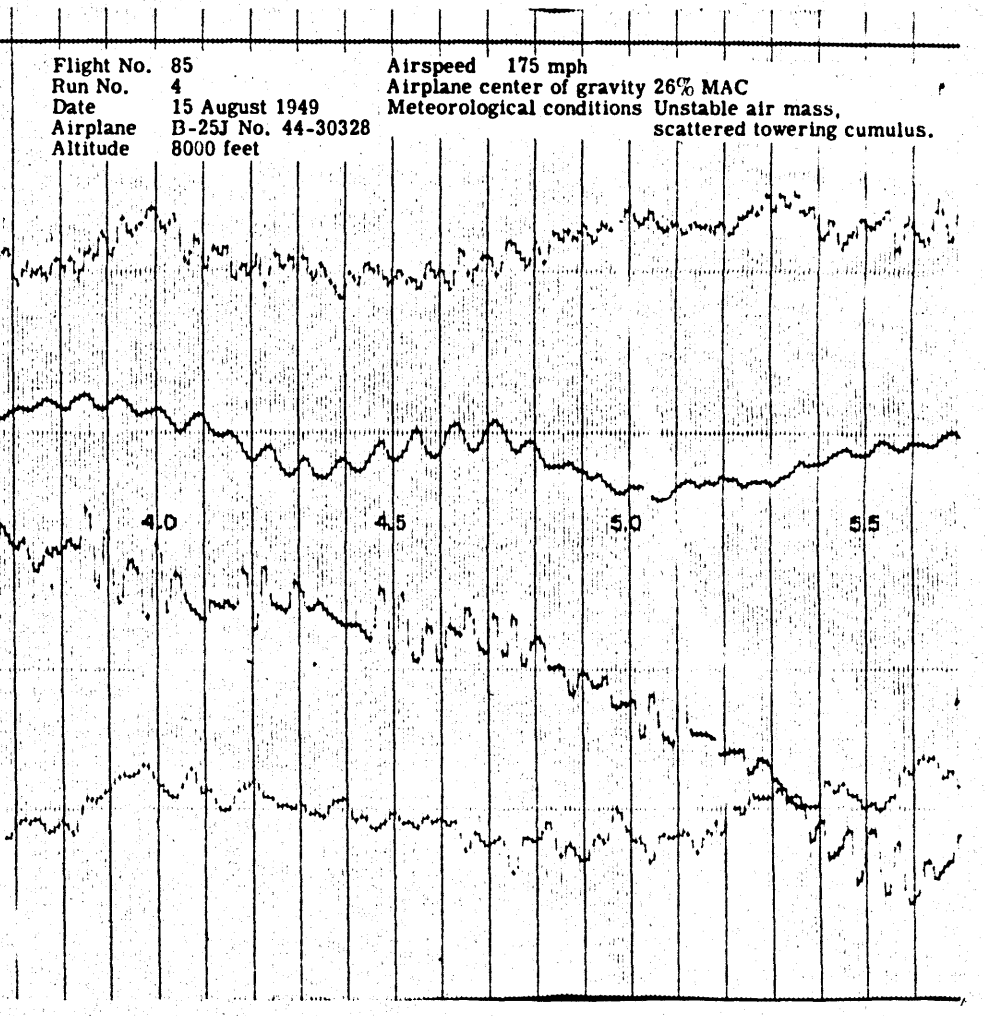




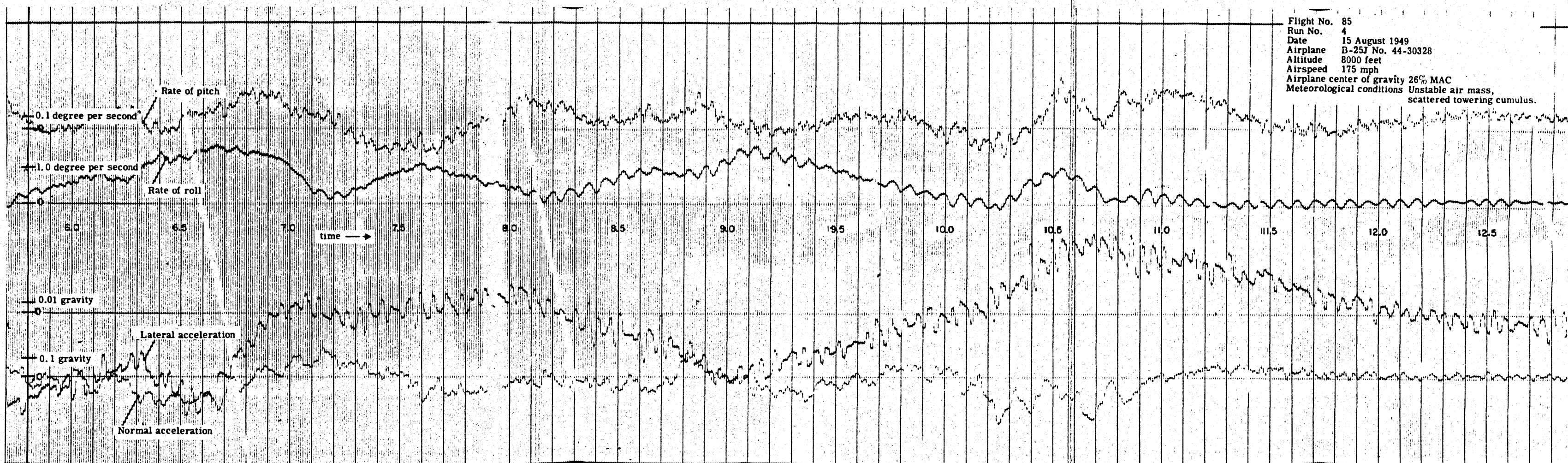
Flight No. 85
 Run No. 3
 Date 15 August 1949
 Airplane B-25J No. 44-30328
 Altitude 8000 feet
 Airspeed 175 mph
 Airplane center of gravity 26% MAC
 Meteorological conditions Unstable air mass, scattered towering cumulus.



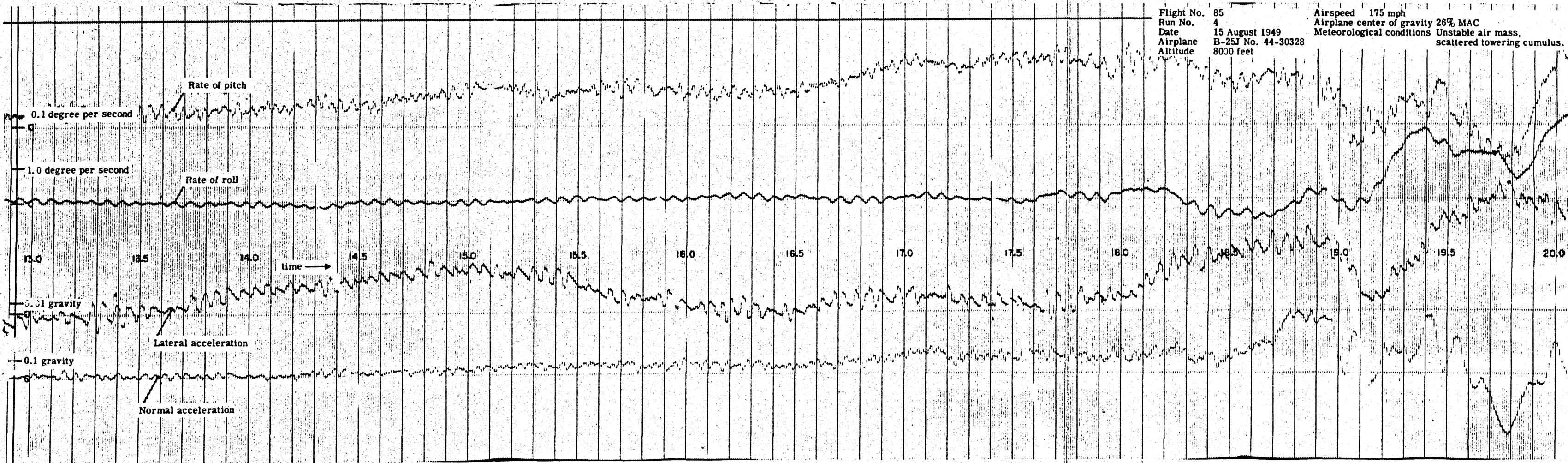
Flight No. 85
 Run No. 4
 Date 15 August 1949
 Airplane B-25J No. 44-30328
 Altitude 8000 feet
 Airspeed 175 mph
 Airplane center of gravity 26% MAC
 Meteorological conditions Unstable air mass, scattered towering cumulus.



Flight No. 85
 Run No. 4
 Date 15 August 1949
 Airplane B-25J No. 44-30328
 Altitude 8000 feet
 Airspeed 175 mph
 Airplane center of gravity 26% MAC
 Meteorological conditions Unstable air mass,
 scattered towering cumulus.

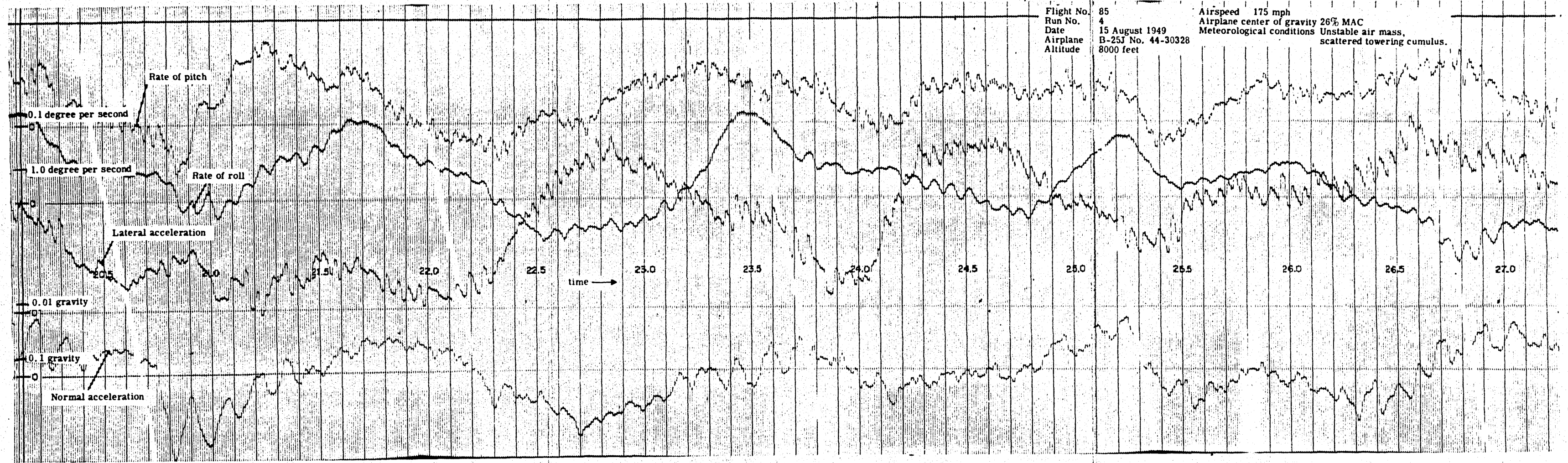


Flight No. 85
 Run No. 4
 Date 15 August 1949
 Airplane B-25J No. 44-30328
 Altitude 8000 feet
 Airspeed 175 mph
 Airplane center of gravity 26% MAC
 Meteorological conditions Unstable air mass,
 scattered towering cumulus.



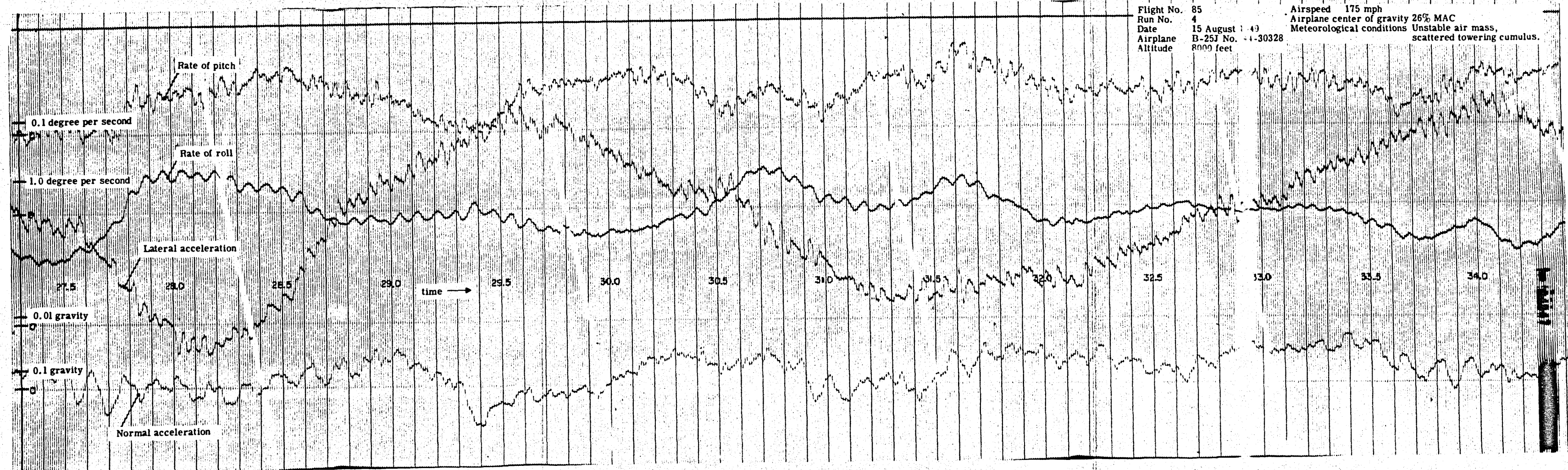
Flight No. 85
Run No. 4
Date 15 August 1949
Airplane B-25J No. 44-30328
Altitude 8000 feet

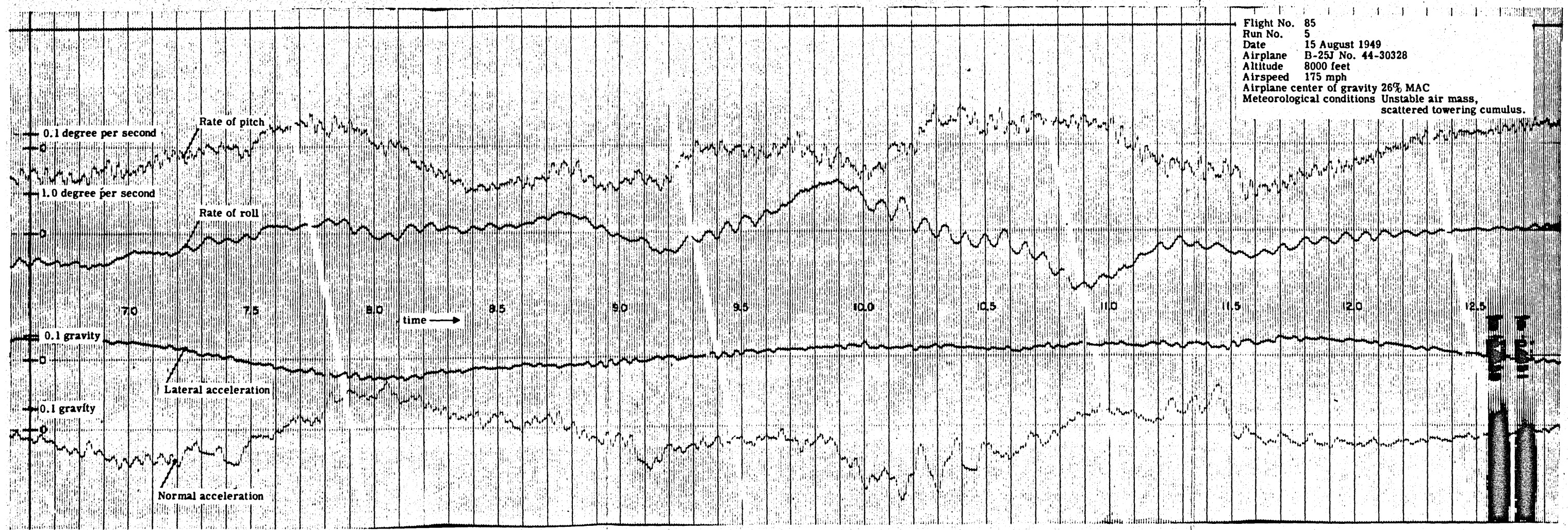
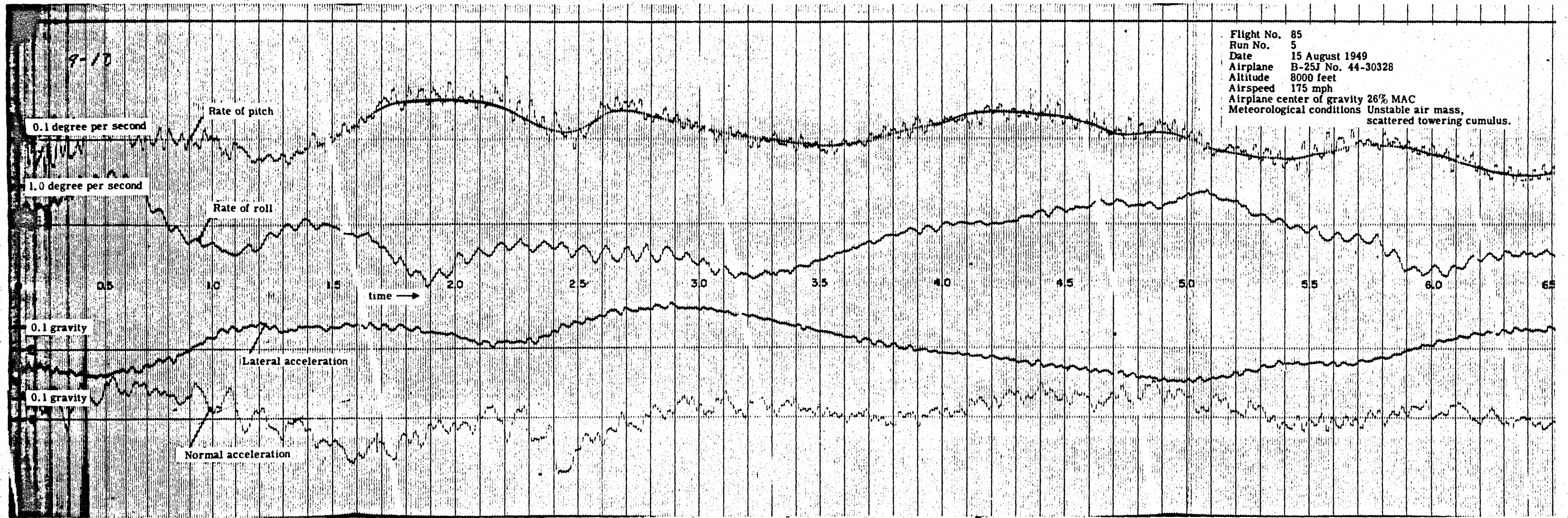
Airspeed 175 mph
Airplane center of gravity 26% MAC
Meteorological conditions Unstable air mass,
scattered towering cumulus.



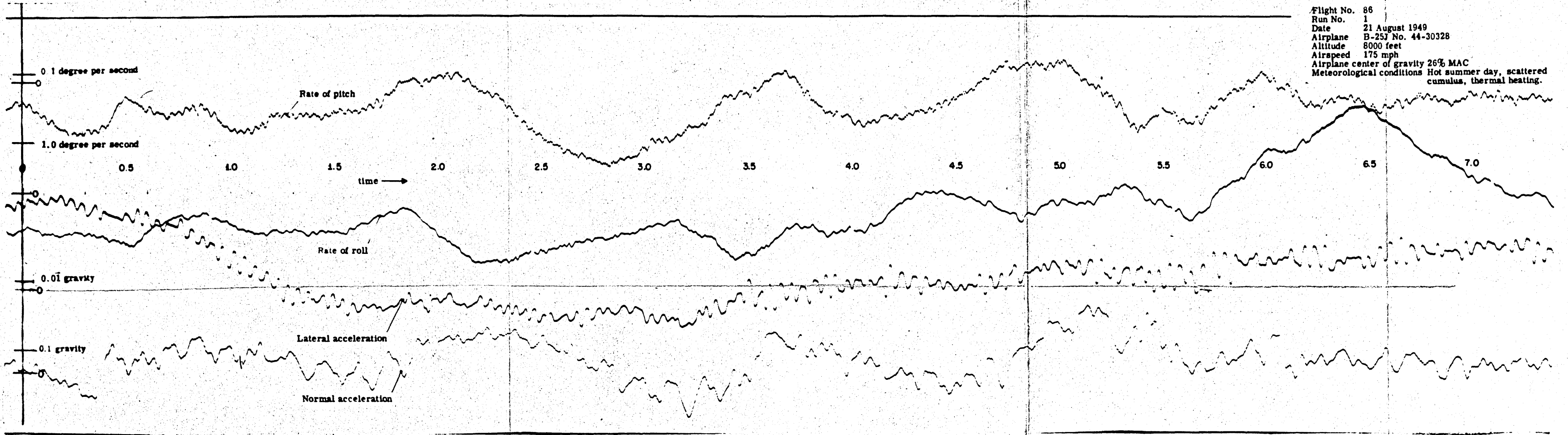
Flight No. 85
Run No. 4
Date 15 August 1949
Airplane B-25J No. 44-30328
Altitude 8000 feet

Airspeed 175 mph
Airplane center of gravity 26% MAC
Meteorological conditions Unstable air mass,
scattered towering cumulus.

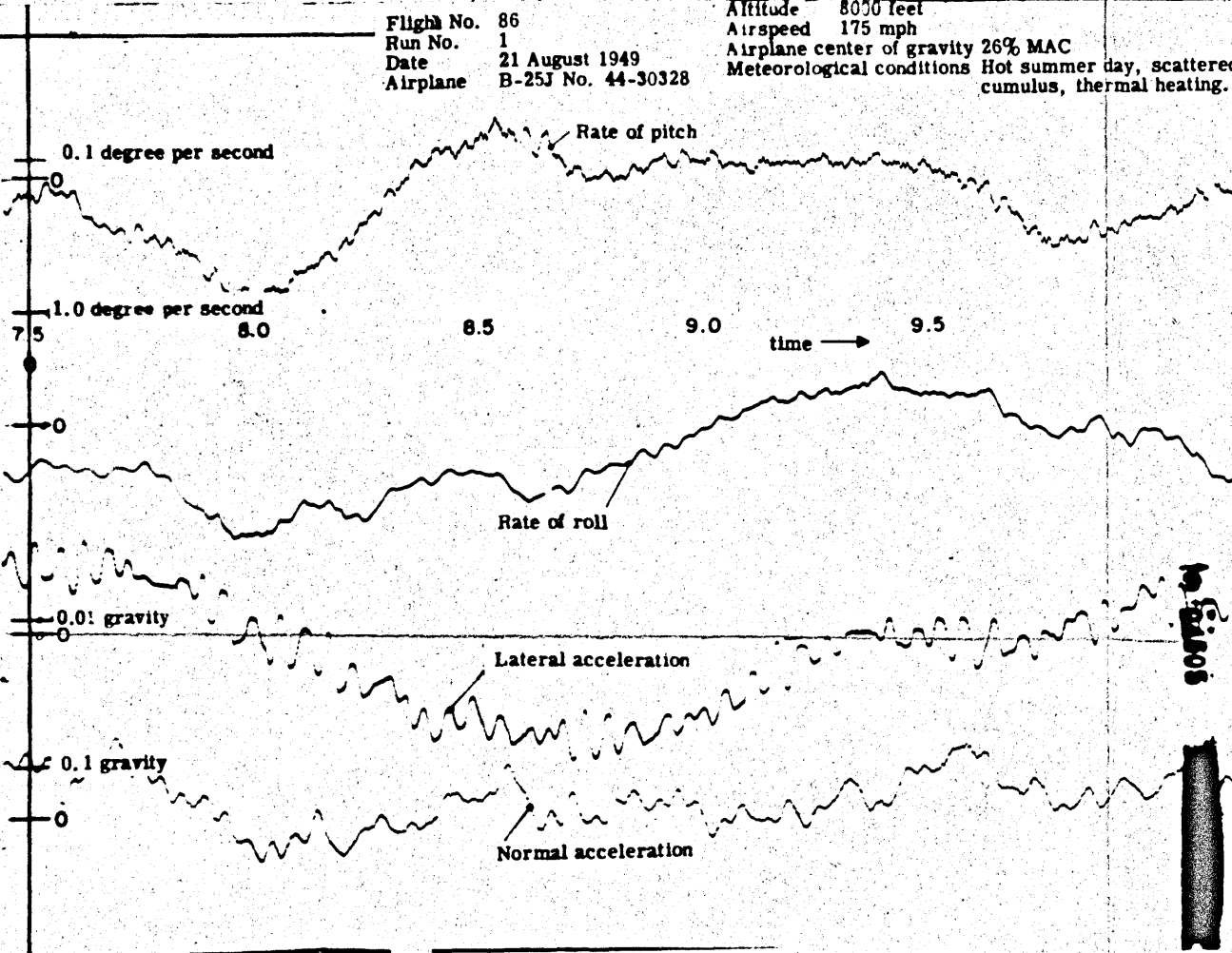




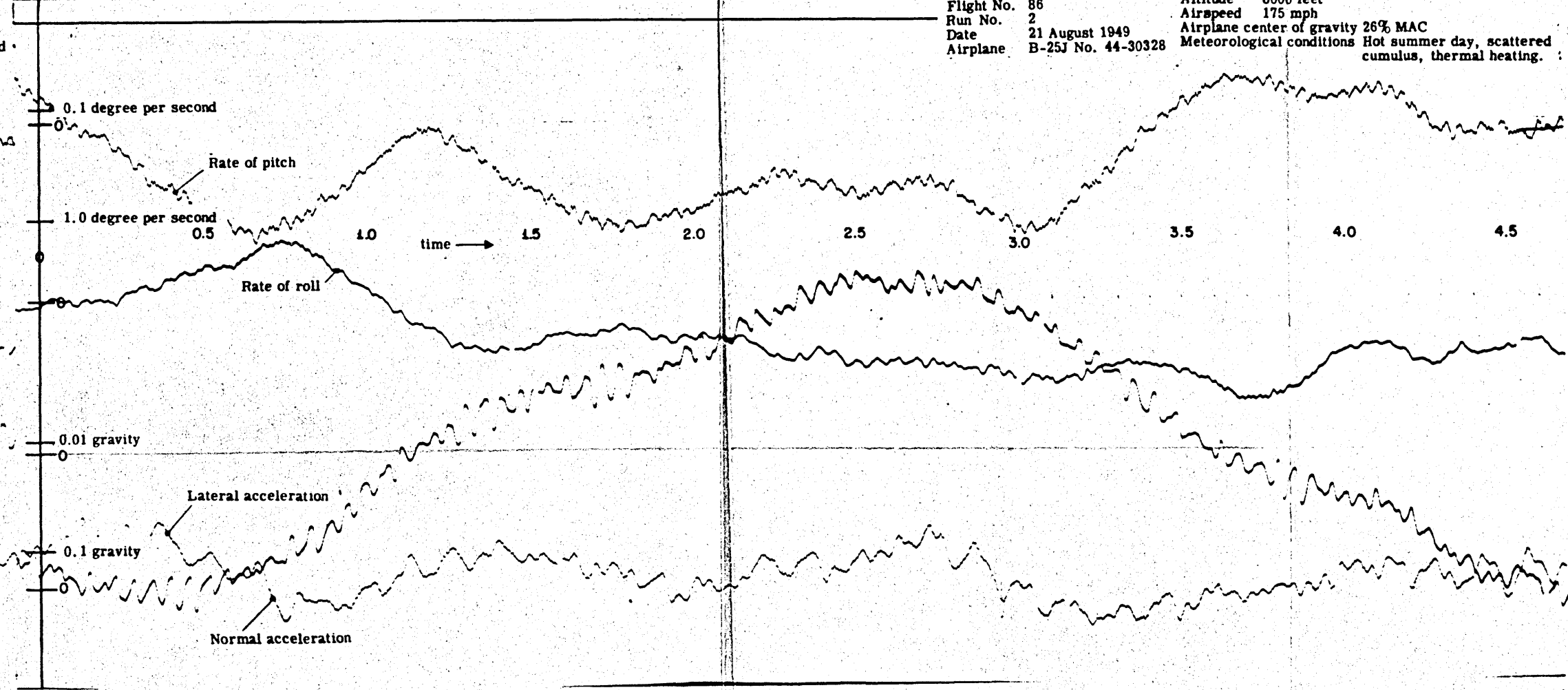
Flight No. 86
 Run No. 1
 Date 21 August 1949
 Airplane B-25J No. 44-30328
 Altitude 8000 feet
 Airspeed 175 mph
 Airplane center of gravity 26% MAC
 Meteorological conditions Hot summer day, scattered cumulus, thermal heating.



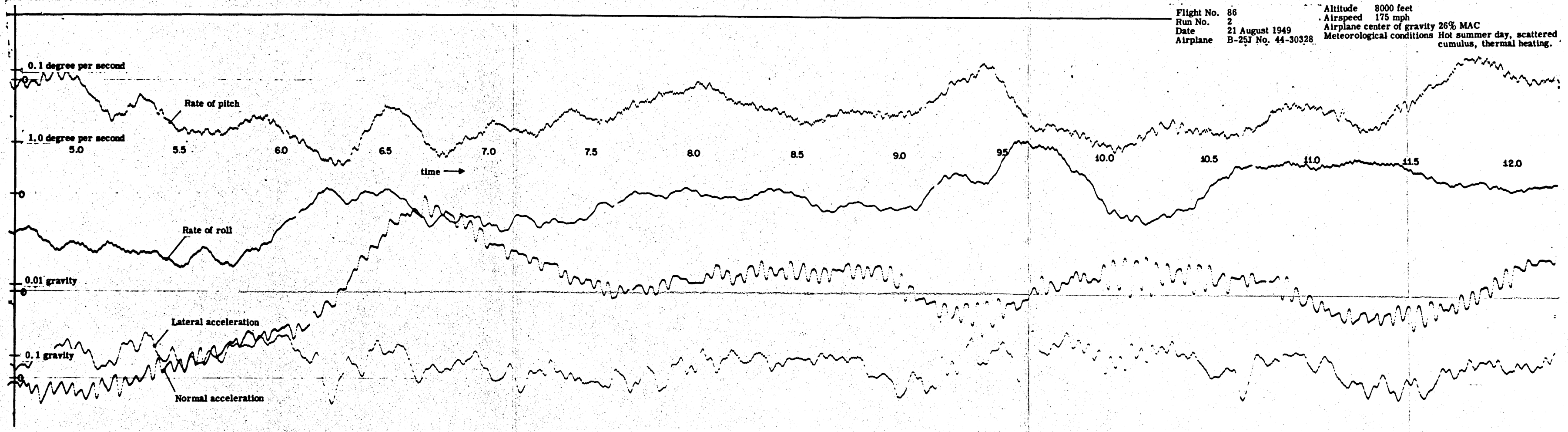
Flight No. 86
 Run No. 1
 Date 21 August 1949
 Airplane B-25J No. 44-30328
 Altitude 8000 feet
 Airspeed 175 mph
 Airplane center of gravity 26% MAC
 Meteorological conditions Hot summer day, scattered cumulus, thermal heating.



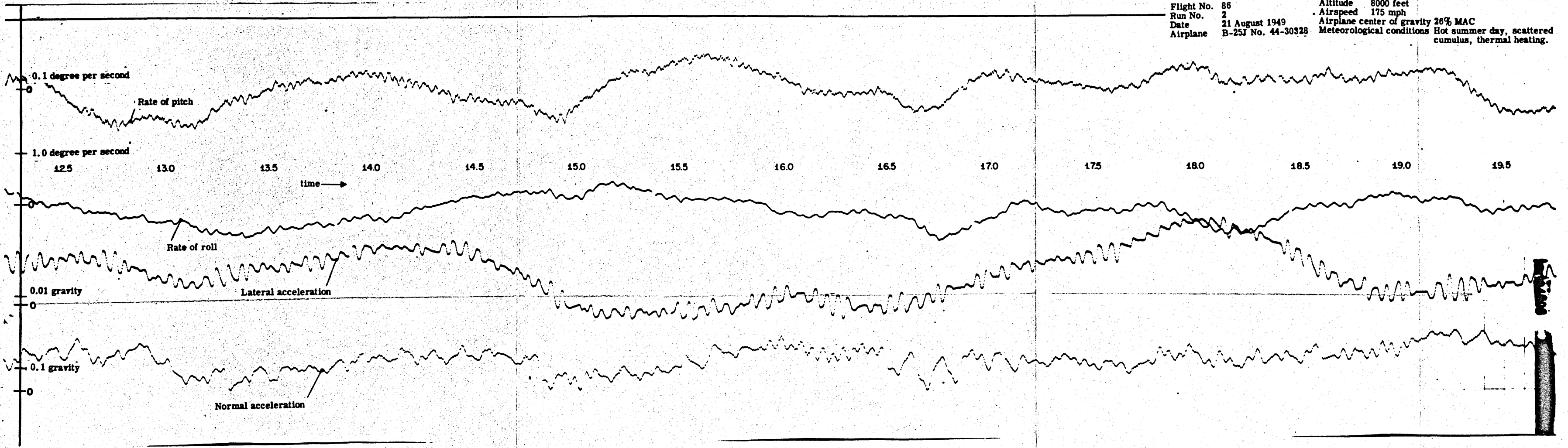
Flight No. 86
 Run No. 2
 Date 21 August 1949
 Airplane B-25J No. 44-30328
 Altitude 8000 feet
 Airspeed 175 mph
 Airplane center of gravity 26% MAC
 Meteorological conditions Hot summer day, scattered cumulus, thermal heating.

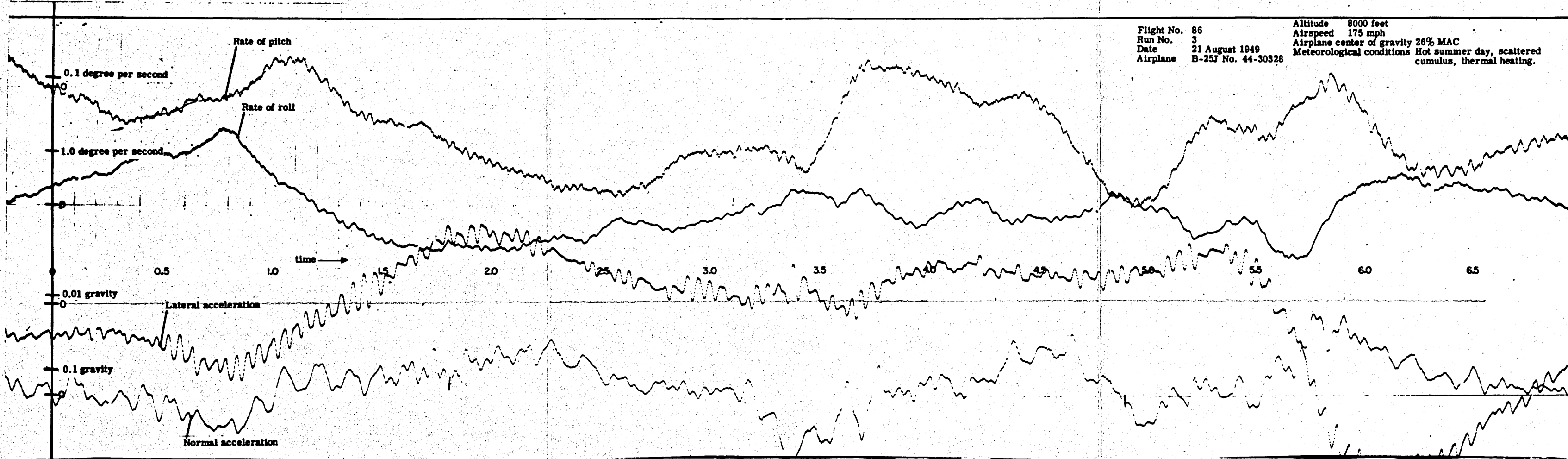


Flight No. 86 Altitude 8000 feet
 Run No. 2 Airspeed 175 mph
 Date 21 August 1949 Airplane center of gravity 26% MAC
 Airplane B-25J No. 44-30328 Meteorological conditions Hot summer day, scattered cumulus, thermal heating.



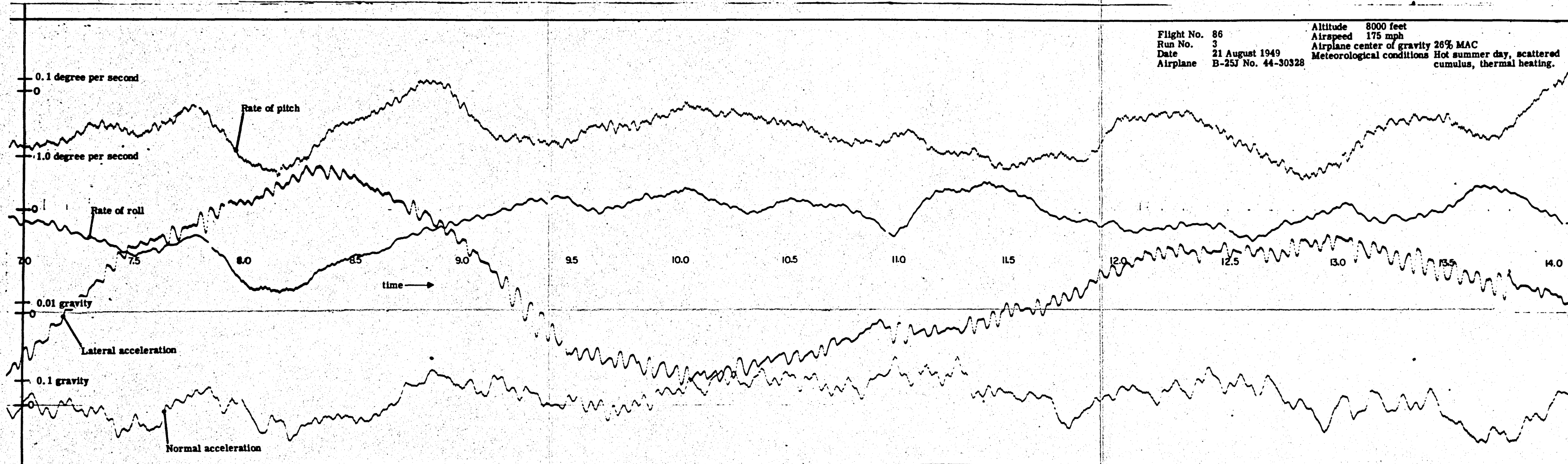
Flight No. 86 Altitude 8000 feet
 Run No. 2 Airspeed 175 mph
 Date 21 August 1949 Airplane center of gravity 26% MAC
 Airplane B-25J No. 44-30328 Meteorological conditions Hot summer day, scattered cumulus, thermal heating.





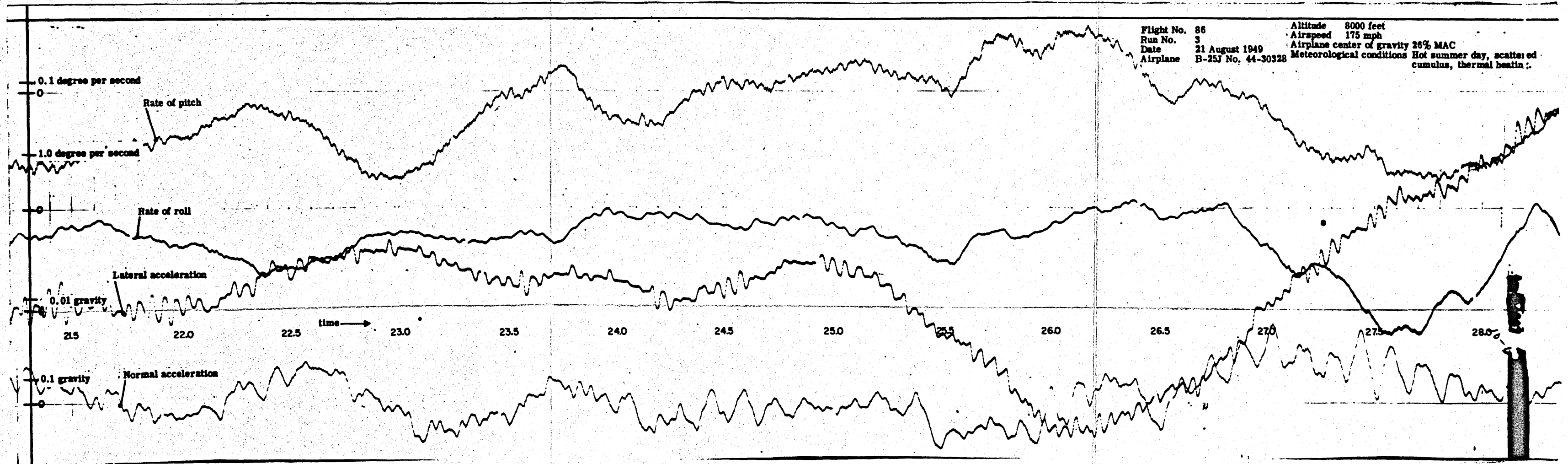
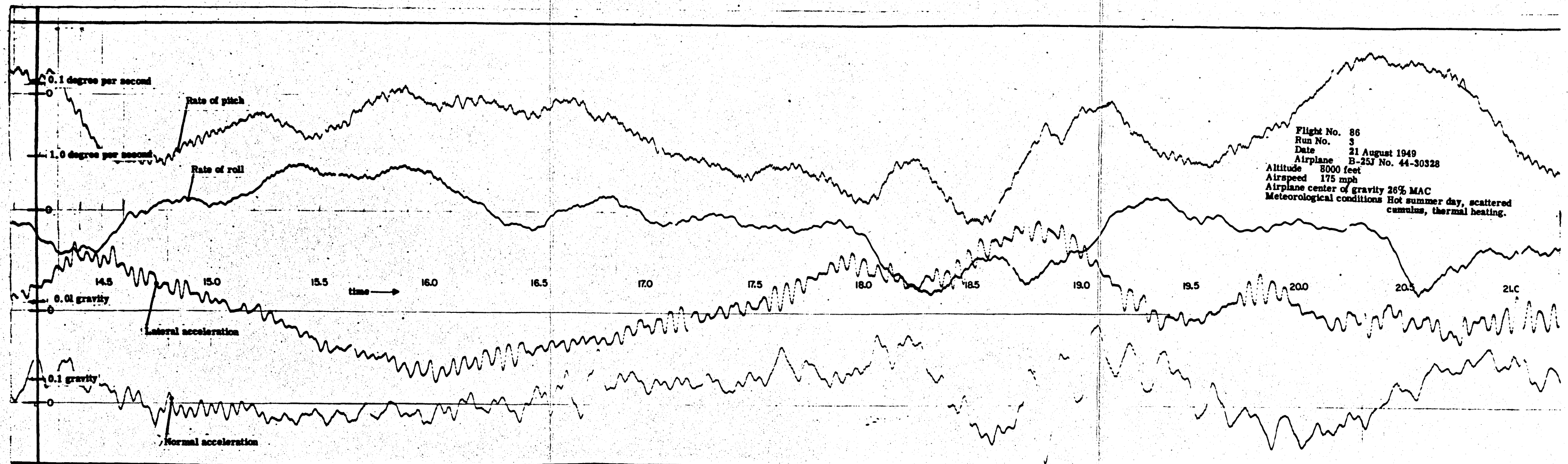
Flight No. 86
 Run No. 3
 Date 21 August 1949
 Airplane B-25J No. 44-30328

Altitude 8000 feet
 Airspeed 175 mph
 Airplane center of gravity 26% MAC
 Meteorological conditions Hot summer day, scattered cumulus, thermal heating.



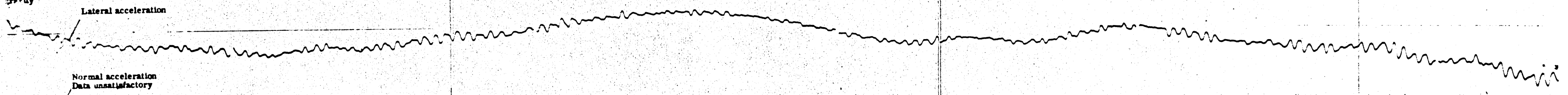
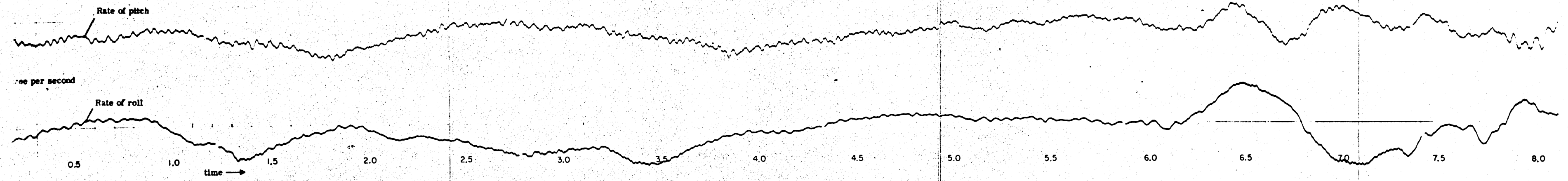
Flight No. 86
 Run No. 3
 Date 21 August 1949
 Airplane B-25J No. 44-30328

Altitude 8000 feet
 Airspeed 175 mph
 Airplane center of gravity 26% MAC
 Meteorological conditions Hot summer day, scattered cumulus, thermal heating.



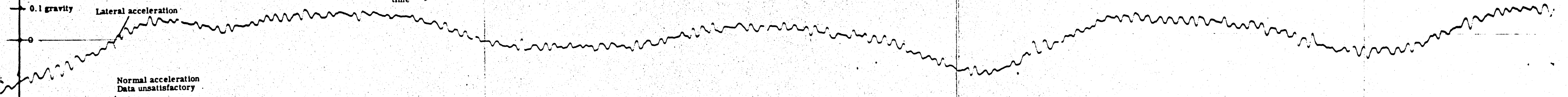
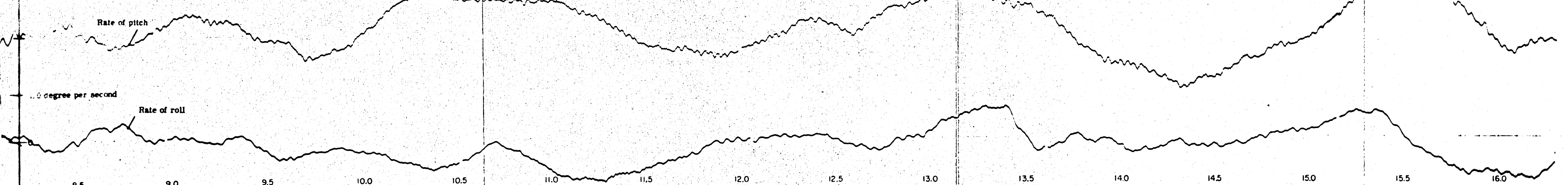
1.0 degree per second

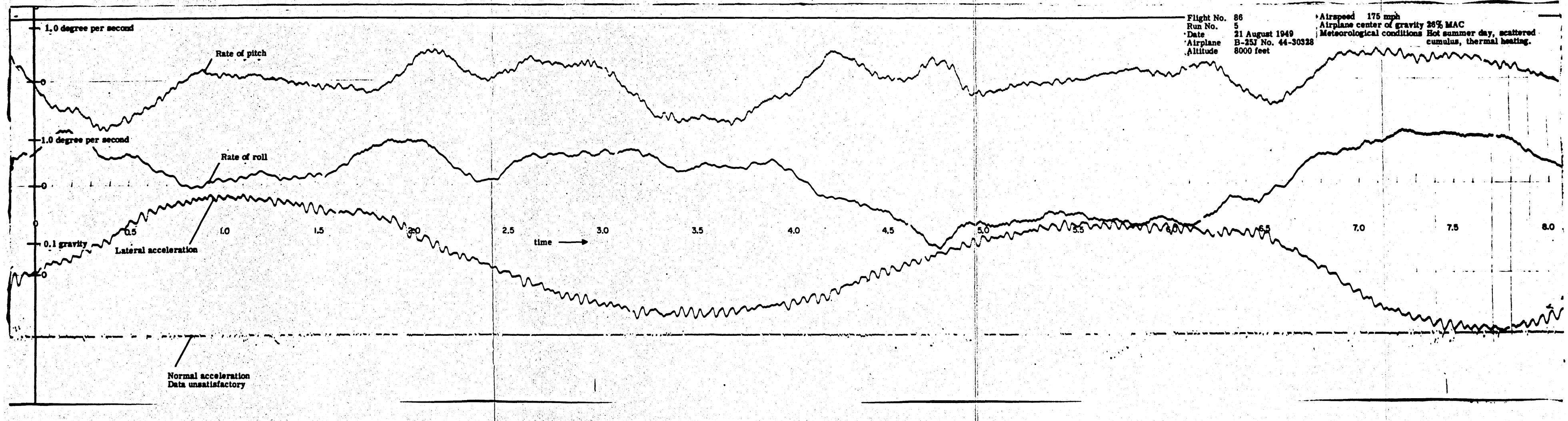
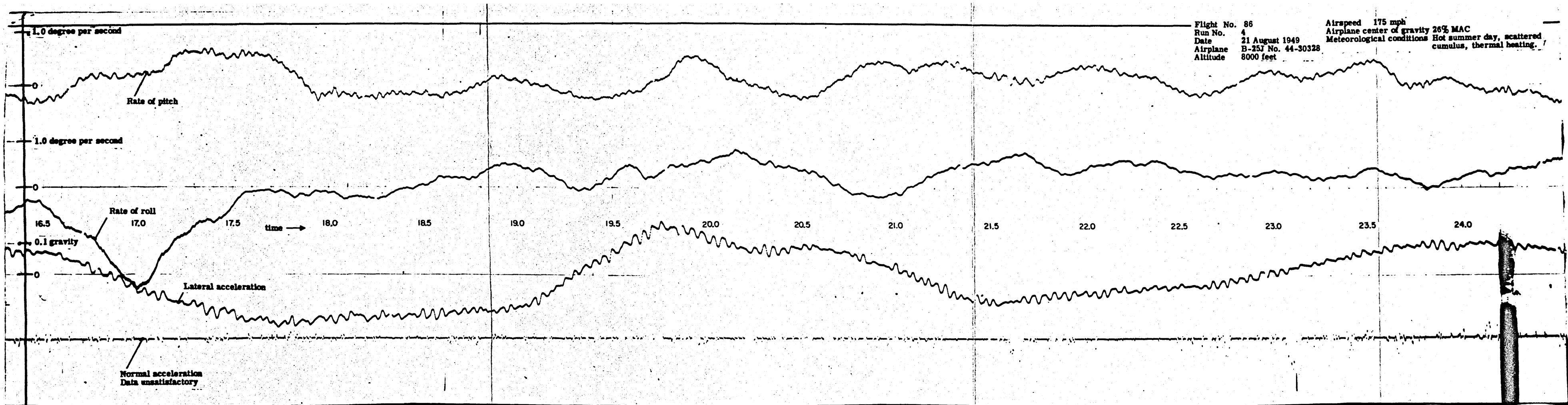
Flight No. 8
Run No. 4
Date 21 August 1949
Airplane B-25J No. 44-30328
Altitude 8000 feet
Airspeed 175 mph
Airplane center of gravity 26% MAC
Meteorological conditions Hot summer day, scattered cumulus, thermal heating.

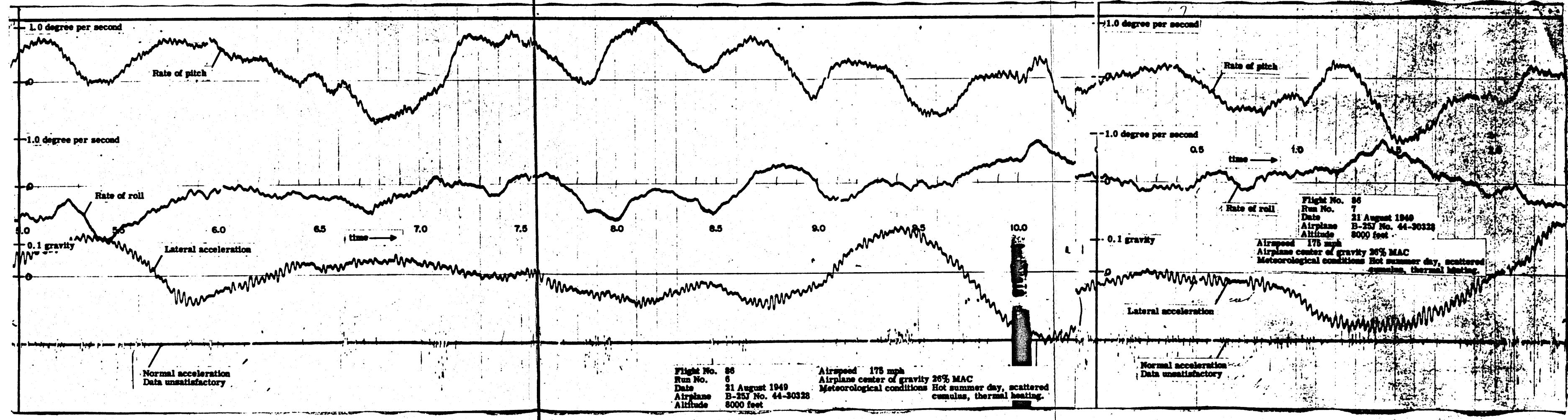
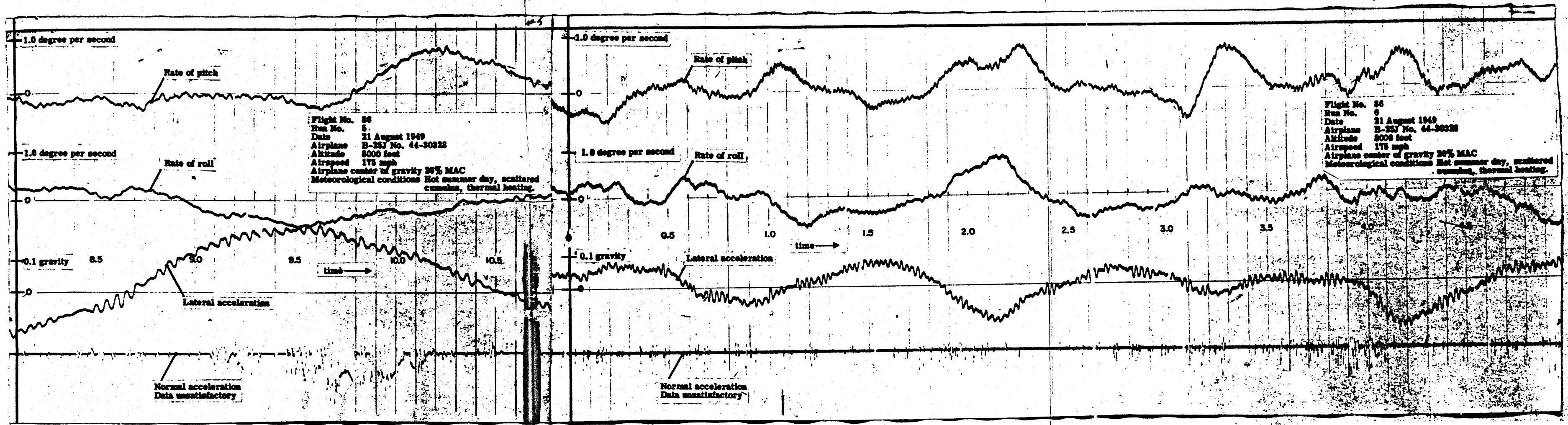


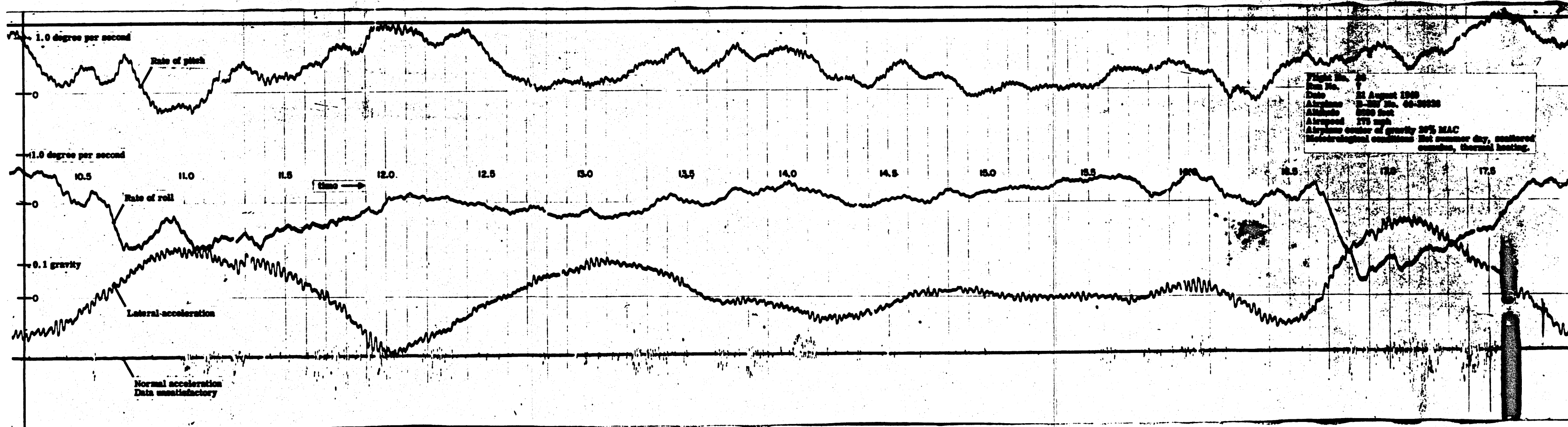
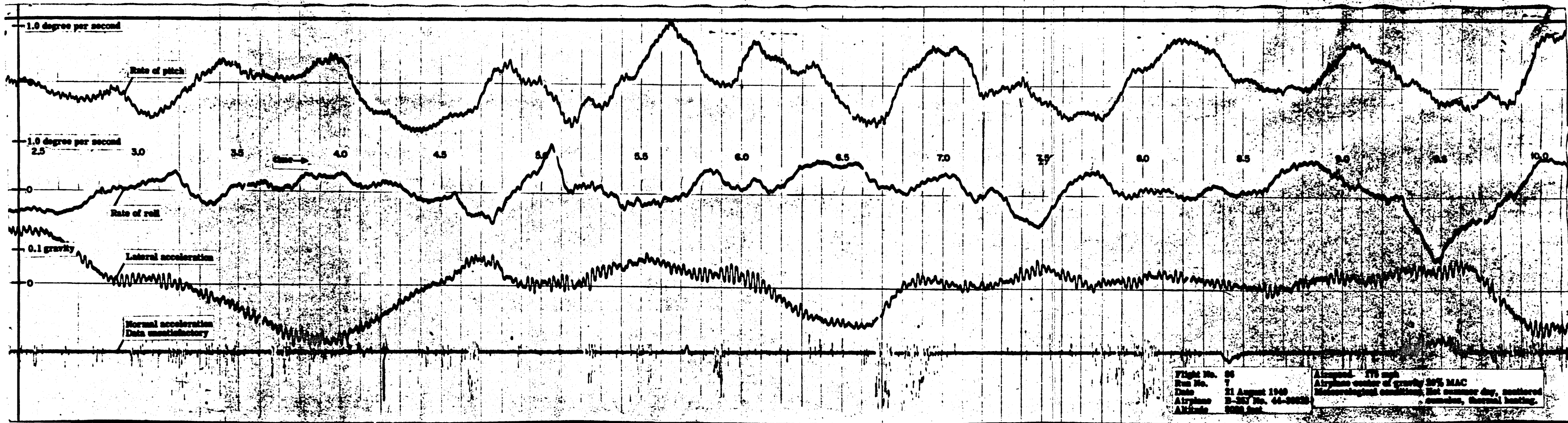
1.0 degree per second

Flight No. 86
Run No. 4
Date 21 August 1949
Airplane B-25J No. 44-30328
Altitude 8000 feet
Airspeed 175 mph
Airplane center of gravity 26% MAC
Meteorological conditions Hot summer day, scattered cumulus, thermal heating.

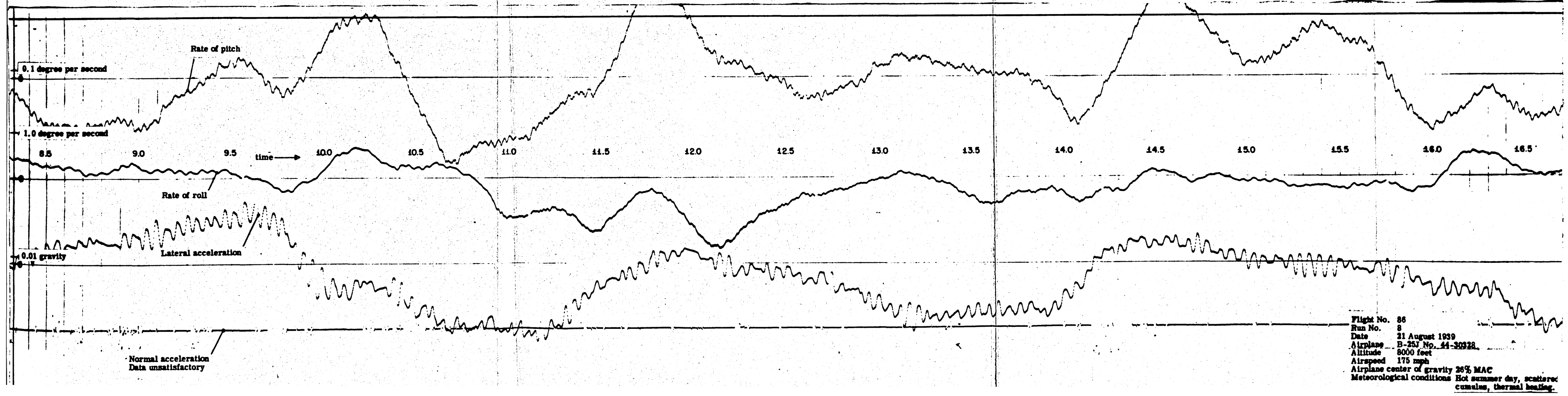
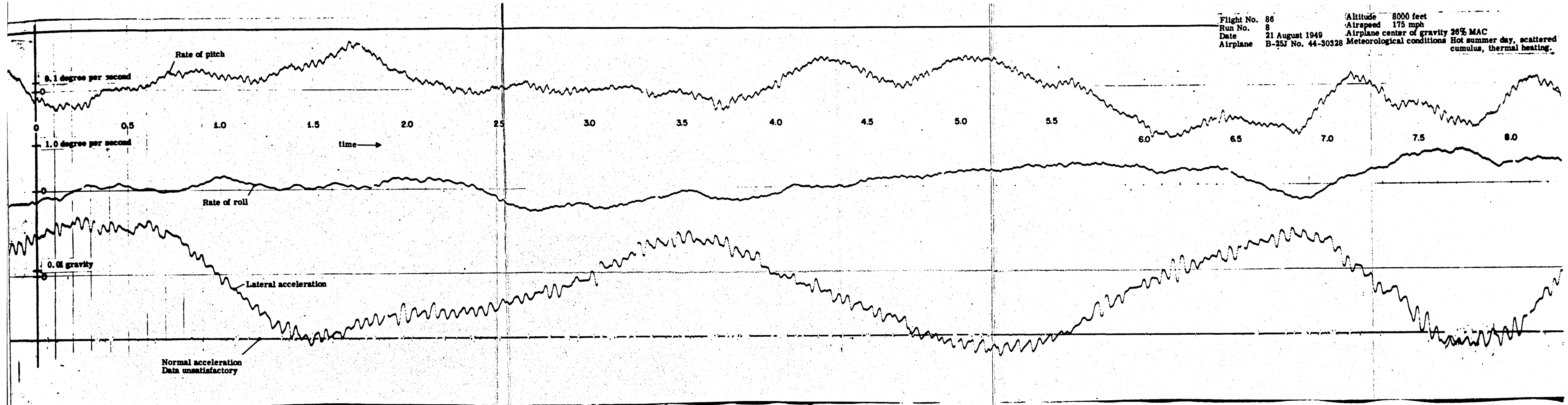




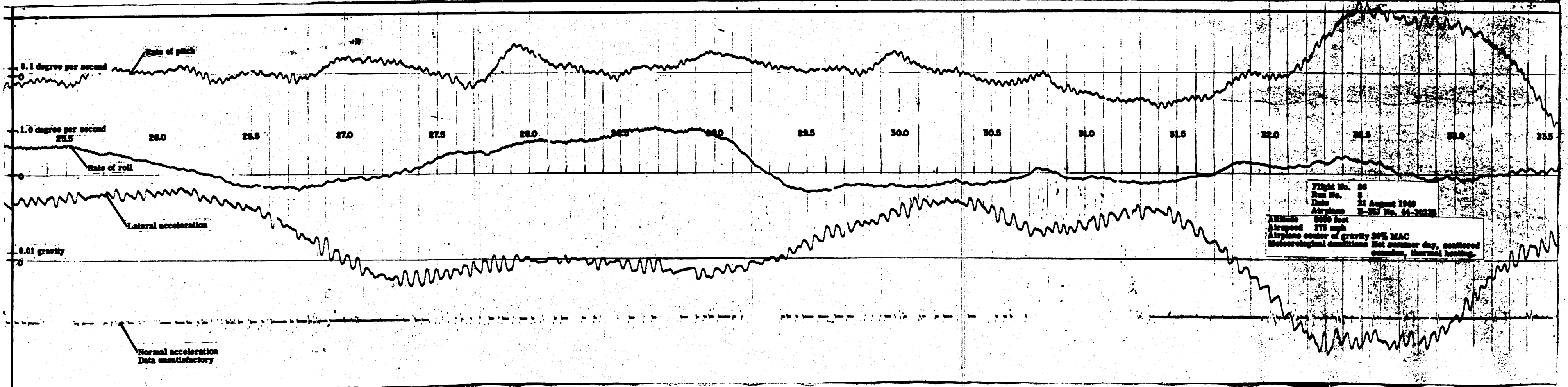
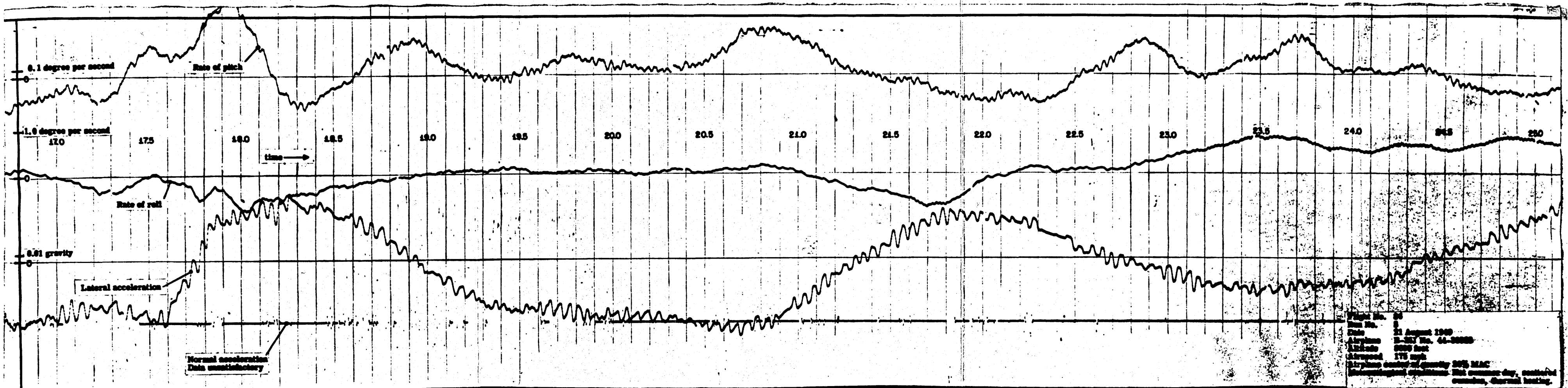


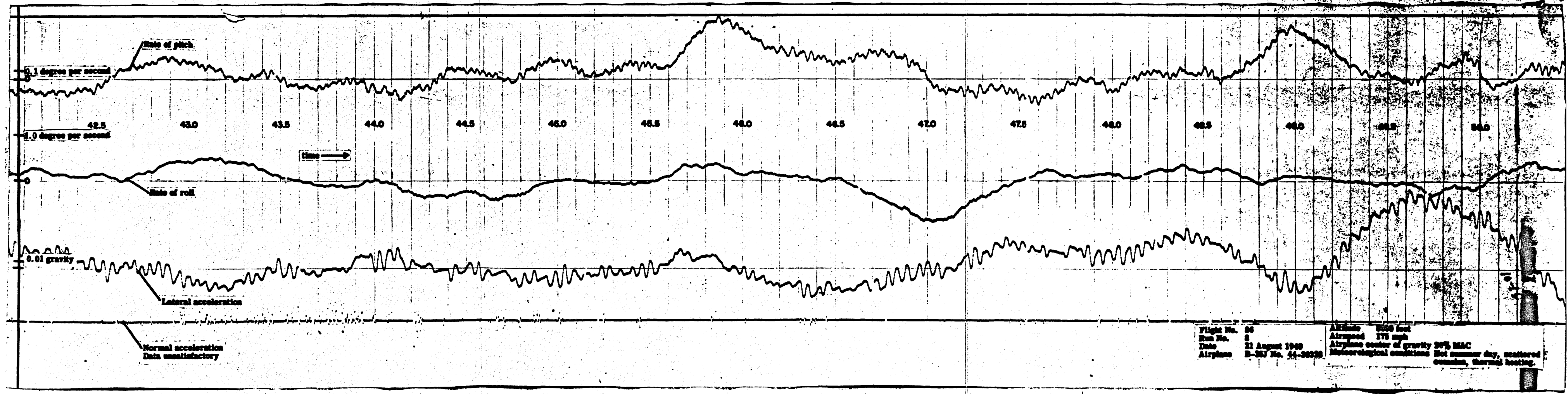


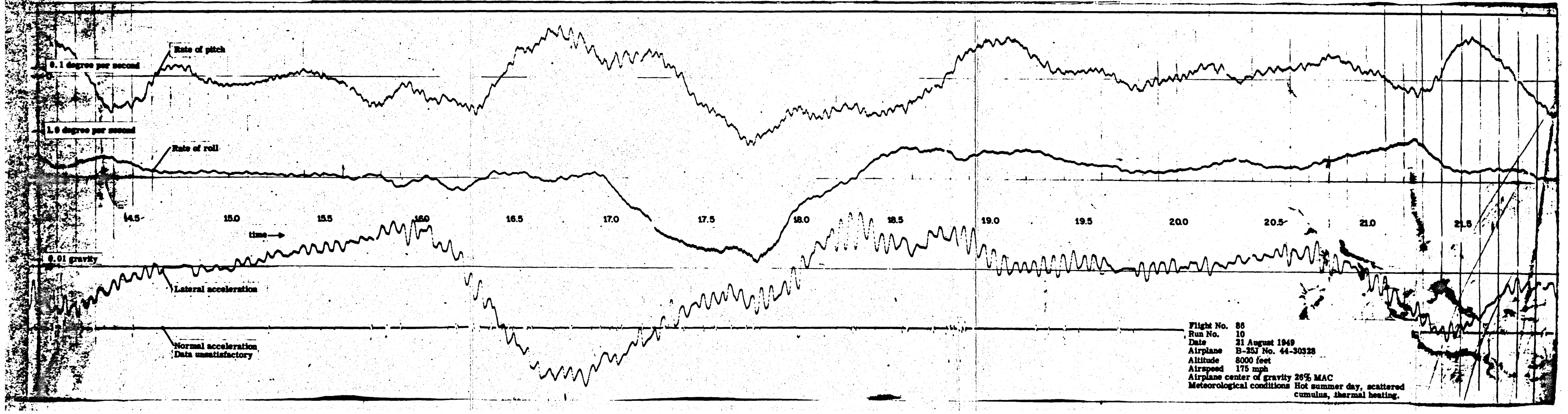
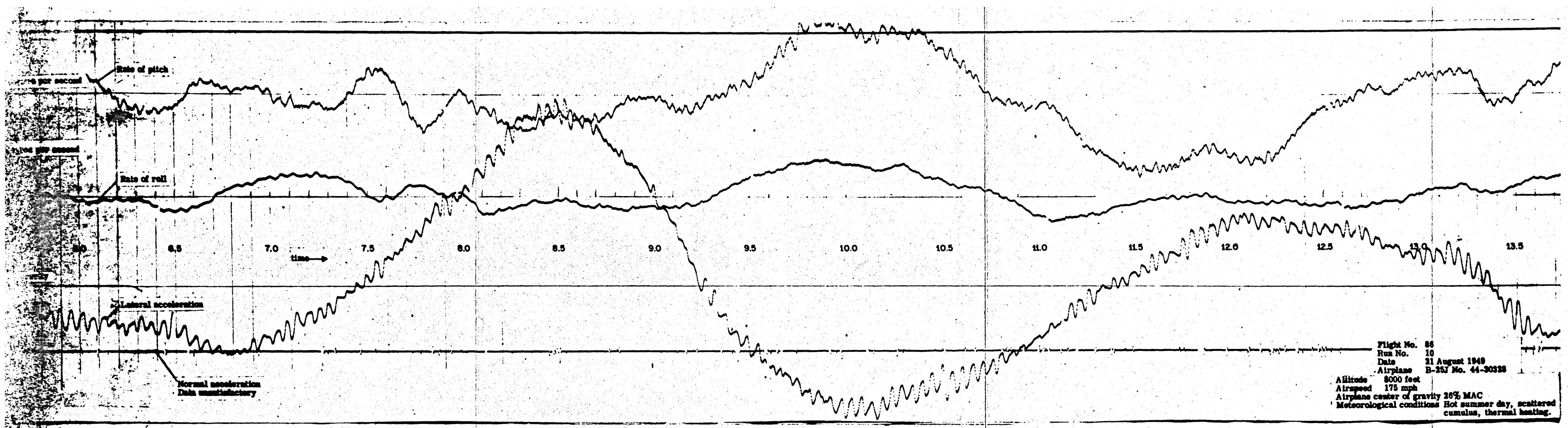
Flight No. 86 Altitude 8000 feet
 Run No. 8 Airspeed 175 mph
 Date 21 August 1949 Airplane center of gravity 26% MAC
 Airplane B-25J No. 44-30328 Meteorological conditions Hot summer day, scattered cumulus, thermal heating.

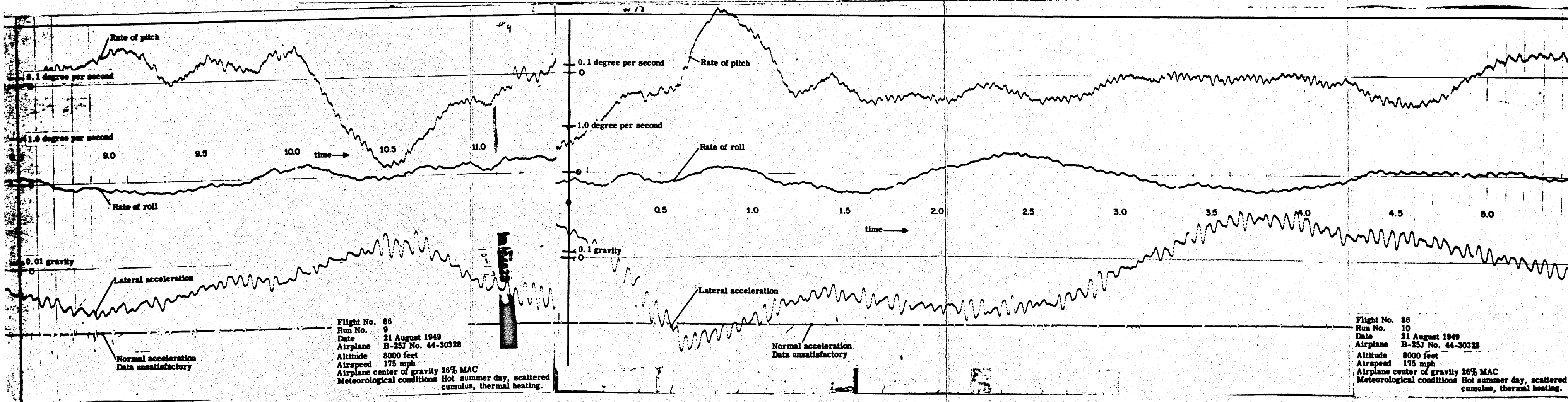
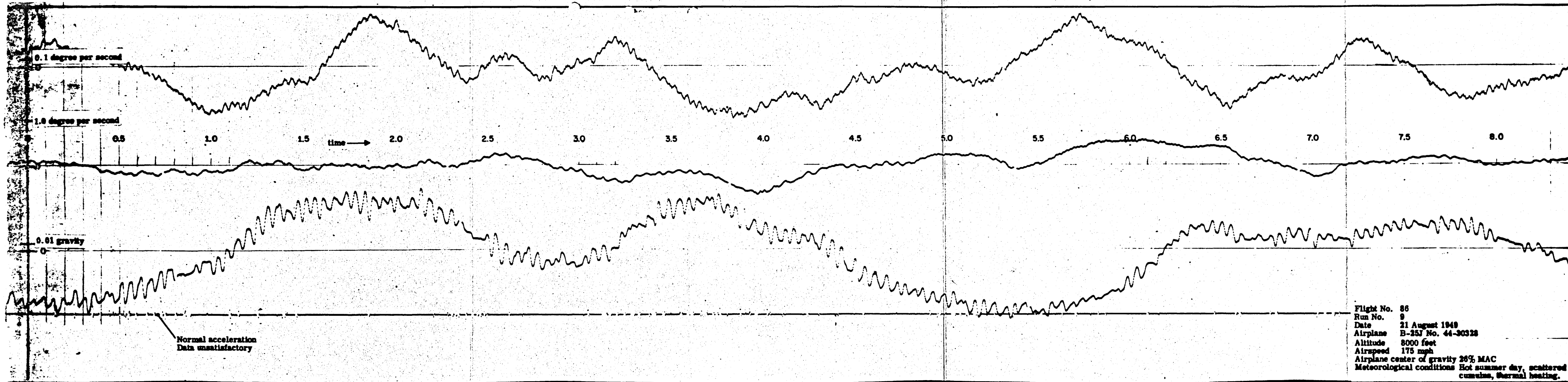


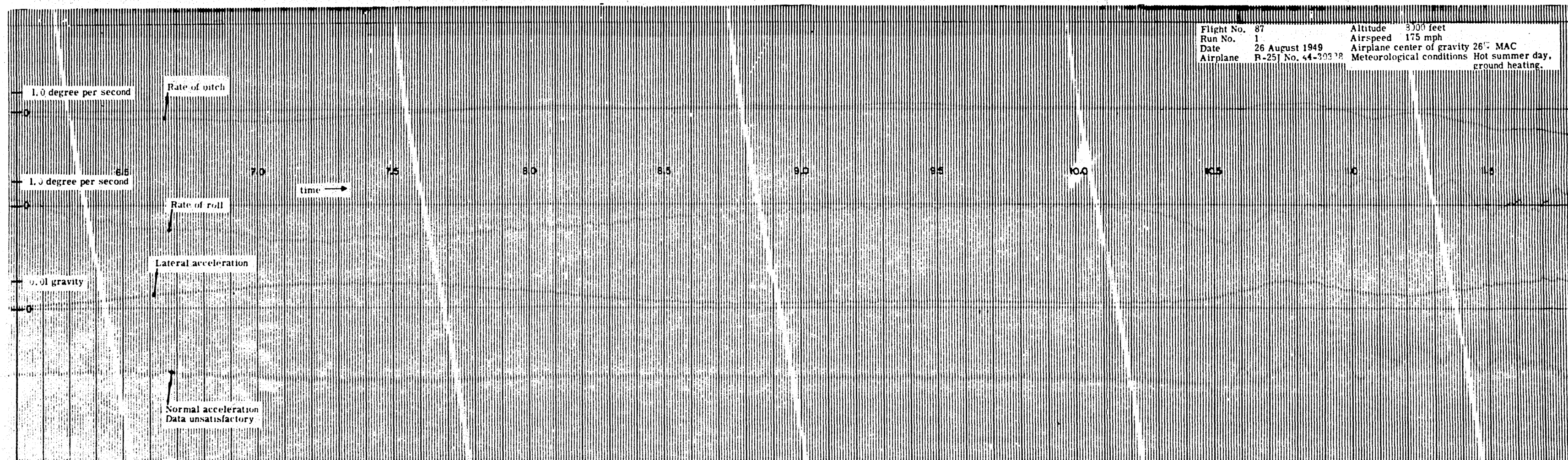
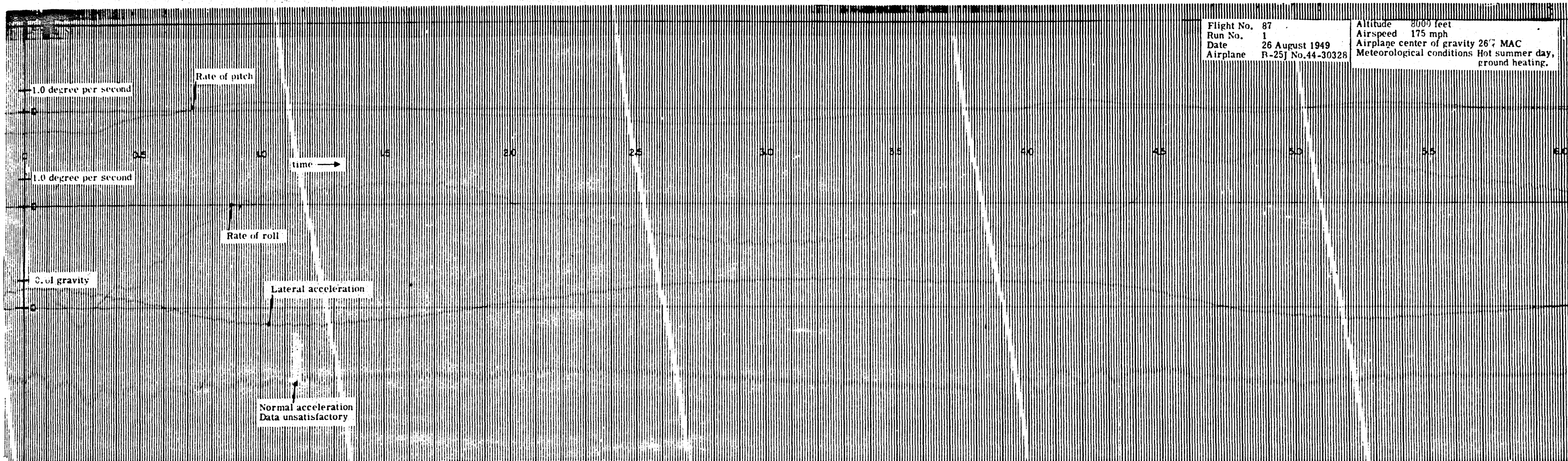
Flight No. 86
 Run No. 8
 Date 21 August 1949
 Airplane B-25J No. 44-30328
 Altitude 8000 feet
 Airspeed 175 mph
 Airplane center of gravity 26% MAC
 Meteorological conditions Hot summer day, scattered cumulus, thermal heating.

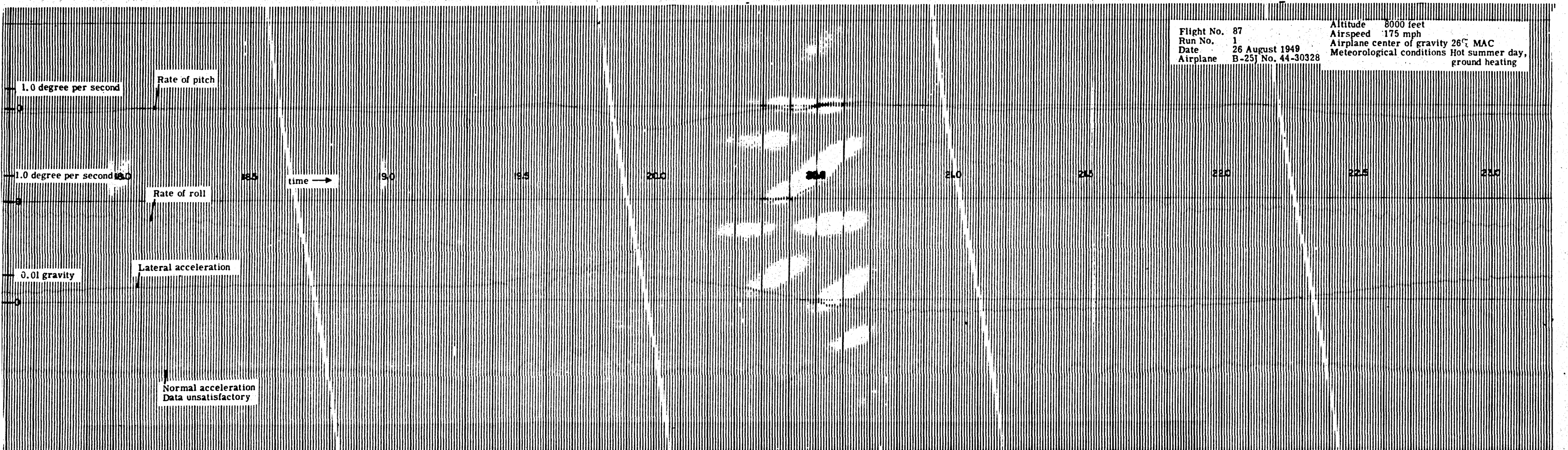
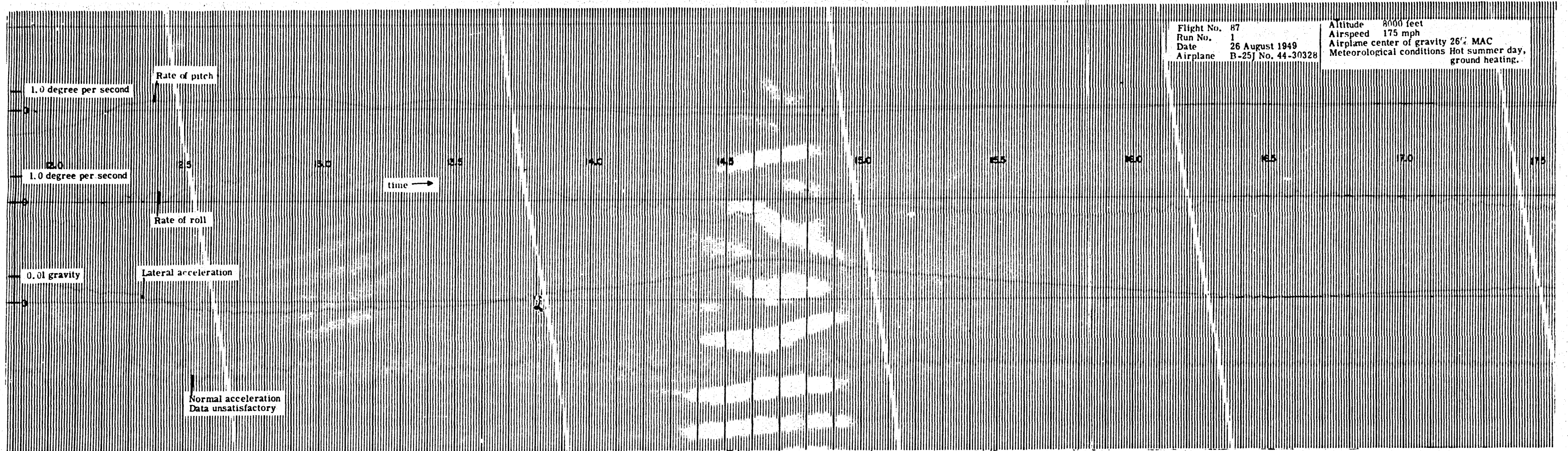


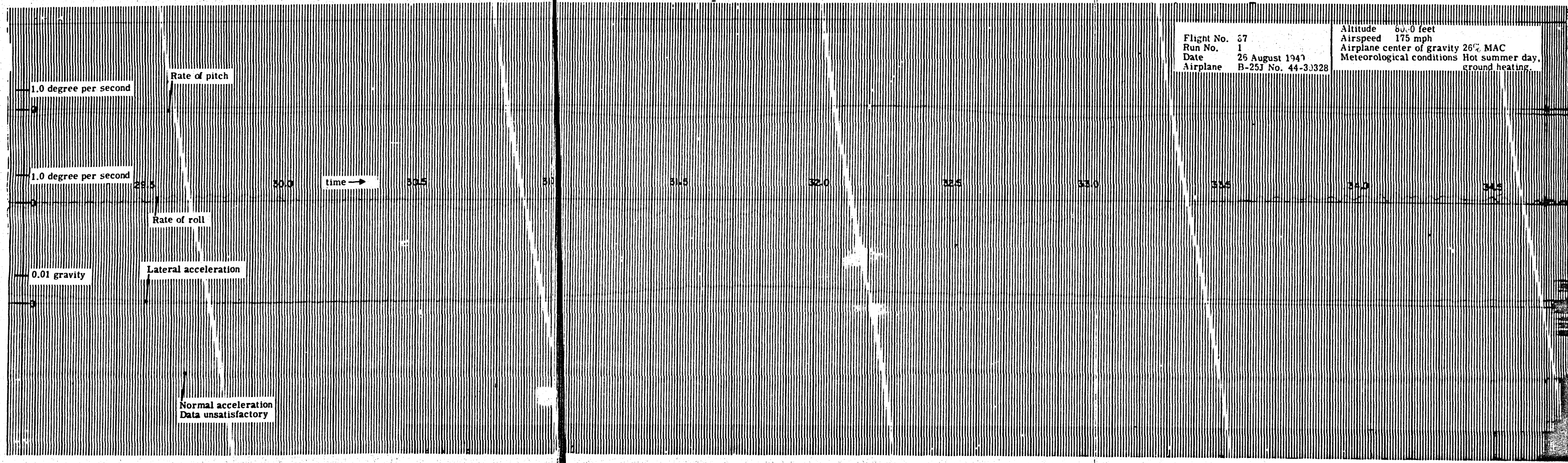
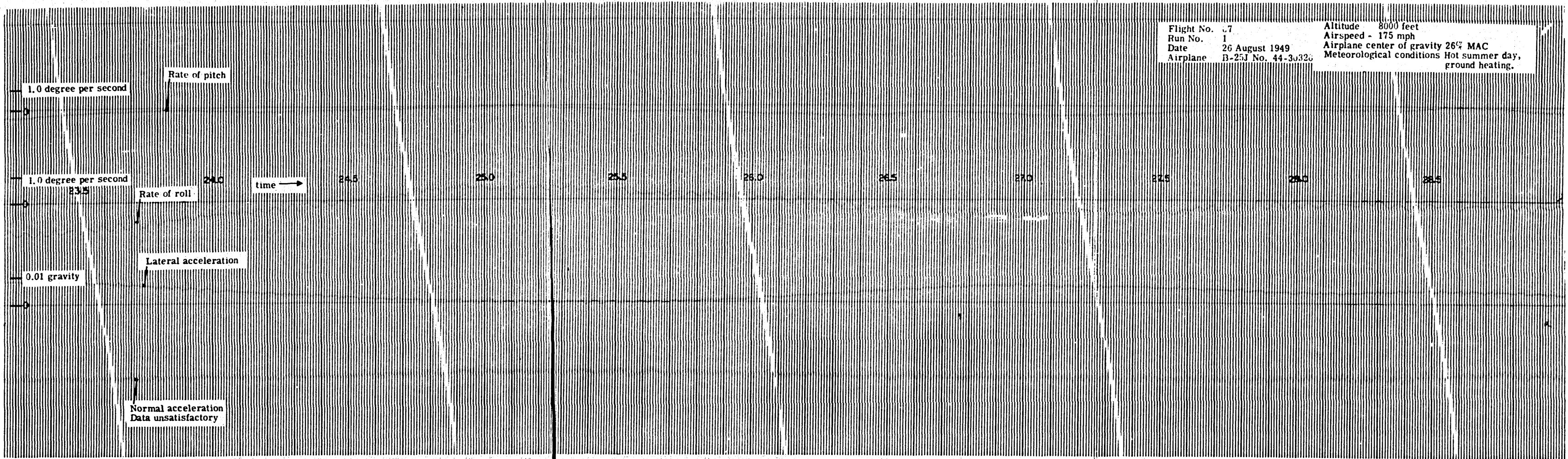


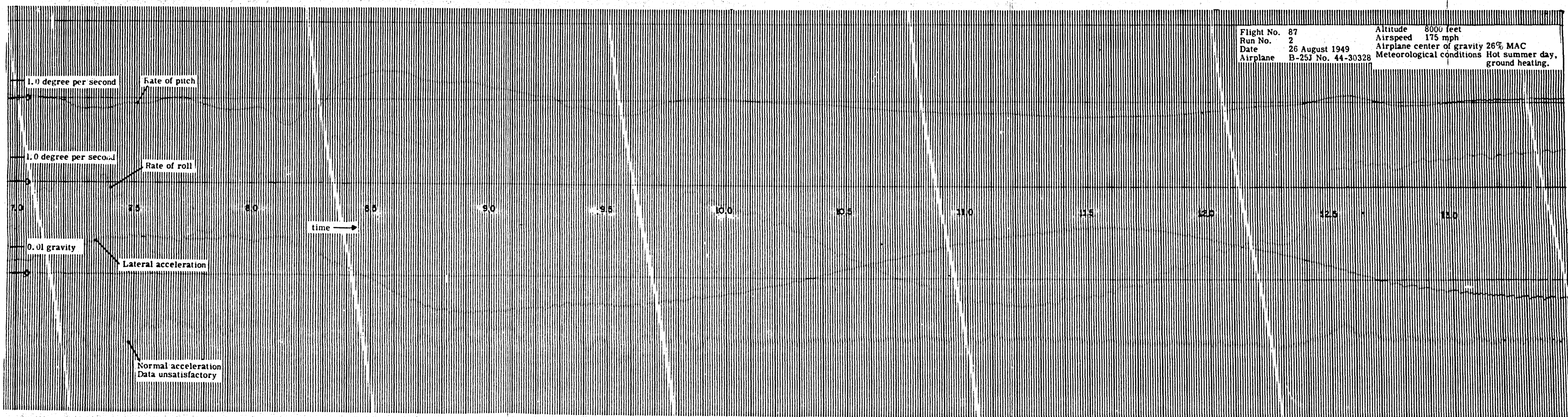
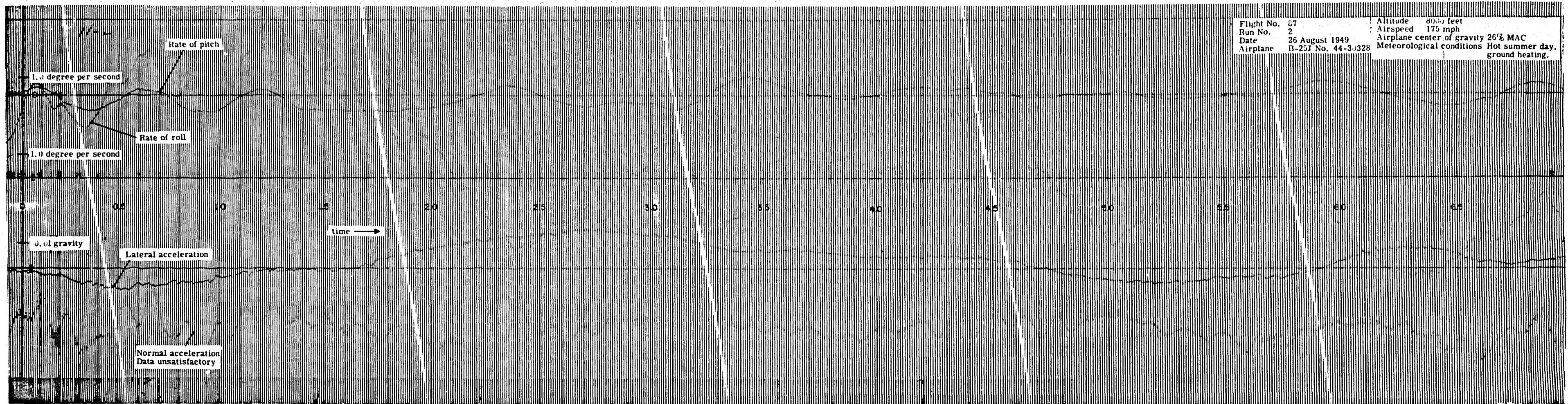


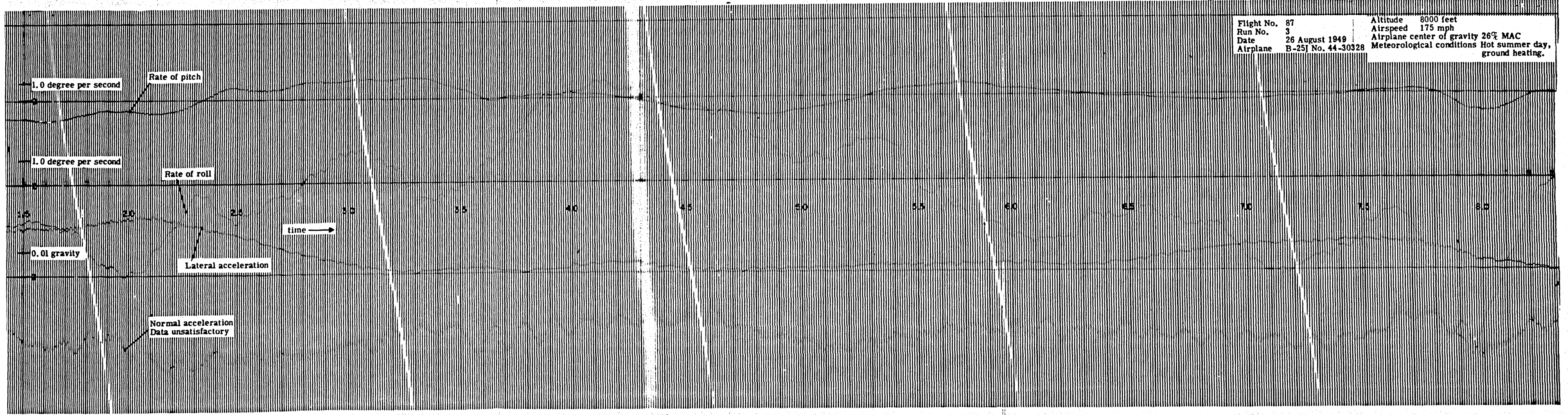
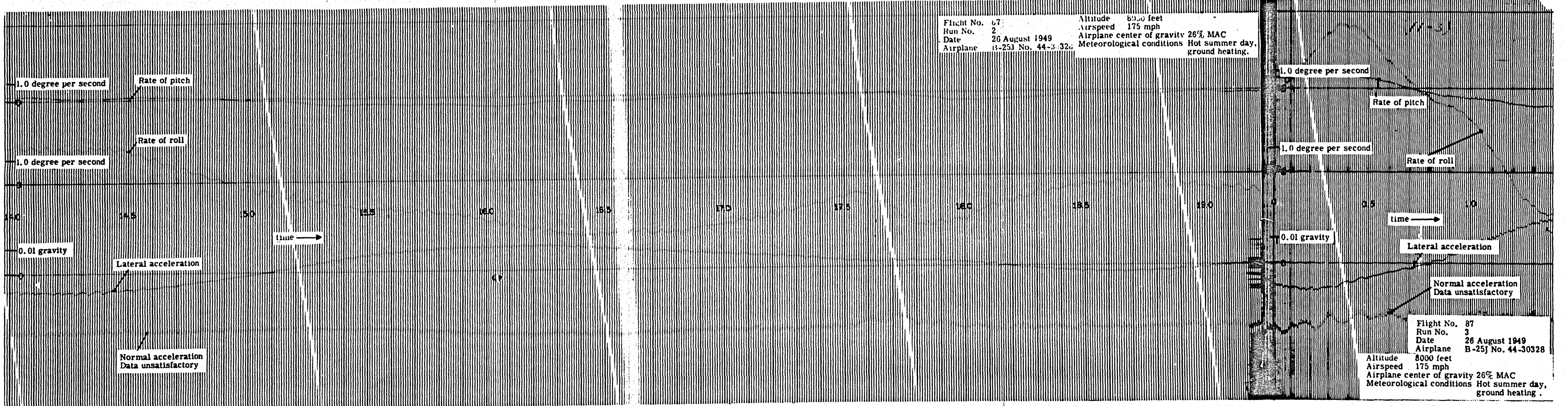




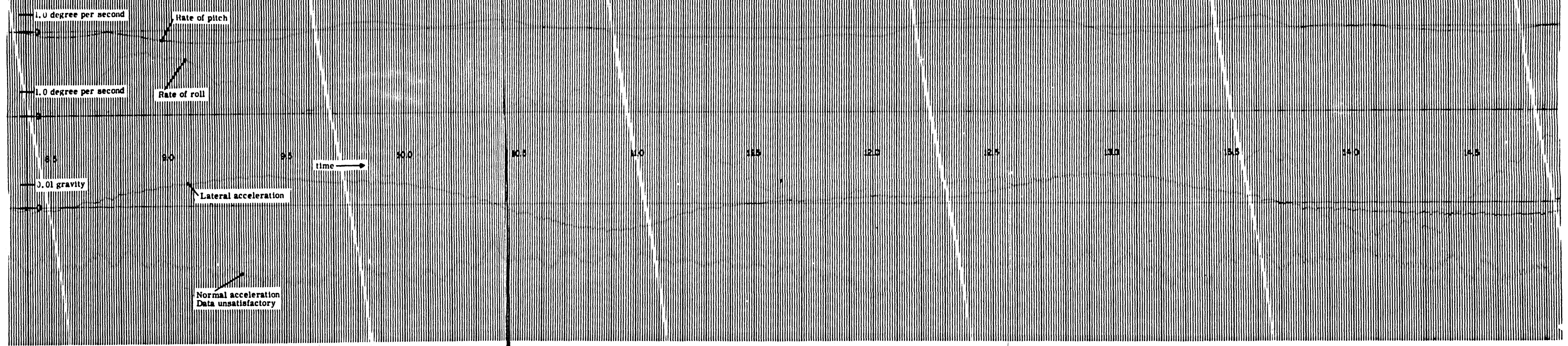




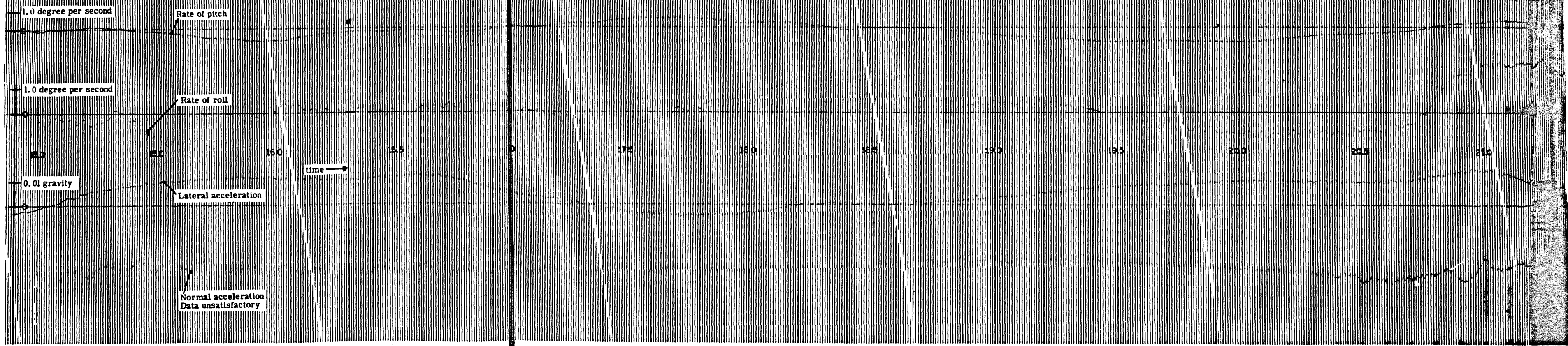


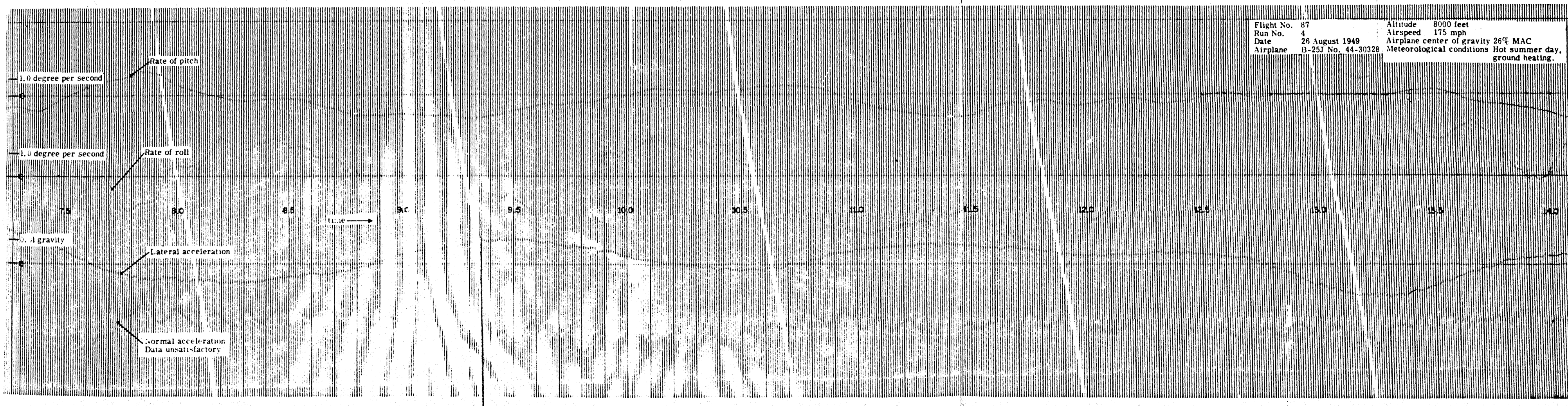
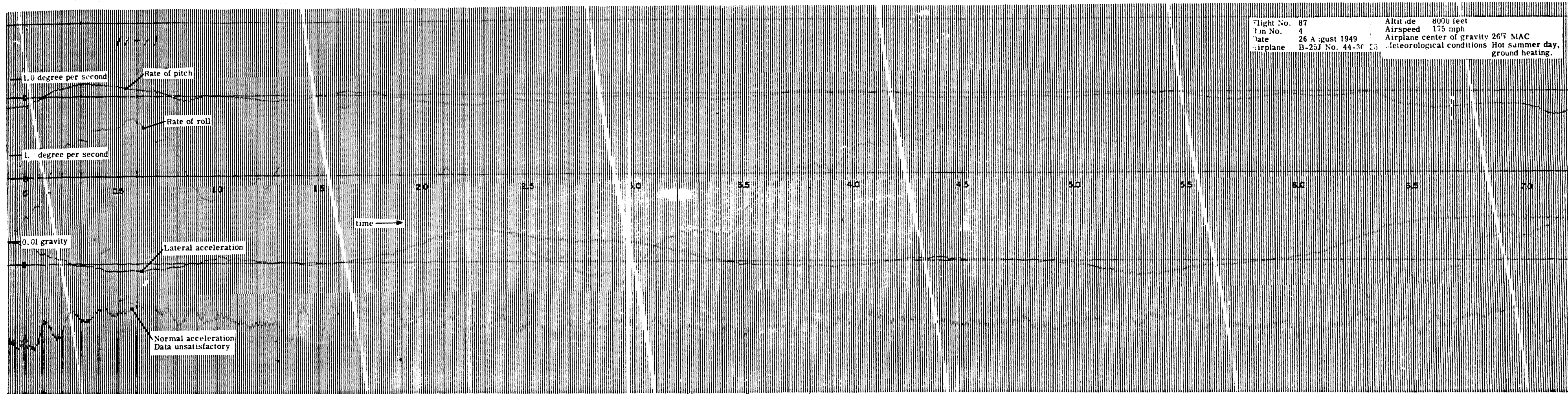


Flight No.	87	Altitude	8000 feet
Run No.	3	Airspeed	175 mph
Date	26 August 1949	Airplane center of gravity	28% MAC
Airplane	B-25J No. 44-30328	Meteorological conditions	Hot summer day, ground heating.



Flight No.	87	Altitude	8000 feet
Run No.	3	Airspeed	175 mph
Date	26 August 1949	Airplane center of gravity	26% MAC
Airplane	B-25J No. 44-30328	Meteorological conditions	Hot summer day, ground heating.



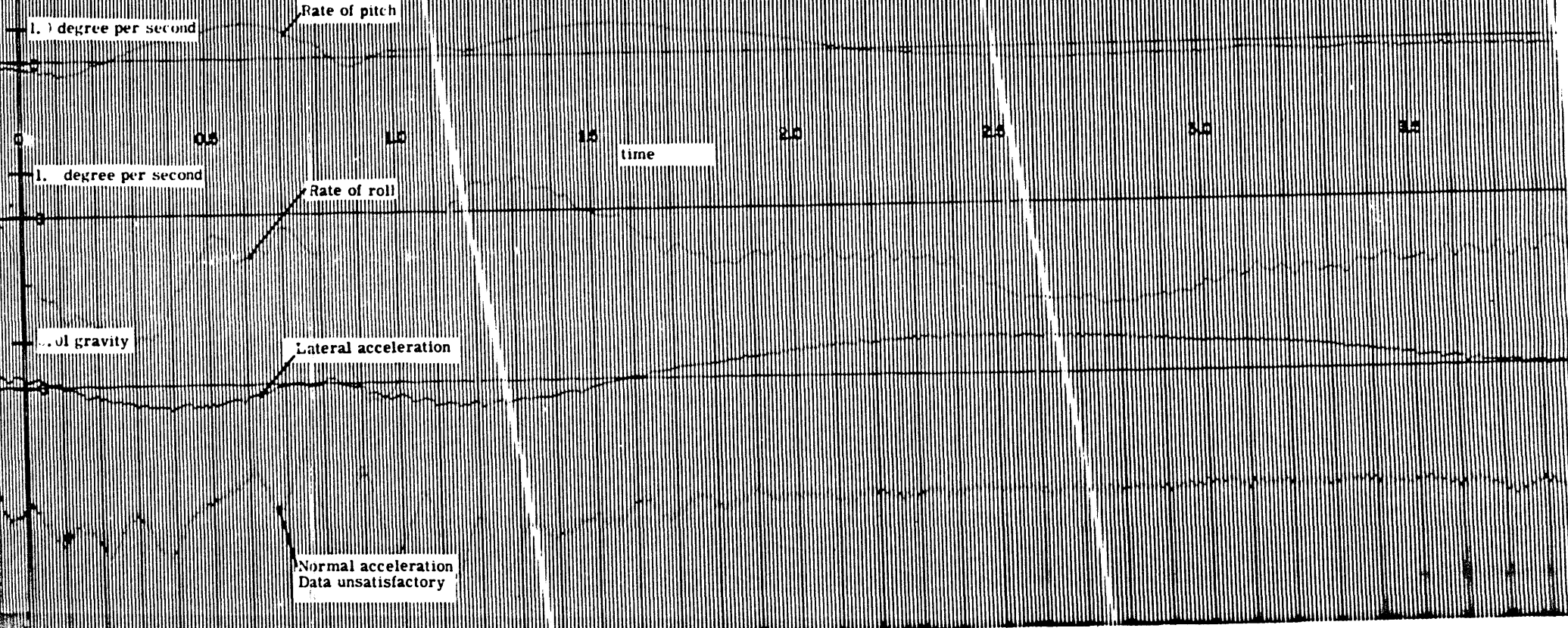
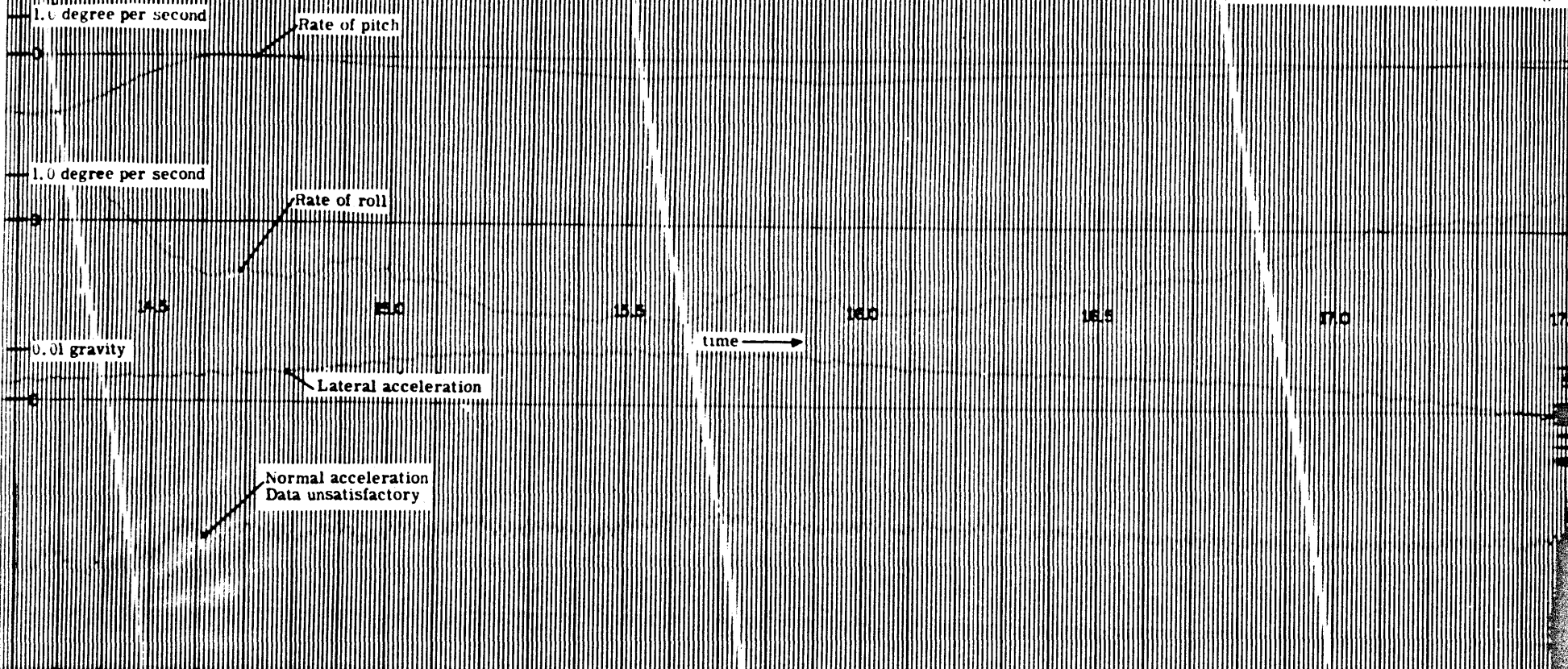


Flight No. 87
Run No. 4
Date 21 August 1949
Airplane B-25J No. 44-30328

Altitude 8000 feet
Airspeed 175 mph
Airplane center of gravity 25% MAC
Meteorological conditions Hot summer day,
ground heating.

Flight No. 87
Run No. 5
Date 26 August 1949
Airplane B-25J No. 44-30328

Altitude 8000 feet
Airspeed 175 mph
Airplane center of gravity 26% MAC
Meteorological conditions Hot summer day,
ground heating.

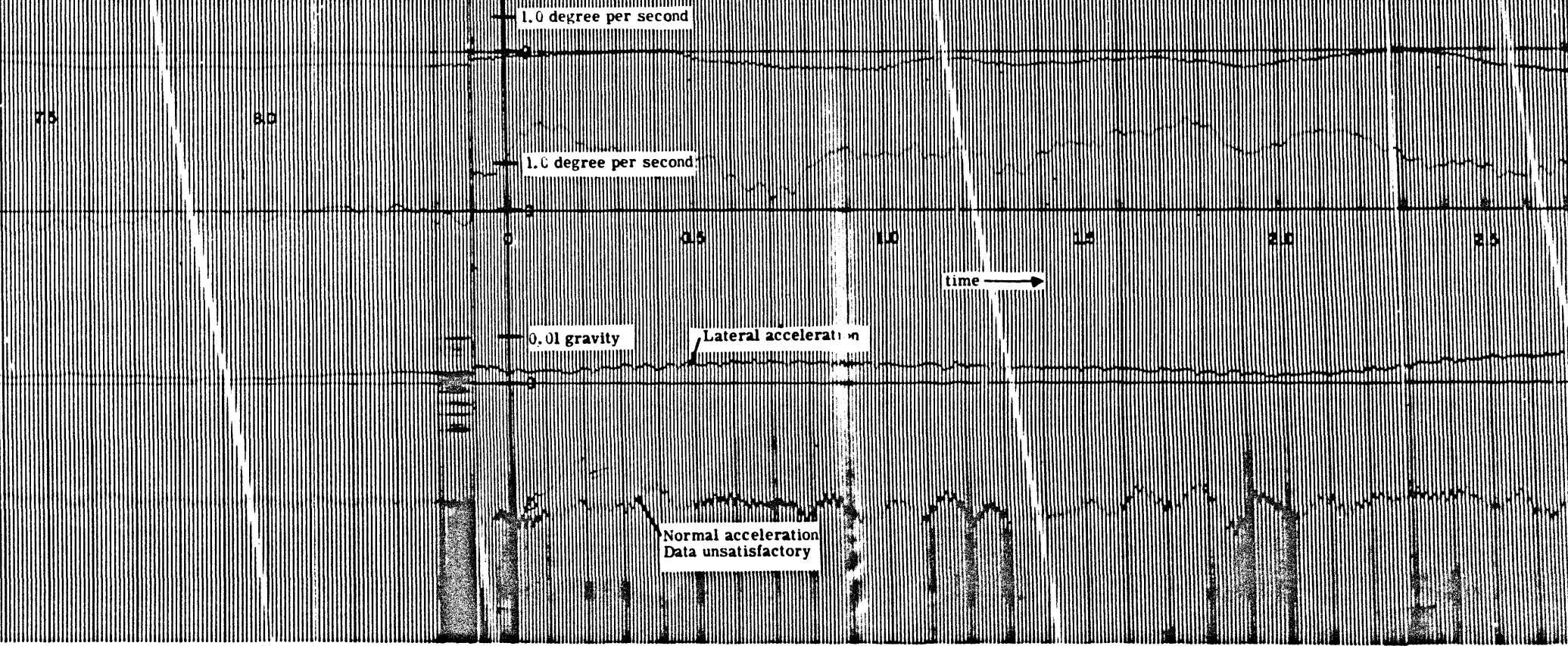
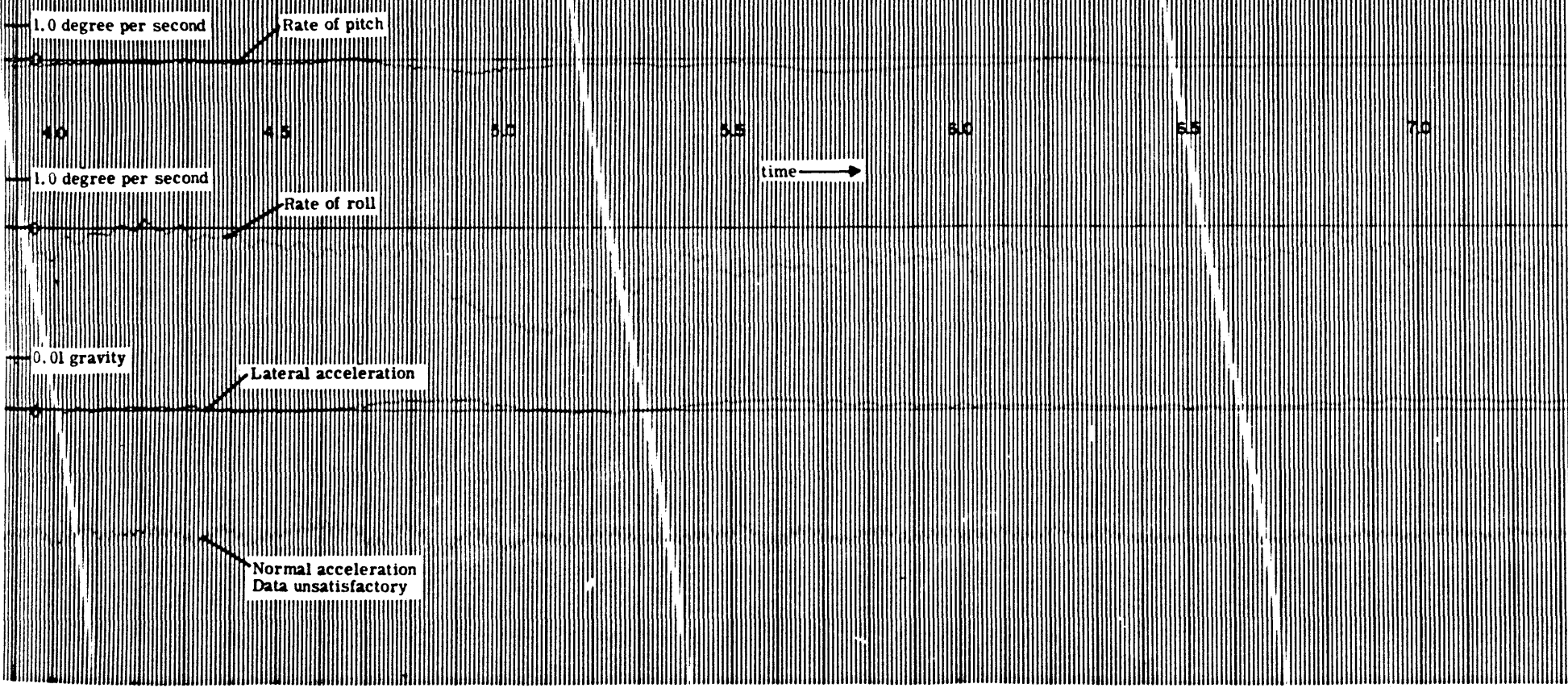


Flight No. 87
Run No. 5
Date 26 August 1949
Airplane B-25J No. 44-30328

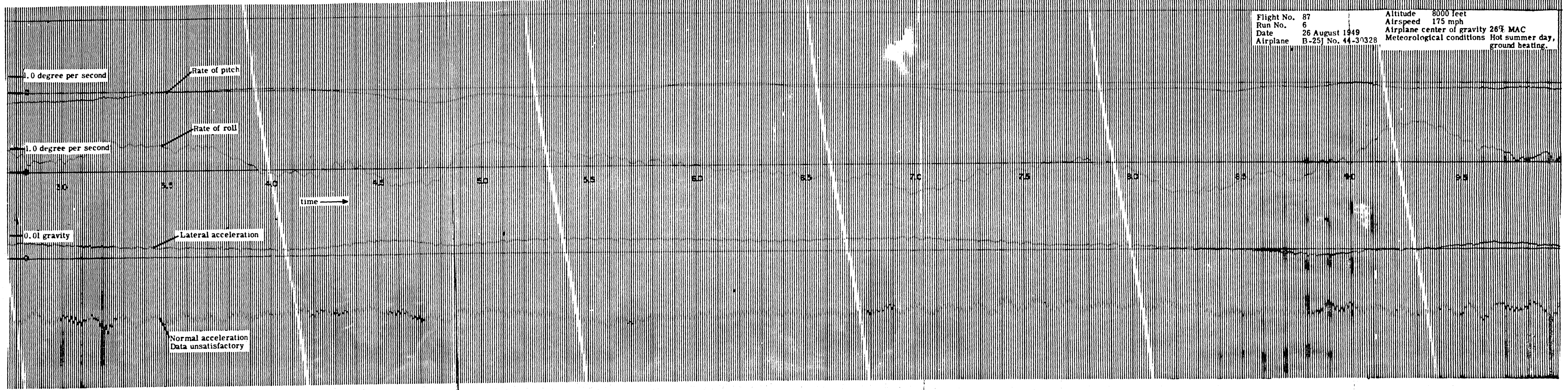
Altitude 8000 feet
Airspeed 175 mph
Airplane center of gravity 26% MAC
Meteorological conditions Hot summer day,
ground heating.

Flight No. 87
Run No. 6
Date 26 August 1949
Airplane B-25J No. 44-30328

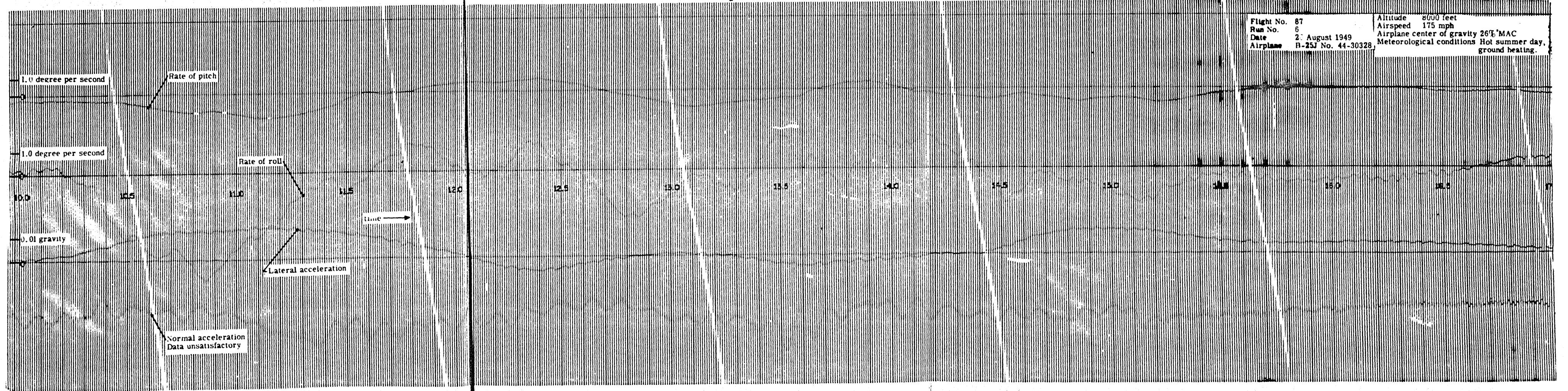
Altitude 8000 feet
Airspeed 175 mph
Airplane center of gravity 26% MAC
Meteorological conditions Hot summer day,
ground heating.

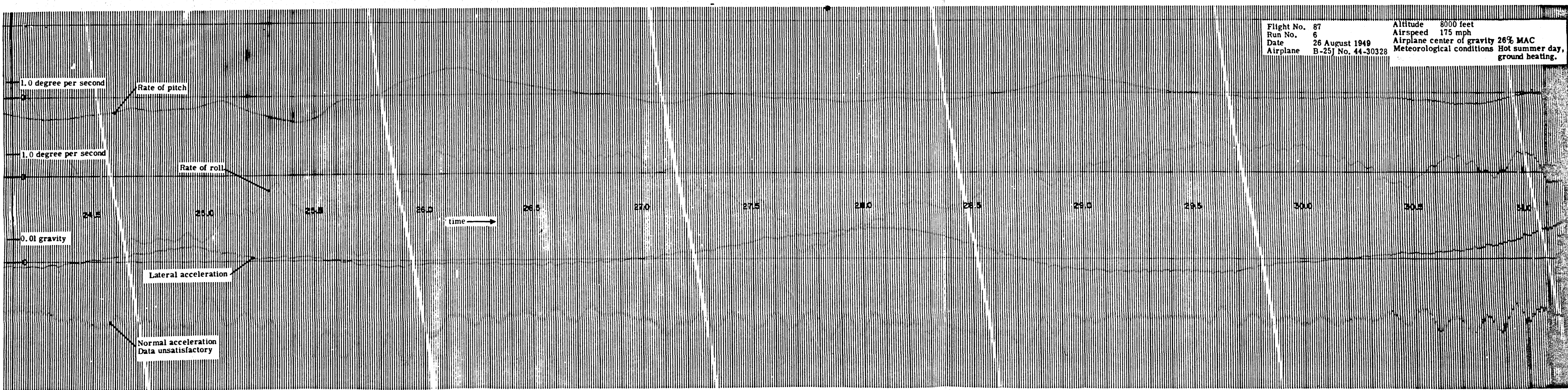
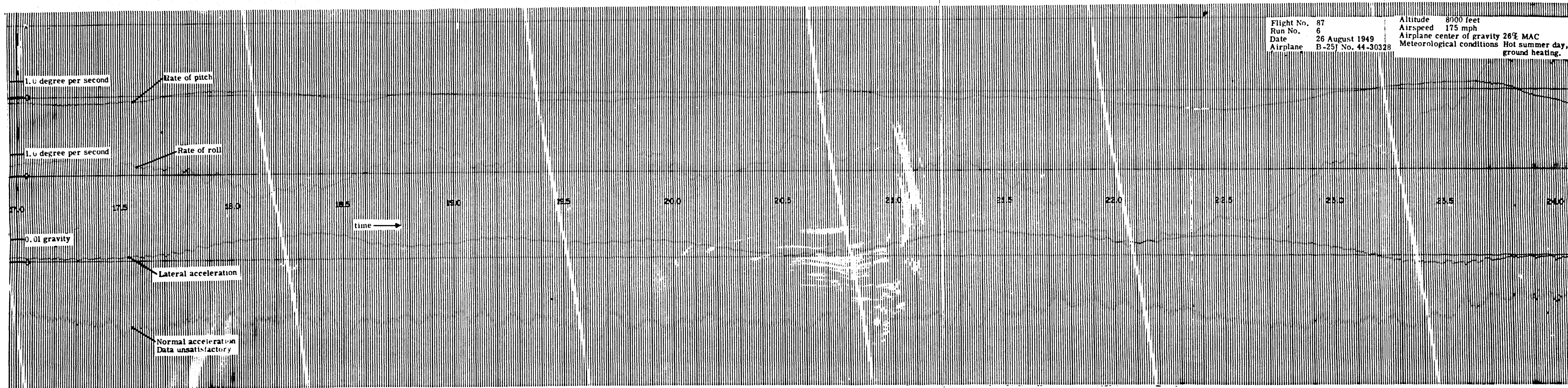


Flight No.	87	Altitude	8000 feet
Run No.	6	Airspeed	175 mph
Date	26 August 1949	Airplane center of gravity	26% MAC
Airplane	B-25J No. 44-30328	Meteorological conditions	Hot summer day, ground heating.



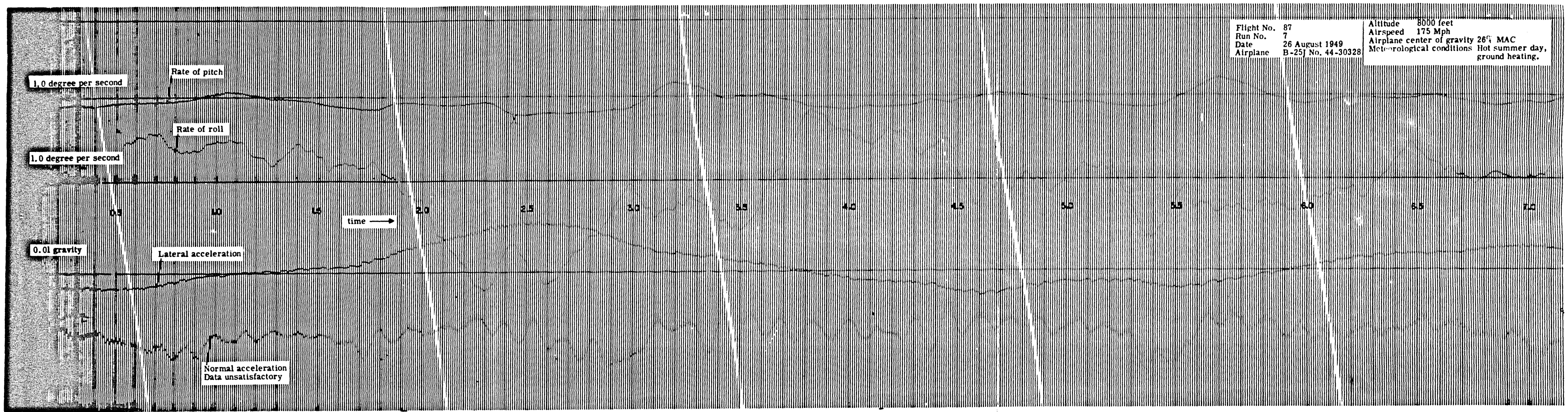
Flight No.	87	Altitude	8000 feet
Run No.	6	Airspeed	175 mph
Date	26 August 1949	Airplane center of gravity	26% MAC
Airplane	B-25J No. 44-30328	Meteorological conditions	Hot summer day, ground heating.





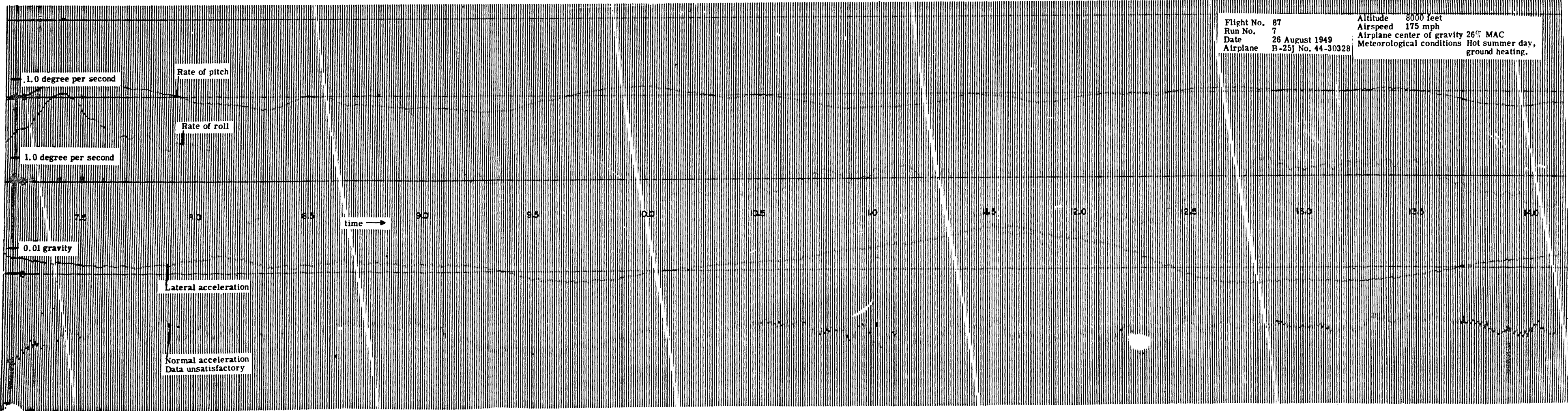
Flight No. 87
Run No. 7
Date 26 August 1949
Airplane B-25J No. 44-30328

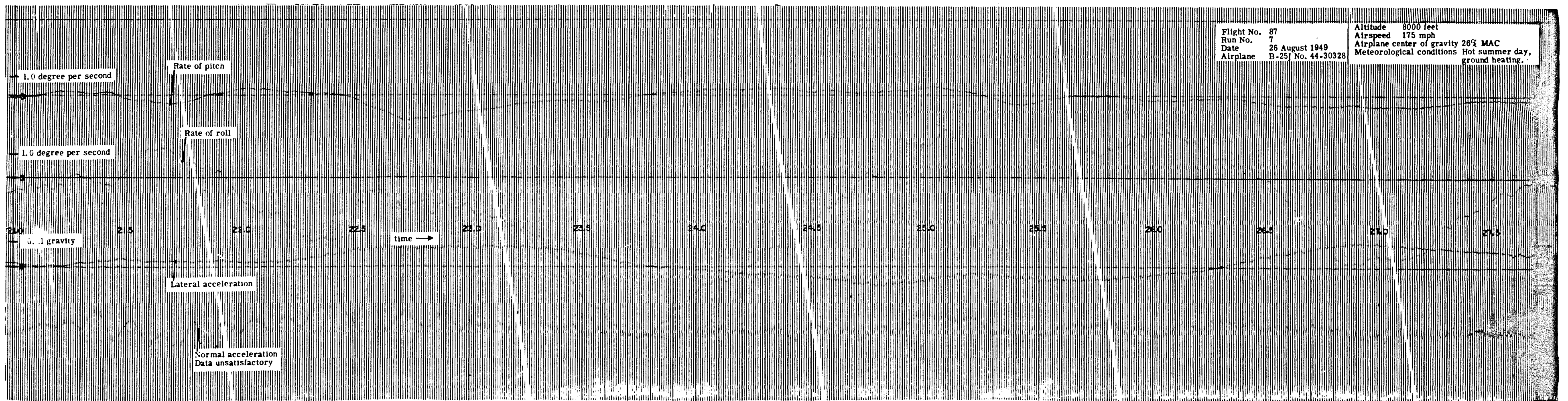
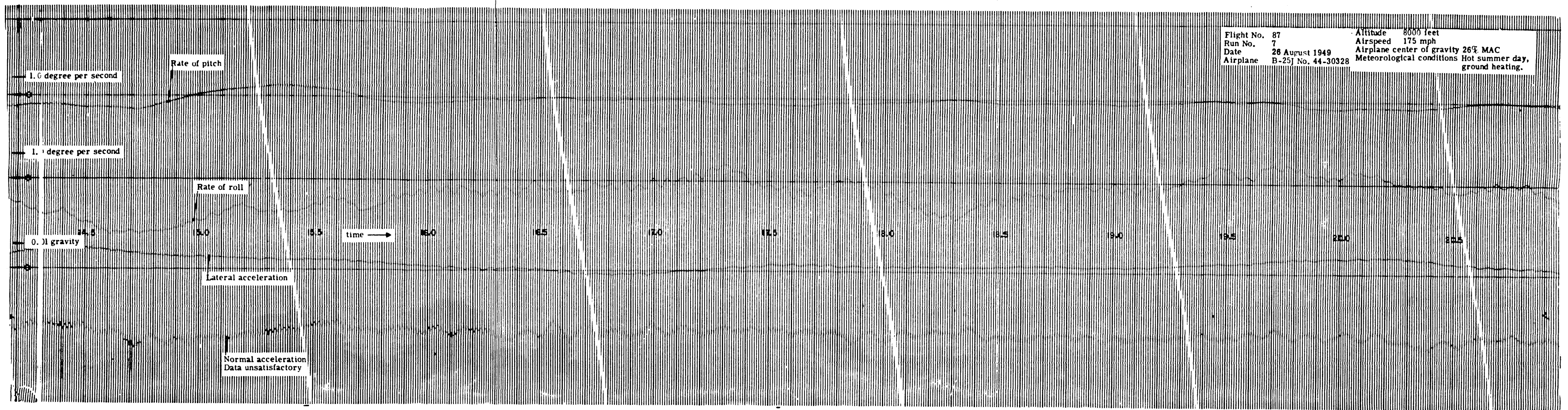
Altitude 8000 feet
Airspeed 175 Mph
Airplane center of gravity 26% MAC
Meteorological conditions Hot summer day,
ground heating.



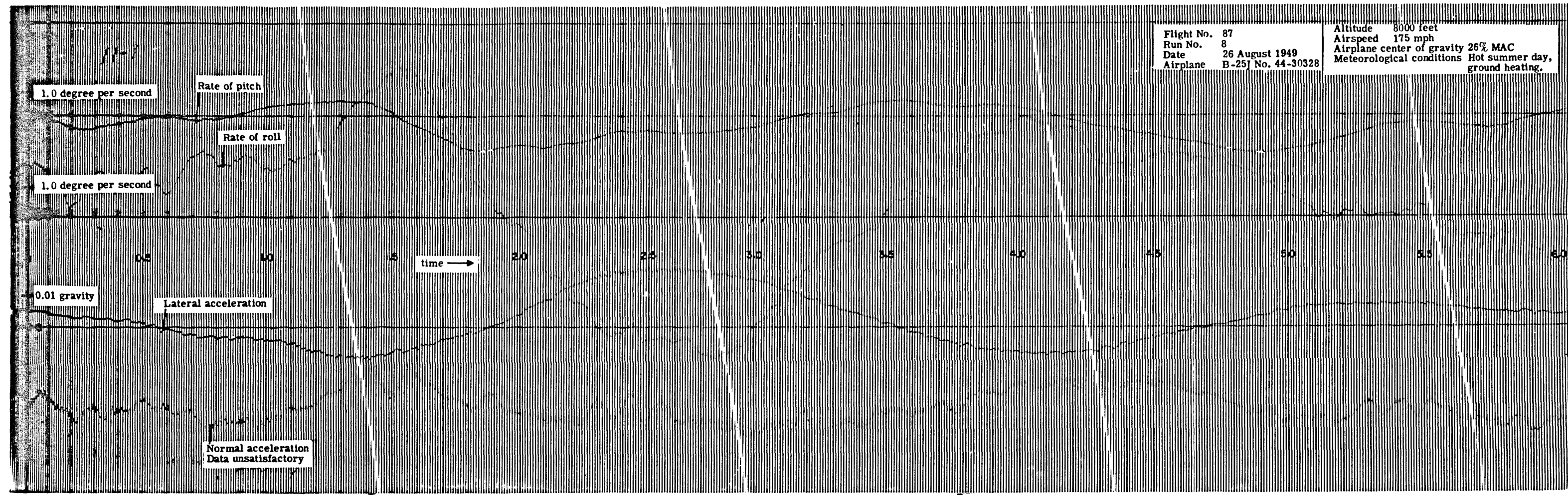
Flight No. 87
Run No. 7
Date 26 August 1949
Airplane B-25J No. 44-30328

Altitude 8000 feet
Airspeed 175 mph
Airplane center of gravity 26% MAC
Meteorological conditions Hot summer day,
ground heating.

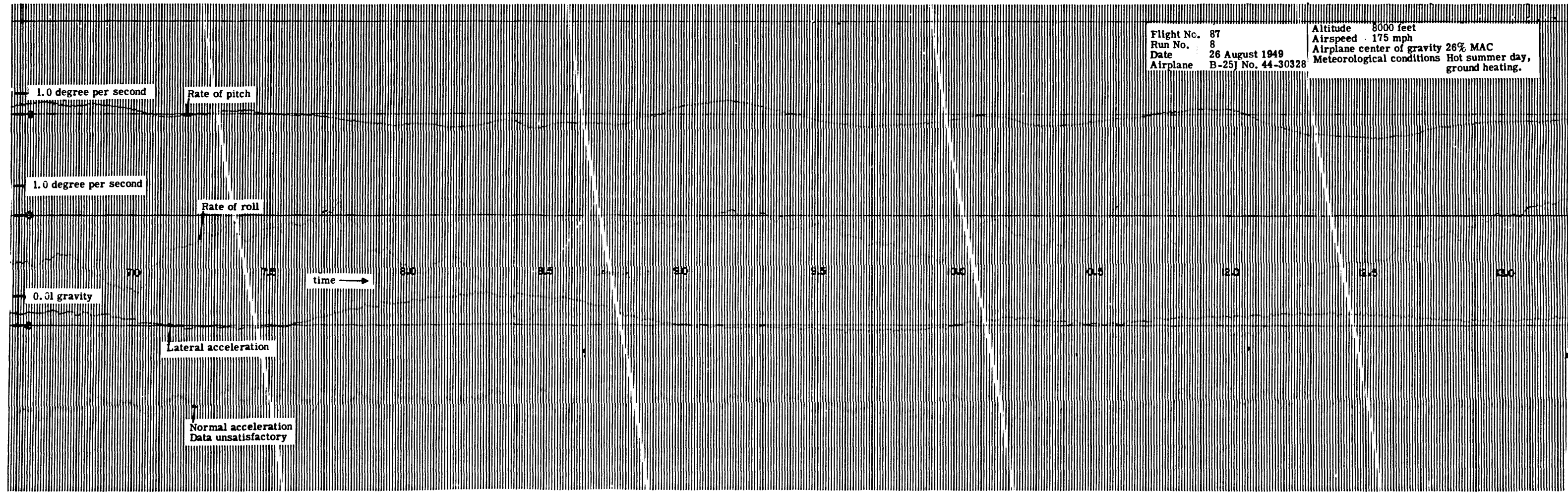


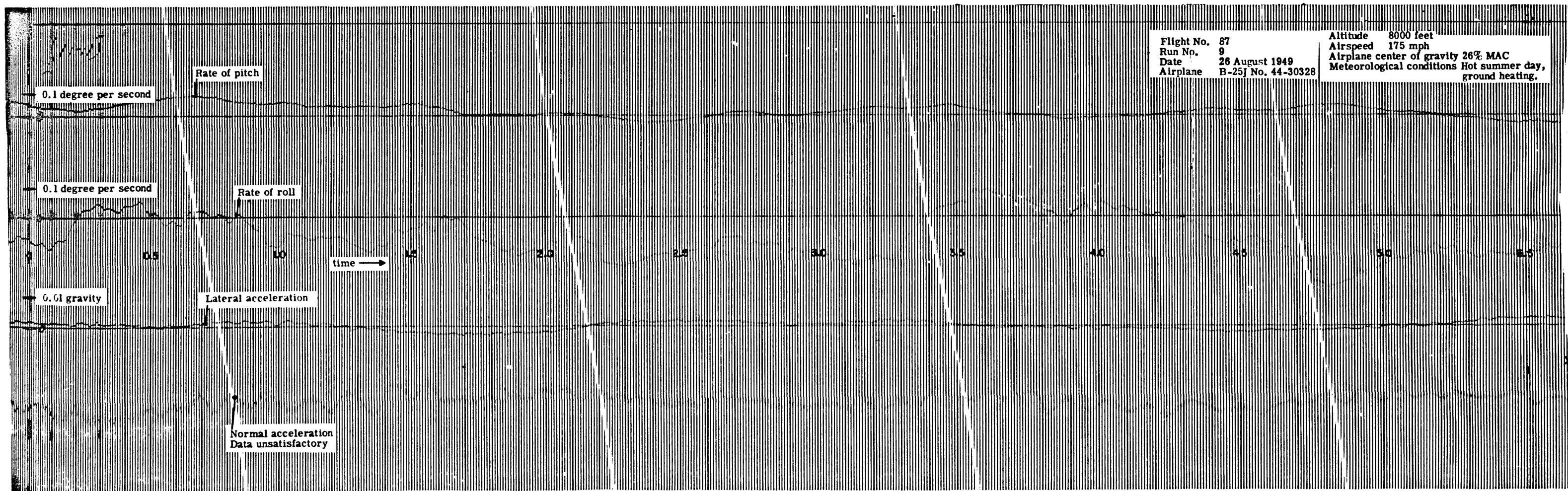


Flight No.	87	Altitude	8000 feet
Run No.	8	Airspeed	175 mph
Date	26 August 1949	Airplane center of gravity	26% MAC
Airplane	B-25J No. 44-30328	Meteorological conditions	Hot summer day, ground heating.



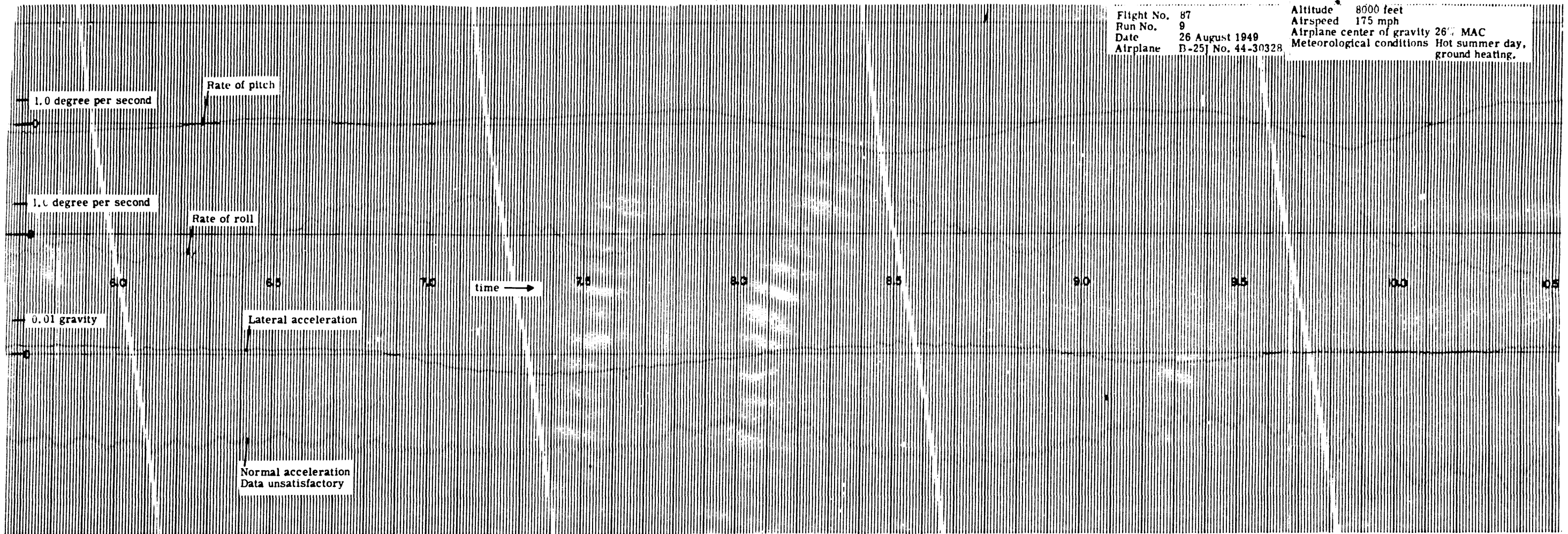
Flight No.	87	Altitude	8000 feet
Run No.	8	Airspeed	175 mph
Date	26 August 1949	Airplane center of gravity	26% MAC
Airplane	B-25J No. 44-30328	Meteorological conditions	Hot summer day, ground heating.





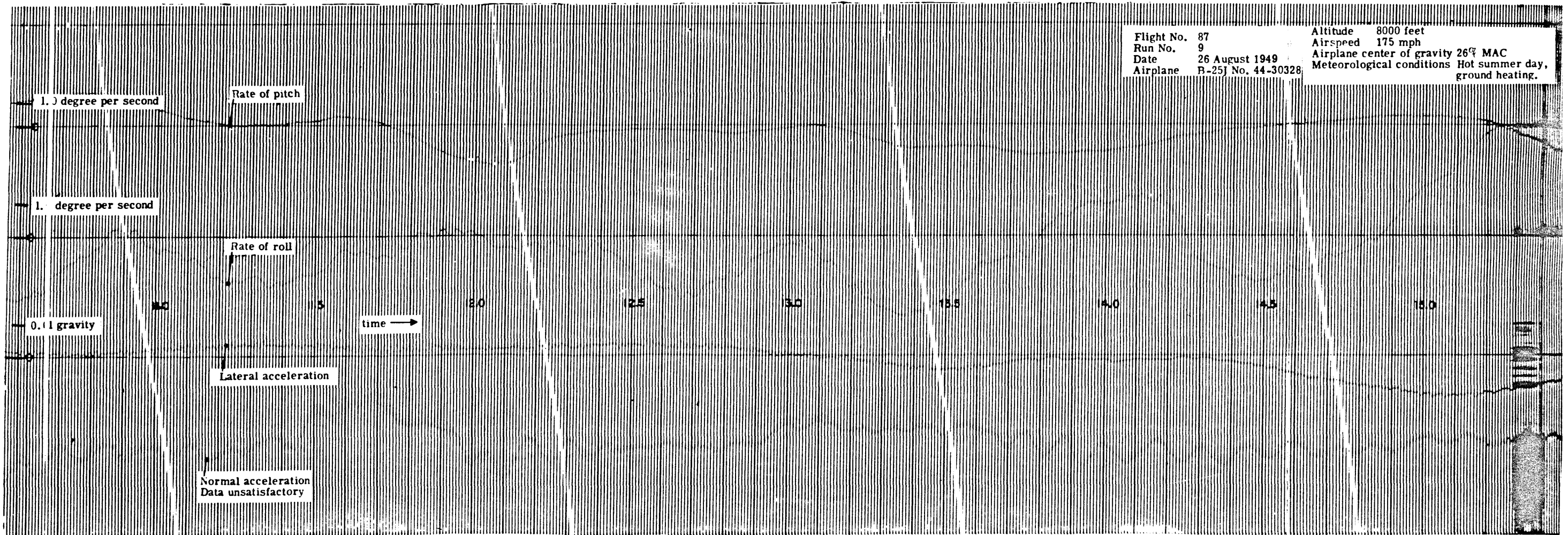
Flight No. 87
Run No. 9
Date 26 August 1949
Airplane B-25J No. 44-30328

Altitude 8000 feet
Airspeed 175 mph
Airplane center of gravity 26% MAC
Meteorological conditions Hot summer day,
ground heating.

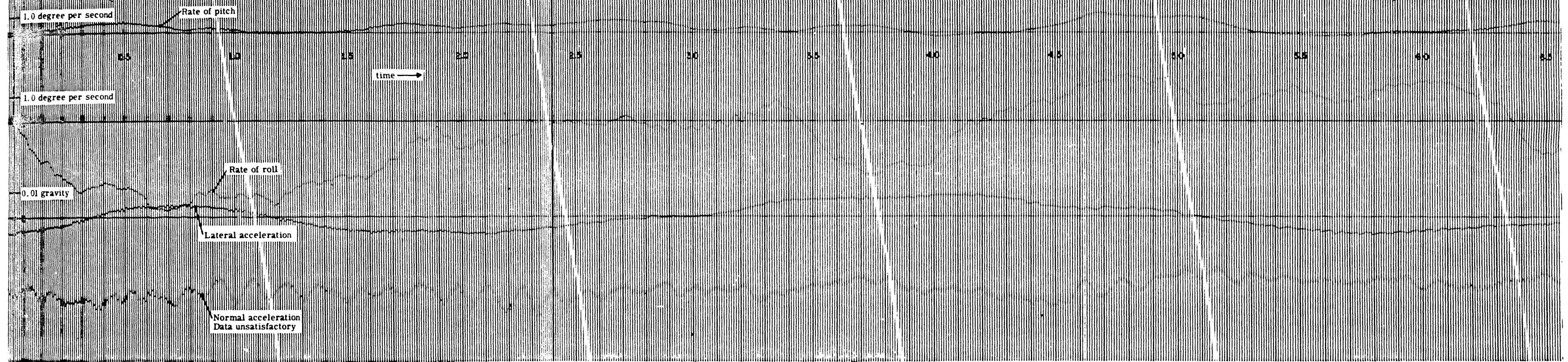


Flight No. 87
Run No. 9
Date 26 August 1949
Airplane B-25J No. 44-30328

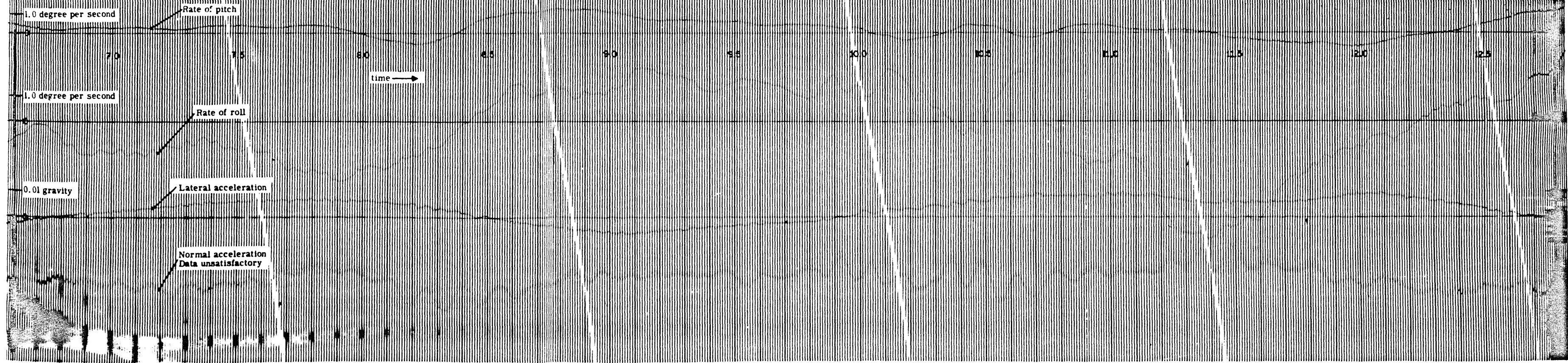
Altitude 8000 feet
Airspeed 175 mph
Airplane center of gravity 26% MAC
Meteorological conditions Hot summer day,
ground heating.



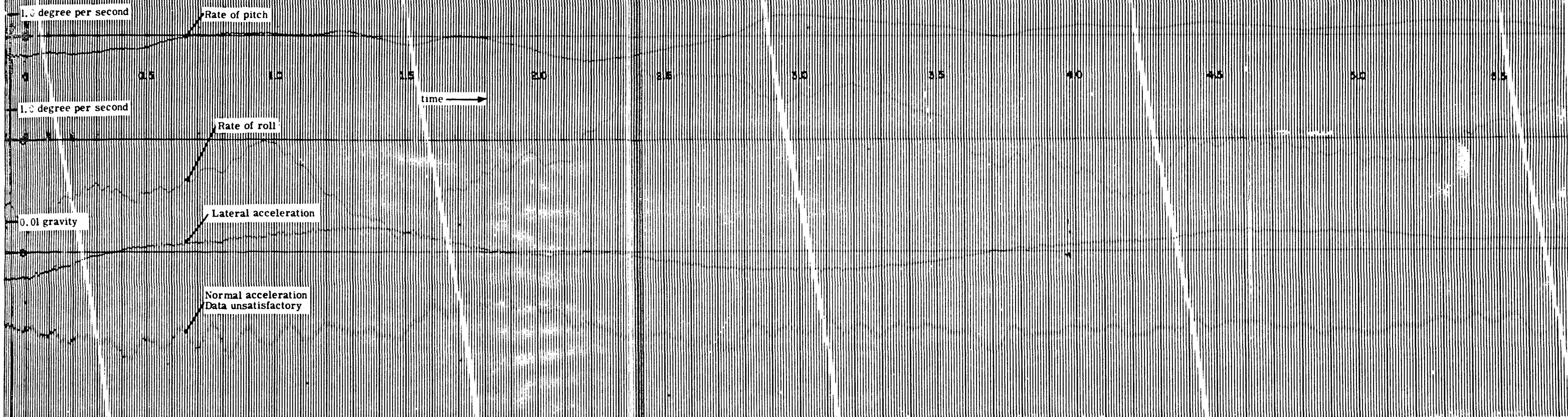
Flight No.	87	Altitude	8000 feet
Run No.	10	Airspeed	175 mph
Date	26 August 1949	Airplane center of gravity	26% MAC
Airplane	B-25J No. 44-30328	Meteorological conditions	Hot summer day, ground heating.



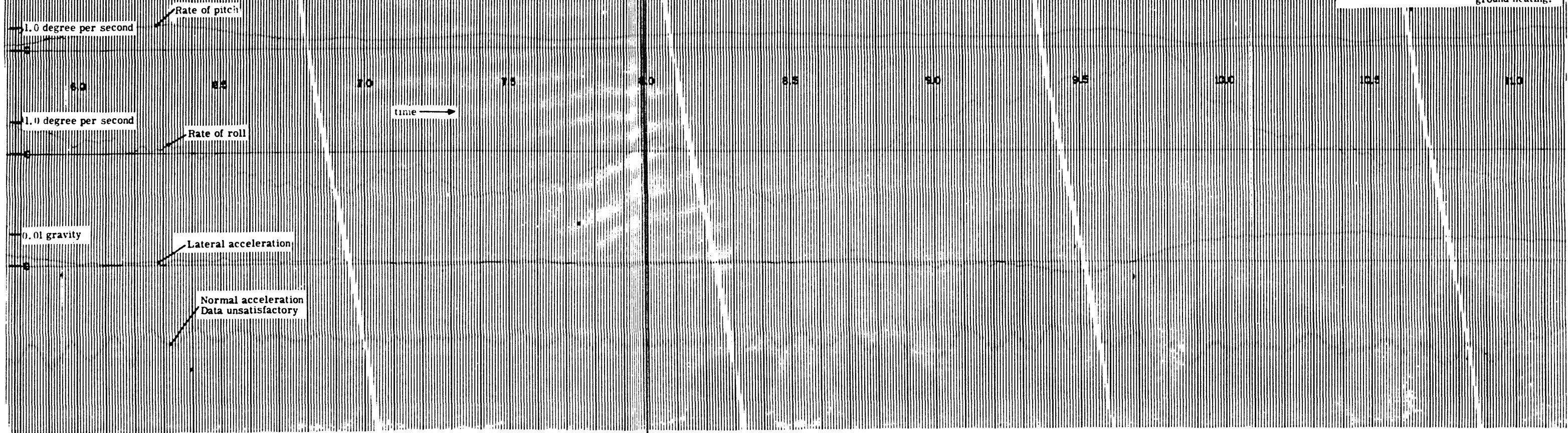
Flight No.	87	Altitude	8000 feet
Run No.	10	Airspeed	175 mph
Date	26 August 1949	Airplane center of gravity	26% MAC
Airplane	B-25J No. 44-30328	Meteorological conditions	Hot summer day, ground heating.



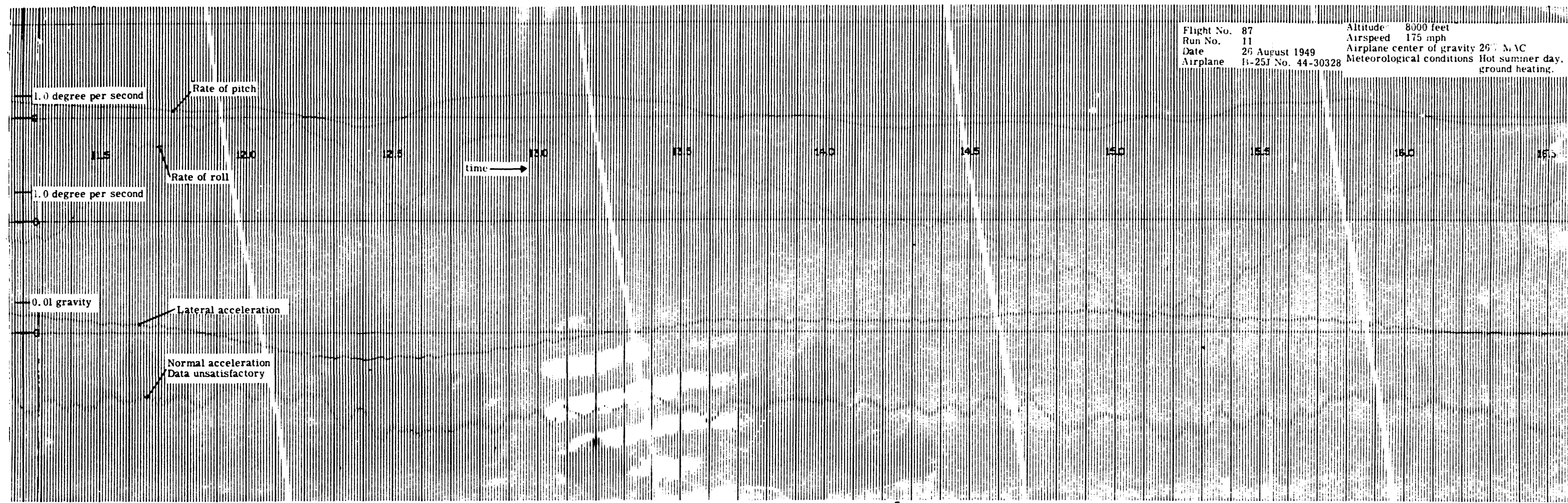
Flight No.	87	Altitude	8000 feet
Run No.	11	Airspeed	175 mph
Date	23 August 1949	Airplane center of gravity	26% MAC
Airplane	B-25J No. 44-30328	Meteorological conditions	Hot summer day, ground heating.



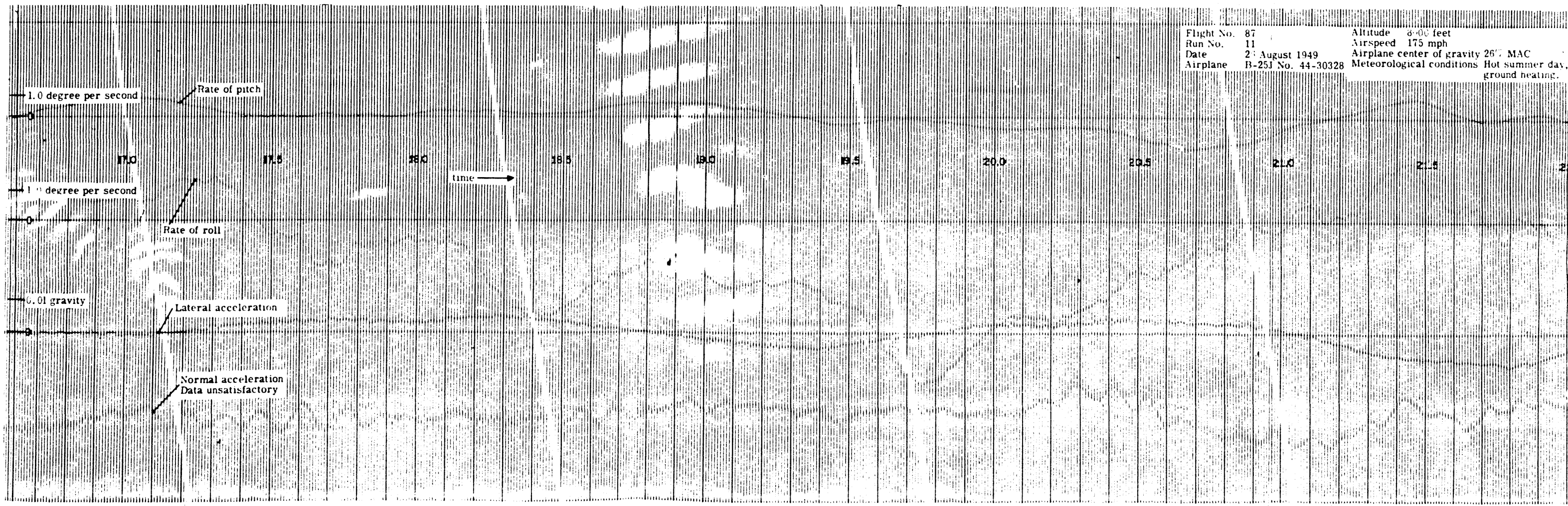
Flight No.	87	Altitude	8000 feet
Run No.	11	Airspeed	175 mph
Date	23 August 1949	Airplane center of gravity	26% MAC
Airplane	B-25J No. 44-30328	Meteorological conditions	Hot summer day, ground heating.



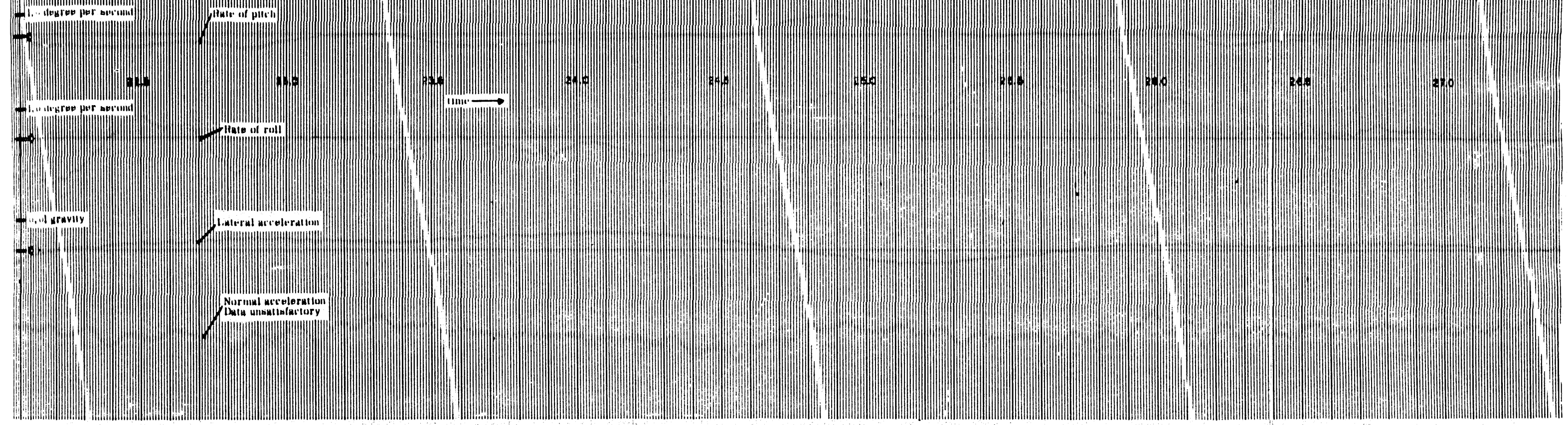
Flight No. 87 Altitude 8000 feet
 Run No. 11 Airspeed 175 mph
 Date 26 August 1949 Airplane center of gravity 26% MAC
 Airplane B-25J No. 44-30328 Meteorological conditions Hot summer day, ground heating.



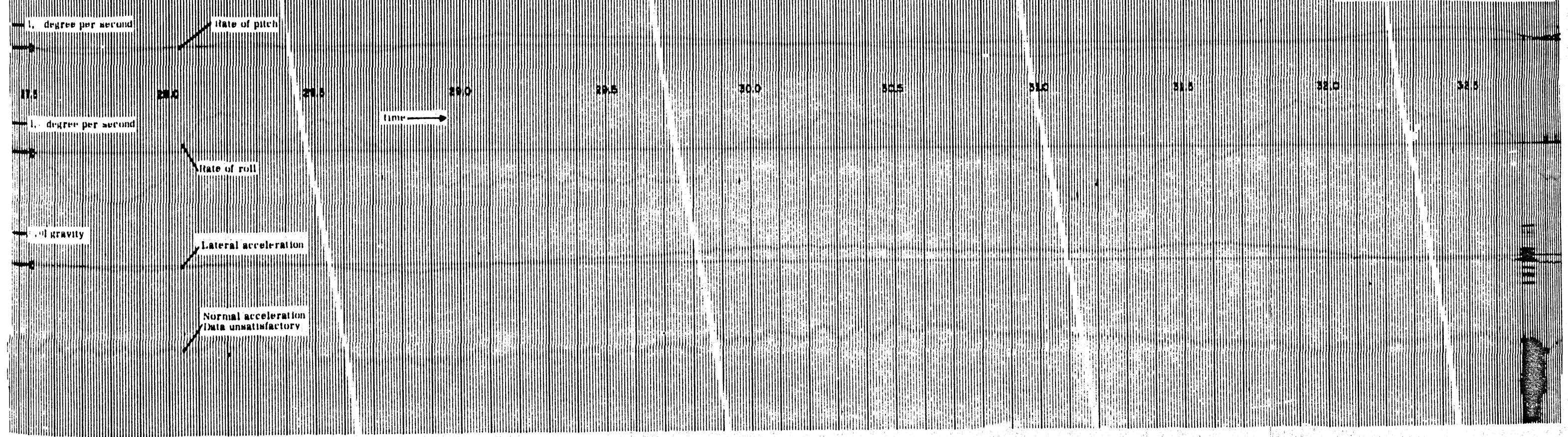
Flight No. 87 Altitude 8000 feet
 Run No. 11 Airspeed 175 mph
 Date 27 August 1949 Airplane center of gravity 26% MAC
 Airplane B-25J No. 44-30328 Meteorological conditions Hot summer day, ground heating.

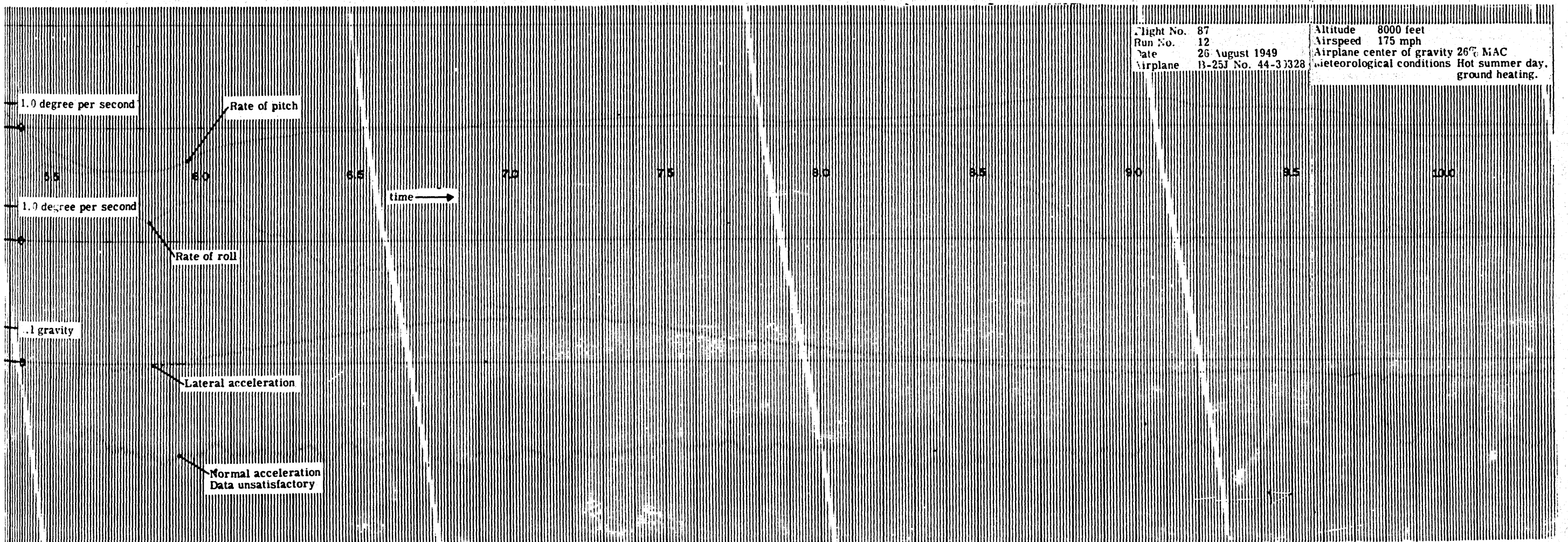
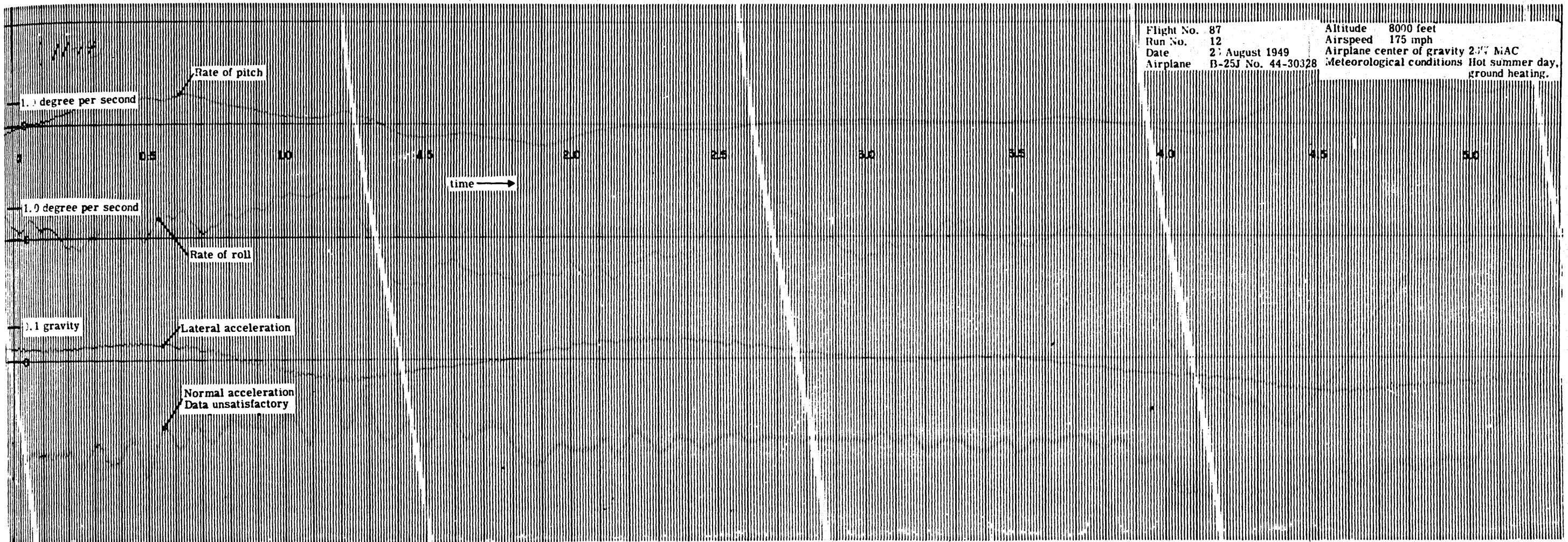


Flight No.	87	Altitude	8000 feet
Run No.	11	Airspeed	175 mph
Date	29 August 1949	Airplane center of gravity	26% MAC
Airplane	B-25J No. 44-3131	Meteorological conditions	Hot summer day, ground heating.

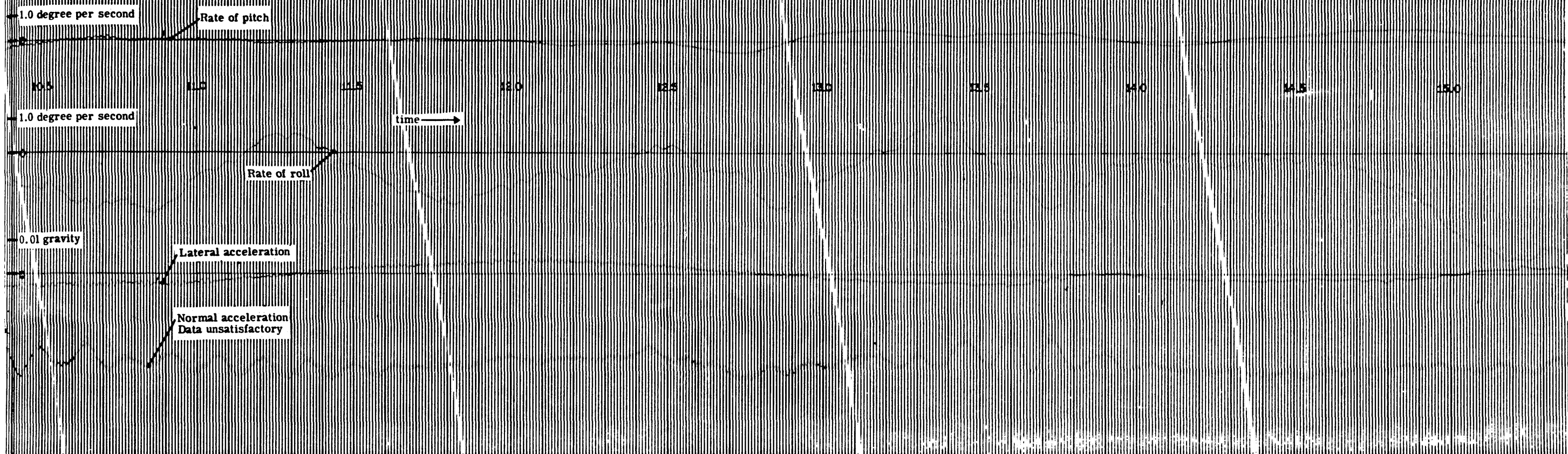


Flight No.	87	Altitude	8000 feet
Run No.	11	Airspeed	175 mph
Date	29 August 1949	Airplane center of gravity	26% MAC
Airplane	B-25J No. 44-30328	Meteorological conditions	Hot summer day, ground heating.

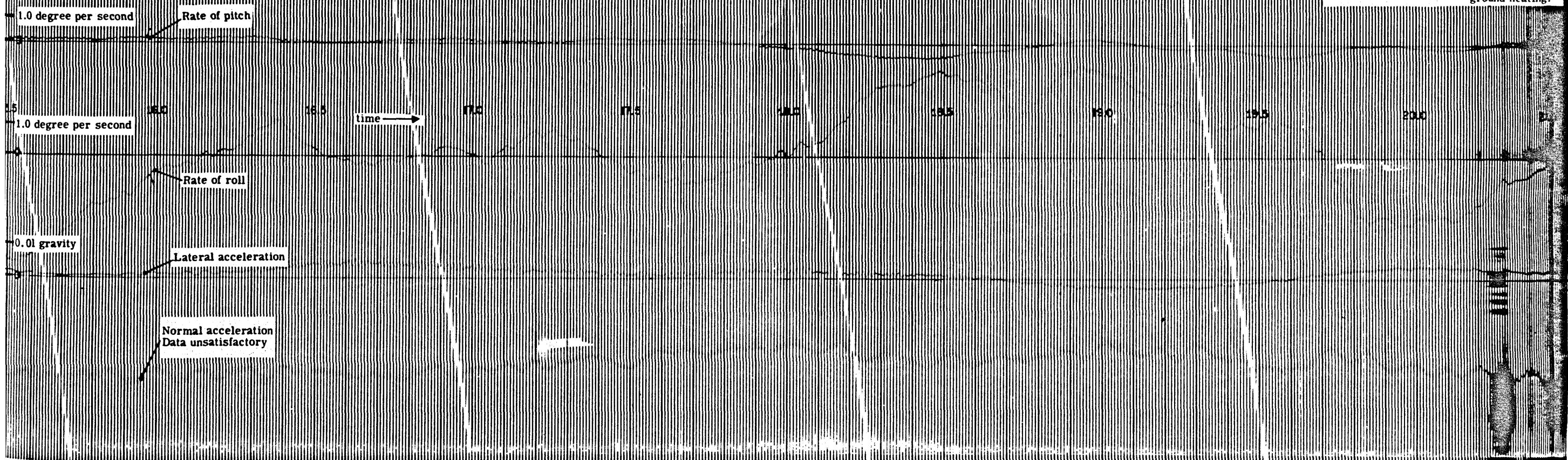




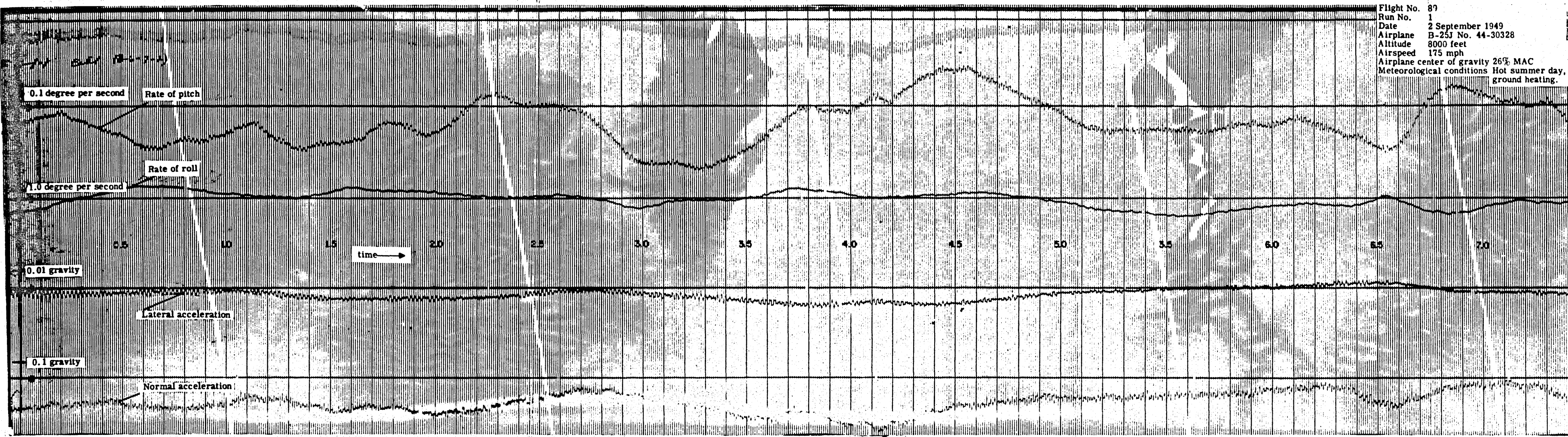
Flight No. 87 Altitude 8000 feet
 Run No. 12 Airspeed 175 mph
 Date 26 August 1949 Airplane center of gravity 26% MAC
 Airplane B-25J No. 44-30328 Meteorological conditions Hot summer day, ground heating.



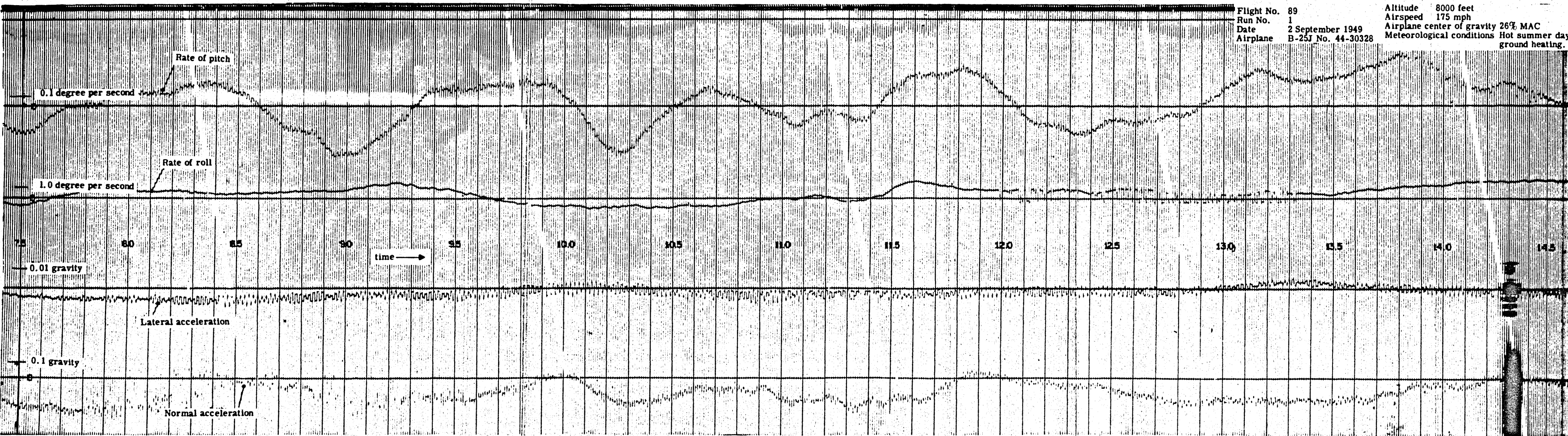
Flight No. 87 Altitude 8000 feet
 Run No. 12 Airspeed 175 mph
 Date 26 August 1949 Airplane center of gravity 26% MAC
 Airplane B-25J No. 44-30328 Meteorological conditions Hot summer day, ground heating.

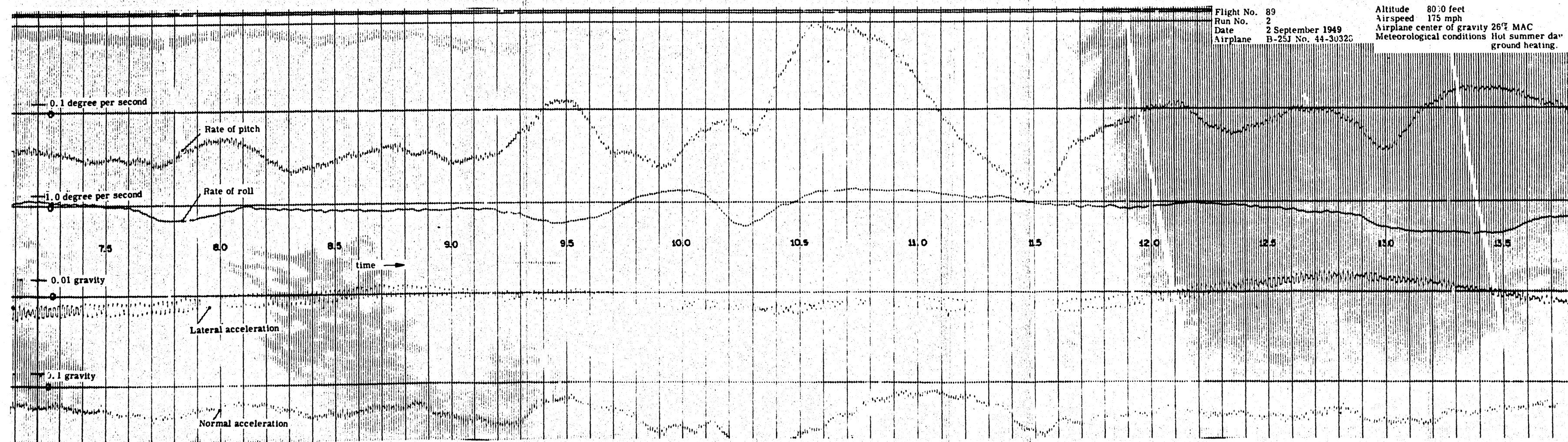
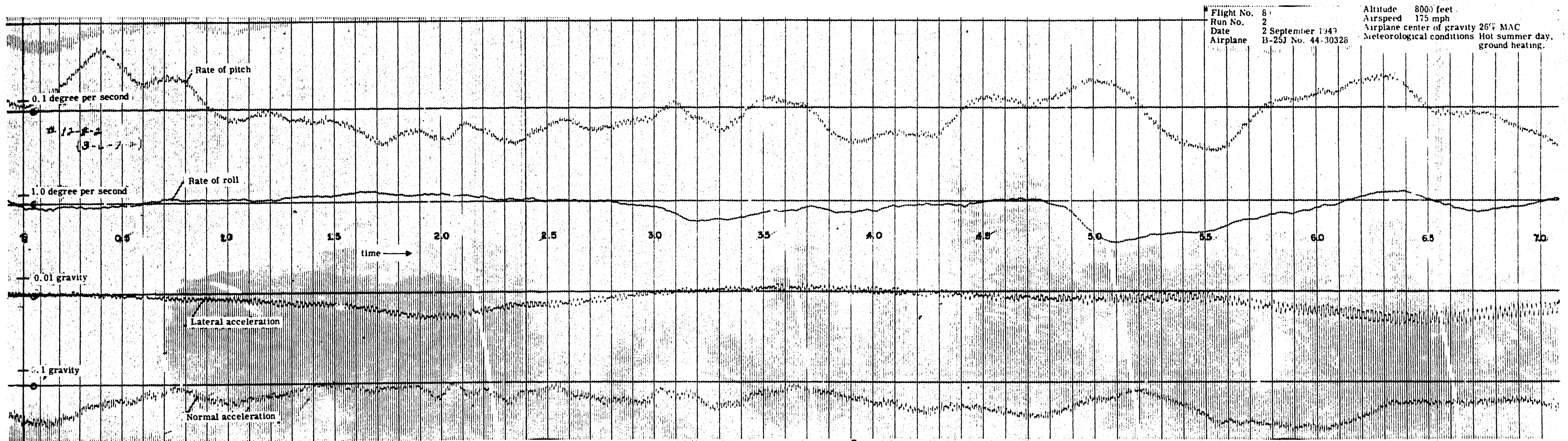


Flight No. 87
 Run No. 1
 Date 2 September 1949
 Airplane B-25J No. 44-30328
 Altitude 8000 feet
 Airspeed 175 mph
 Airplane center of gravity 26% MAC
 Meteorological conditions Hot summer day,
 ground heating.

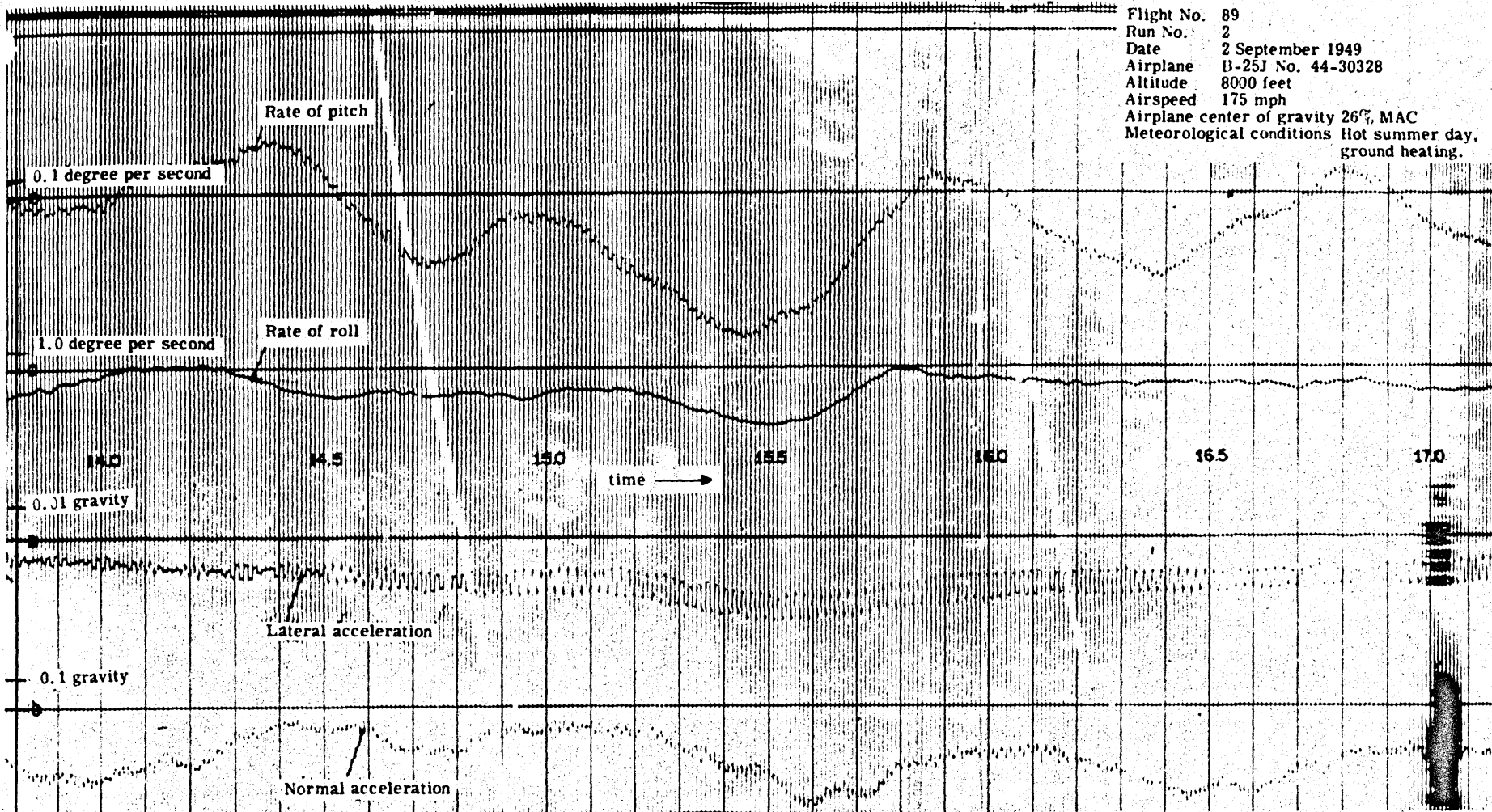


Flight No. 89
 Run No. 1
 Date 2 September 1949
 Airplane B-25J No. 44-30328
 Altitude 8000 feet
 Airspeed 175 mph
 Airplane center of gravity 26% MAC
 Meteorological conditions Hot summer day,
 ground heating.

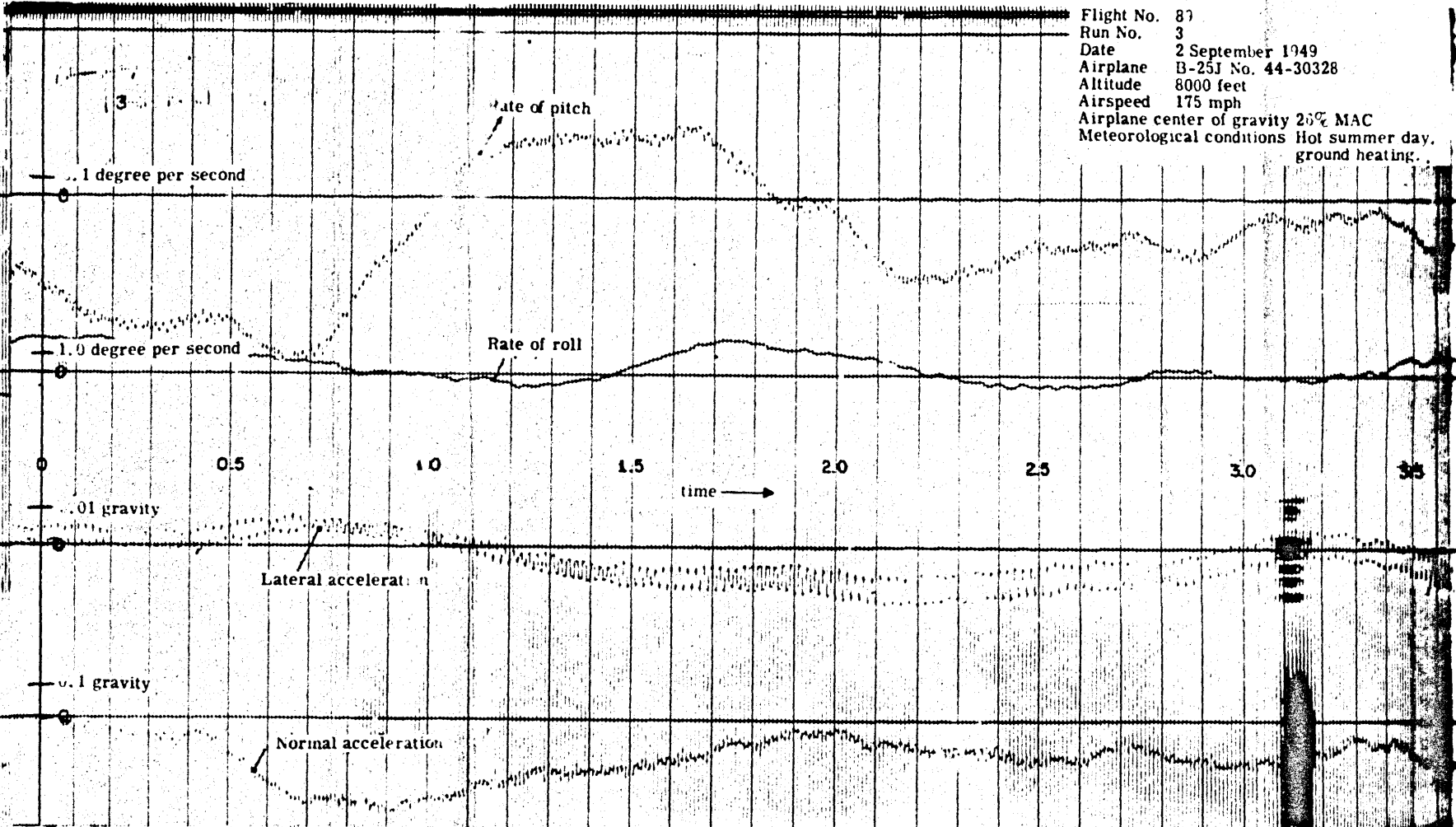




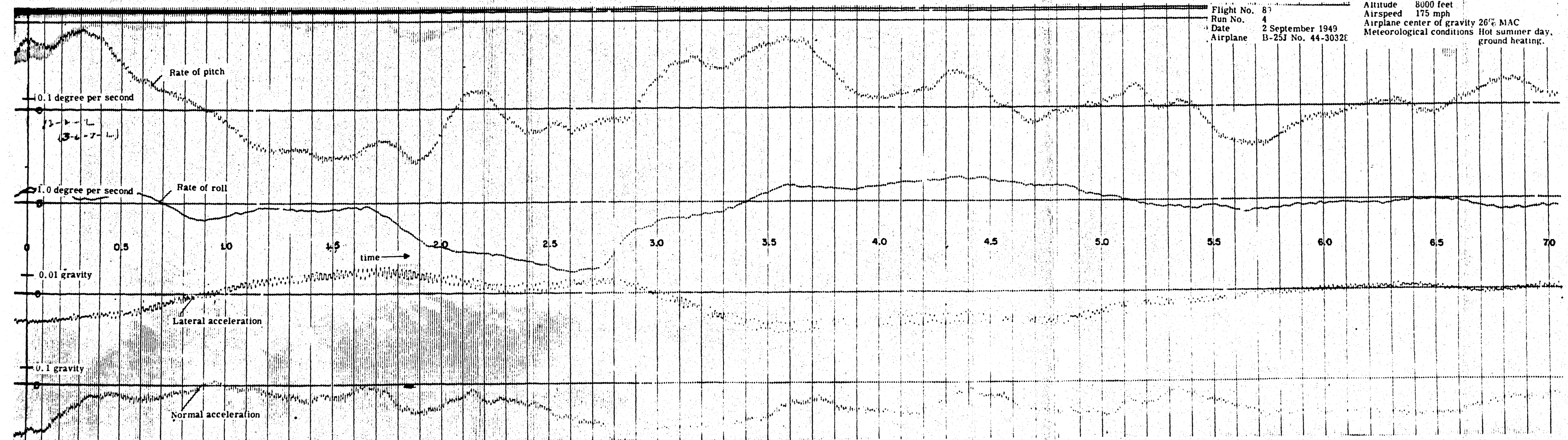
Flight No. 89
 Run No. 2
 Date 2 September 1949
 Airplane B-25J No. 44-30328
 Altitude 8000 feet
 Airspeed 175 mph
 Airplane center of gravity 26% MAC
 Meteorological conditions Hot summer day,
 ground heating.

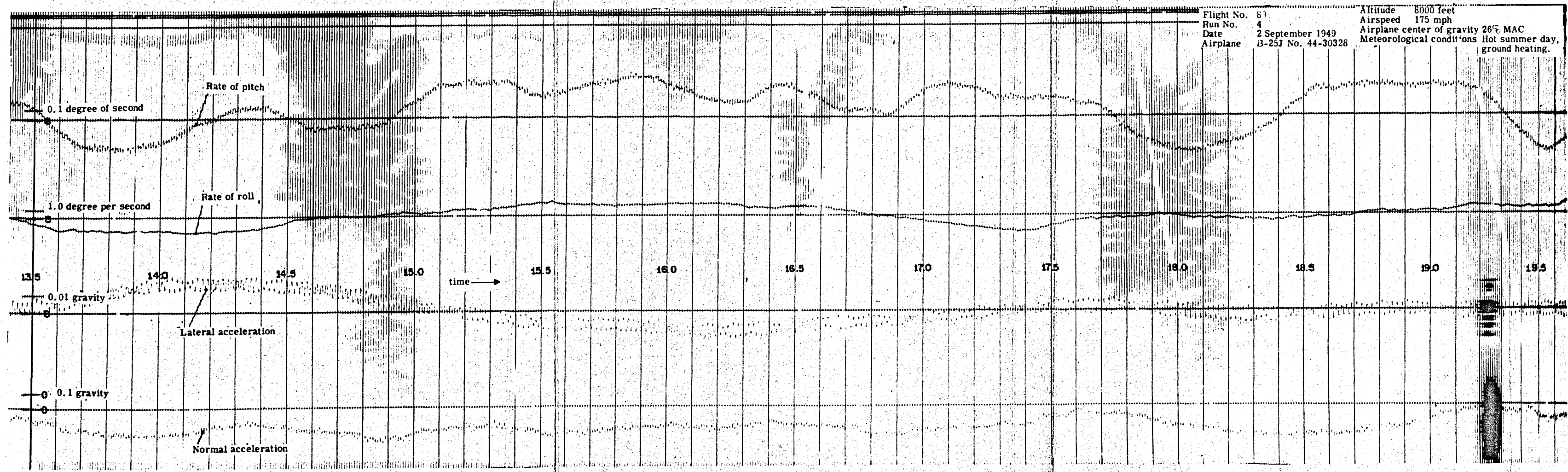
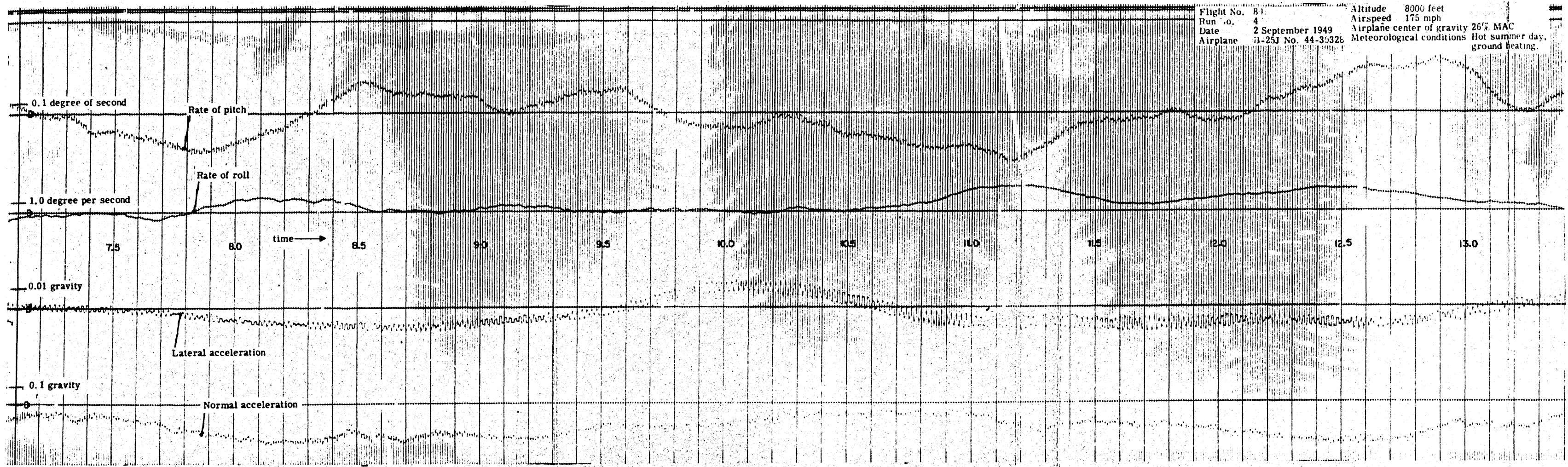


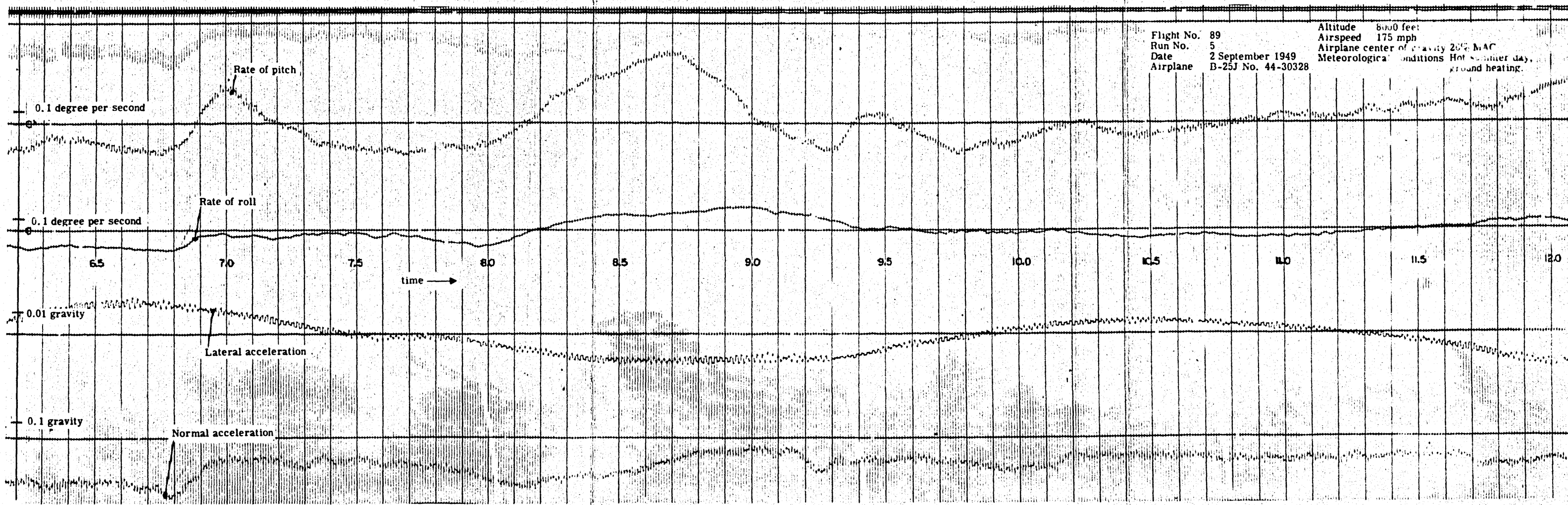
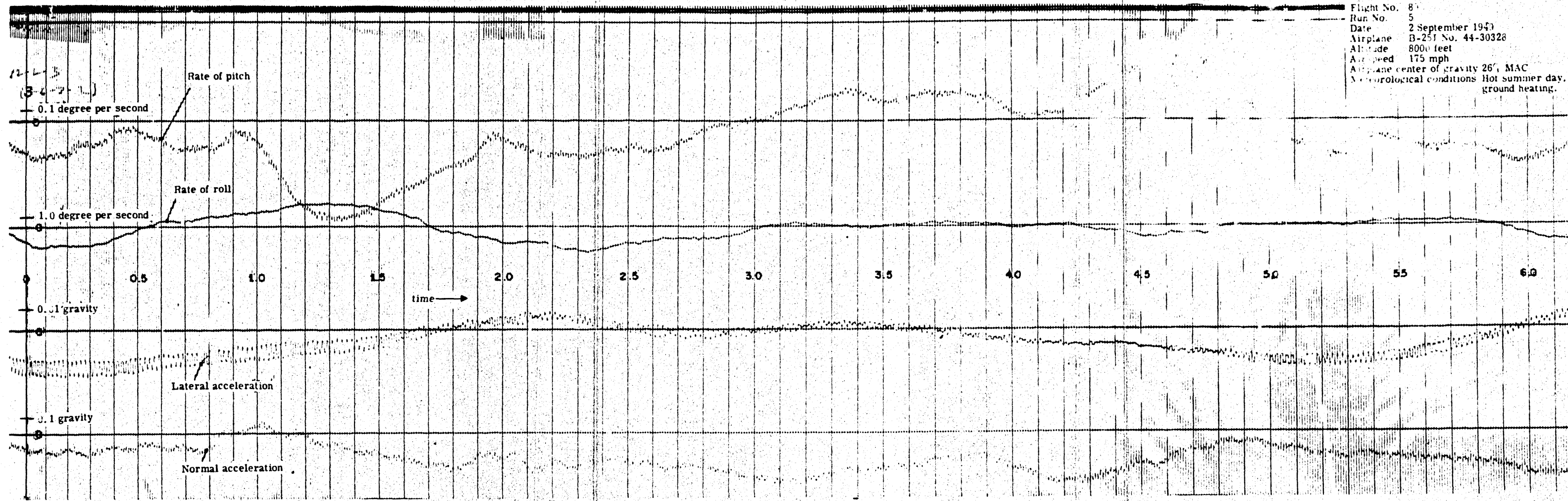
Flight No. 87
 Run No. 3
 Date 2 September 1949
 Airplane B-25J No. 44-30328
 Altitude 8000 feet
 Airspeed 175 mph
 Airplane center of gravity 26% MAC
 Meteorological conditions Hot summer day,
 ground heating.



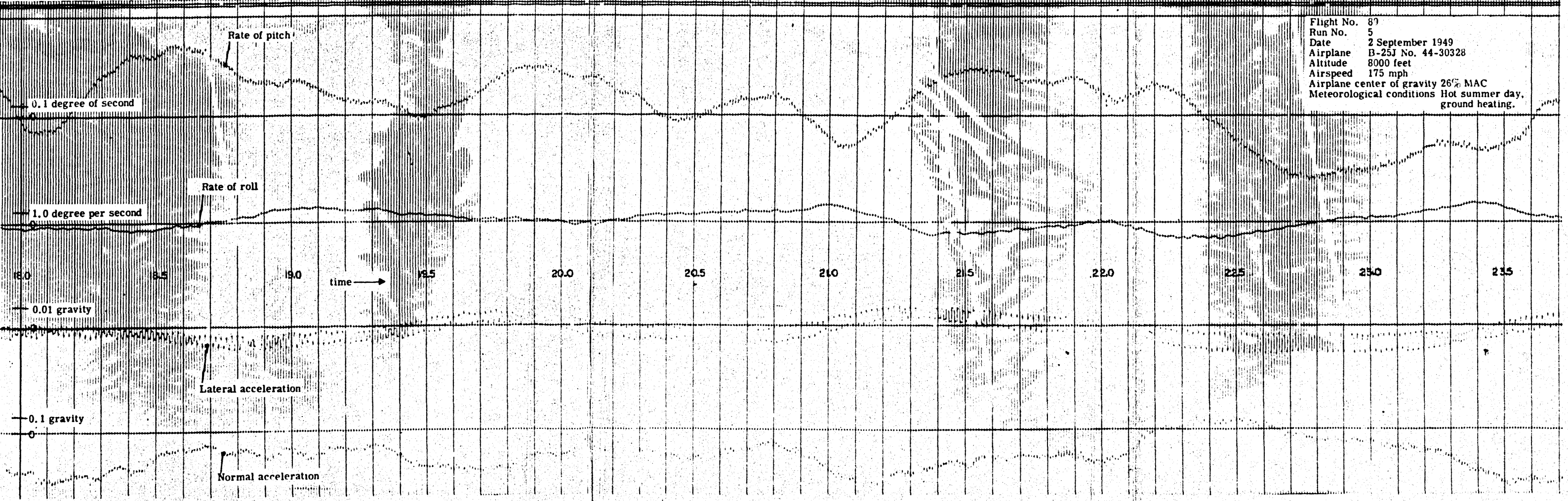
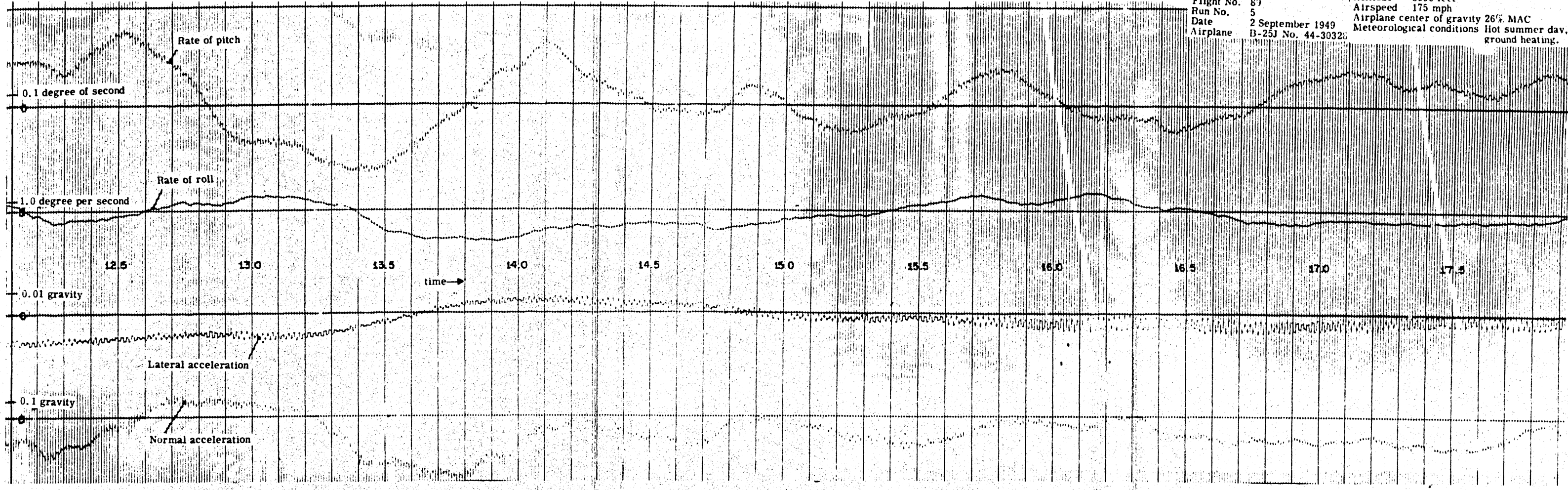
Flight No. 87
 Run No. 4
 Date 2 September 1949
 Airplane B-25J No. 44-30328
 Altitude 8000 feet
 Airspeed 175 mph
 Airplane center of gravity 26% MAC
 Meteorological conditions Hot summer day,
 ground heating.



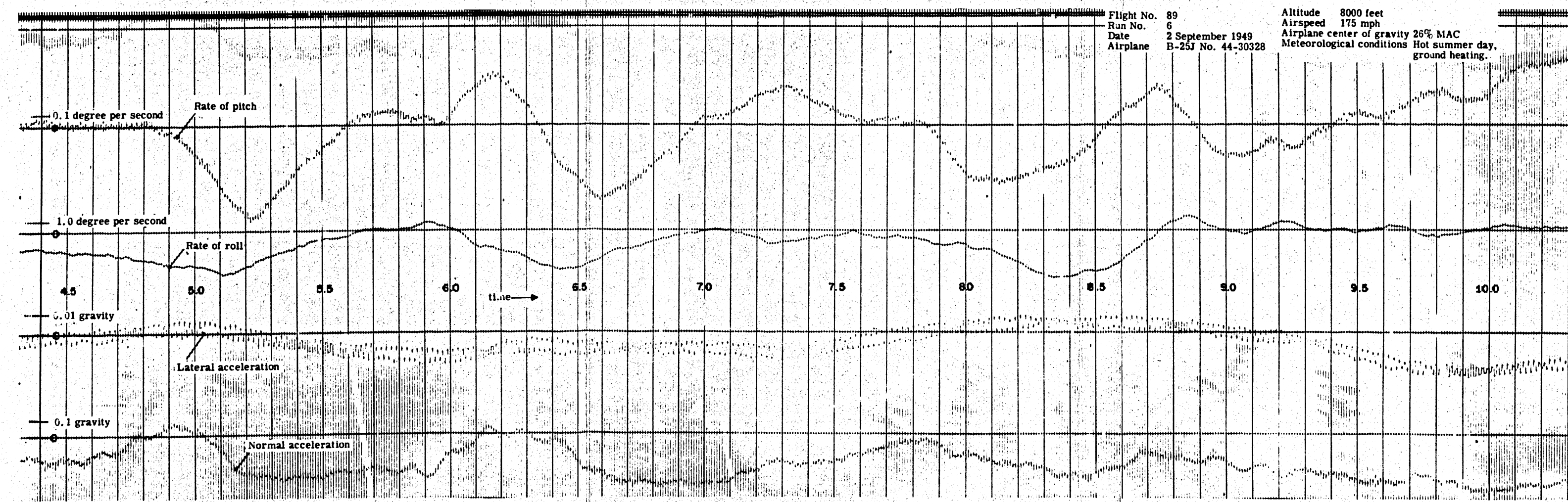
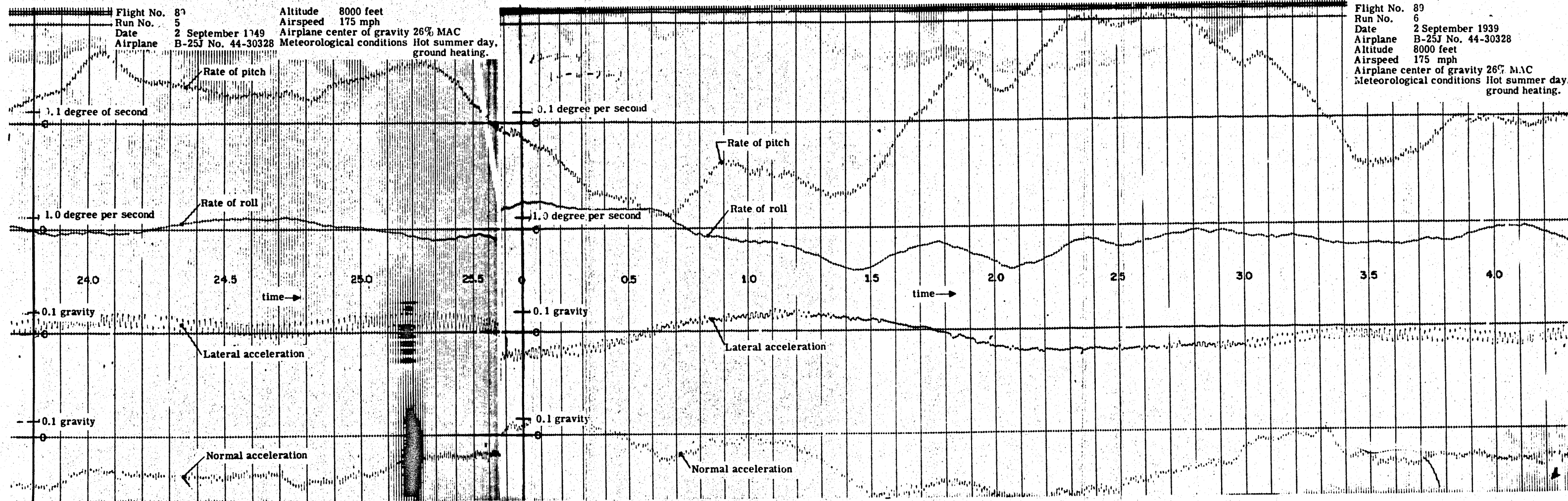




Flight No. 89 Altitude 8000 feet
 Run No. 5 Airspeed 175 mph
 Date 2 September 1949 Airplane center of gravity 26% MAC
 Airplane B-25J No. 44-30328 Meteorological conditions Hot summer day, ground heating.

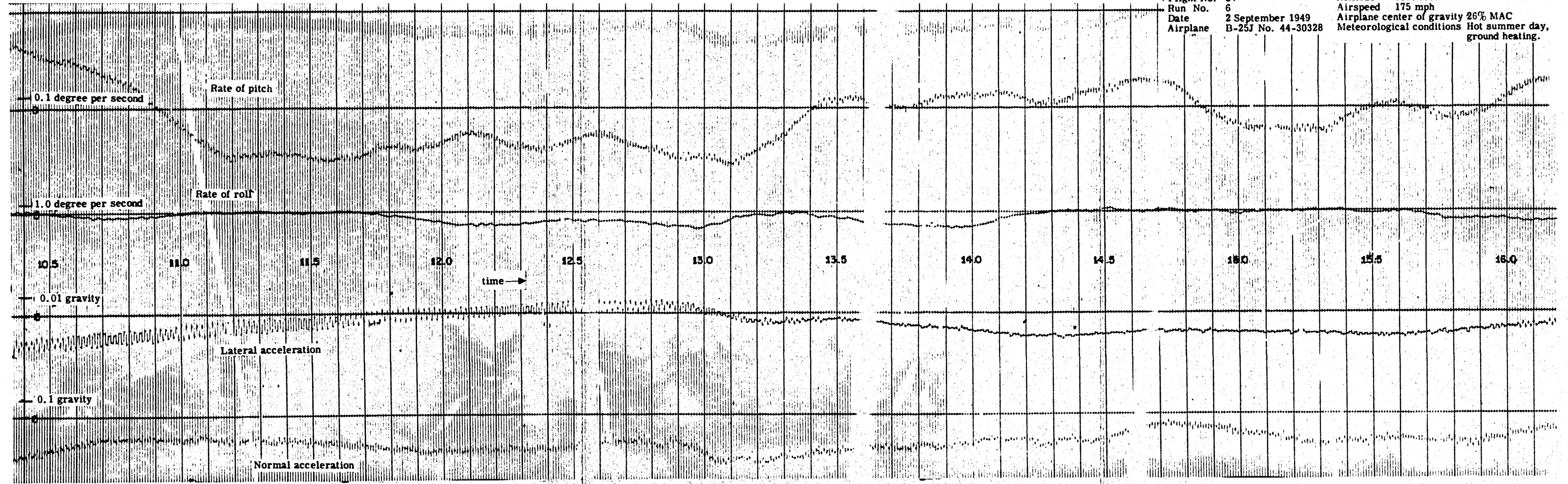


Flight No. 89
 Run No. 5
 Date 2 September 1949
 Airplane B-25J No. 44-30328
 Altitude 8000 feet
 Airspeed 175 mph
 Airplane center of gravity 26% MAC
 Meteorological conditions Hot summer day, ground heating.



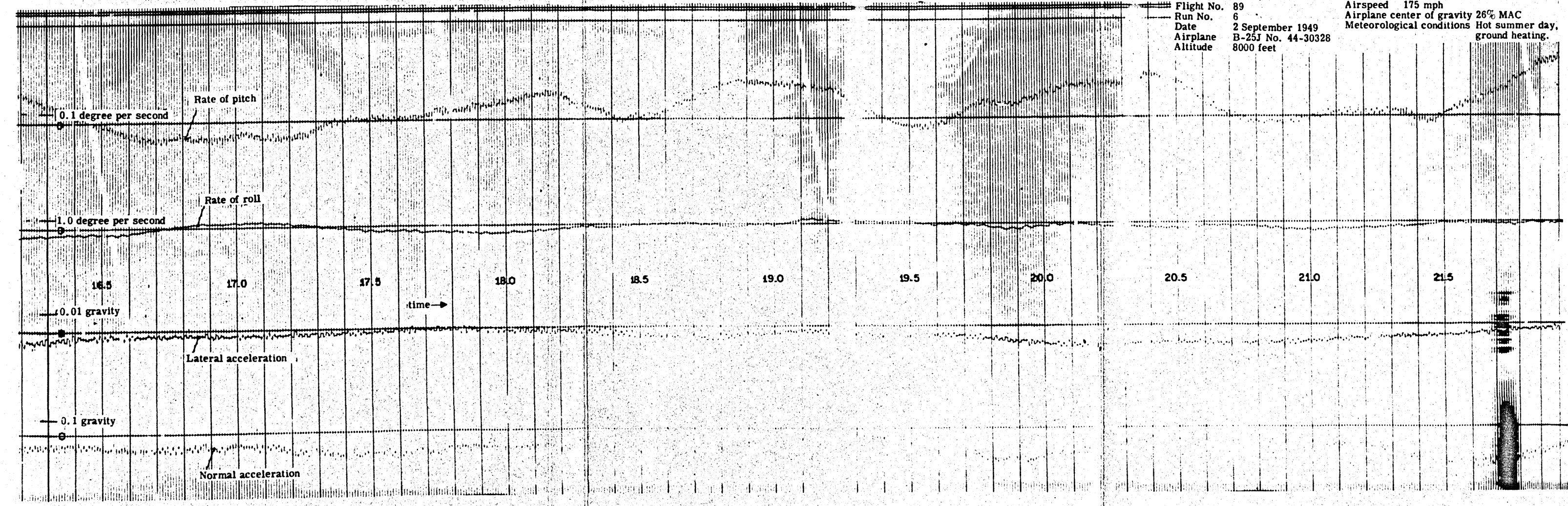
Flight No. 89
 Run No. 6
 Date 2 September 1949
 Airplane B-25J No. 44-30328

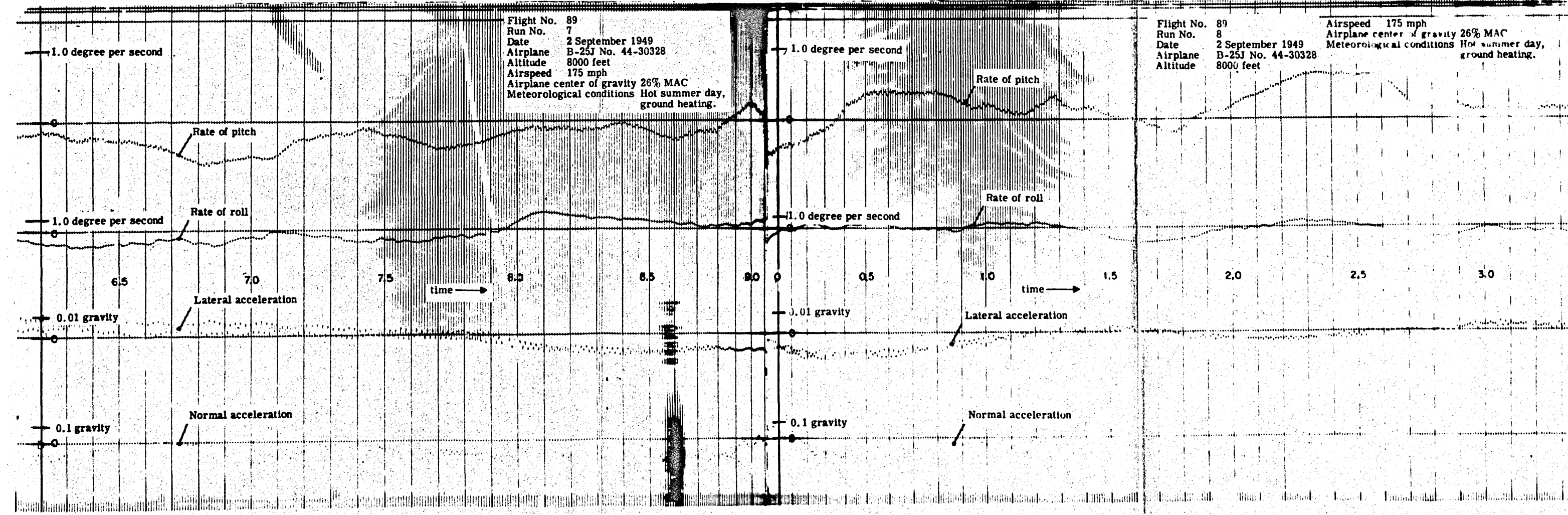
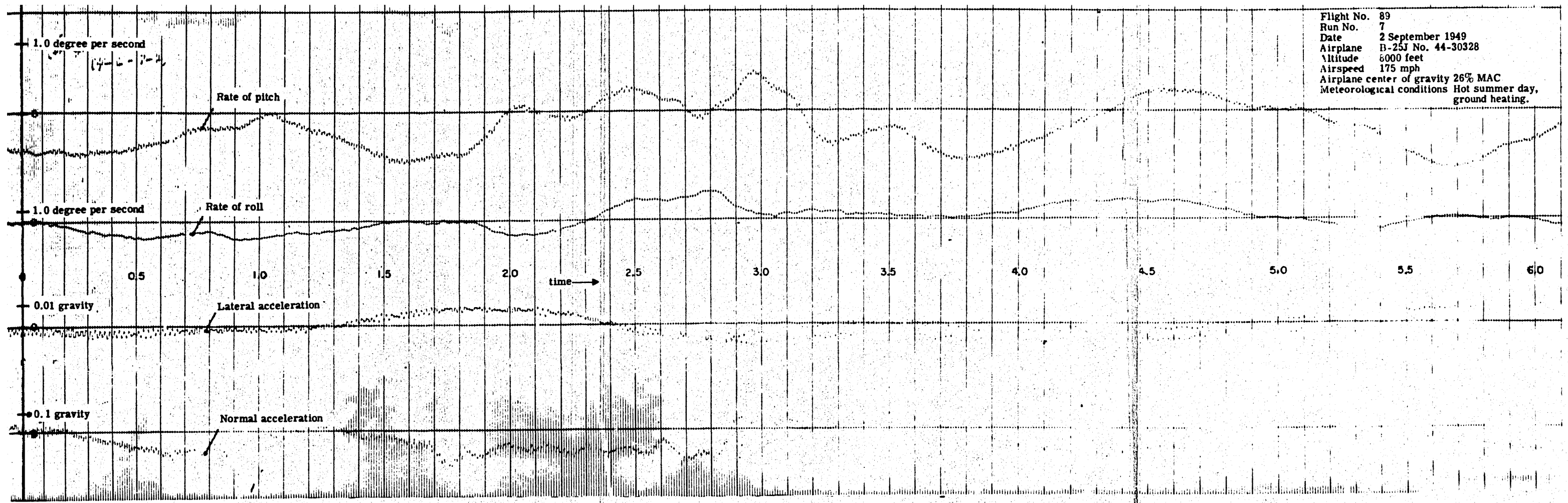
Altitude 8000 feet
 Airspeed 175 mph
 Airplane center of gravity 26% MAC
 Meteorological conditions Hot summer day, ground heating.

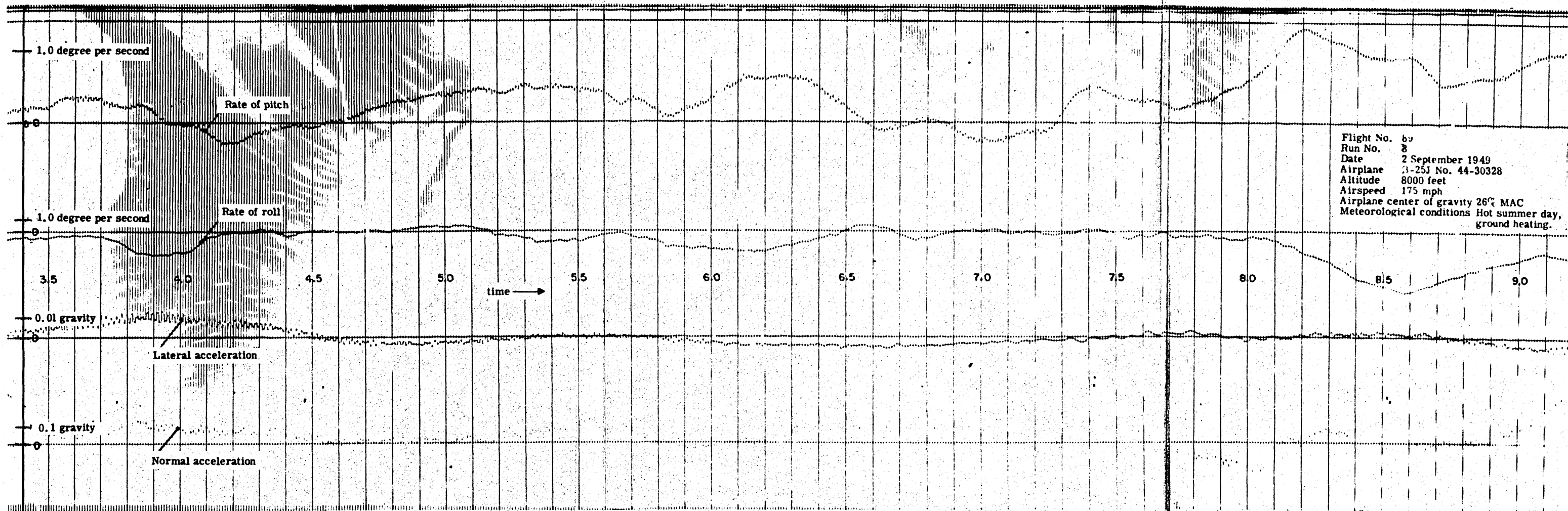


Flight No. 89
 Run No. 6
 Date 2 September 1949
 Airplane B-25J No. 44-30328
 Altitude 8000 feet

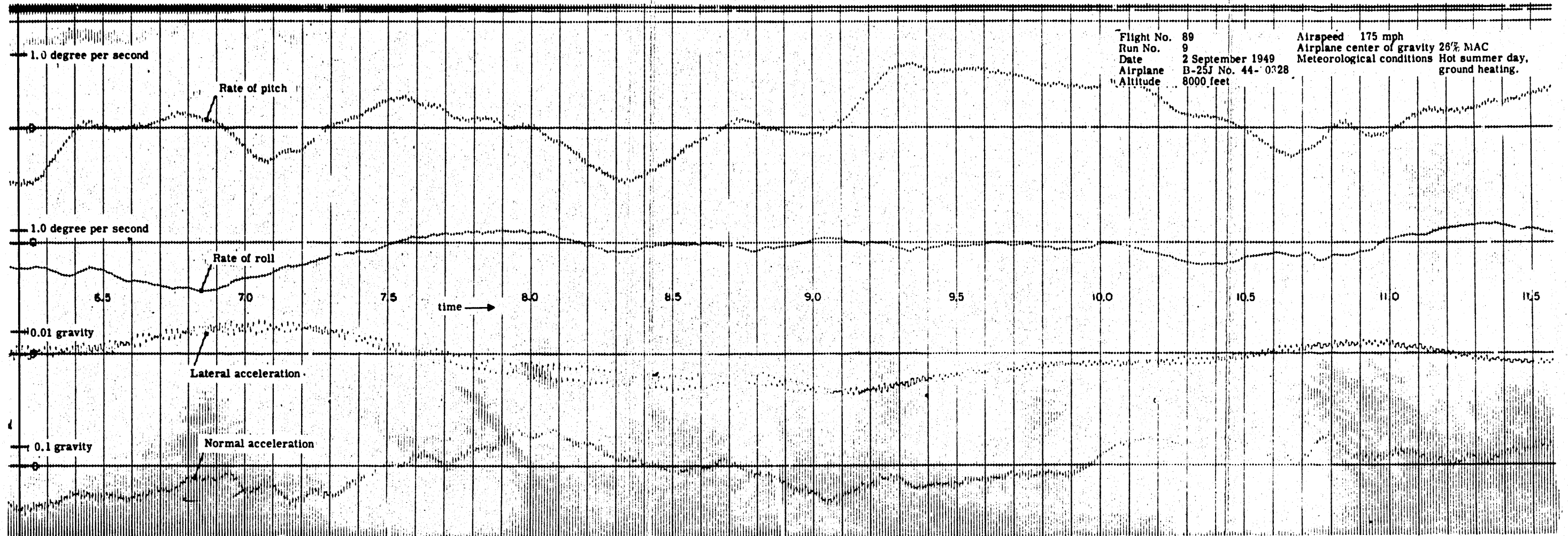
Airspeed 175 mph
 Airplane center of gravity 26% MAC
 Meteorological conditions Hot summer day, ground heating.



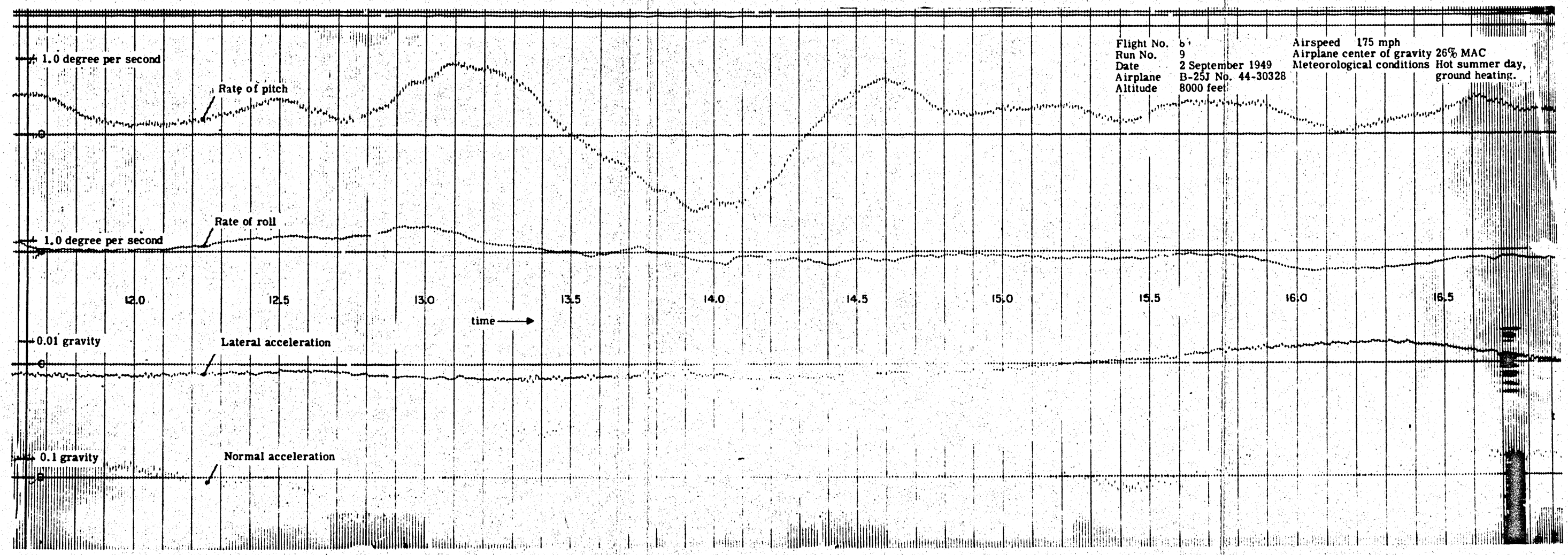


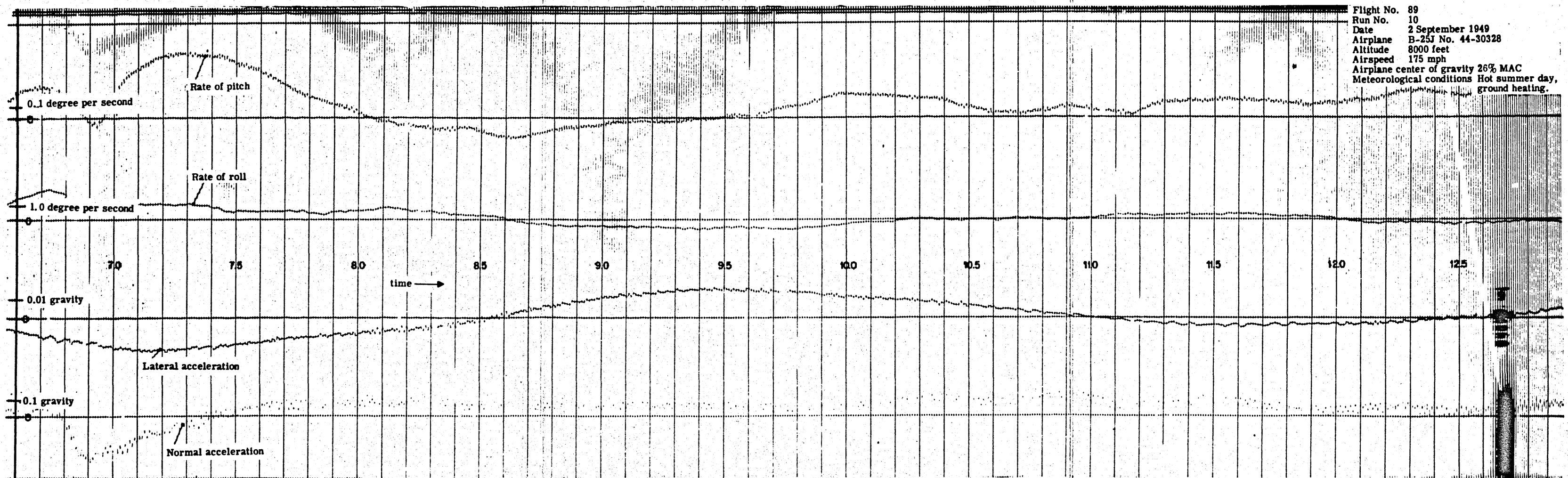
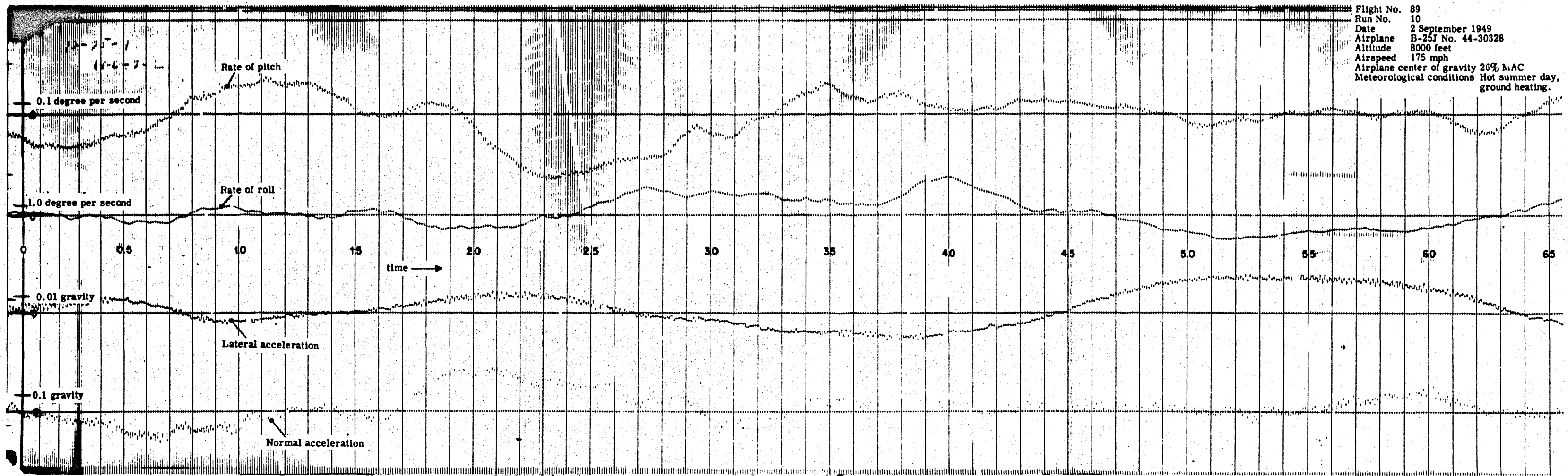


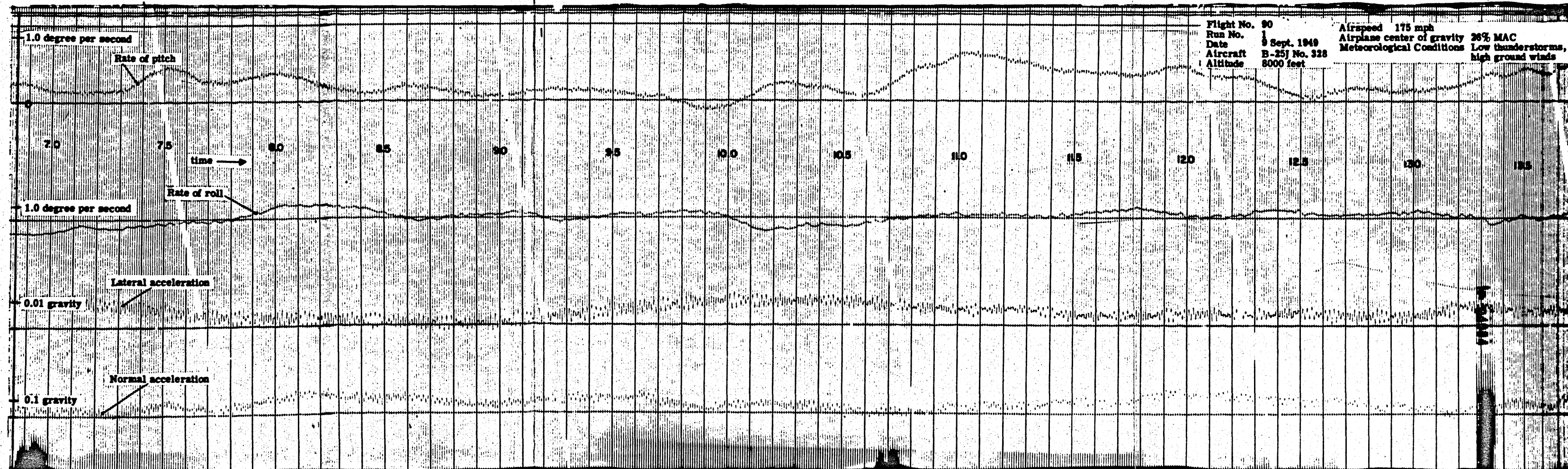
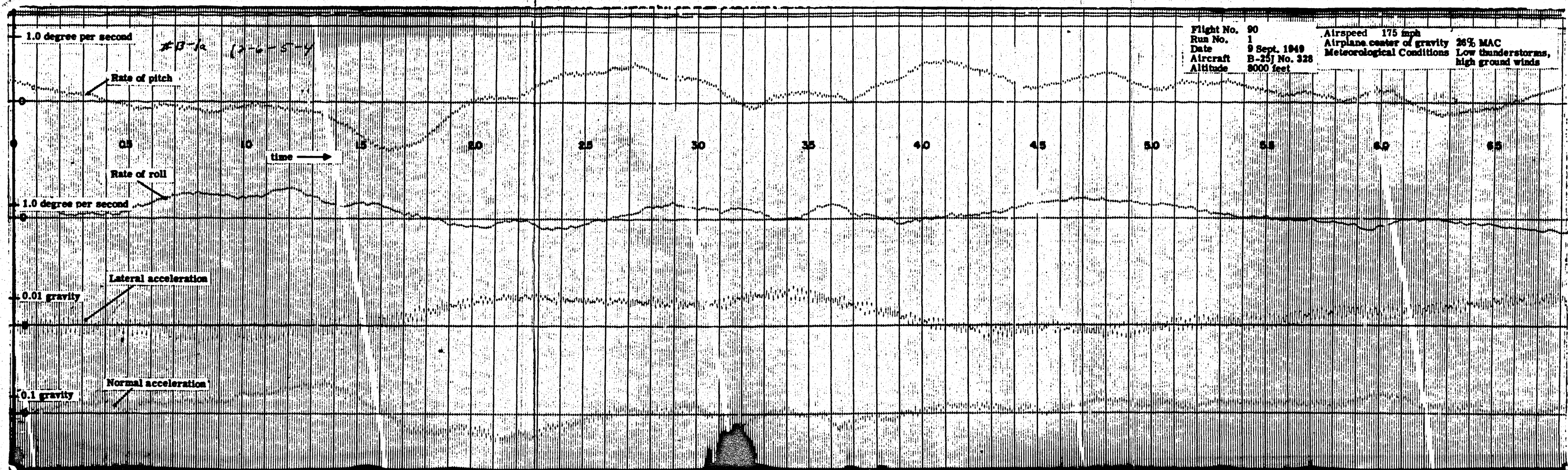
Flight No. 89 Airspeed 175 mph
 Run No. 9 Airplane center of gravity 26% MAC
 Date 2 September 1949 Meteorological conditions Hot summer day,
 Airplane B-25J No. 44-0328 ground heating.
 Altitude 8000 feet

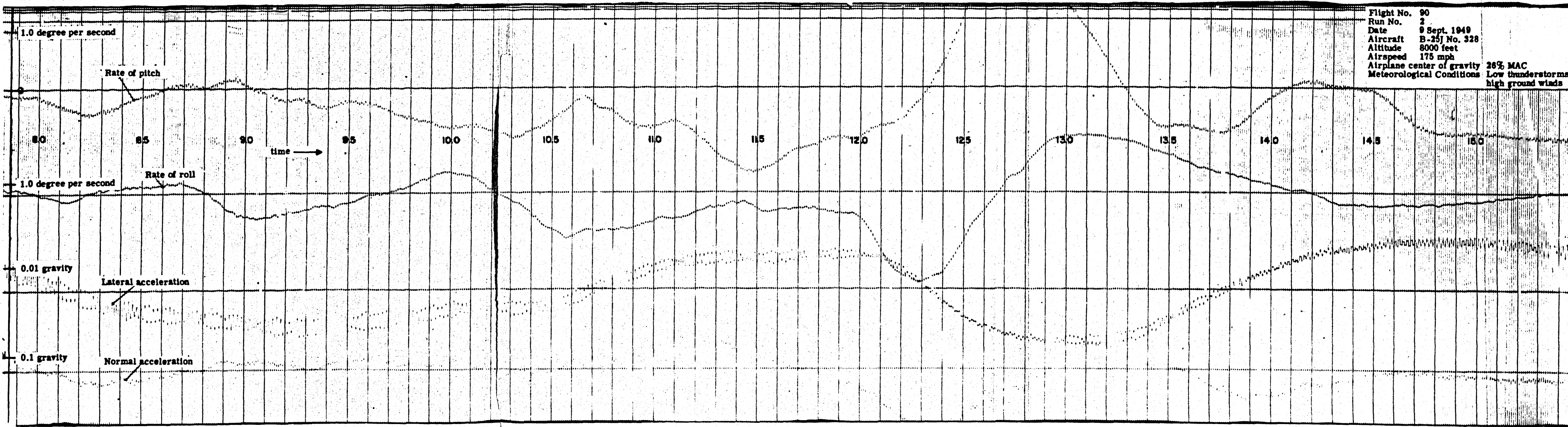
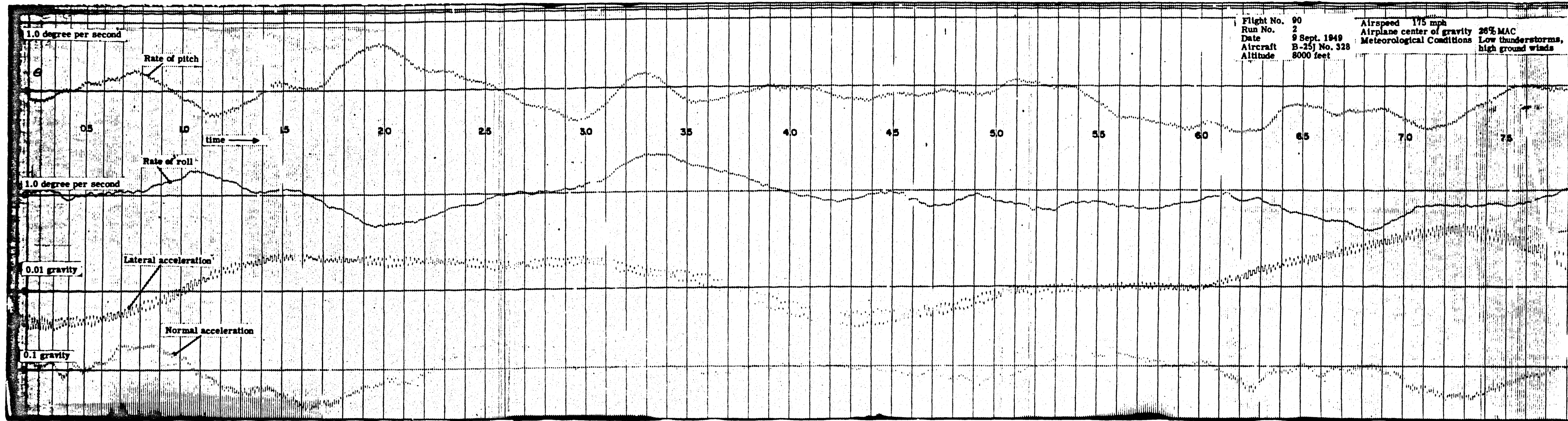


Flight No. 61 Airspeed 175 mph
 Run No. 9 Airplane center of gravity 26% MAC
 Date 2 September 1949 Meteorological conditions Hot summer day,
 Airplane B-25J No. 44-30328 ground heating.
 Altitude 8000 feet



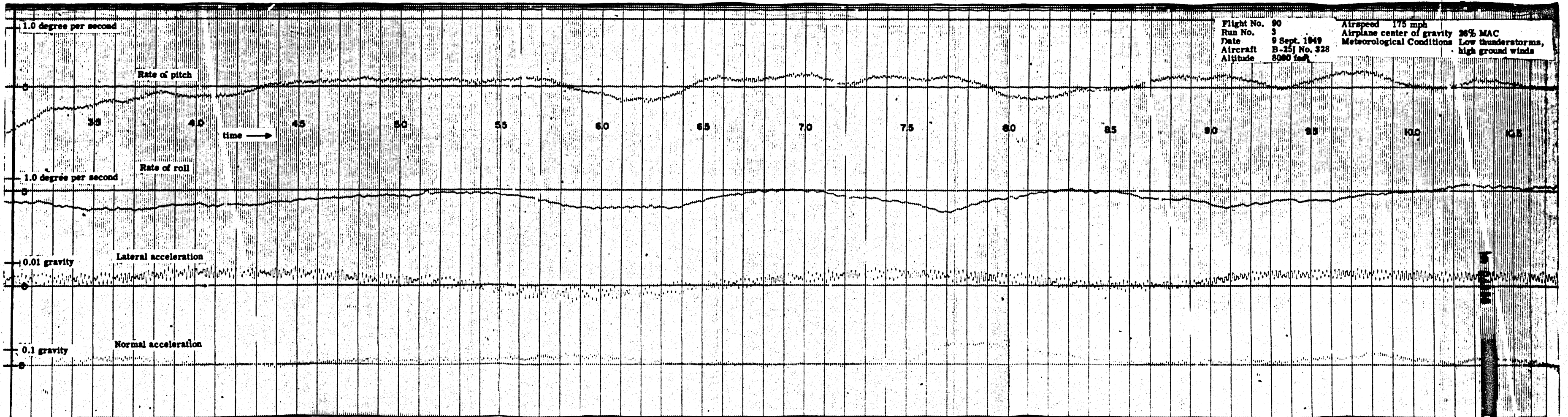
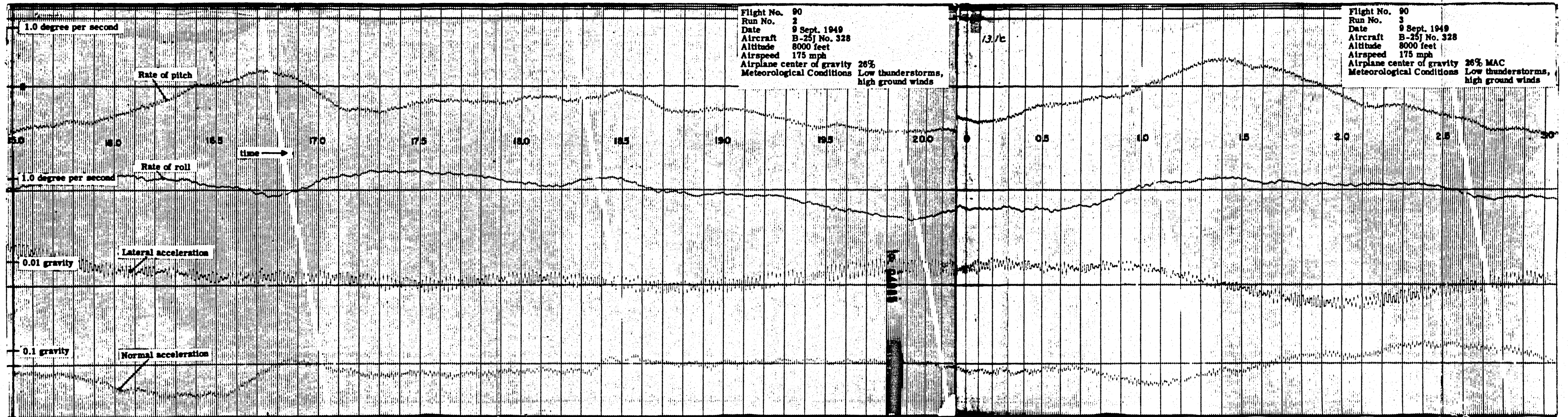


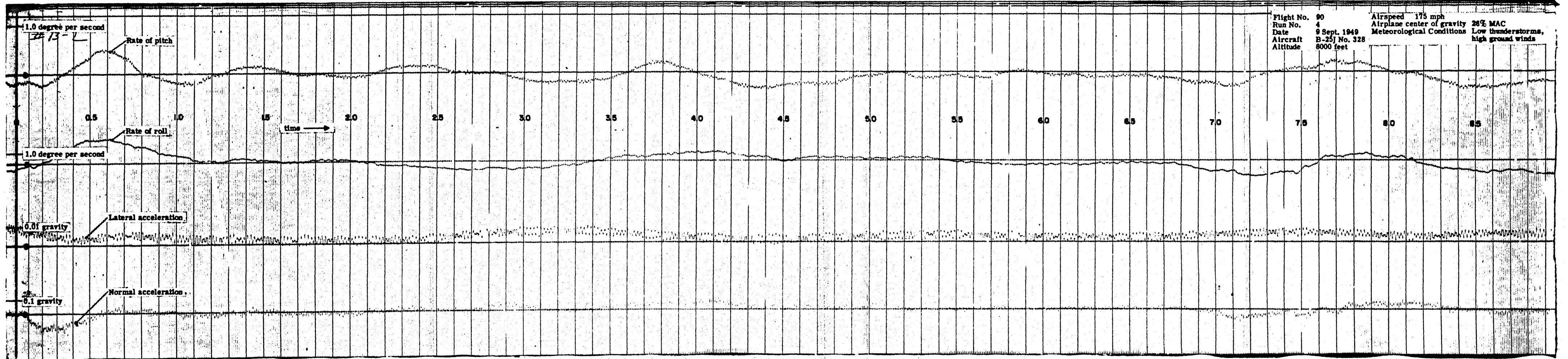


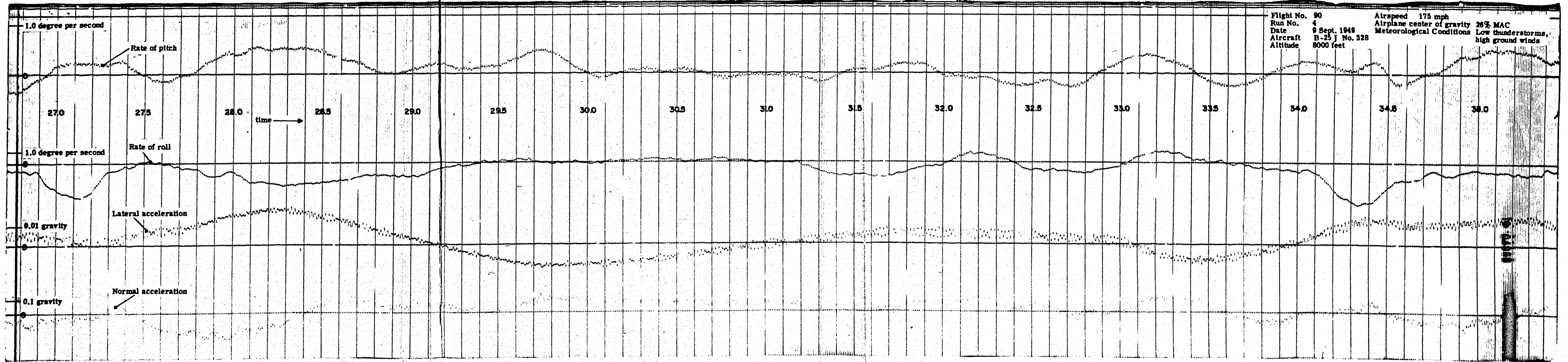
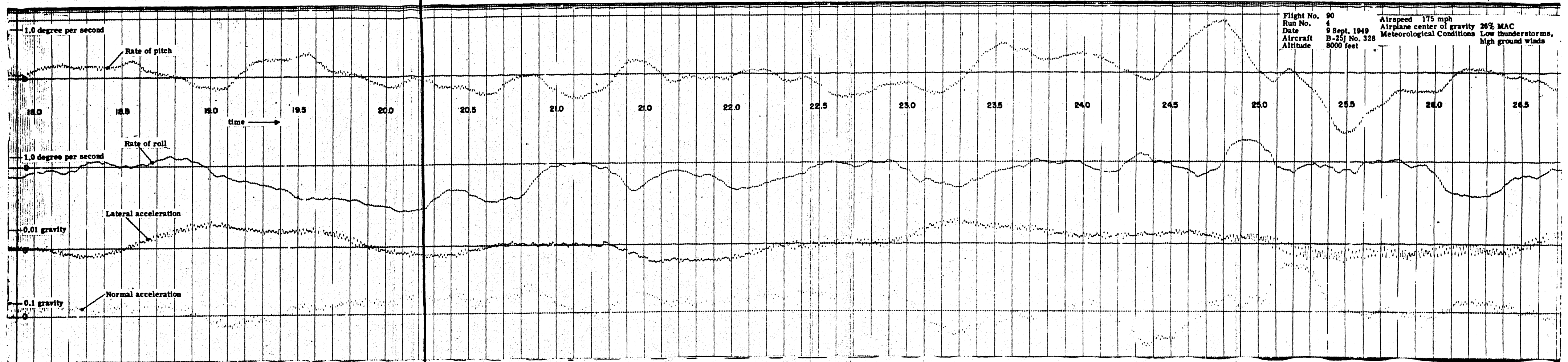


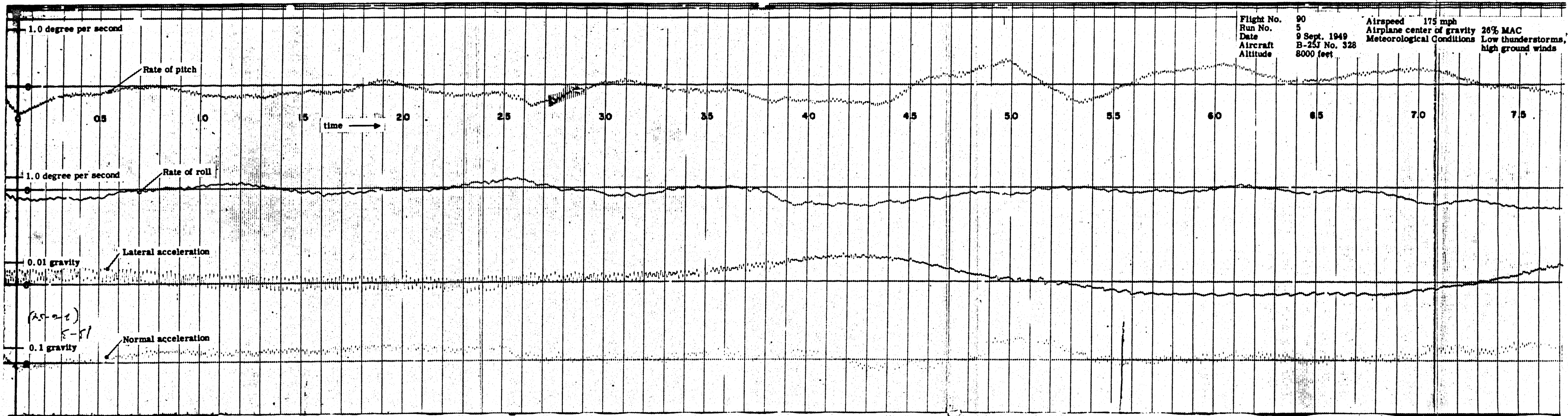
Flight No. 90
 Run No. 2
 Date 9 Sept. 1949
 Aircraft B-25j No. 328
 Altitude 8000 feet
 Airspeed 175 mph
 Airplane center of gravity 26%
 Meteorological Conditions Low thunderstorms,
 high ground winds

Flight No. 90
 Run No. 3
 Date 9 Sept. 1949
 Aircraft B-25j No. 328
 Altitude 8000 feet
 Airspeed 175 mph
 Airplane center of gravity 26% MAC
 Meteorological Conditions Low thunderstorms,
 high ground winds



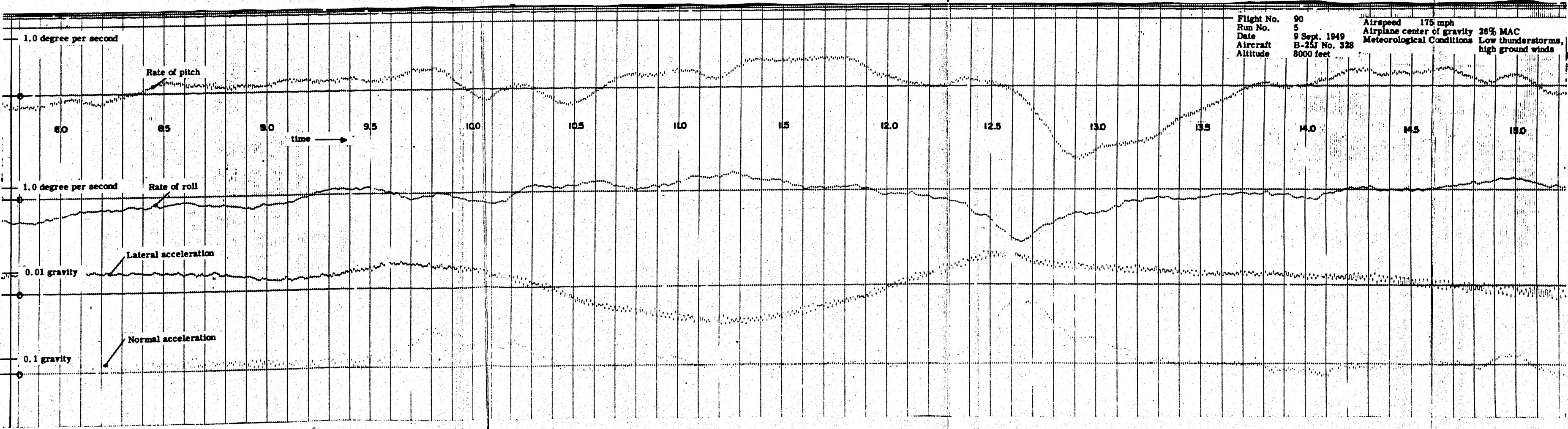






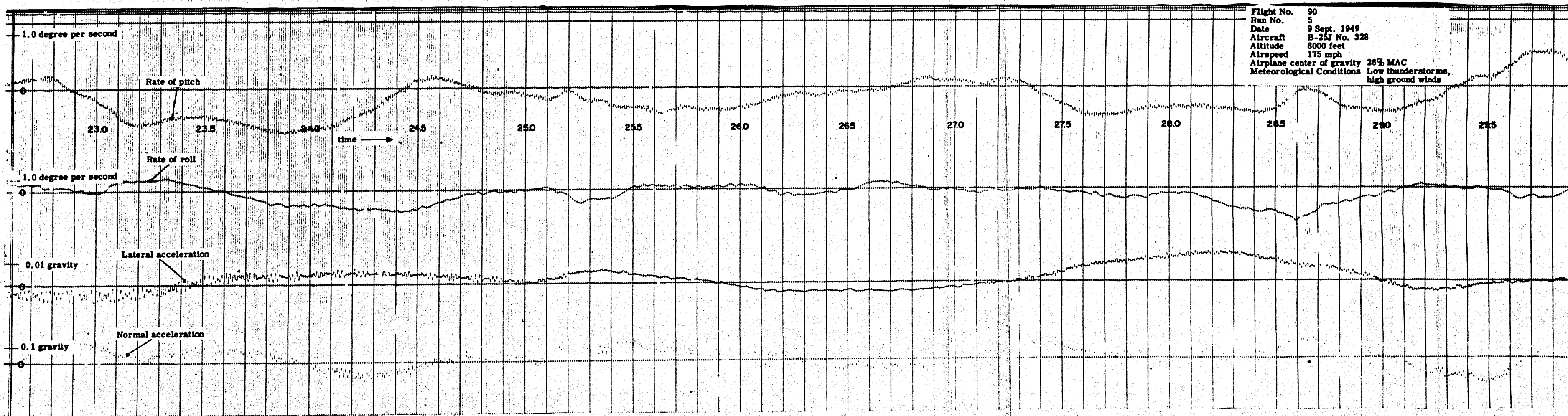
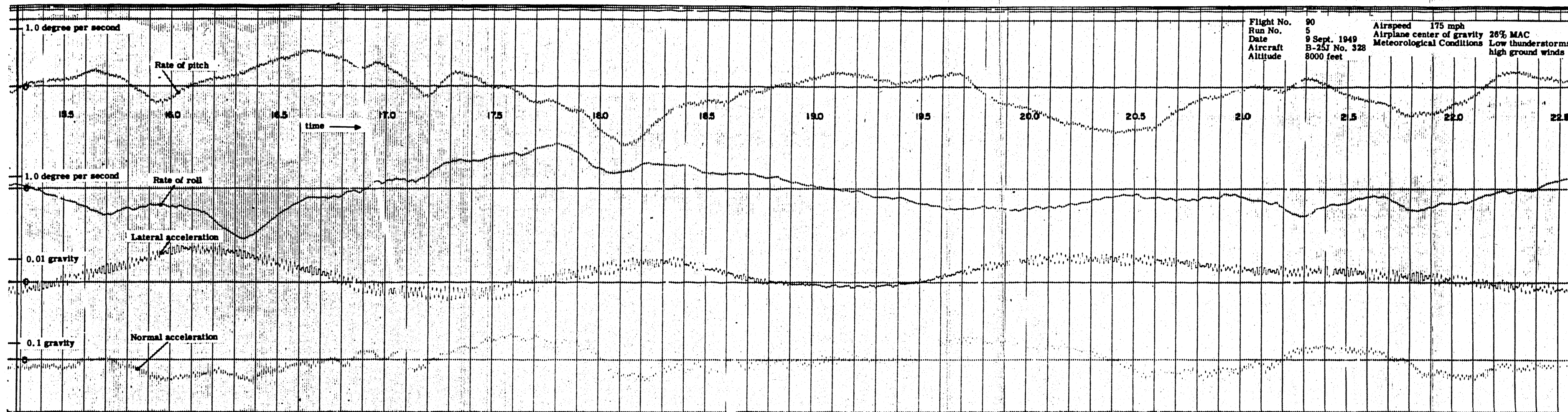
Flight No. 90
Run No. 5
Date 9 Sept. 1949
Aircraft B-25J No. 328
Altitude 8000 feet

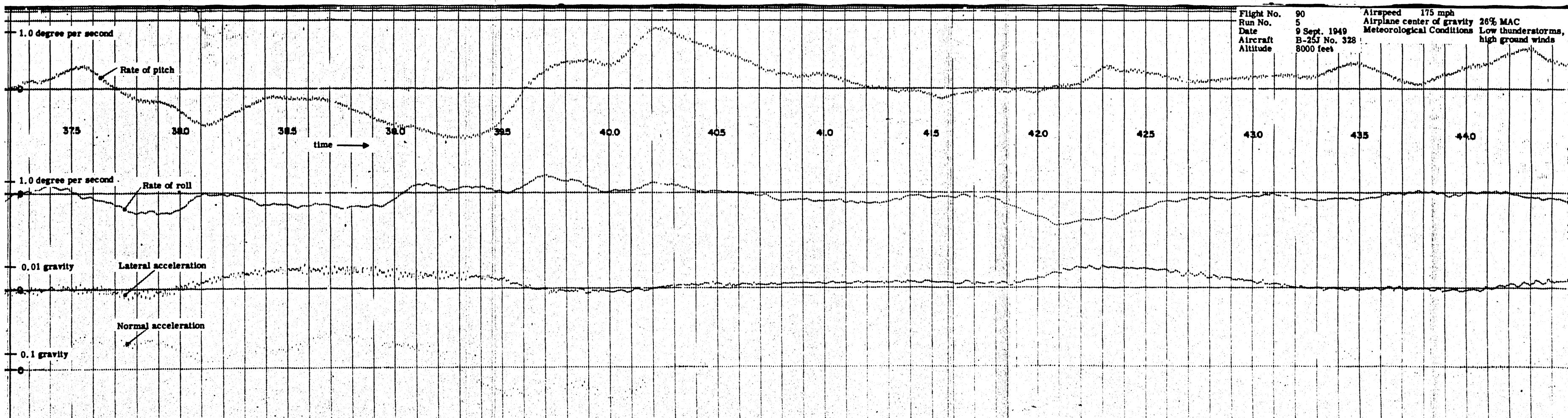
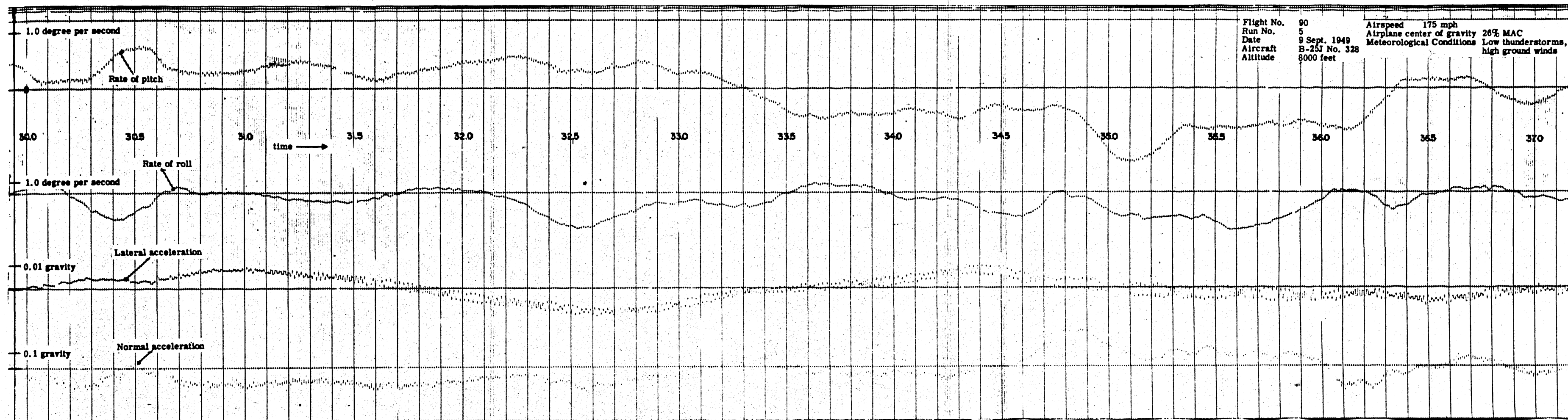
Airspeed 175 mph
Airplane center of gravity 26% MAC
Meteorological Conditions Low thunderstorms, high ground winds

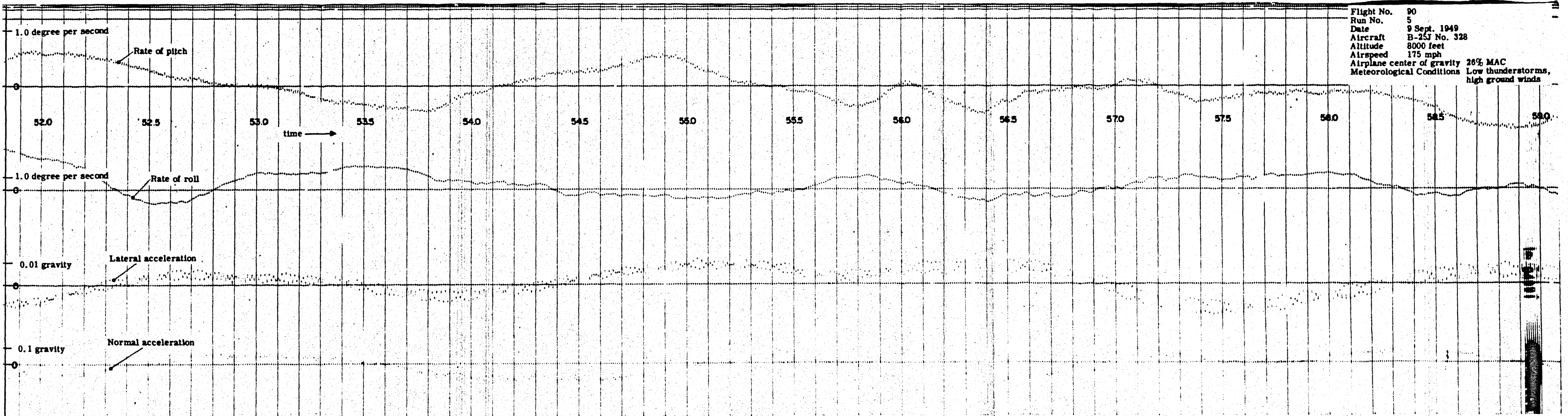
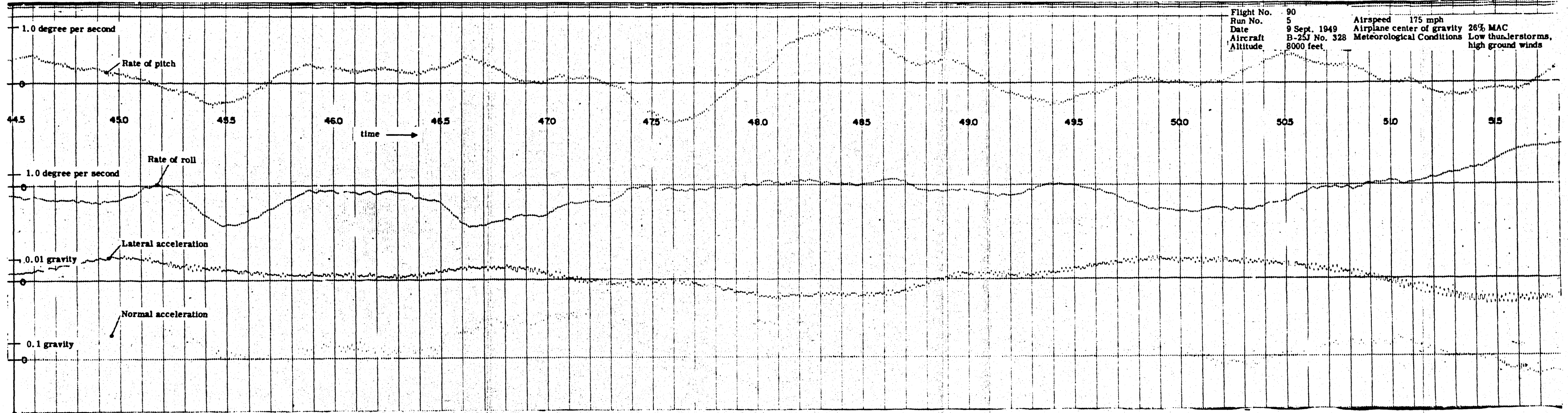


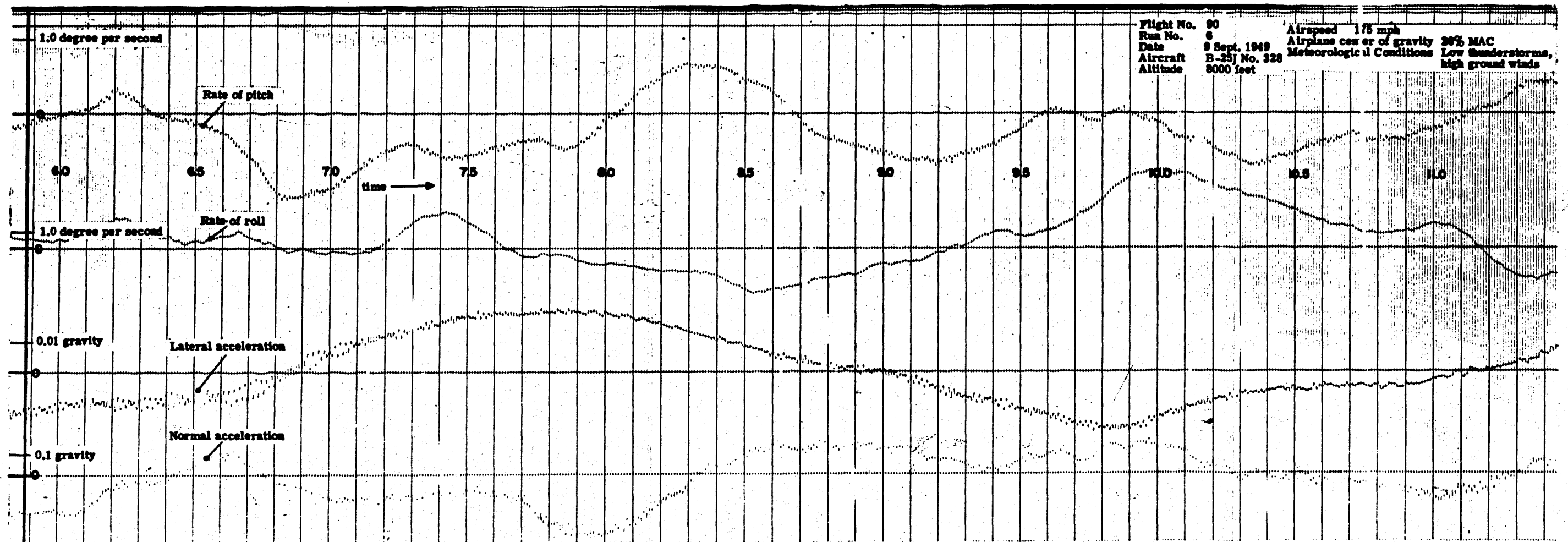
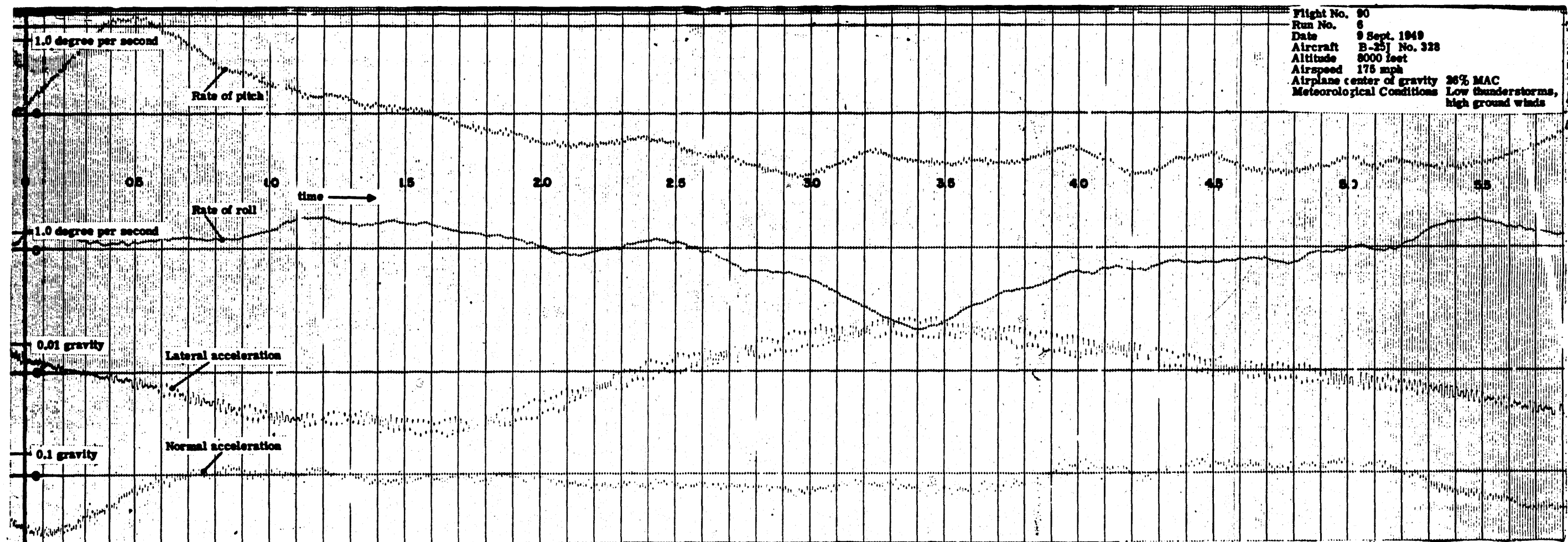
Flight No. 90
Run No. 5
Date 9 Sept. 1949
Aircraft B-25J No. 328
Altitude 8000 feet

Airspeed 175 mph
Airplane center of gravity 26% MAC
Meteorological Conditions Low thunderstorms, high ground winds

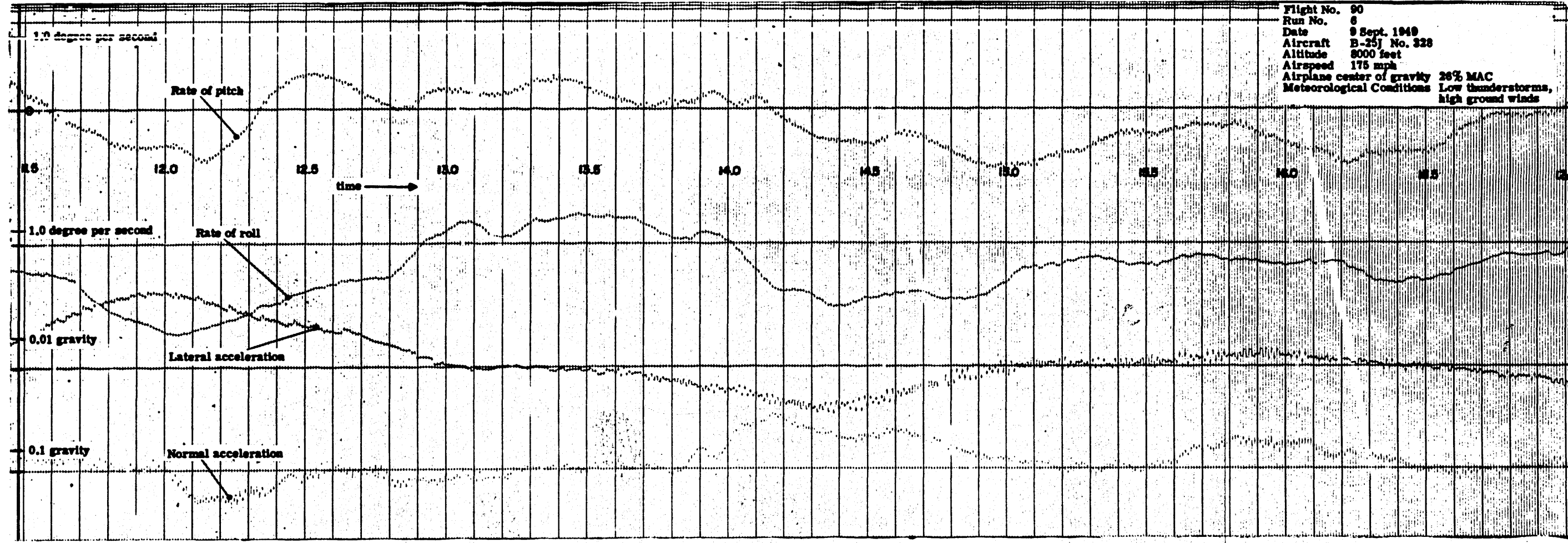




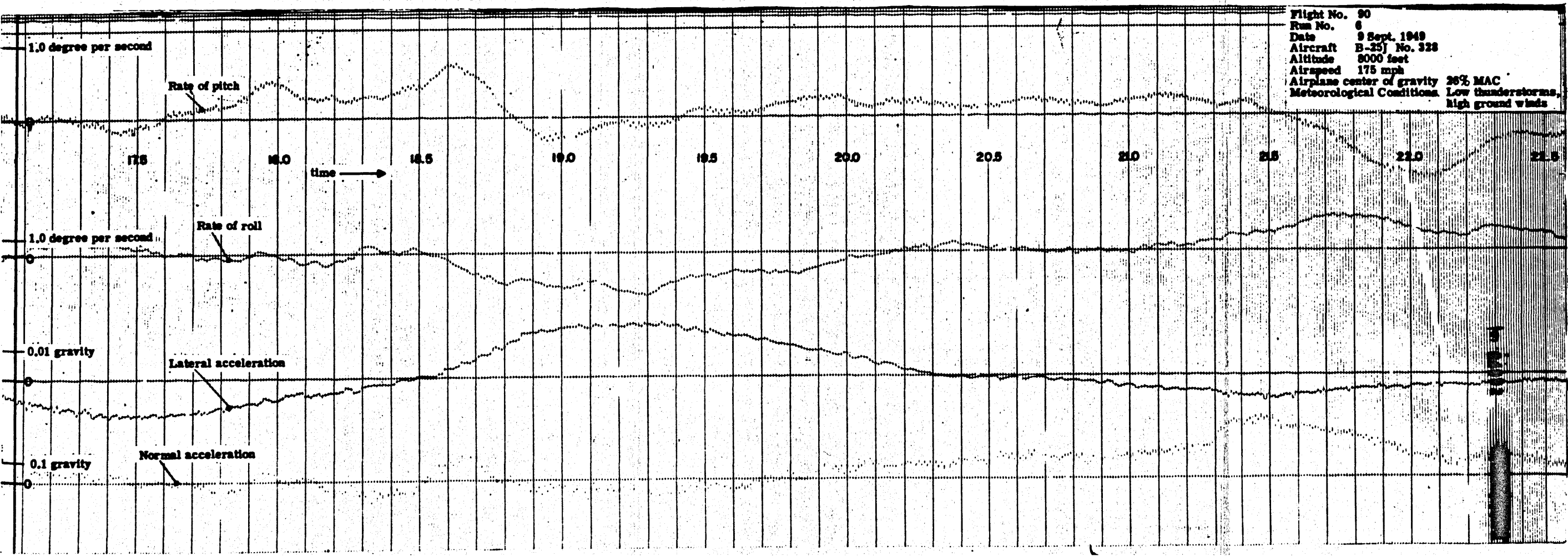


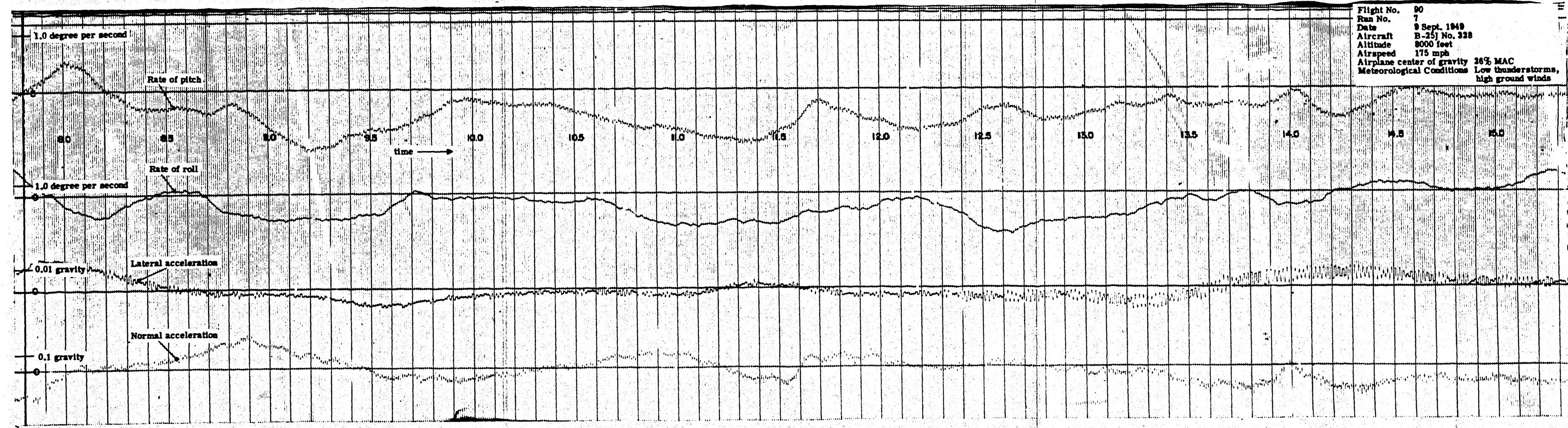
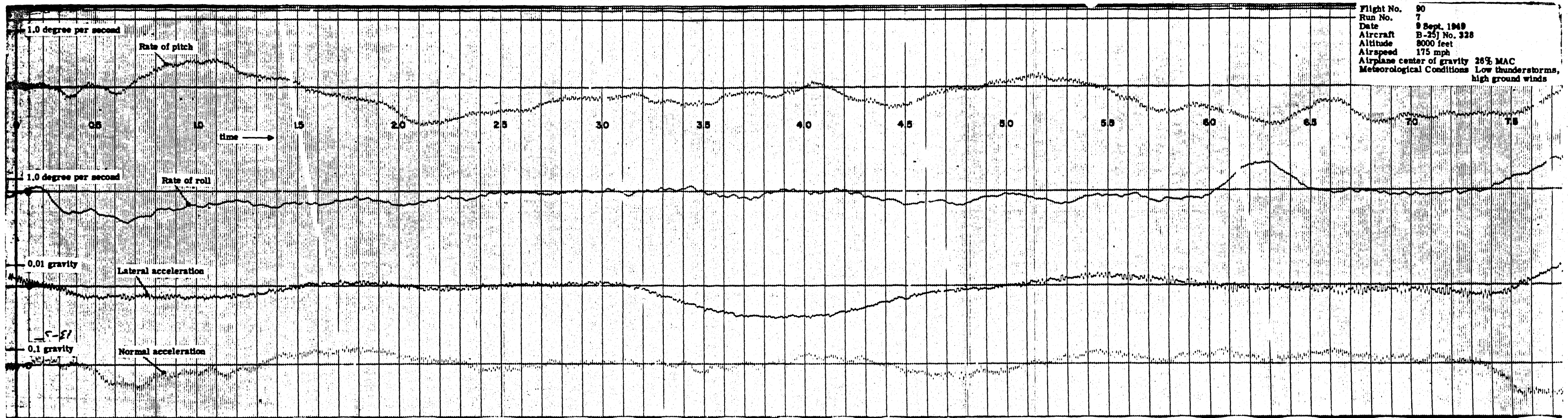


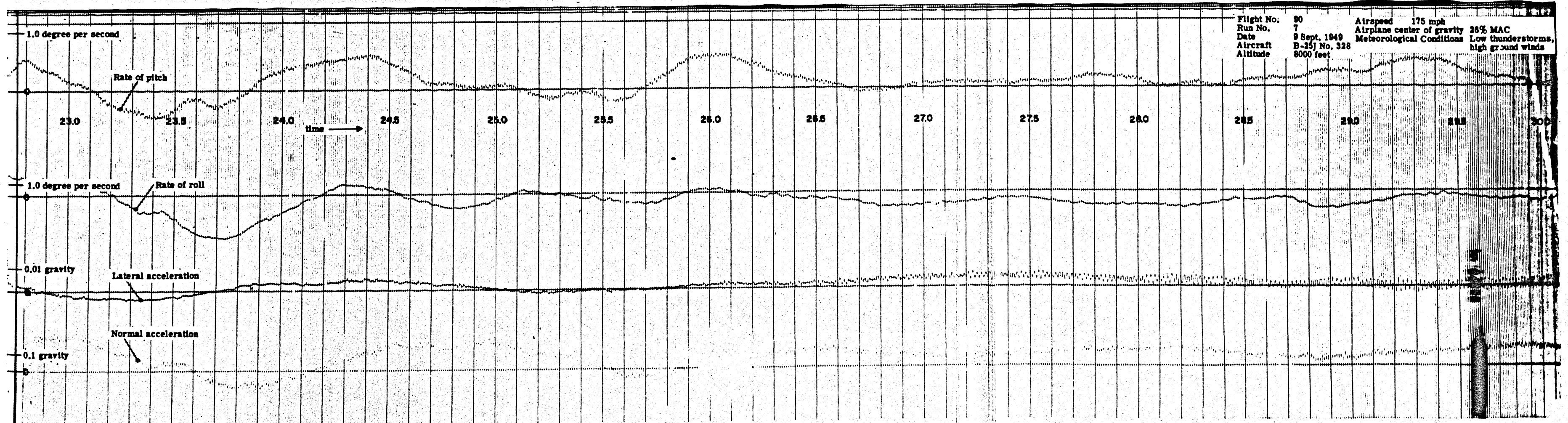
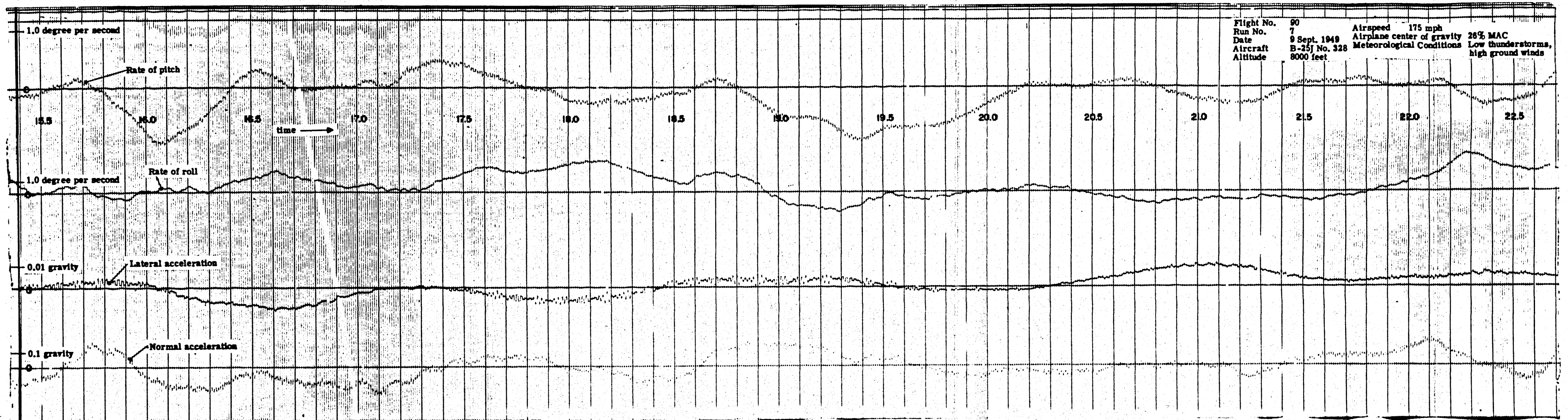
Flight No. 90
 Run No. 6
 Date 9 Sept. 1949
 Aircraft B-25J No. 328
 Altitude 8000 feet
 Airspeed 175 mph
 Airplane center of gravity 26% MAC
 Meteorological Conditions Low thunderstorms,
 high ground winds

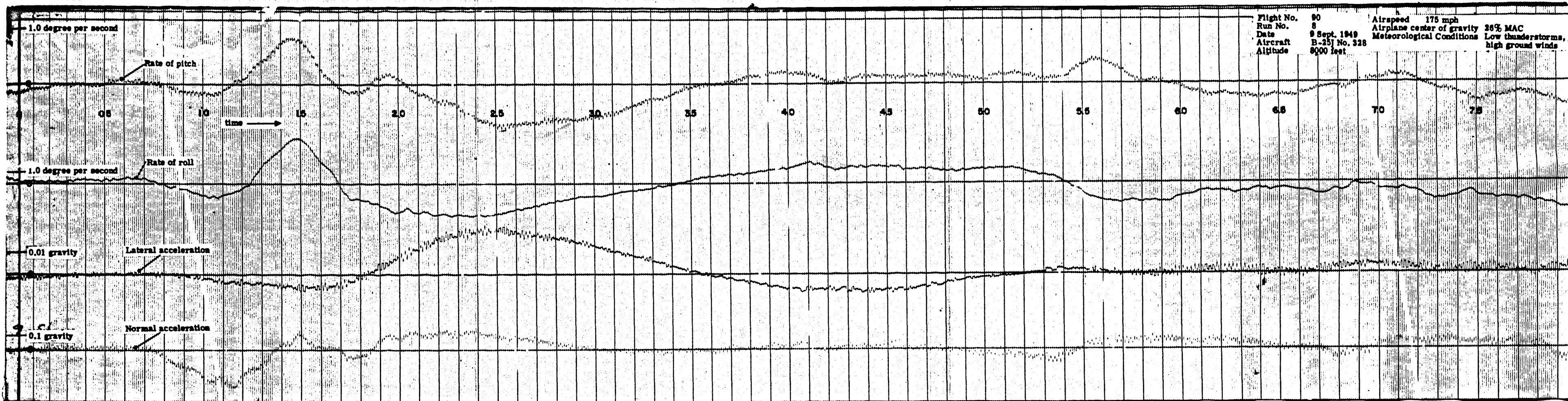


Flight No. 90
 Run No. 6
 Date 9 Sept. 1949
 Aircraft B-25J No. 328
 Altitude 8000 feet
 Airspeed 175 mph
 Airplane center of gravity 26% MAC
 Meteorological Conditions Low thunderstorms,
 high ground winds

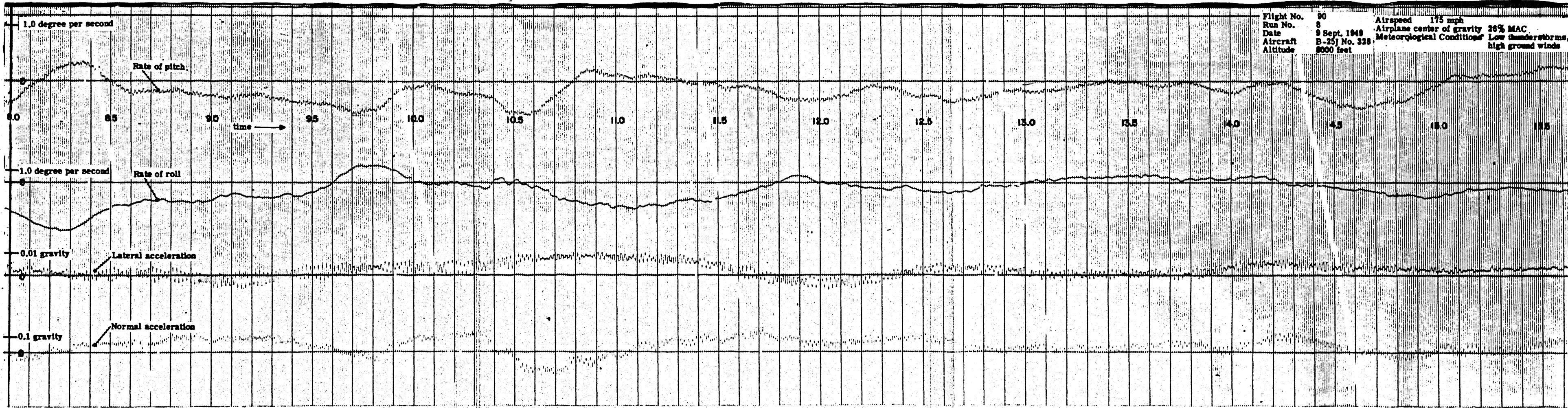




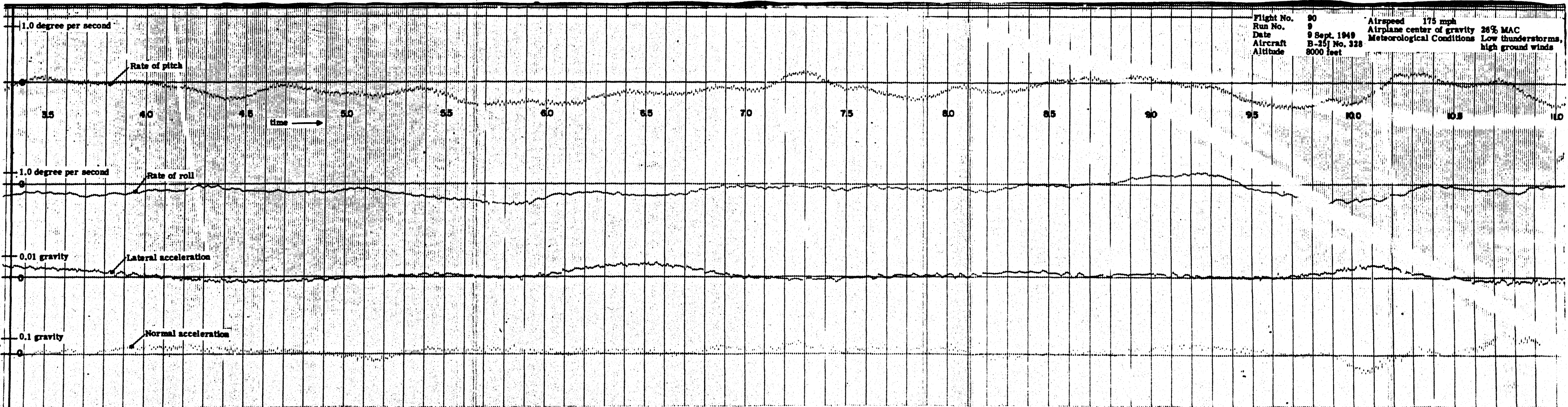
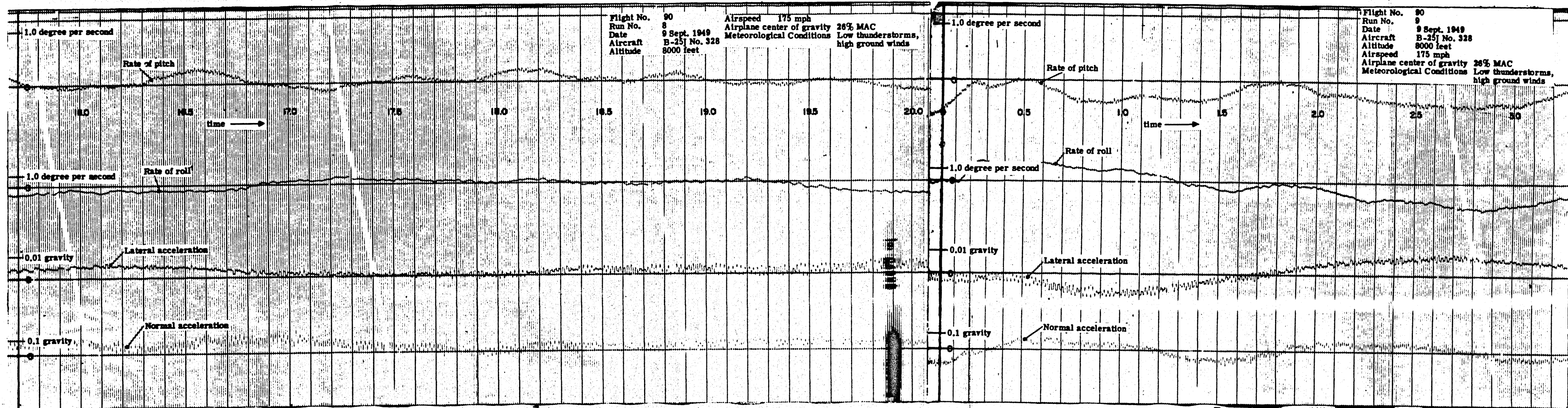




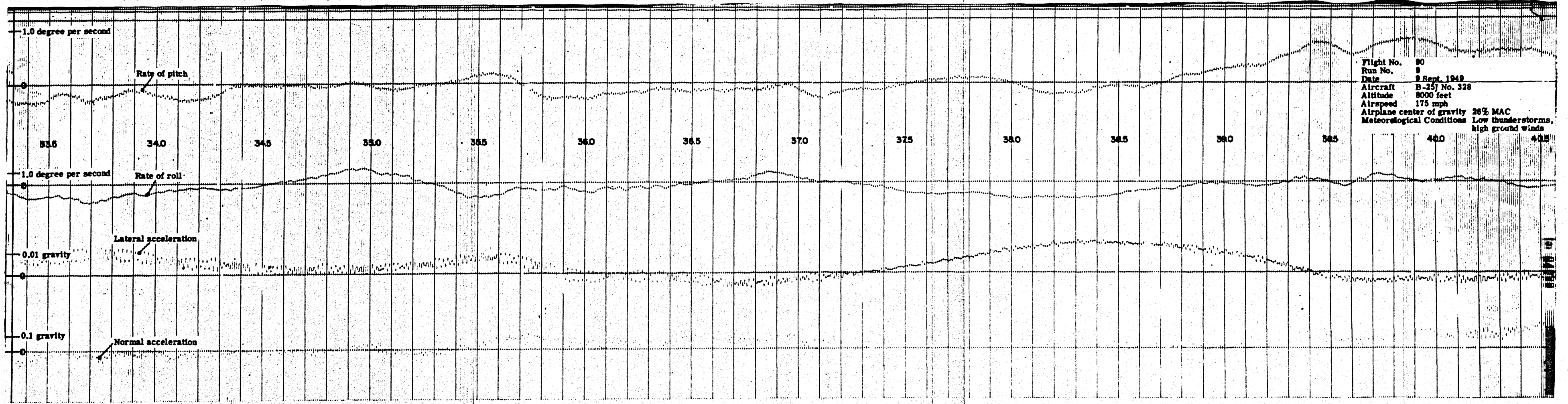
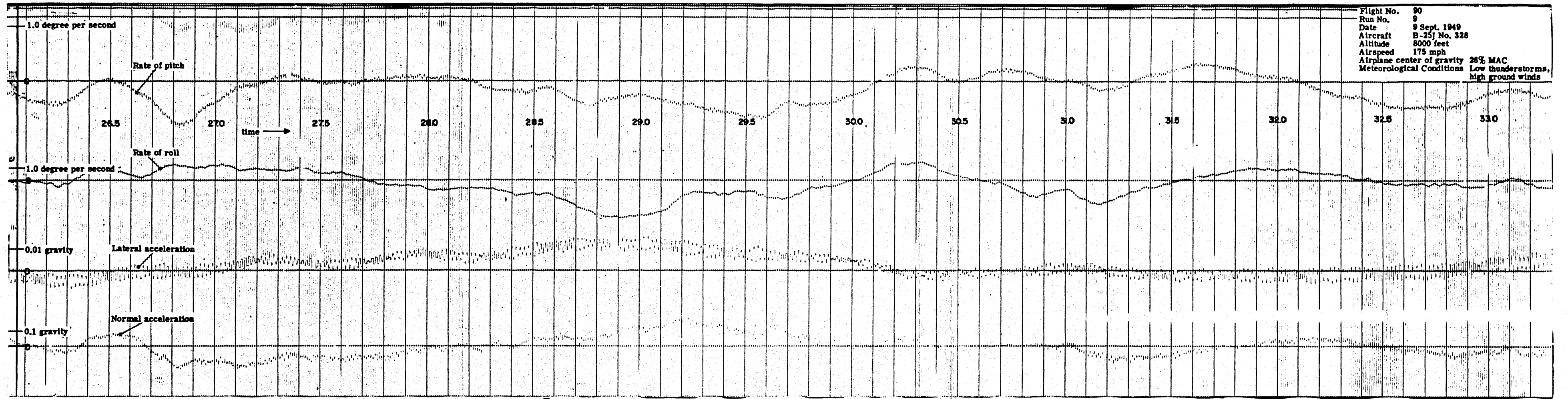
Flight No. 90 Airspeed 175 mph
 Run No. 8 Airplane center of gravity 26% MAC
 Date 9 Sept. 1949 Meteorological Conditions Low thunderstorms,
 Aircraft B-25J No. 328 high ground winds
 Altitude 8000 feet

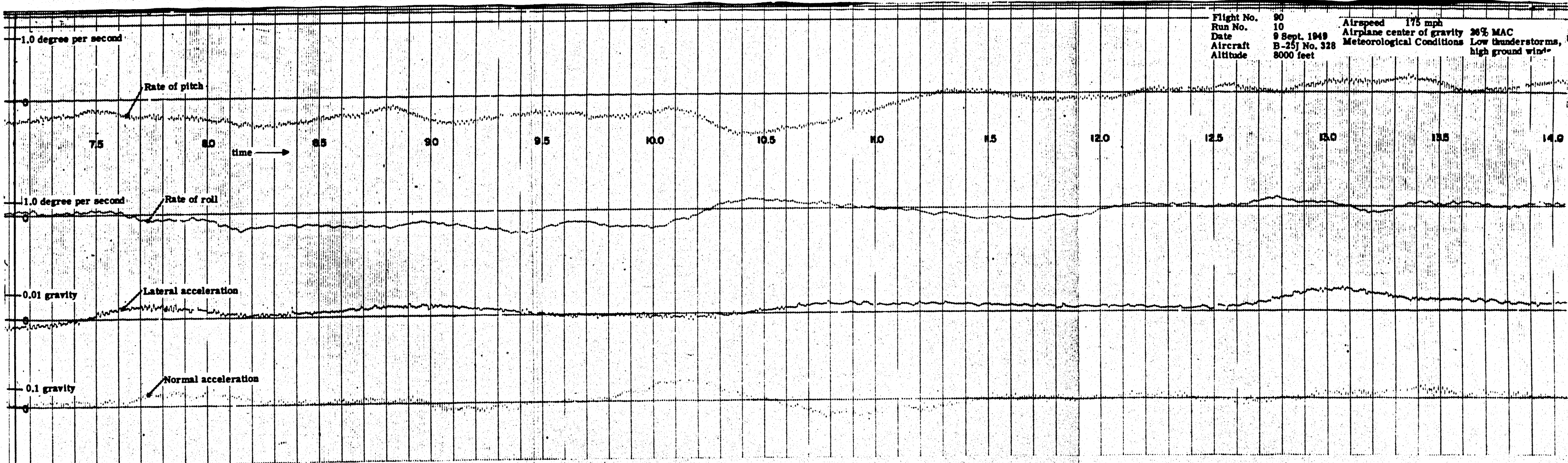


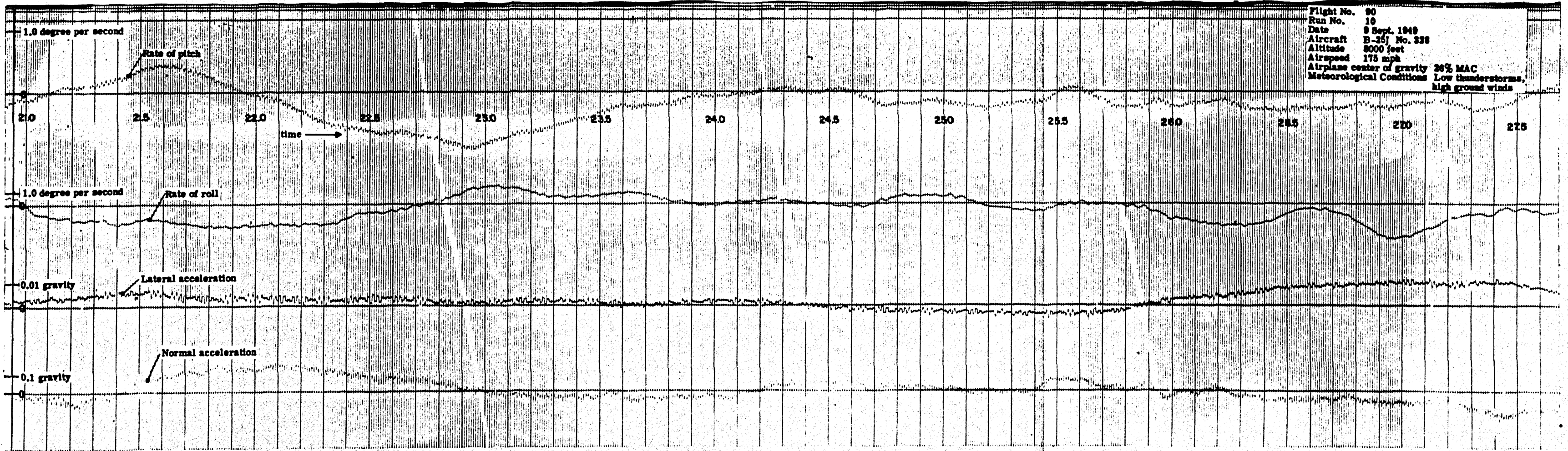
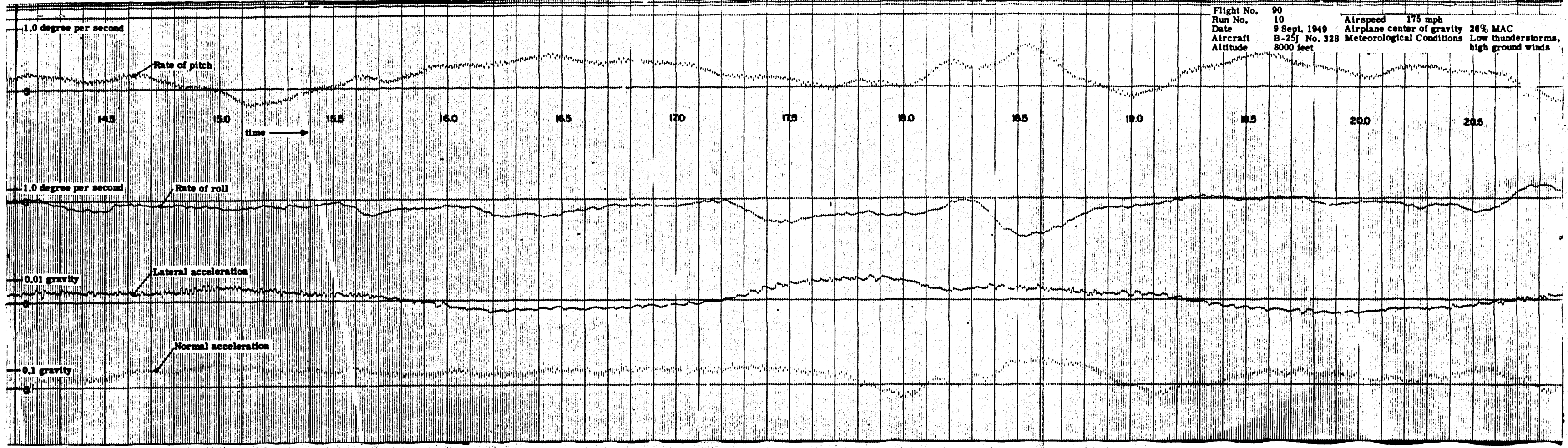
Flight No. 90 Airspeed 175 mph
 Run No. 8 Airplane center of gravity 26% MAC
 Date 9 Sept. 1949 Meteorological Conditions Low thunderstorms,
 Aircraft B-25J No. 328 high ground winds
 Altitude 8000 feet

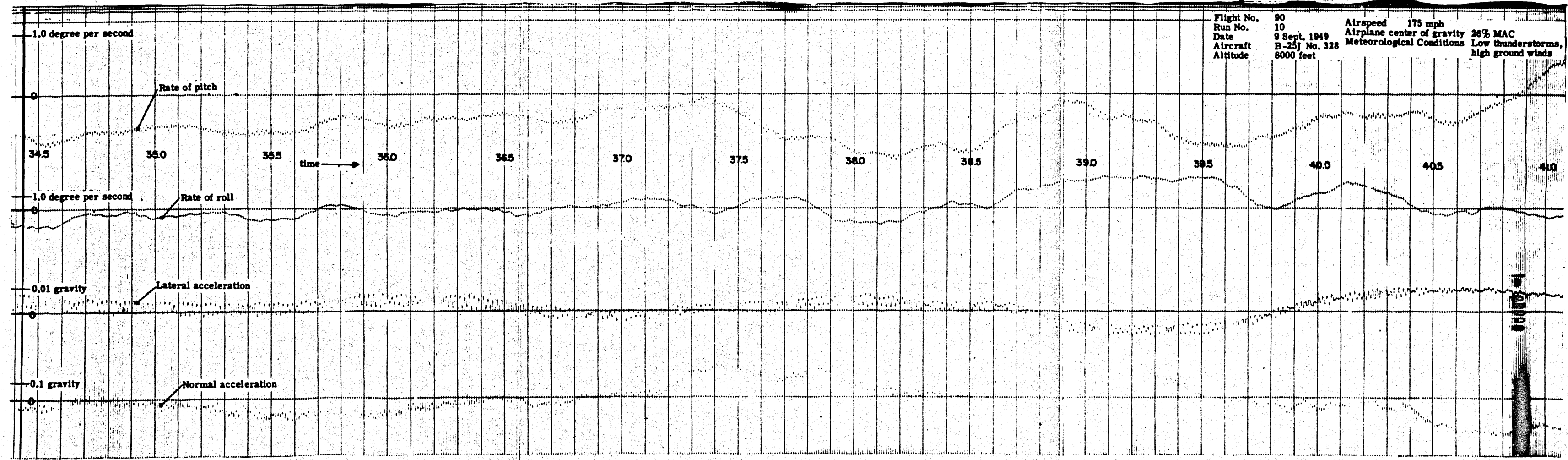
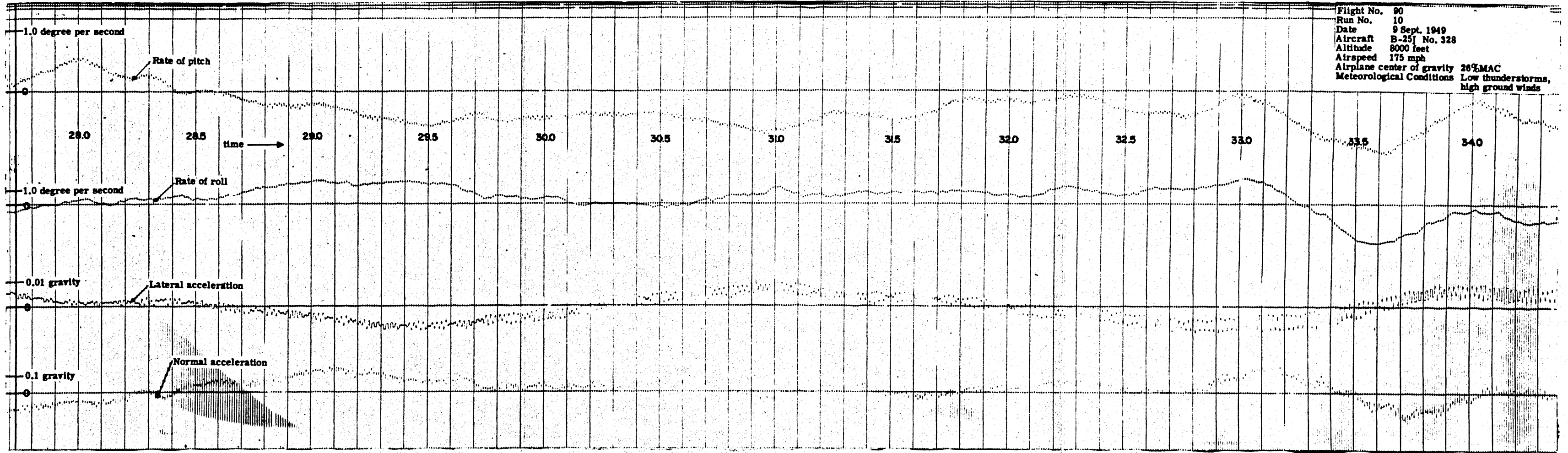


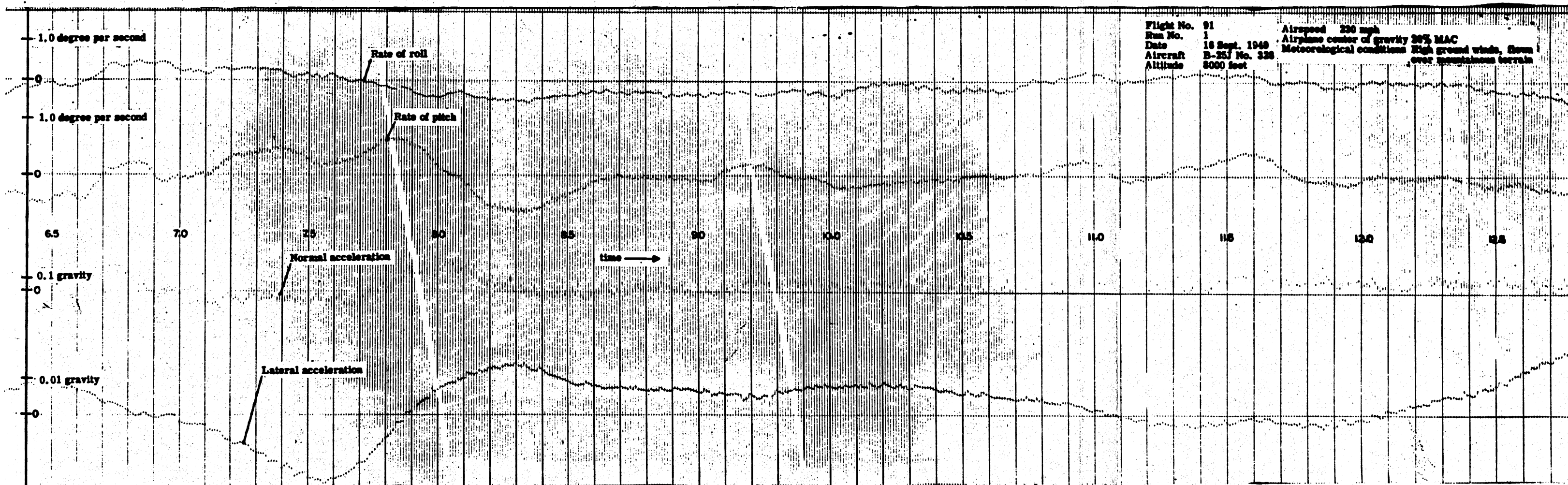
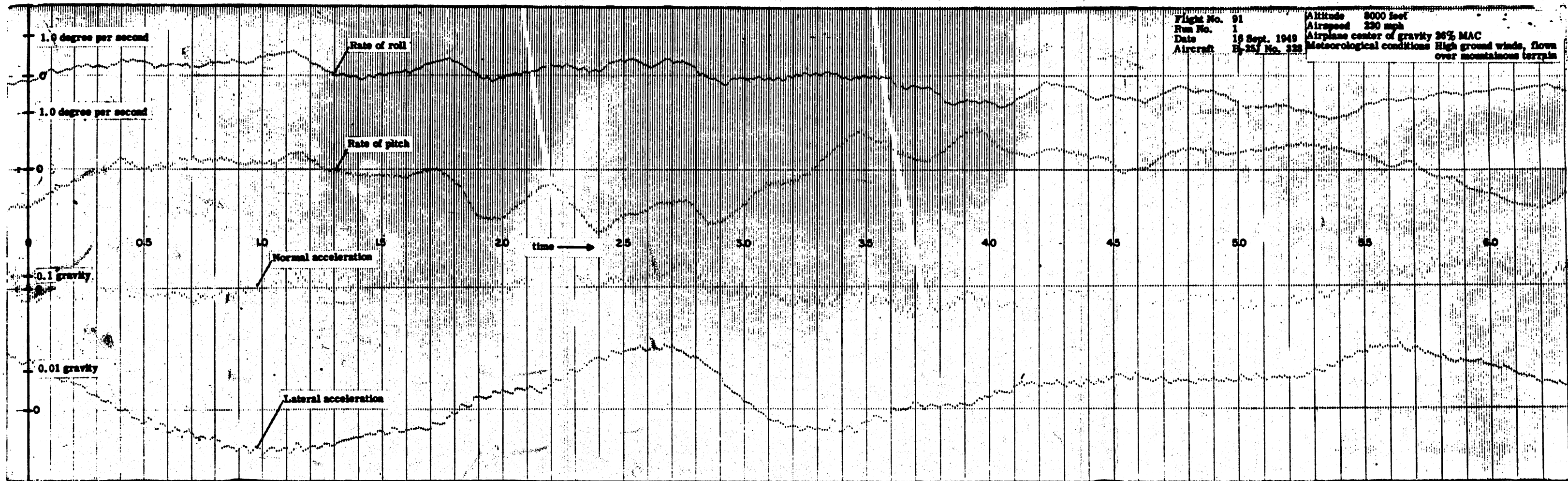


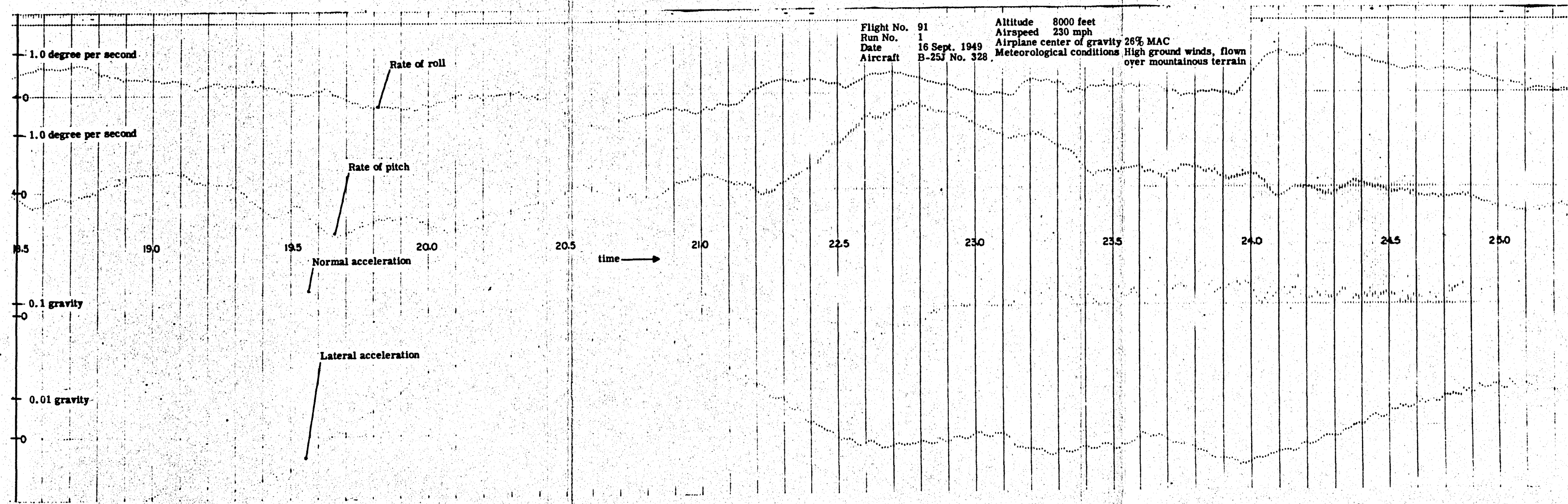
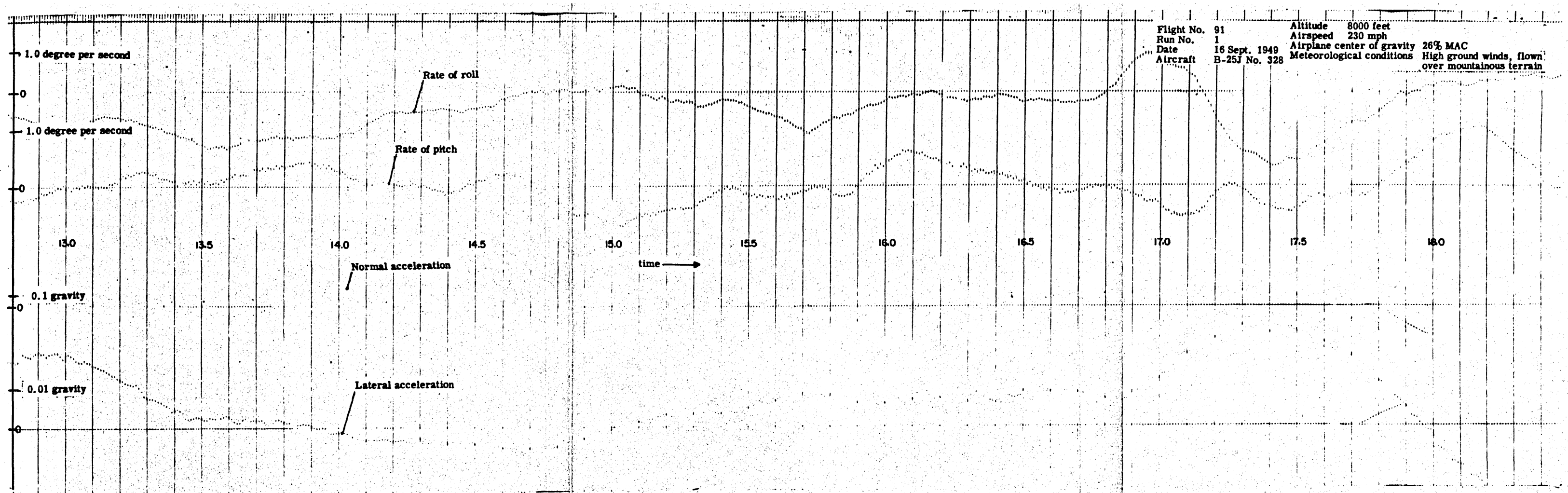


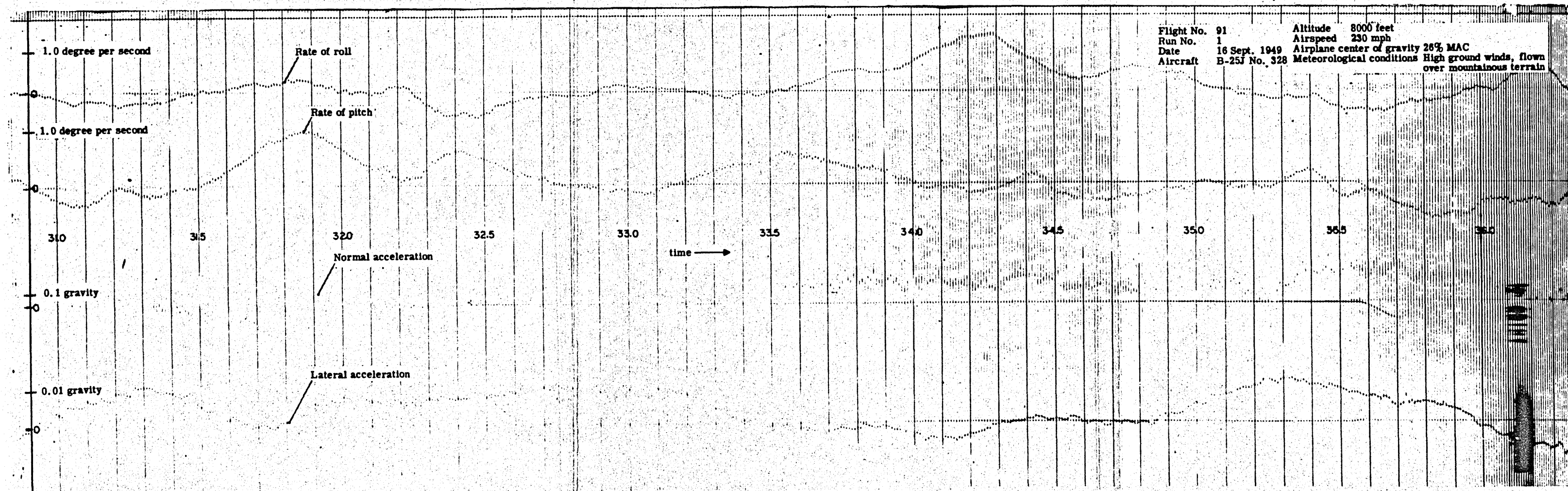
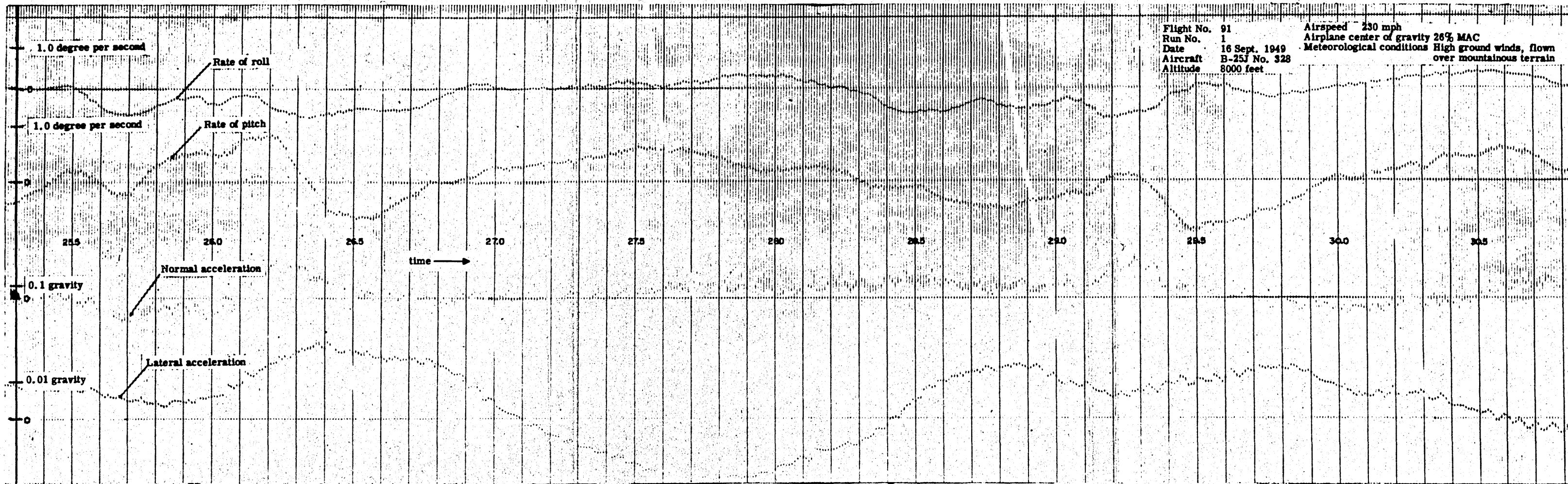


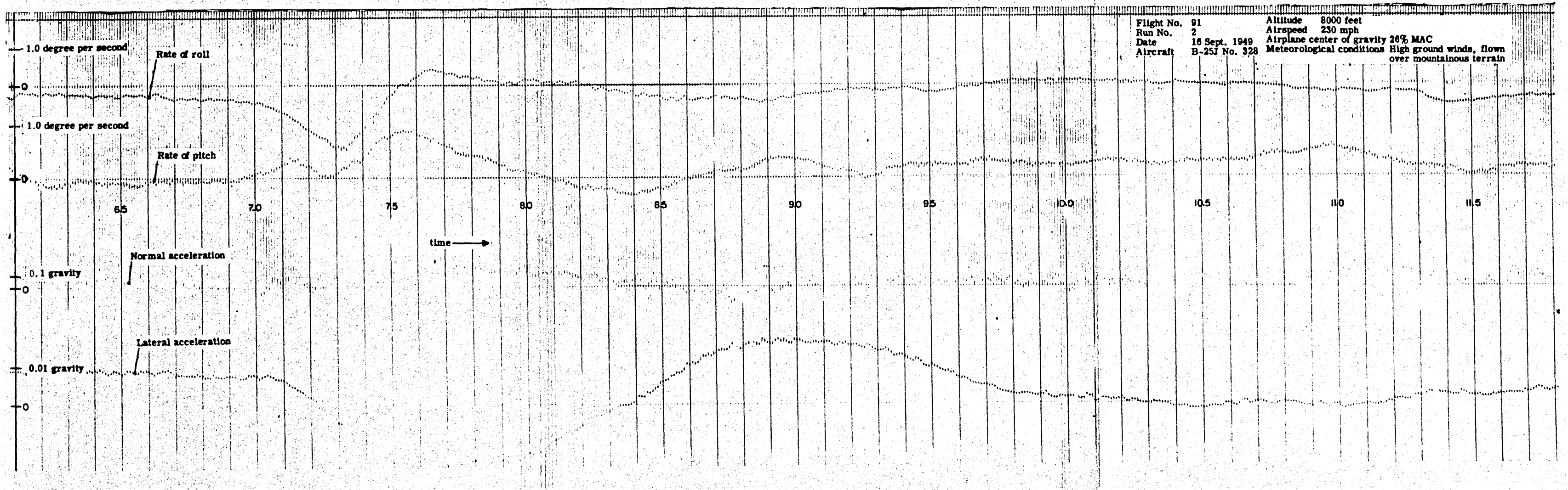
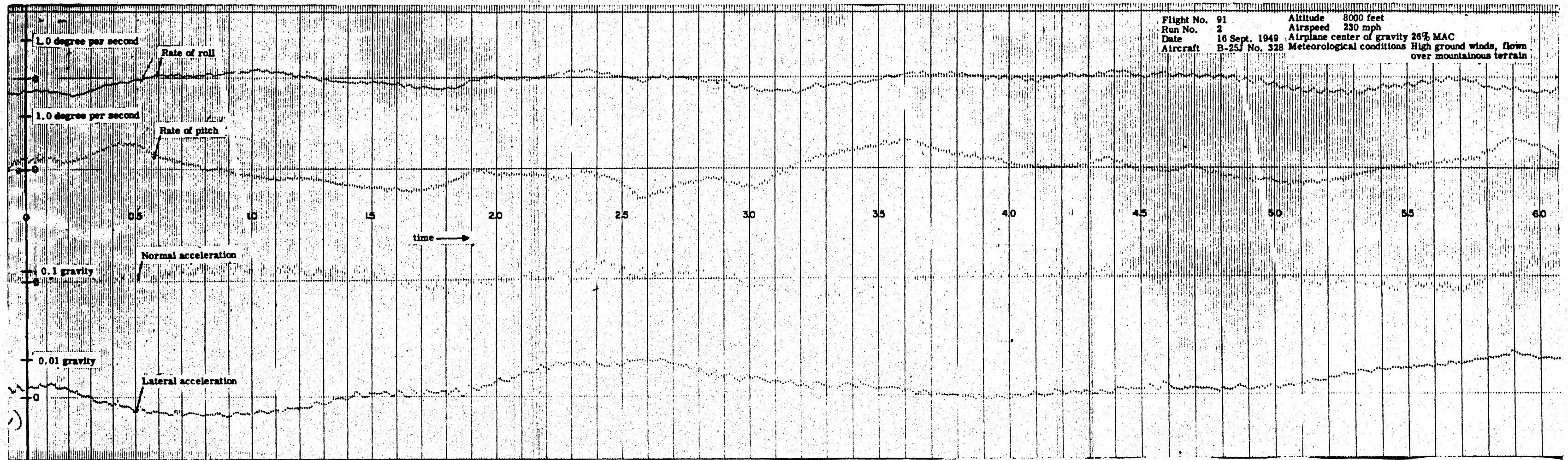


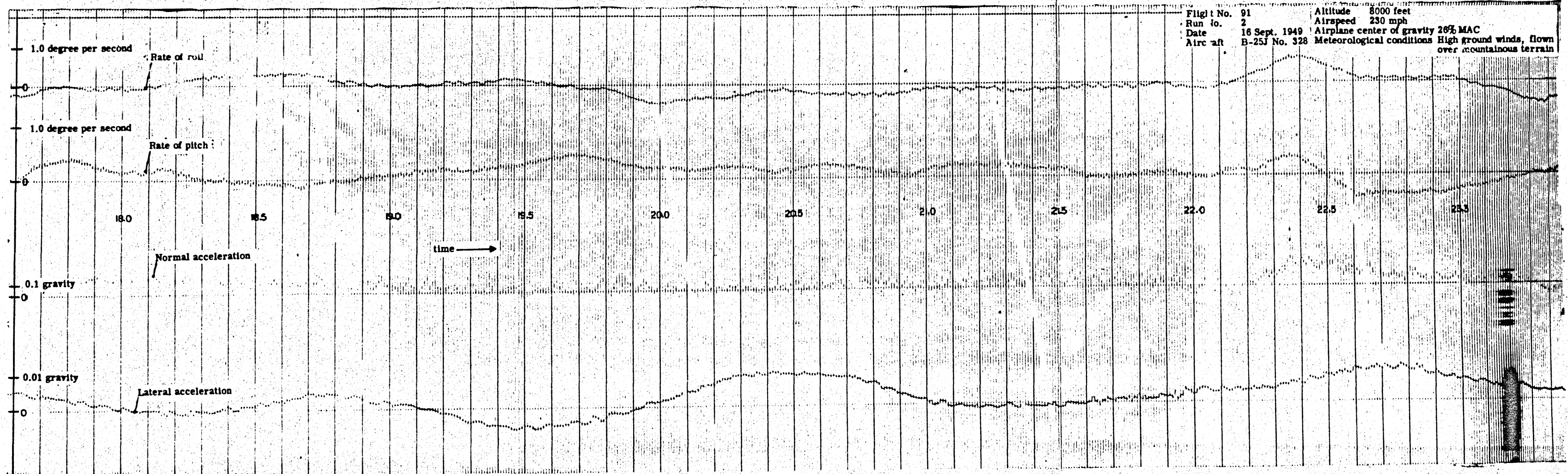
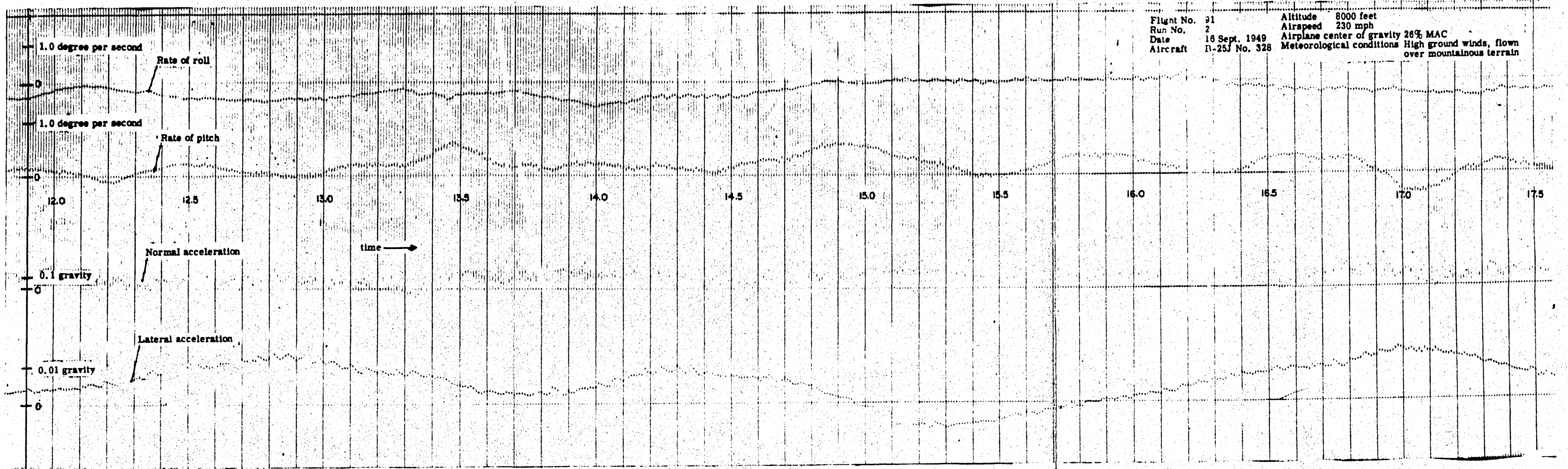


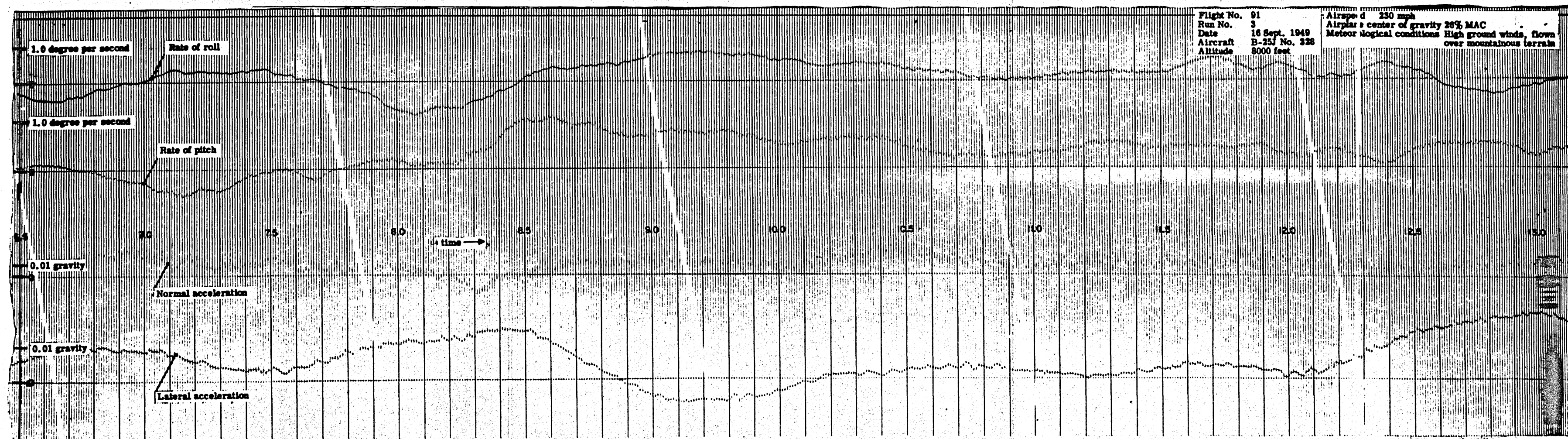
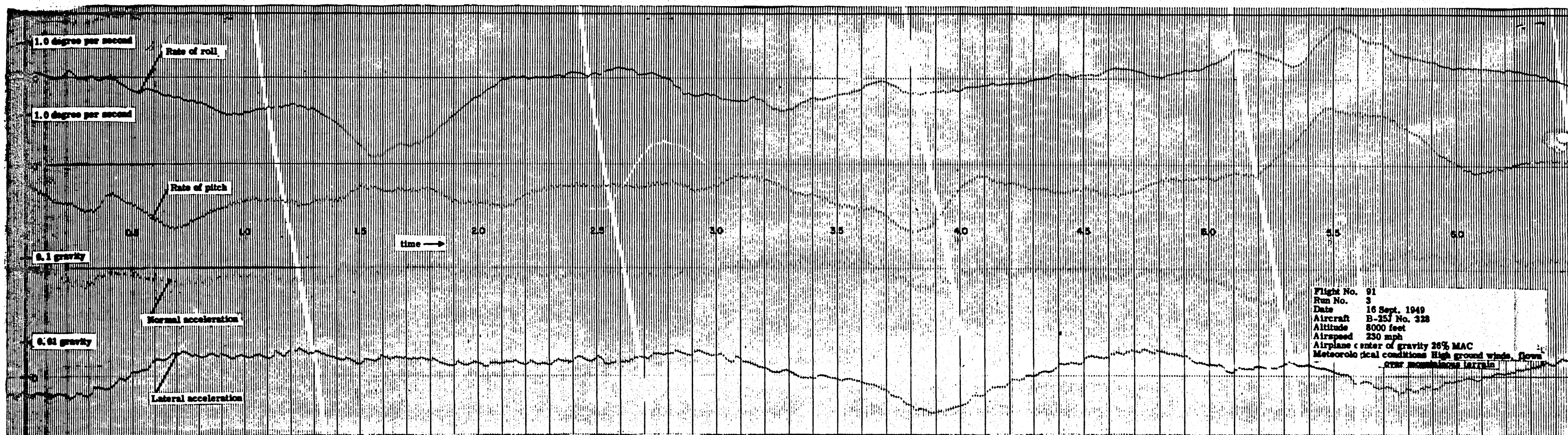


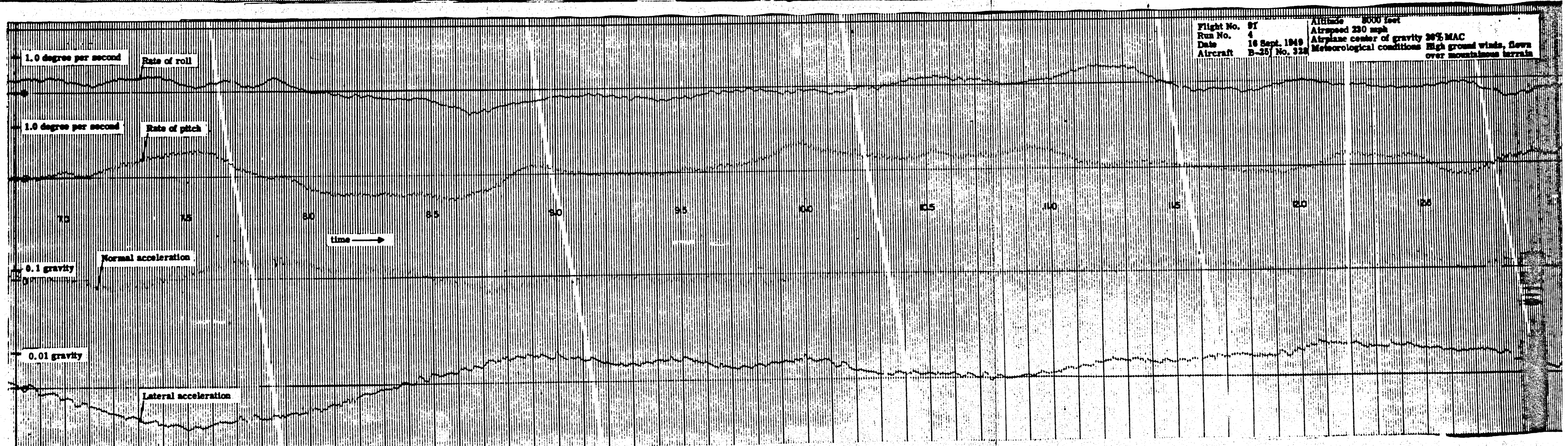
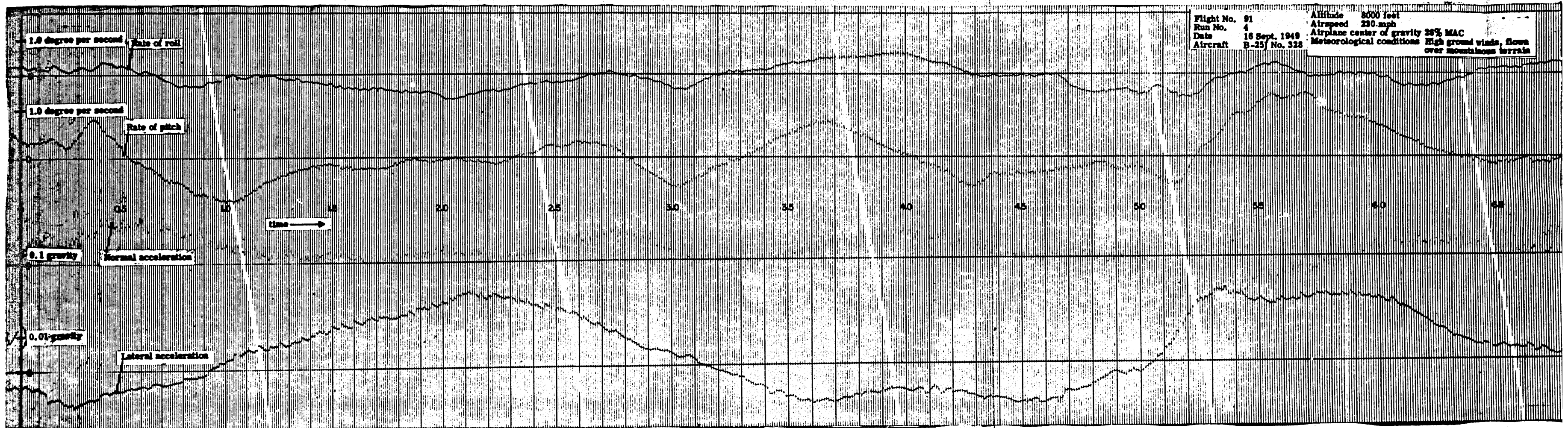


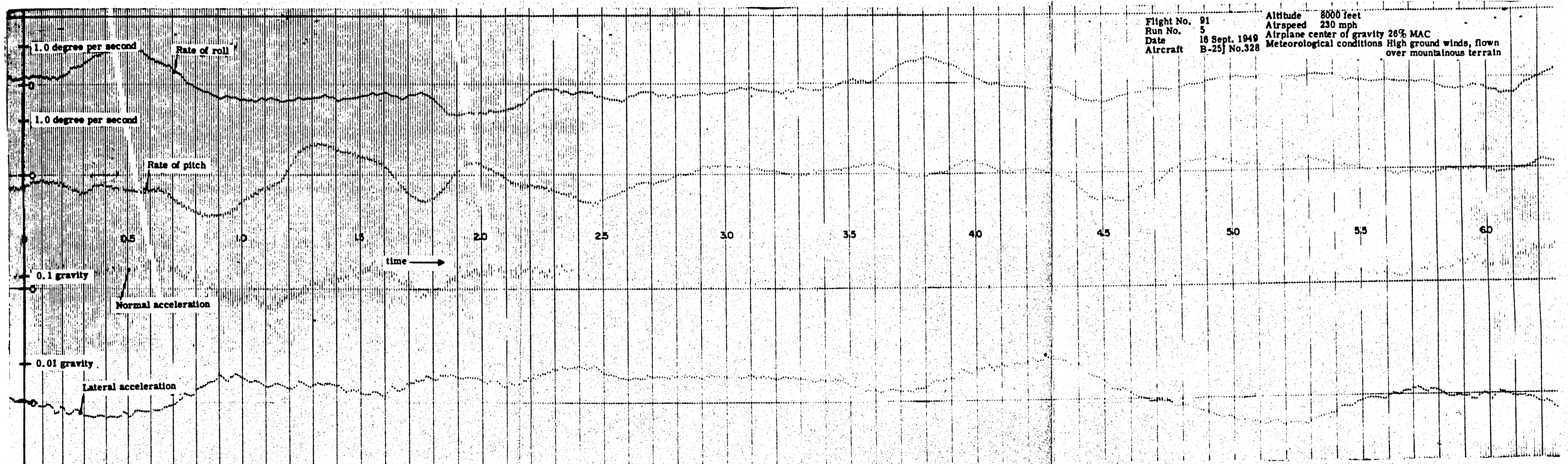






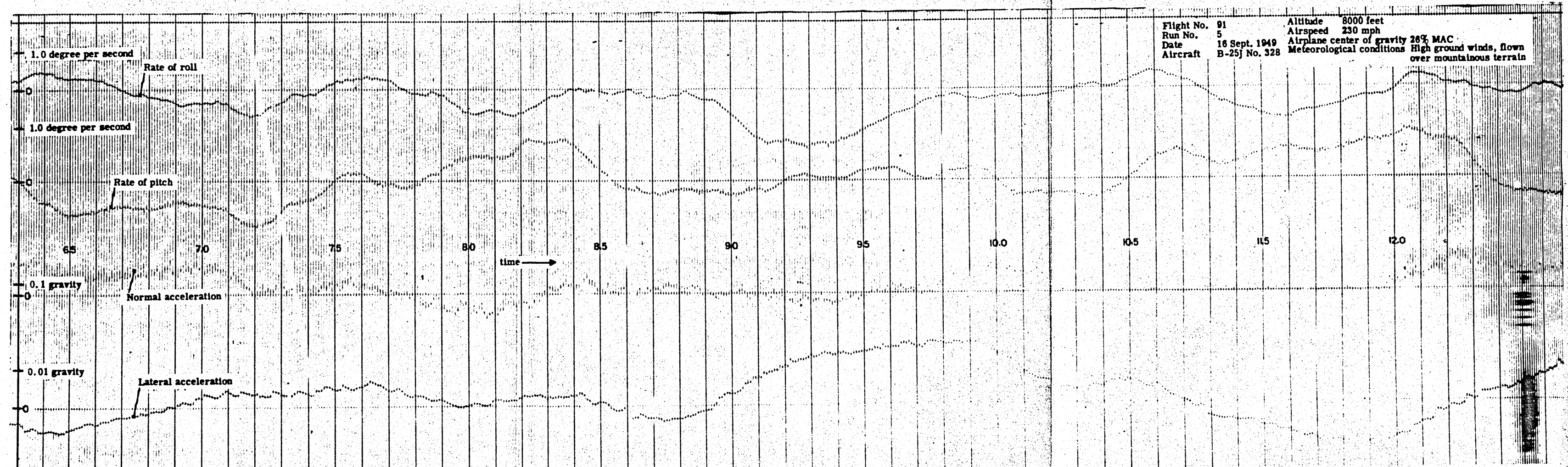






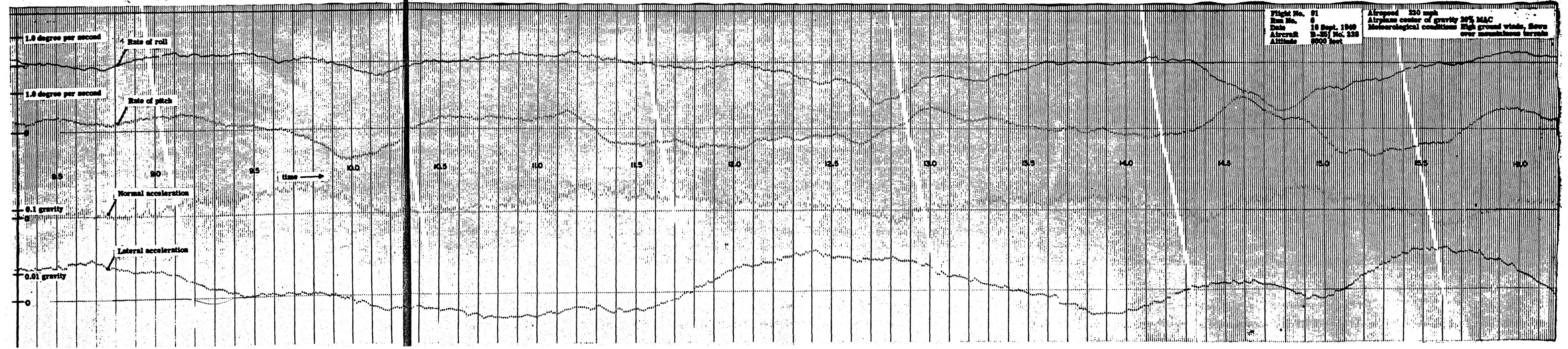
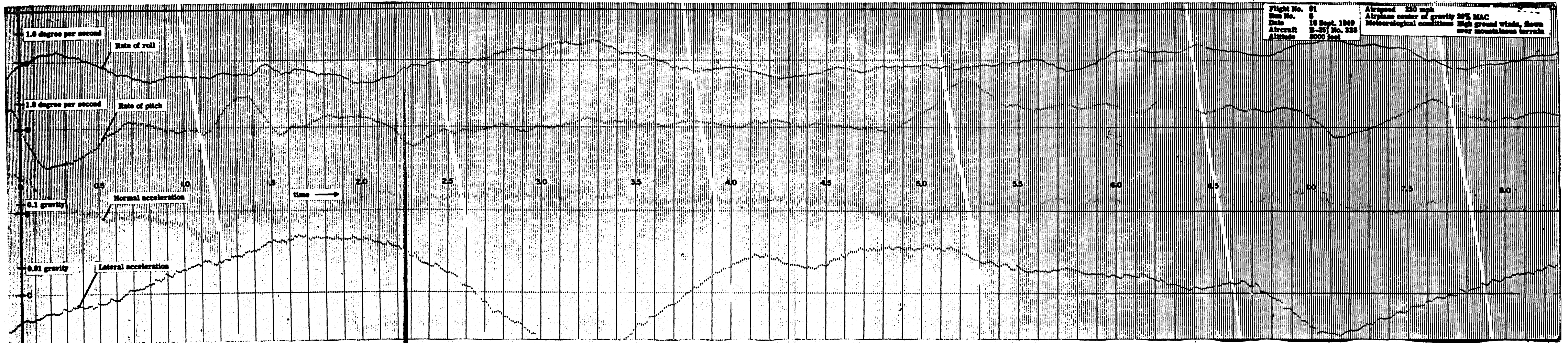
Flight No. 91
 Run No. 5
 Date 16 Sept. 1949
 Aircraft B-25j No. 328

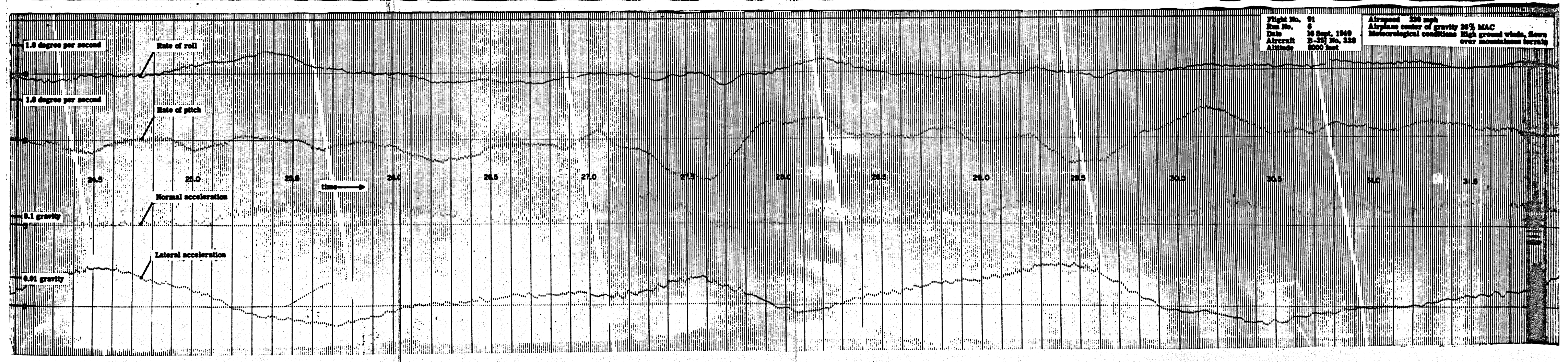
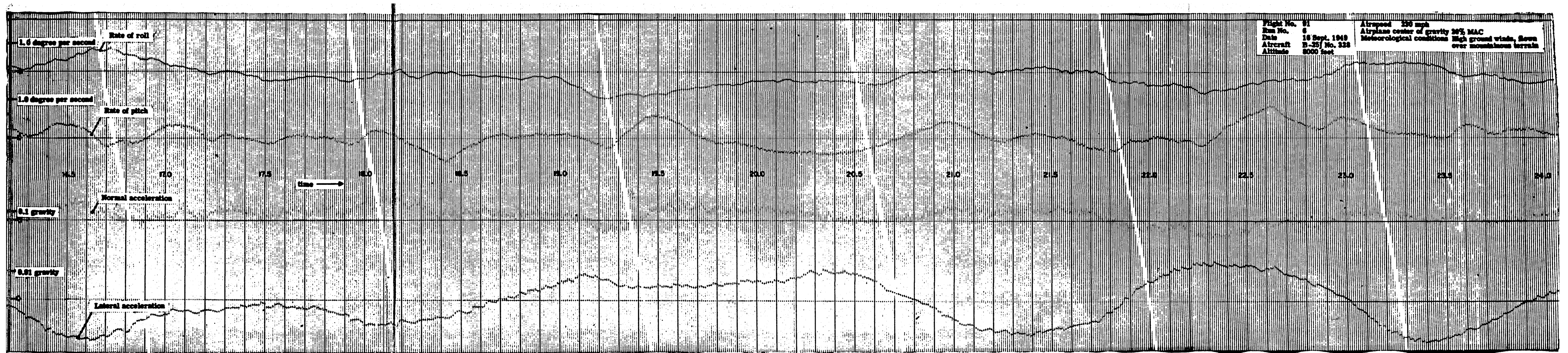
Altitude 8000 feet
 Airspeed 230 mph
 Airplane center of gravity 26% MAC
 Meteorological conditions High ground winds, flown over mountainous terrain

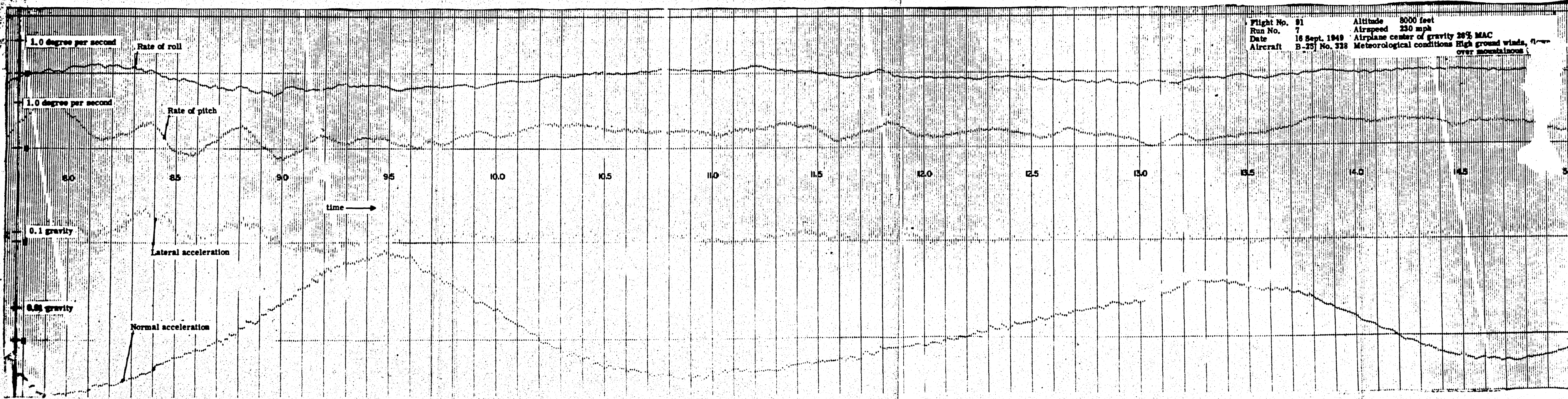
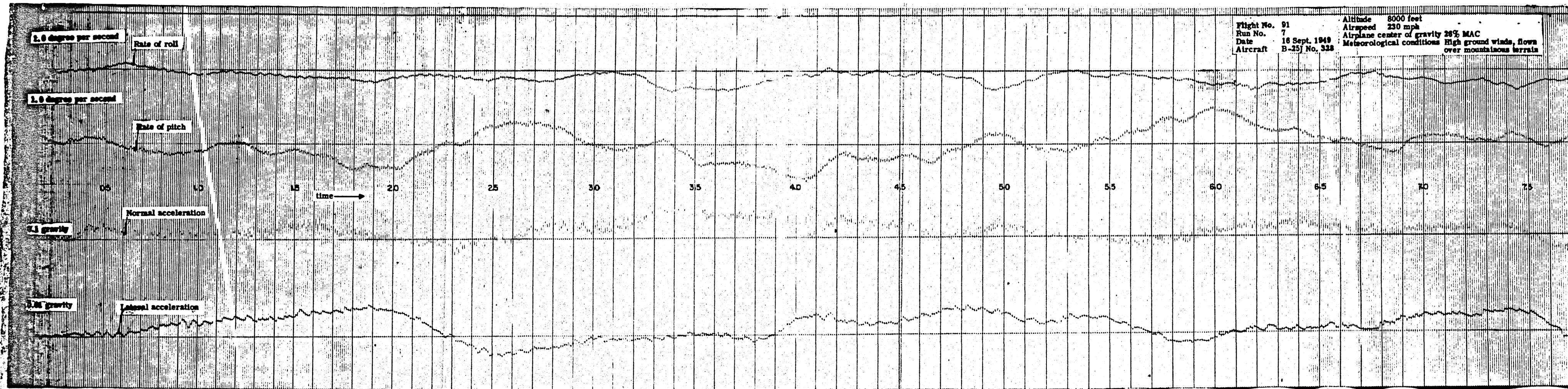


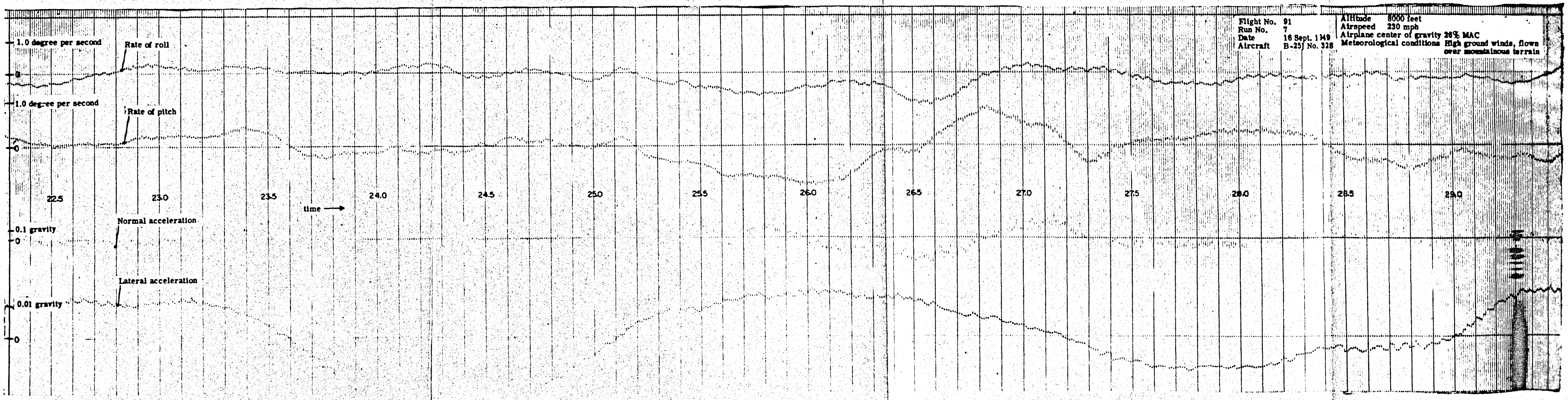
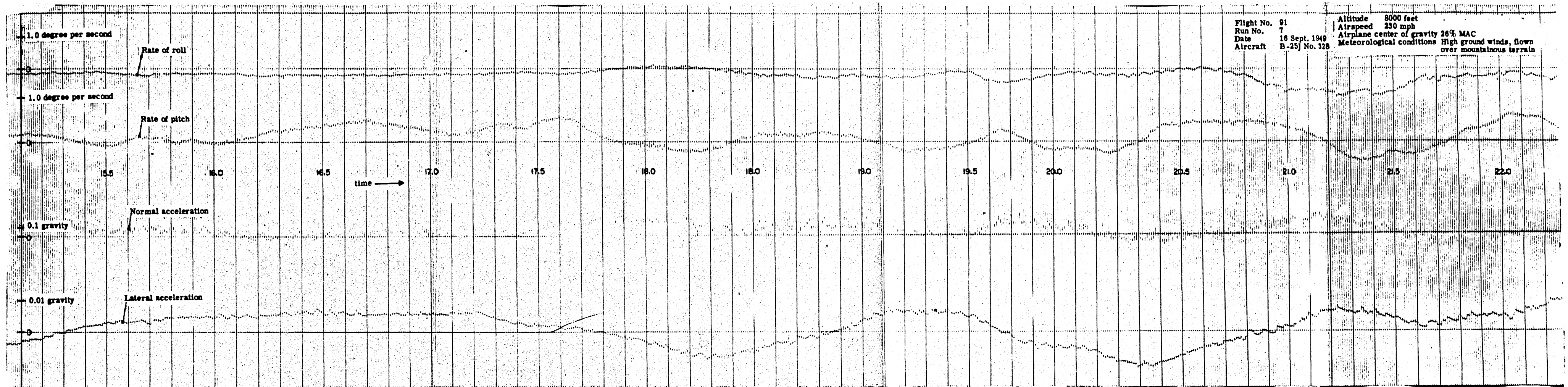
Flight No. 91
 Run No. 5
 Date 16 Sept. 1949
 Aircraft B-25j No. 328

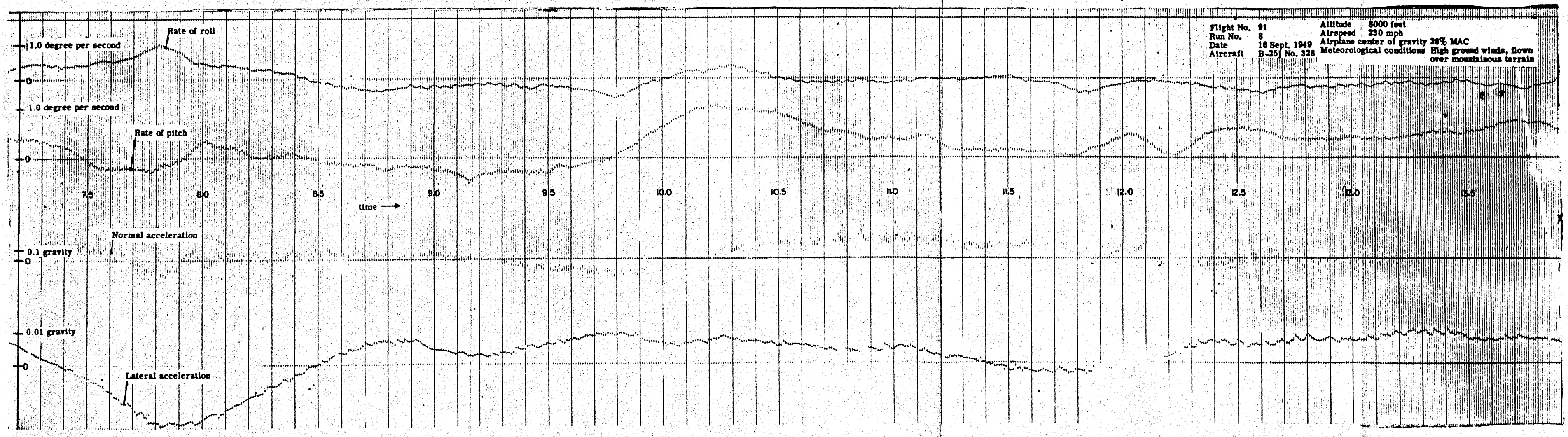
Altitude 8000 feet
 Airspeed 230 mph
 Airplane center of gravity 26% MAC
 Meteorological conditions High ground winds, flown over mountainous terrain

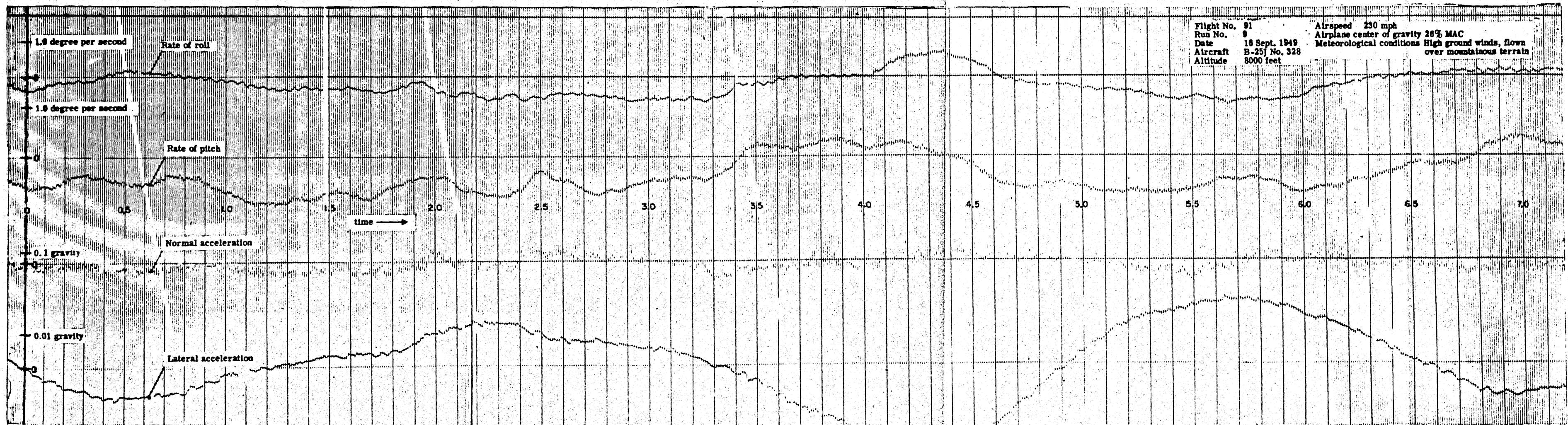
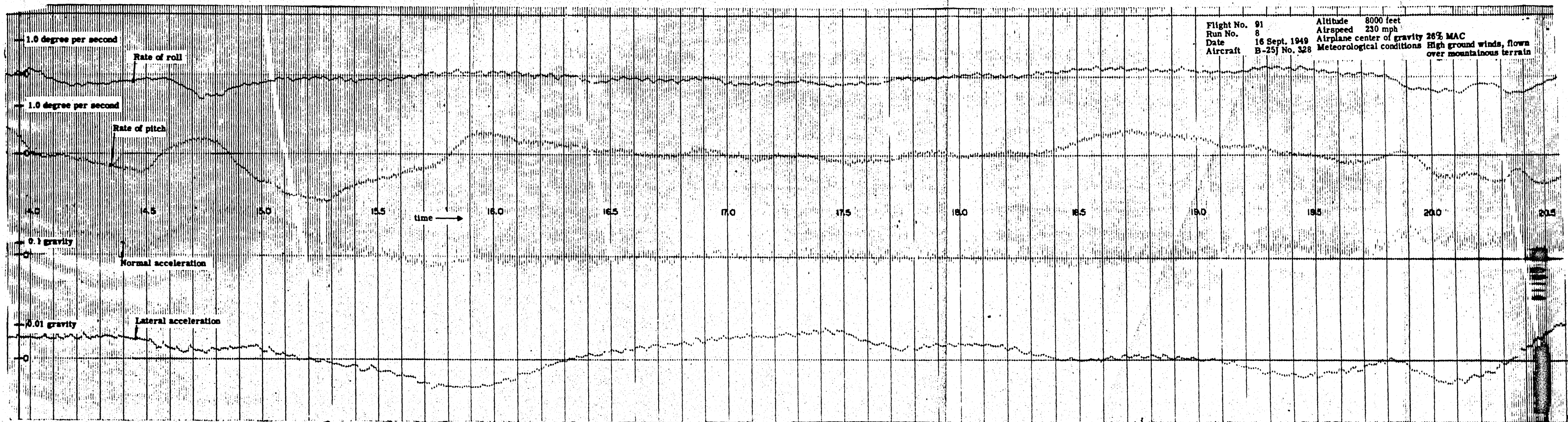


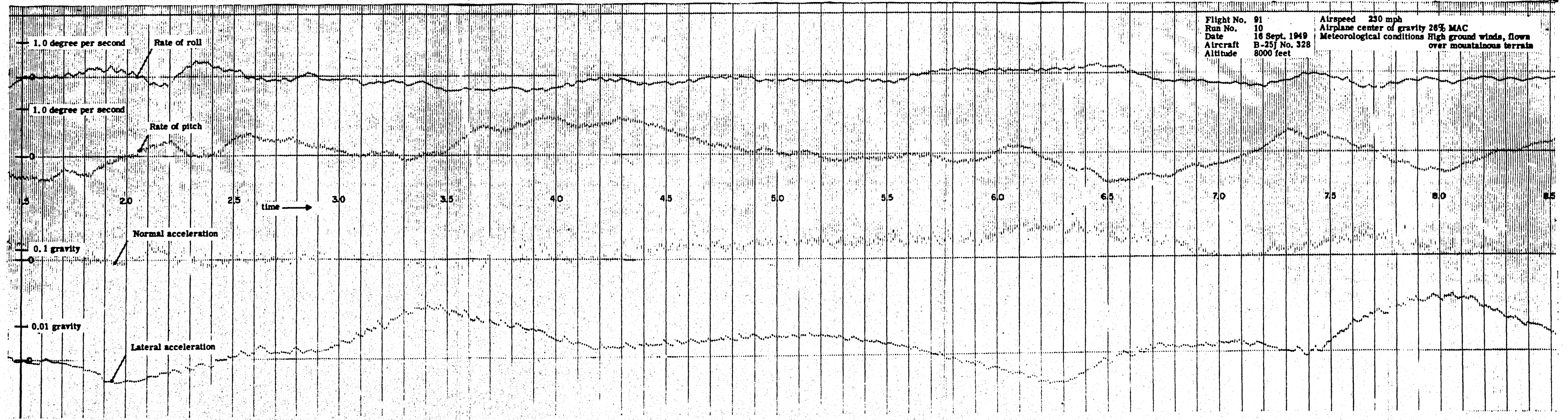
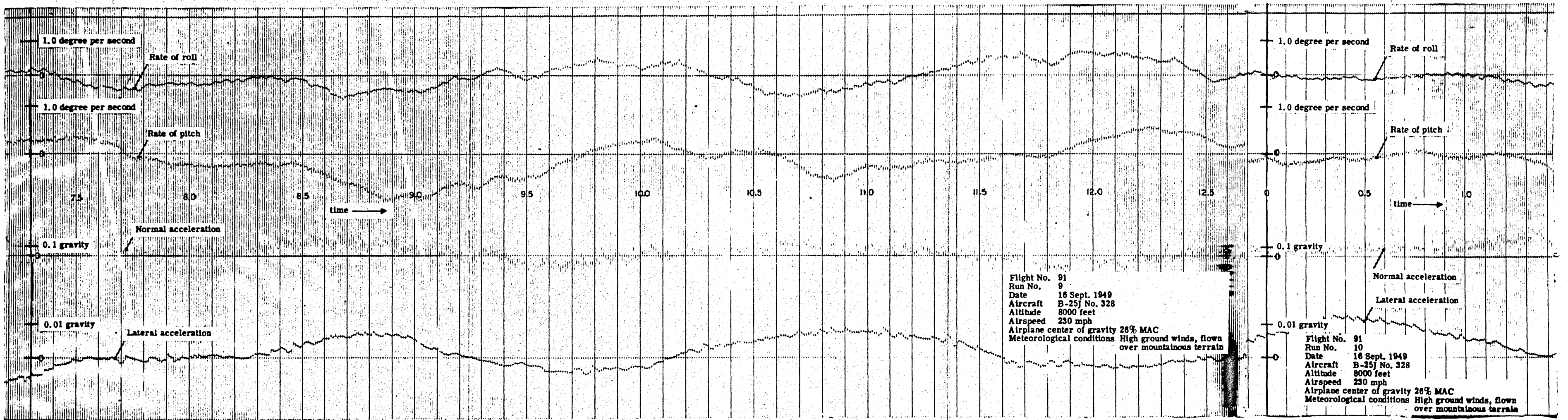


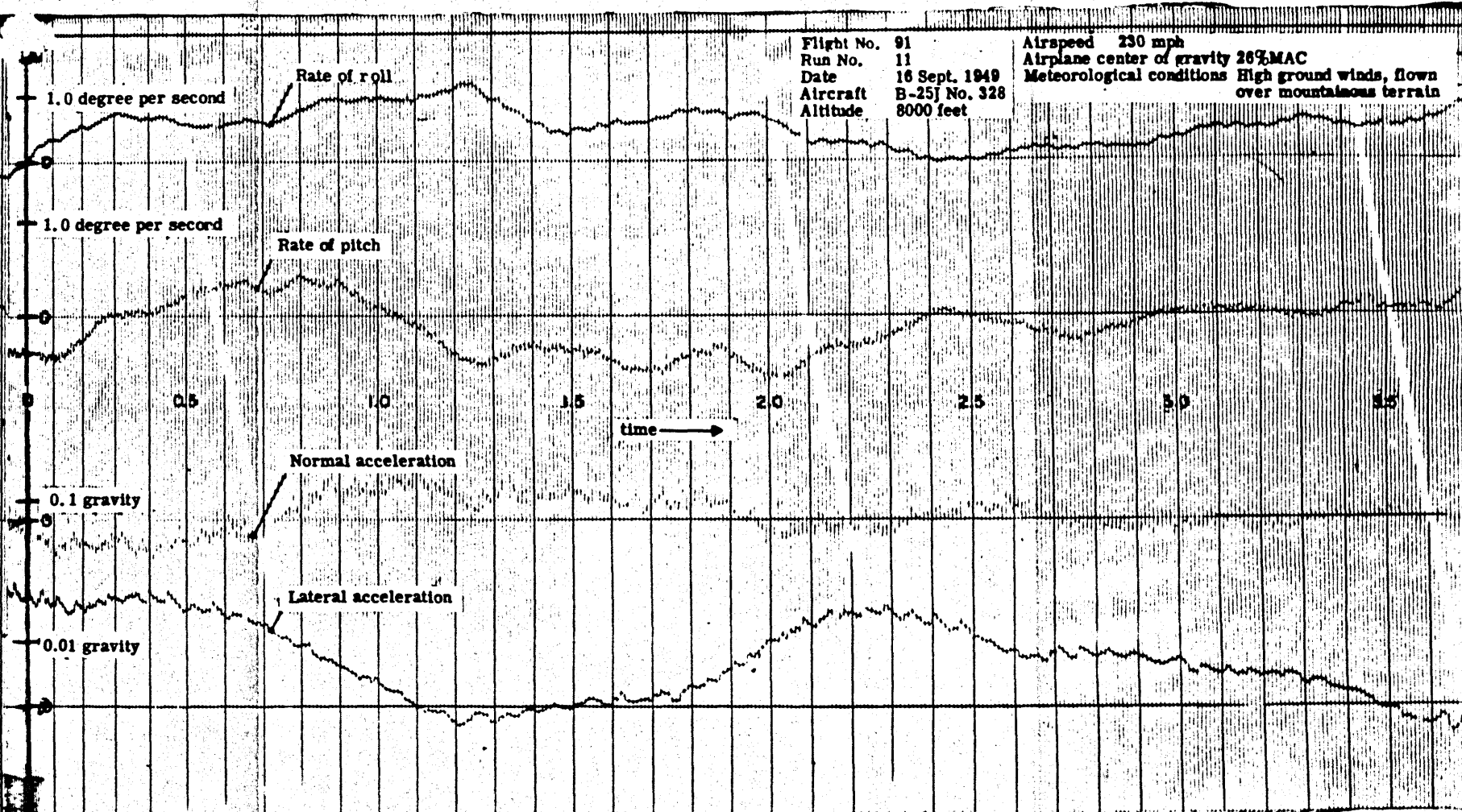
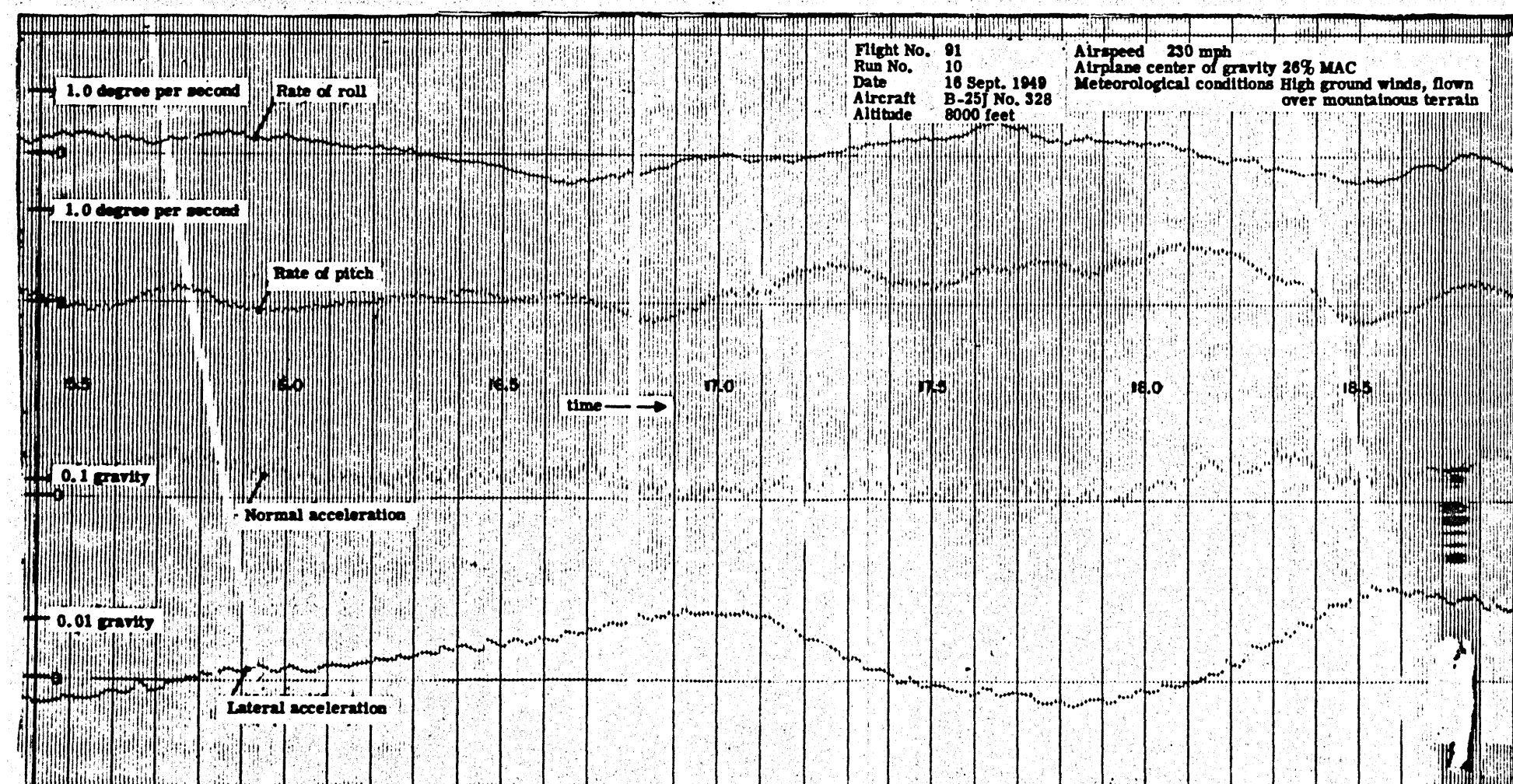
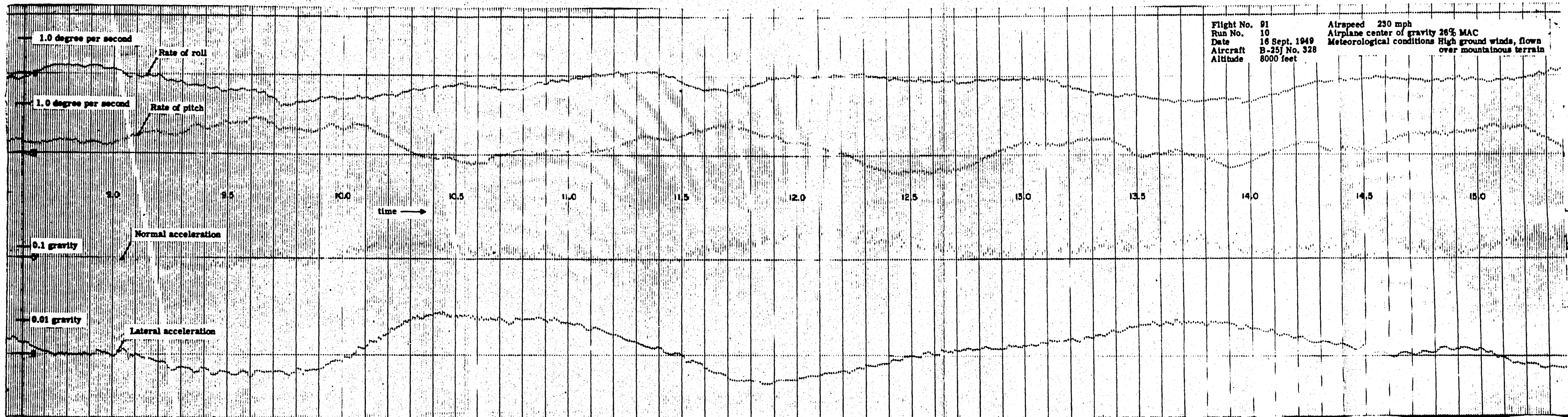


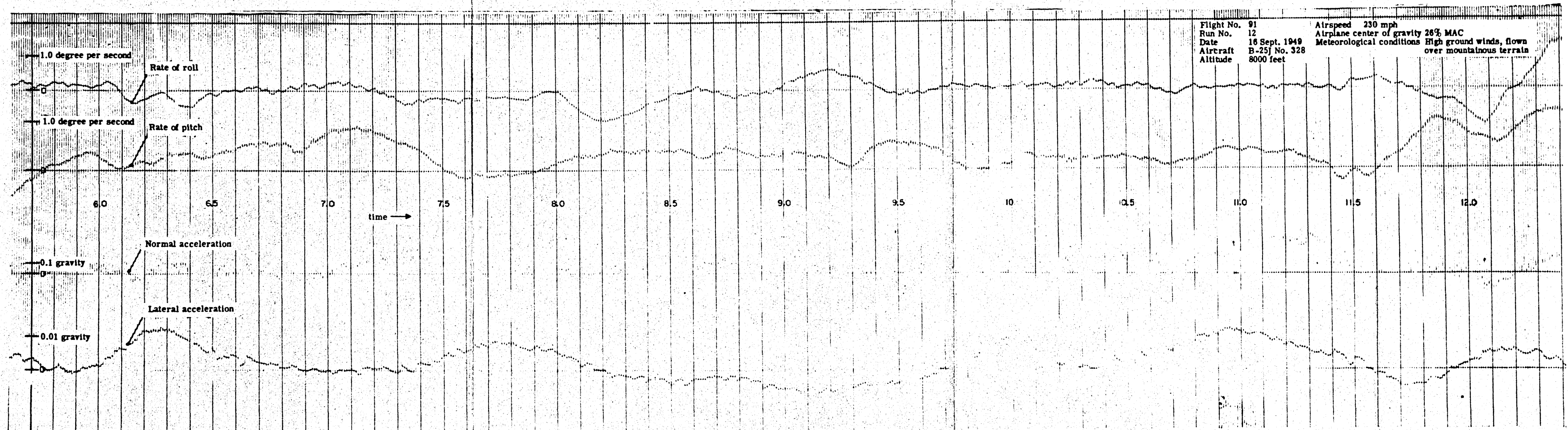
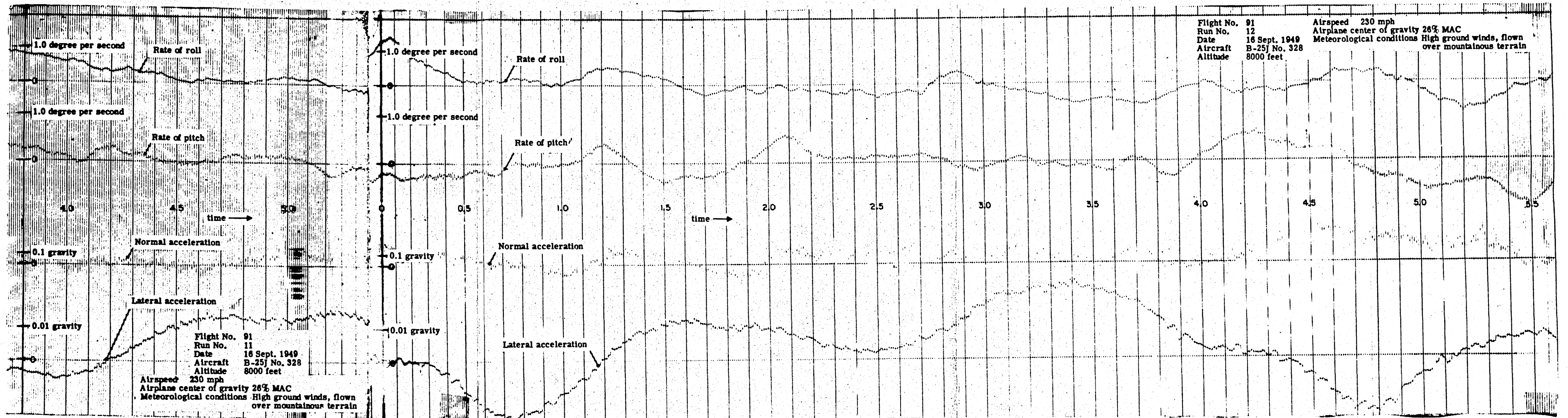


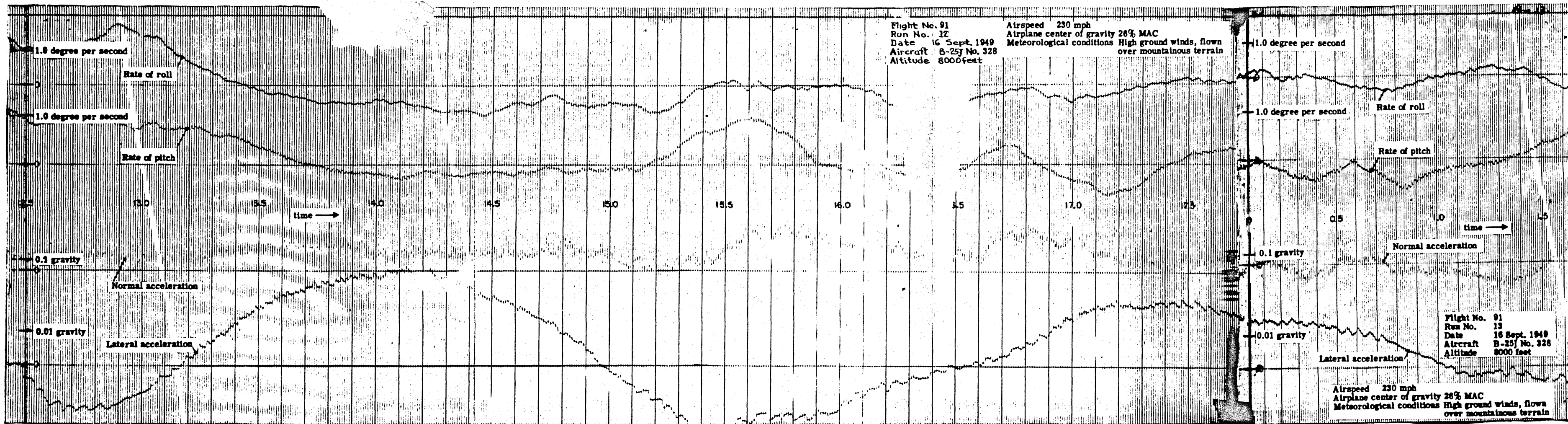


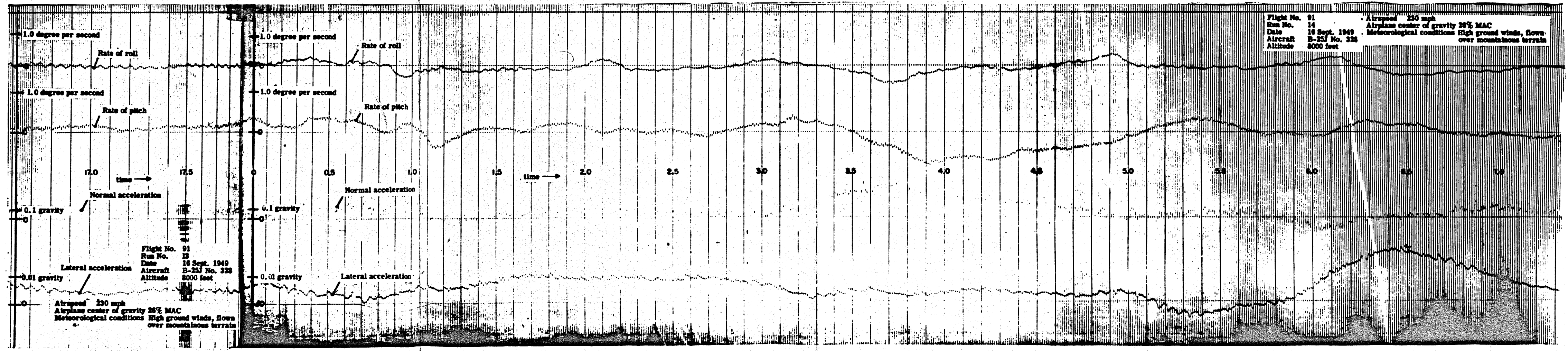
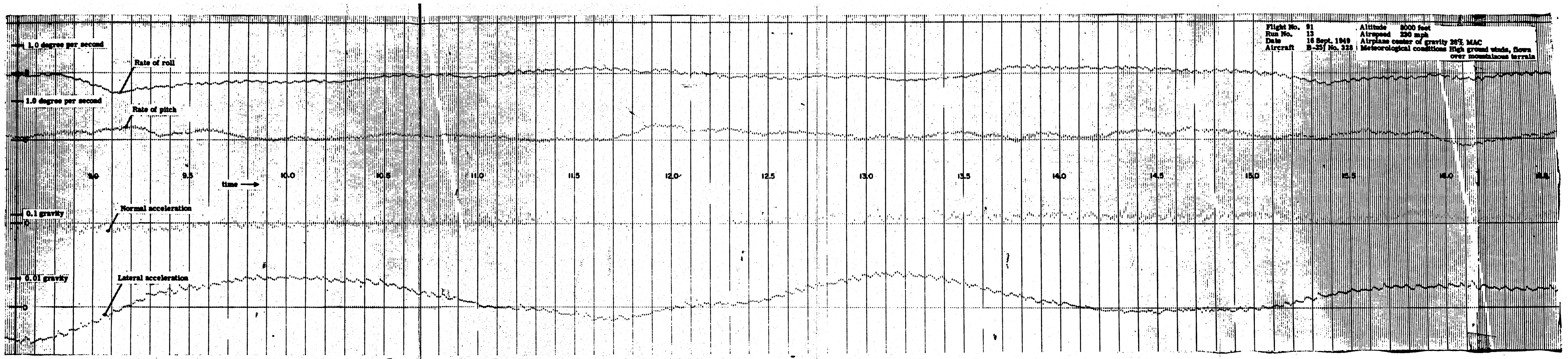


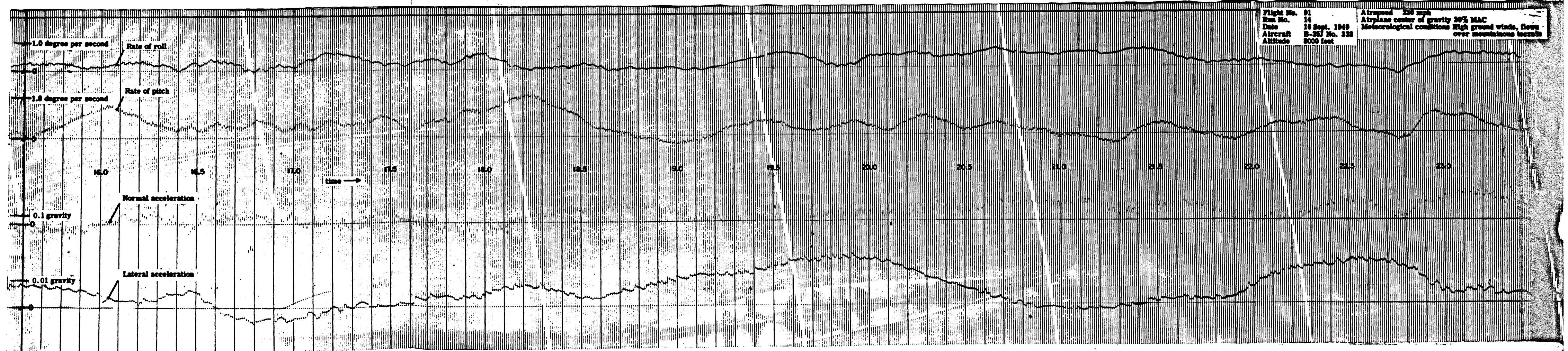
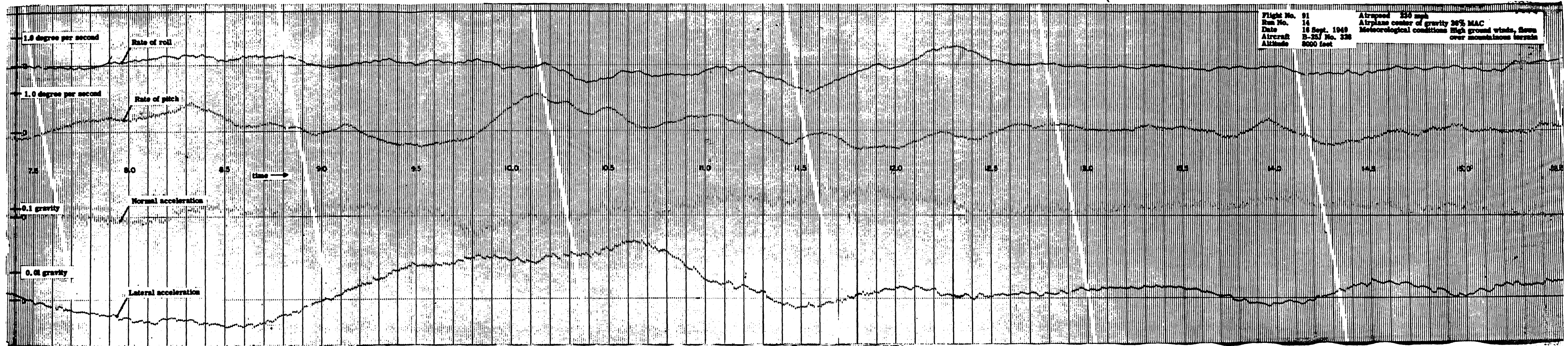


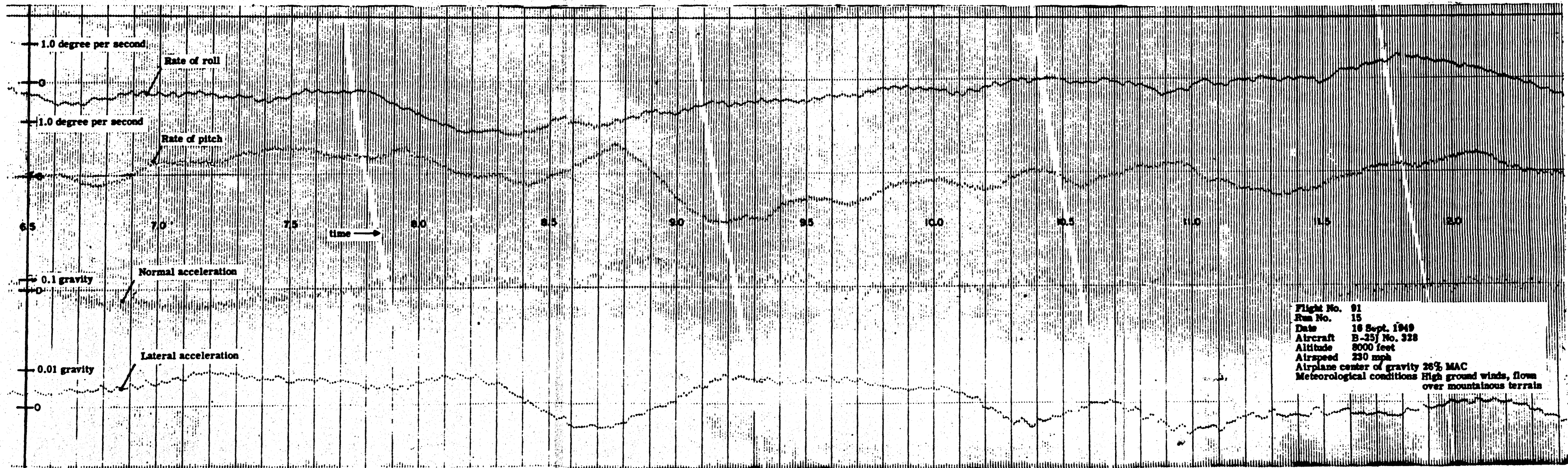
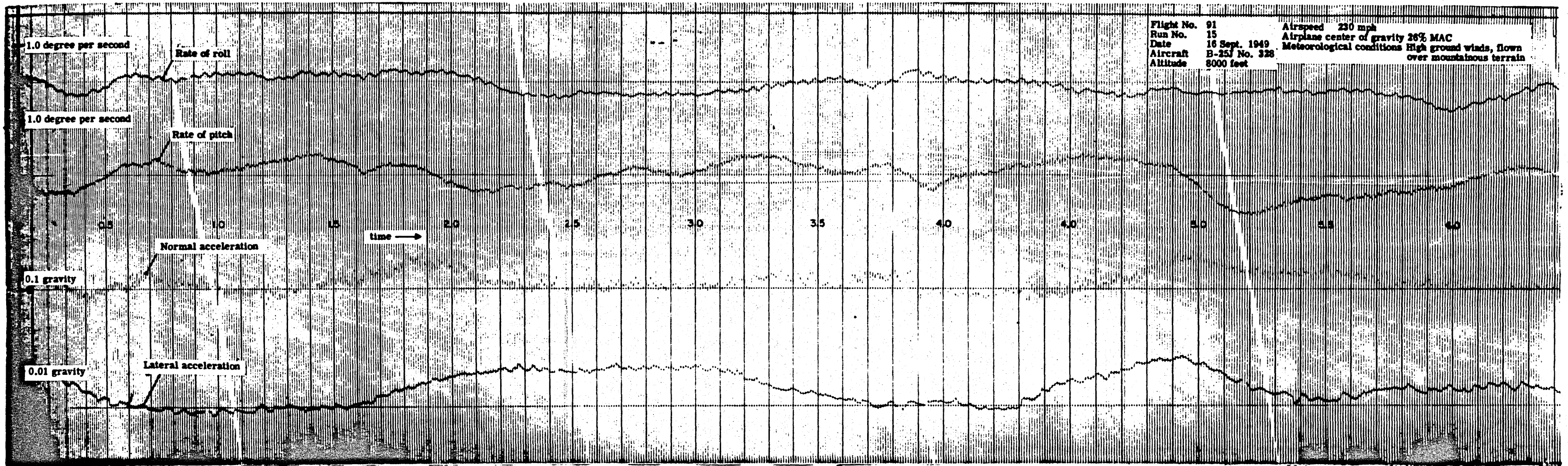


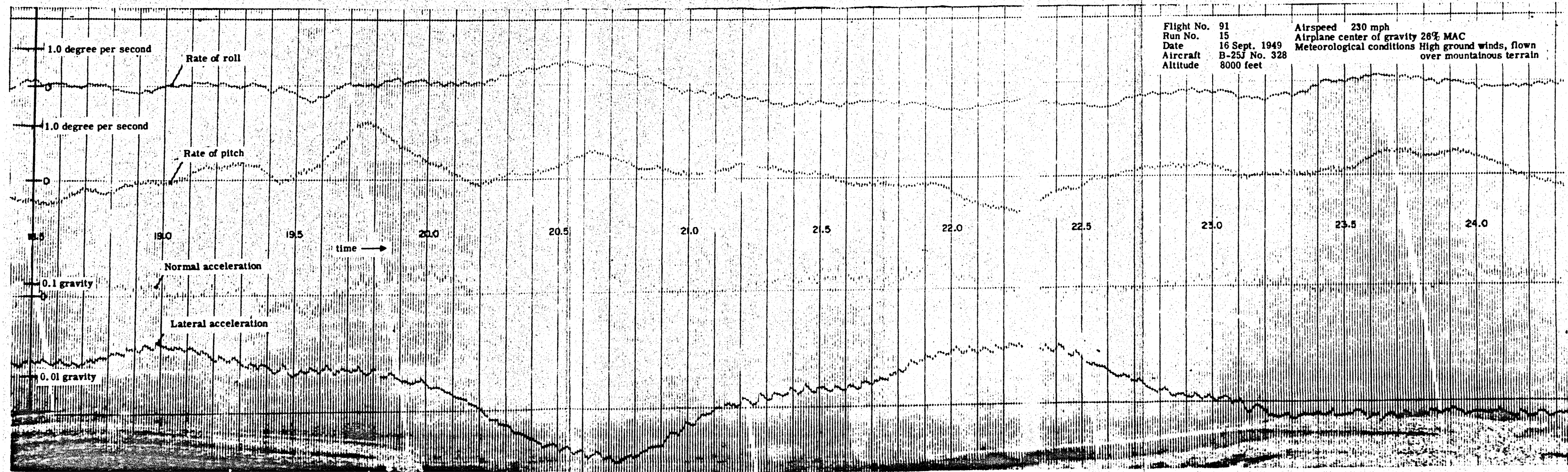
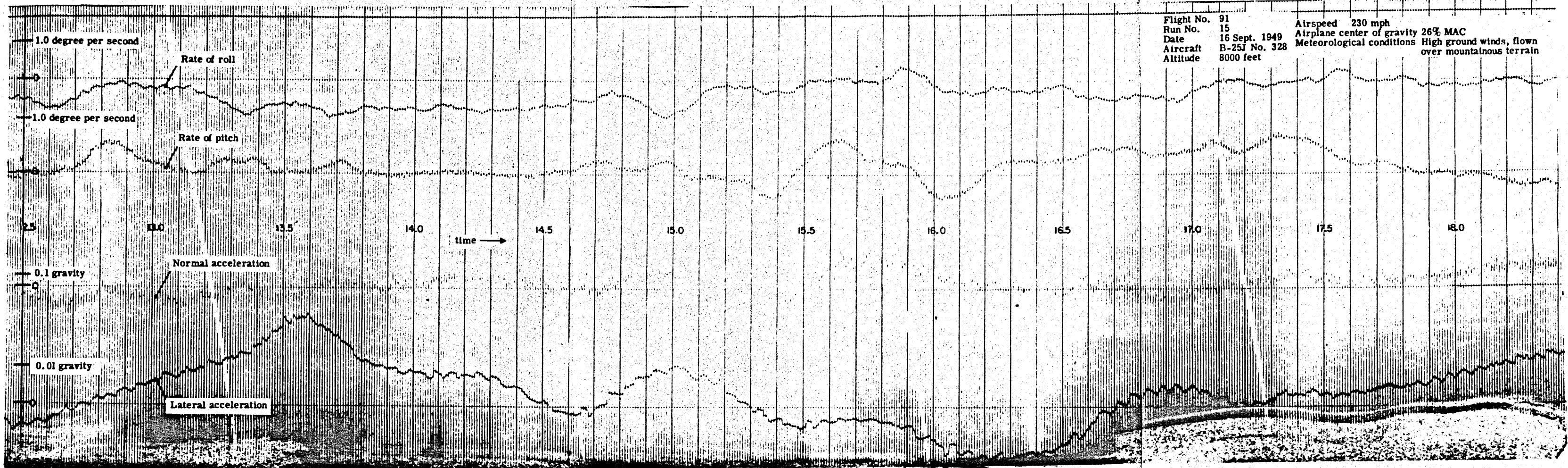


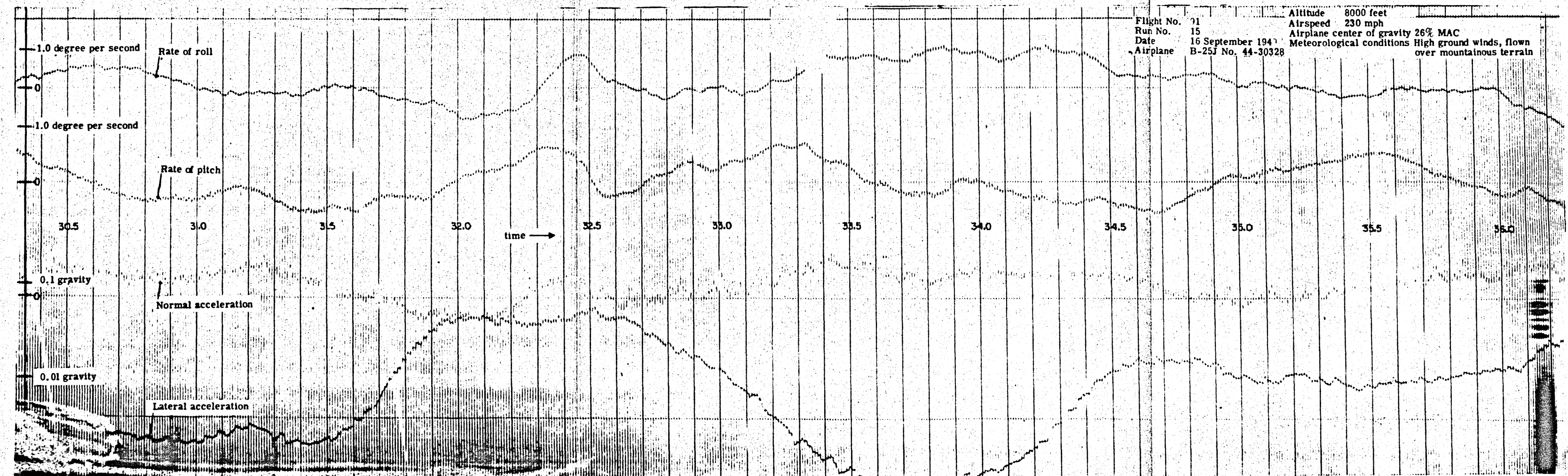
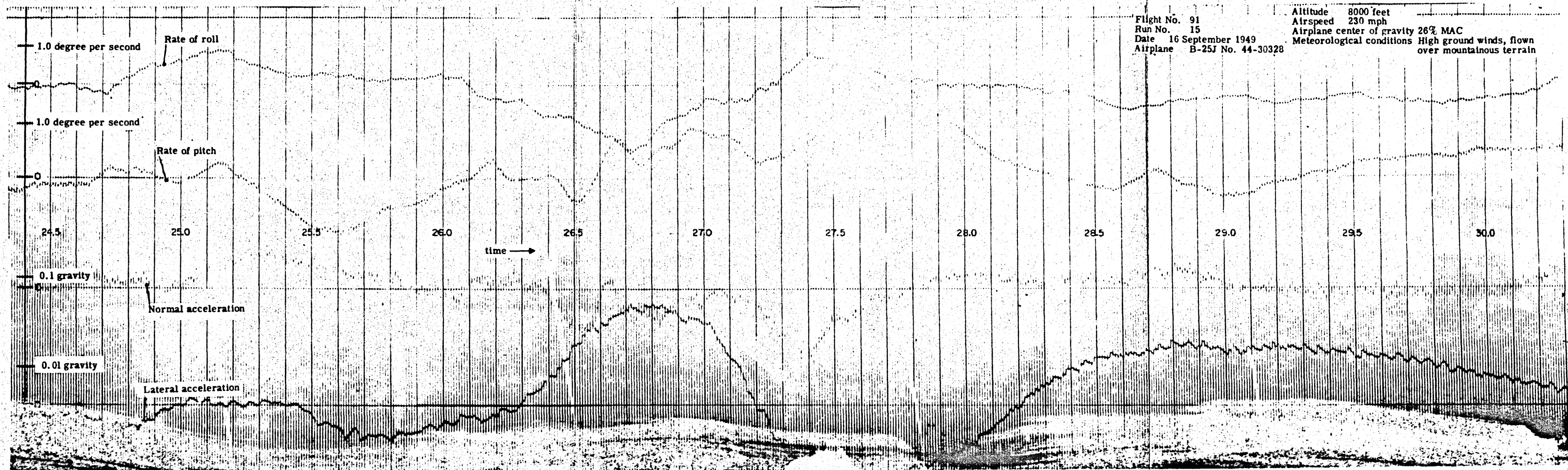


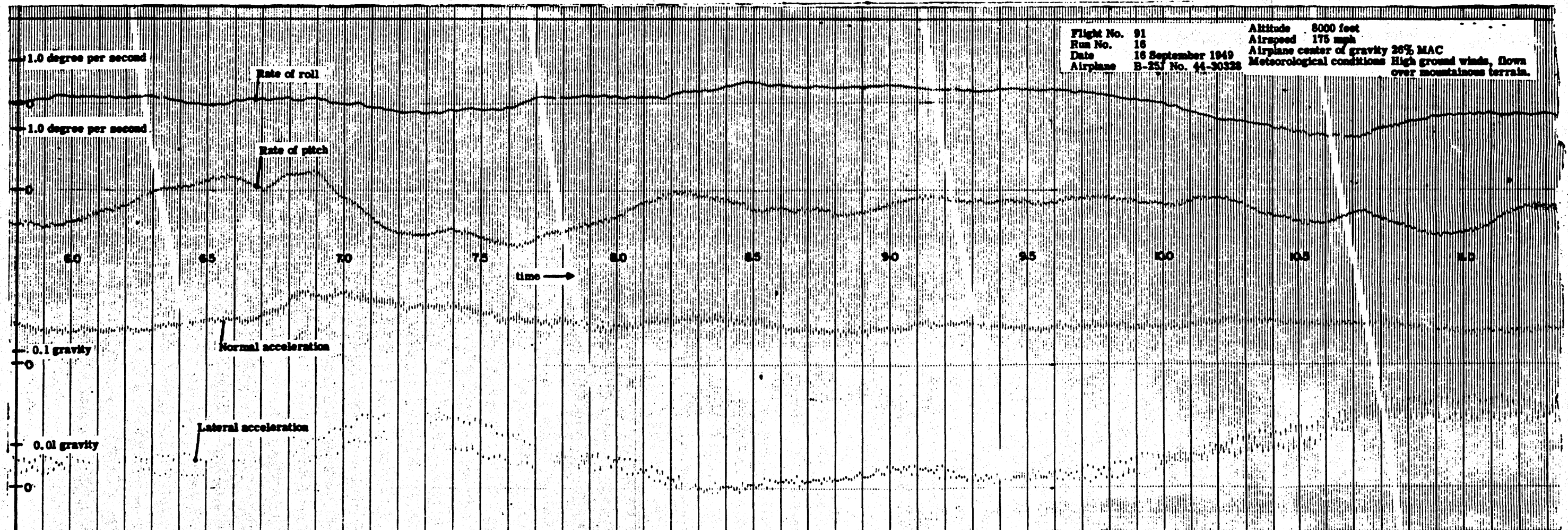
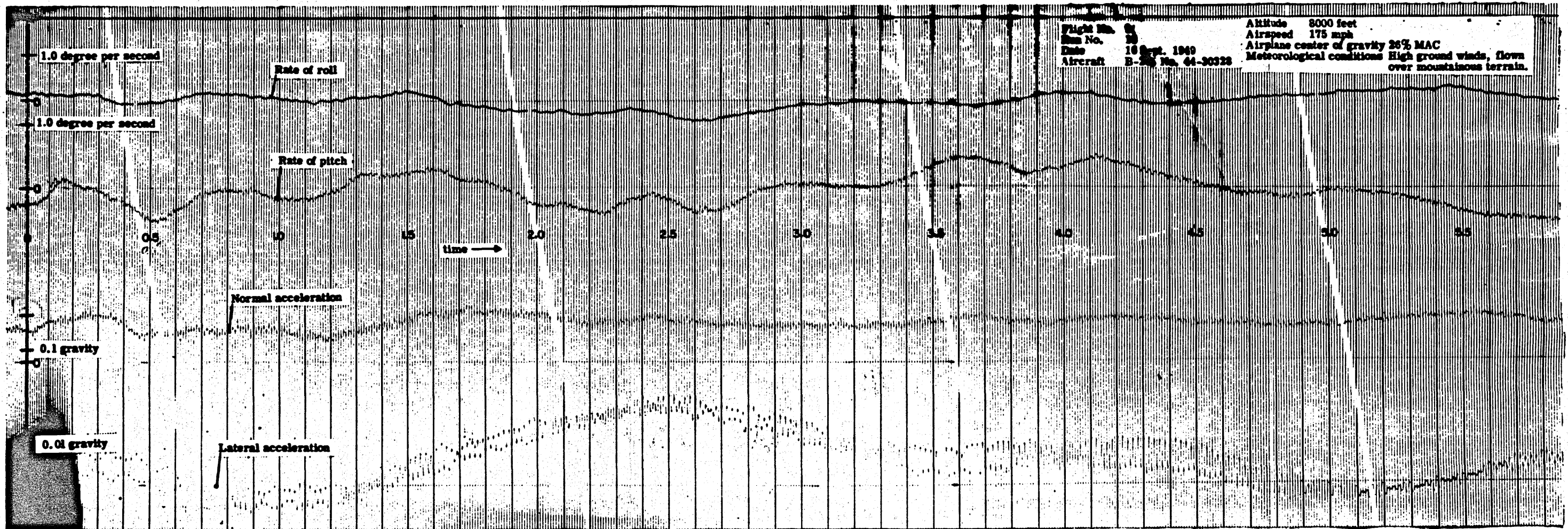


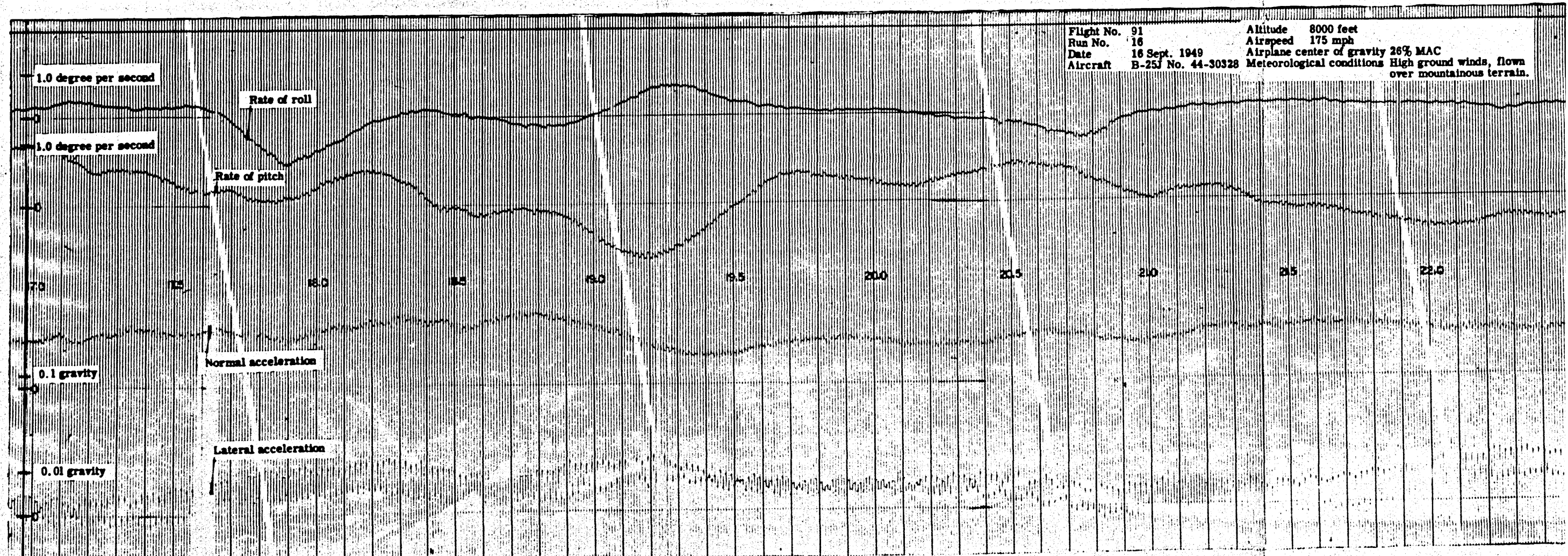
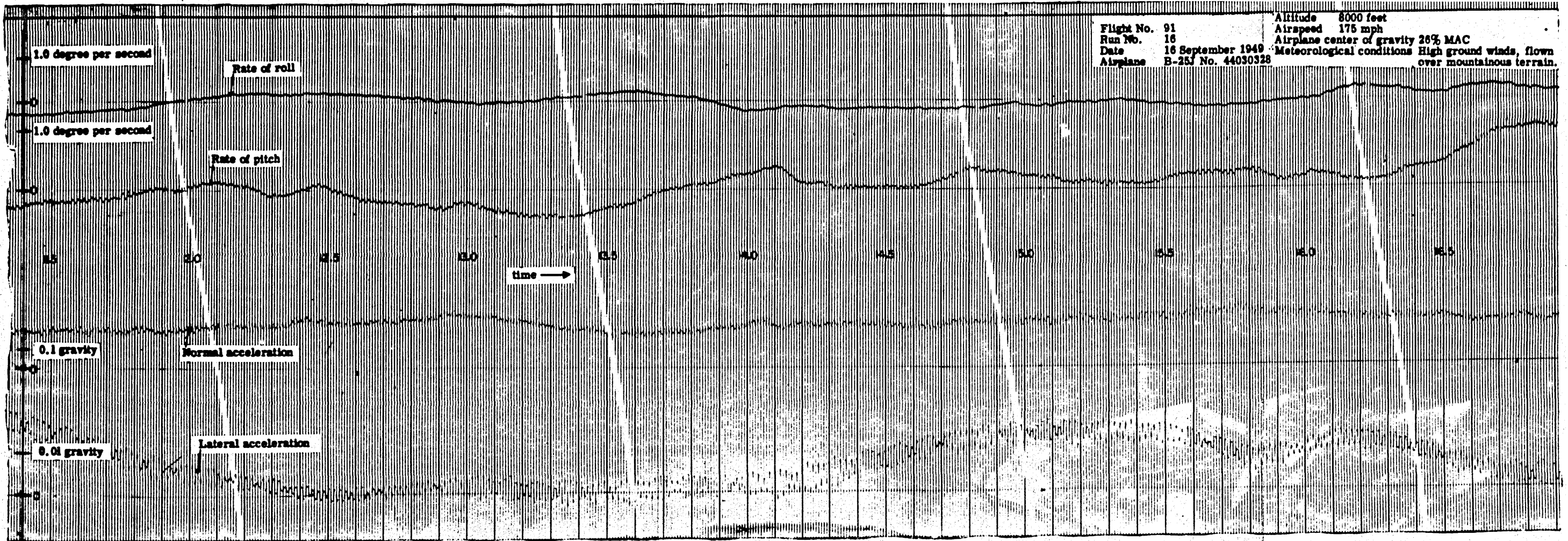


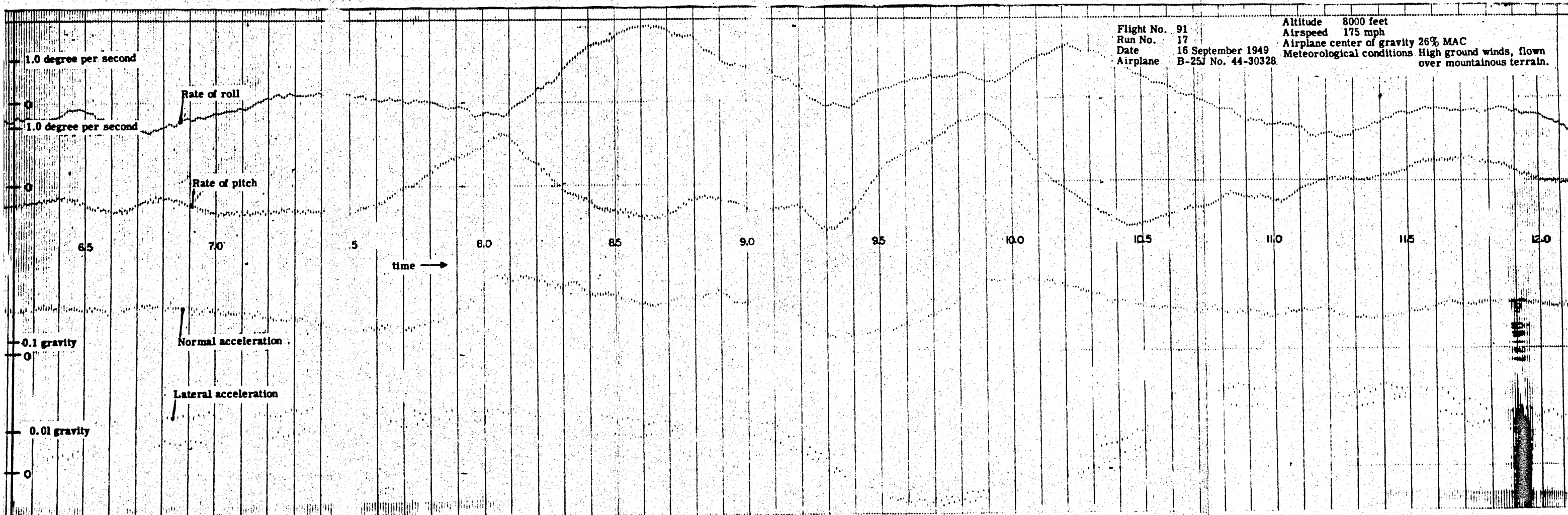
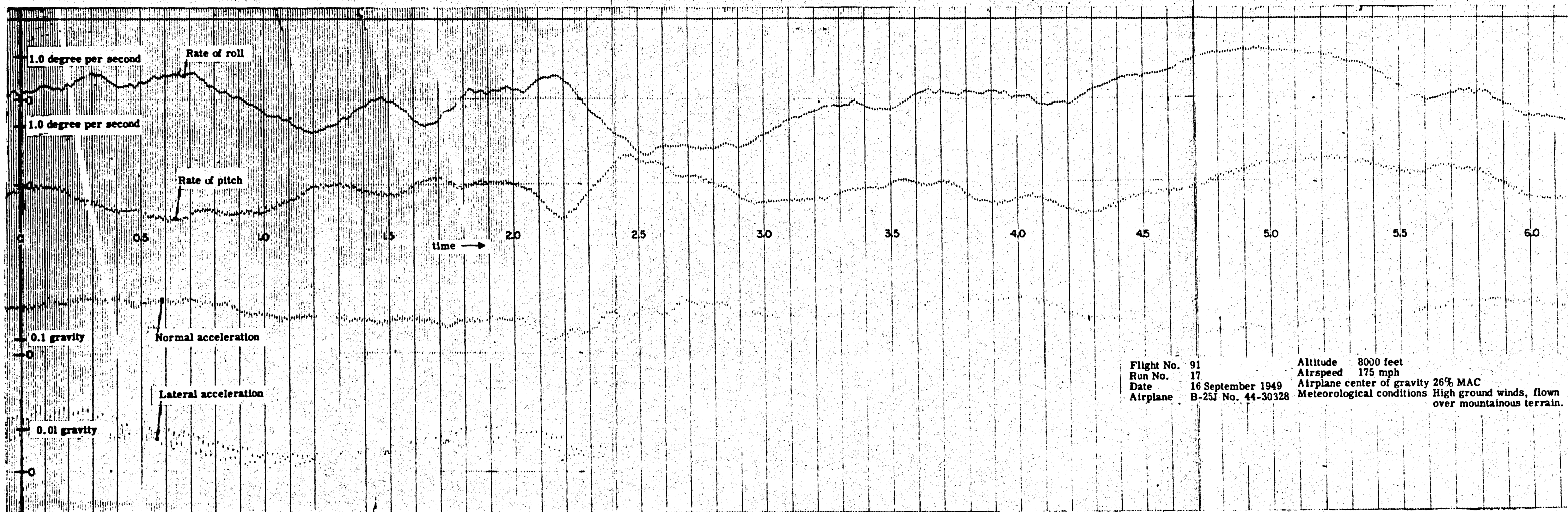


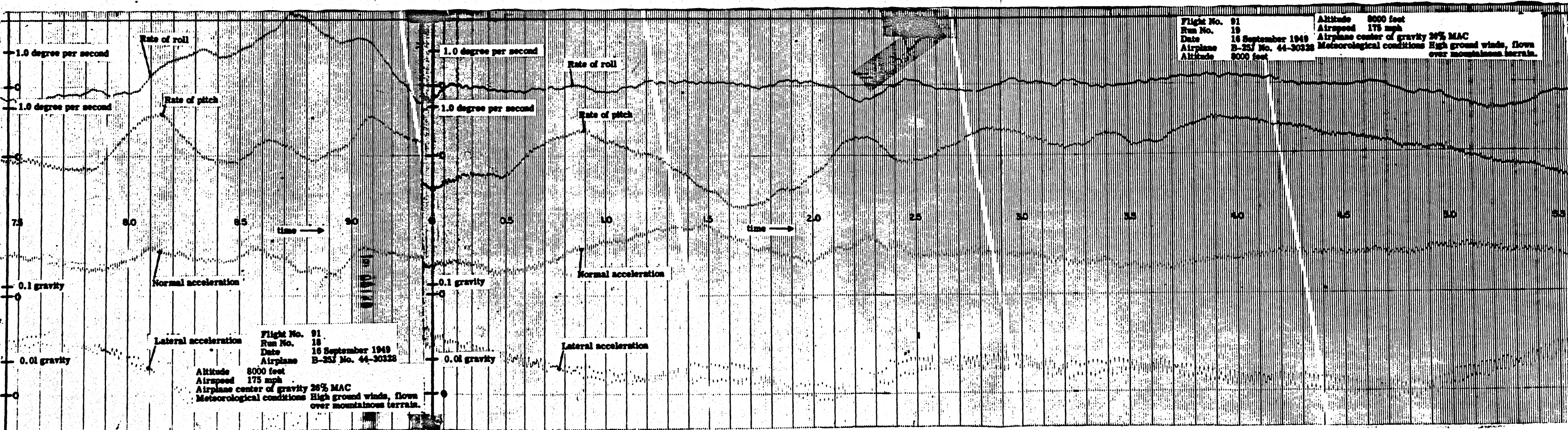
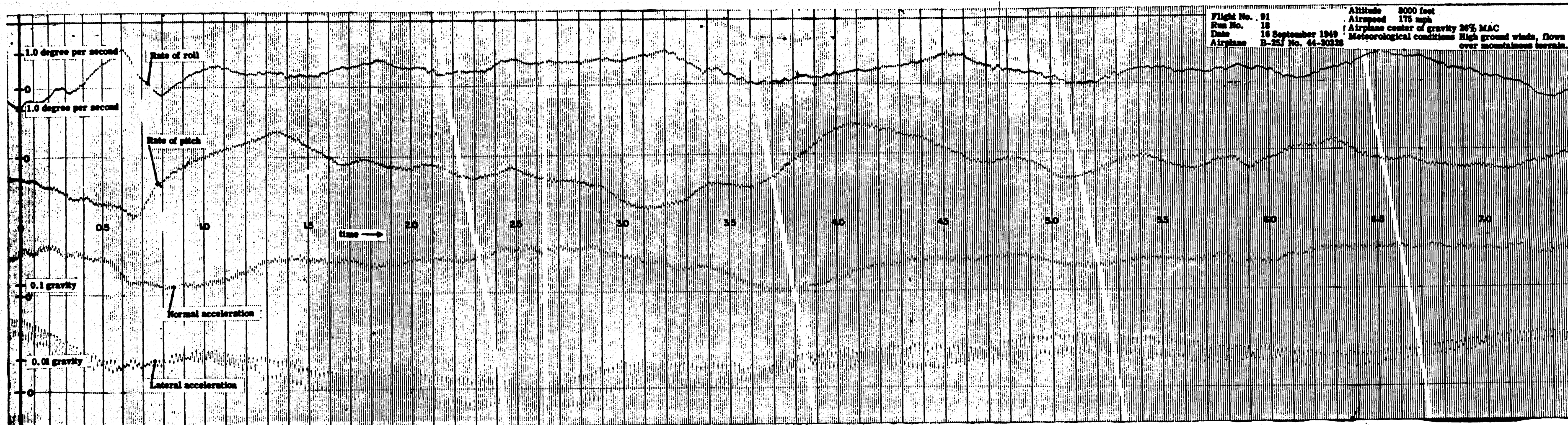


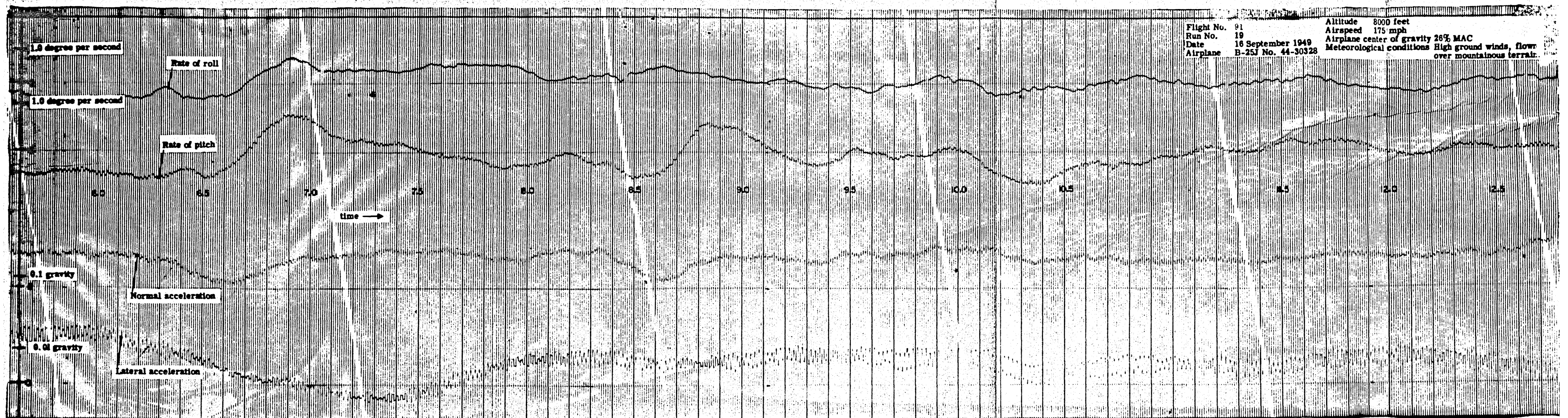




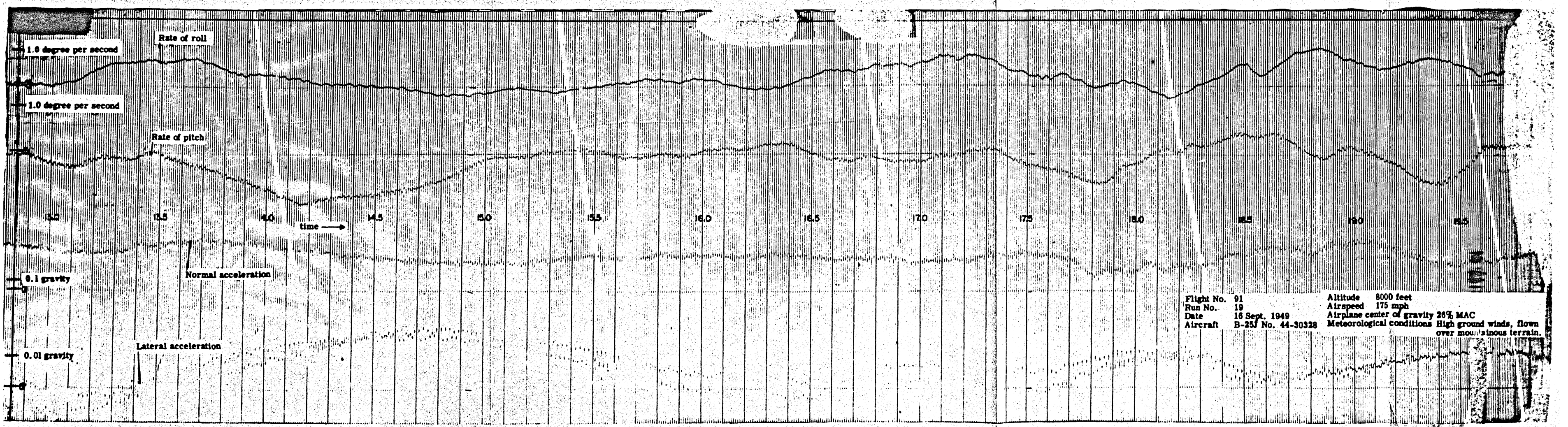








Flight No. 91 Altitude 8000 feet
 Run No. 19 Airspeed 175 mph
 Date 16 September 1949 Airplane center of gravity 26% MAC
 Airplane B-25J No. 44-30328 Meteorological conditions High ground winds, flow over mountainous terrain.



Flight No. 91 Altitude 8000 feet
 Run No. 19 Airspeed 175 mph
 Date 16 Sept. 1949 Airplane center of gravity 26% MAC
 Aircraft B-25J No. 44-30328 Meteorological conditions High ground winds, flow over mountainous terrain.

